PB 201 646

AEROSPACE REPORT NO
TOR-0059(6769-01)-2. VOL. II

Final Report
Hybrid Heat Engine / Electric Systems Study
Volume II: Appendices A through F

71 JUN 01

Prepared for DIVISION OF ADVANCED AUTOMOTIVE
POWER SYSTEMS DEVELOPMENT
U. S. ENVIRONMENTAL PROTECTION AGENCY
Ann Arbor, Michigan

Contract No. F04701-70-C-0059

Reproduced by
NATIONAL TECHNICAL
INFORMATION SERVICE
Springfield, Va. 22151

Office of Corporate Planning
THE AEROSPACE CORPORATION
El Segundo, California

313

PB 201 646

BIBLIOGRAPHIC DATA SHEET

1. Report No. TOR-0059(6769-01)-2 -V.2

3. Recipient's Accession No.

4. Title and Subtitle
Hybrid Heat Engine/Electric Systems Study Volume II

5. Report Date
June 1971

6.

7. Author(s)
Joseph Meltzer, Donald Lapedes

8. Performing Organization Rept. No.

9. Performing Organization Name and Address
The Aerospace Corporation
2350 East El Segundo Blvd.
El Segundo, California 90245

10. Project/Task/Work Unit No.

11. Contract/Grant No.
F04701-70-C-0059

12. Sponsoring Organization Name and Address
Division of Advanced Automotive Power Systems Development
U.S. Environmental Protection Agency
5 Research Drive
Ann Arbor, Michigan 48103

13. Type of Report & Period Covered
Final Report
June '70 to June '71

14.

15. Supplementary Notes

16. Abstracts

The report contains supplementary data forming the appendices for Volume I of the Final Report with the same title.

17. Key Words and Document Analysis. 17a. Descriptors

Electric Automobiles 1306
BT Automobiles
Electric Vehicles
Air Borne Wastes
RT Air Pollution
Combustion Products
Exhaust Gases

17b. Identifiers/Open-Ended Terms

17c. COSATI Field/Group Propulsion and Fuels/Air Breathing Engines

18. Availability Statement
Release un limited

19. Security Class (This Report)
UNCLASSIFIED

20. Security Class (This Page)
UNCLASSIFIED

21. No. of Pages
319

22. Price
$6.00

FORM NTIS-35 (10-70)

USCOMM-DC 40329-P71

Report No.
TOR-0059(6769-01)-2,
Vol. II

FINAL REPORT
HYBRID HEAT ENGINE/ELECTRIC SYSTEMS STUDY

Volume II: Appendices A through F

71 JUN 01

Office of Corporate Planning
THE AEROSPACE CORPORATION
El Segundo, California

Prepared for

Division of Advanced Automotive Power Systems Development
U.S. ENVIRONMENTAL PROTECTION AGENCY
Ann Arbor, Michigan

Contract No. F04701-70-C-0059

FOREWORD

Basic to analyzing the performance of the hybrid vehicle was the importance of understanding the characteristics of each major component since each would be operating in a nonstandard mode required by the hybrid arrangement. In addition, the potential for improvement had to be understood to predict the performance of advanced designs. This report, therefore, contains two types of information: (a) hybrid system analysis and results; and (b) major component state-of-the-art discussions, characteristics used in this study, and advanced technology assessments. Heat engine operating characteristics, mechanical parameters, and exhaust emissions are covered extensively because of both their primary importance and the difficulty involved in collecting a reliable comprehensive set of data; this should relieve future investigators making studies of nonconventional propulsion systems of the necessity of repeating the burdensome task of assembling a data bank.

It should be recognized that calculated results are based on data compiled in this study. The magnitude and trends were established on the basis of a comprehensive survey and evaluation of the best data from both the open literature and current available unpublished data sources. These data are considered suitable for use in the feasibility study conducted under this contract. However, for further detailed design a substantial refinement of the data base would be necessary.

The report is organized to give a logical build-up of information starting with study specification, analytical techniques, and component characteristics and concluding with system performance results and recommendations for development. However, selective reading of major systems performance results is possible and to assist those so interested, the following brief guide is presented:

Section 1	Summary of study results and recommendations
Sections 2, 3, 10, and 11	Presentation of study objectives, design specifications, and results
Sections 3 and 4	Description of computational techniques and performance requirements
Sections 6 through 9	Review of contemporary and projected technology of major components
Section 12	Cost estimates for high-volume production of hybrid cars
Section 13	Presentation of a technological plan for component and system development

This report is published in two volumes for convenience; however, separation of the material is made with due regard to organization. Volume I consists of Sections 1 through 13 and presents the essential study information, while Volume II consists of Appendices A through F and presents supplementary data.

The period of performance for this study was June 1970 through June 1971.

ACKNOWLEDGMENTS

The extensive diversity in technological capabilities necessary for a thorough evaluation of the hybrid electric vehicle has required the reliance for support and expertise on select members of The Aerospace Corporation technical staff as well as members of the national technical community. Recognition of this effort is expressed herewith:

The Aerospace Corporation

Mr. Dan Bernstein	Electrical System-Control System
Mr. Lester Forrest	Heat Engines (Internal Combustion)
Mr. Gerald Harju	Programming for Computations
Mr. Merrill Hinton	Vehicle Specifications/Conceptual Design and Sizing Studies
Dr. Toru Iura	Heat Engines (Internal Combustion) Heat Engine Exhaust Emissions Vehicle Exhaust Emissions Test Program
Mr. Dennis Kelly	Electrical System - Motor and Generator
Mr. Jack Kettler	Electrical System - Batteries Heat Engines (External Combustion)
Mr. Harry Killian	Computational Techniques Electrical System - Batteries
Mr. Robert La France	Electrical System - Motor, Generator, Control Systems
Mrs. Roberta Nichols	Vehicle Exhaust Emission Test Program
Mr. Wolfgang Roessler	Heat Engine Exhaust Emissions Vehicle Exhaust Emission Test Program
Dr. Henry Sampson	Vehicle Specifications Computational Techniques Vehicle Power Requirements
Mr. Raymond Schult	Electrical System - Motor, Generator, Control Systems

University of California, Berkeley

Dr. Robert Sawyer	Heat Engine Exhaust Emissions

University of California, Irvine

Dr. Robert M. Saunders	Electrical System - Motor Generator, Control Systems

It is to be noted that considerable data of great value to this study were kindly provided by individuals in industry, universities, and government agencies. Acknowledgment of these data sources is given in Appendix F to this report.

Donald E. Lapedes

Donald E. Lapedes
Manager, Hybrid Vehicle Program

Joseph Meltzer
Director, Pollution and Resources
Programs
Office of Corporate Planning

CONTENTS

The major sections and appendices of Volumes I and II are listed below. For detailed tables of contents and lists of illustrations see the individual sections and appendices.

Volume I

Section | Page

1. Summary 1-1
2. Introduction 2-1
3. Vehicle Specifications and Study Methodology 3-1
4. Computational Techniques 4-1
5. Vehicle Power Requirements 5-1
6. Electrical System - Motor, Generator, and Control Systems 6-1
7. Electrical System - Battery Characteristics and Operation. 7-1
8. Heat Engine Performance Characteristics and Operation . . . 8-1
9. Heat Engine Exhaust Emissions 9-1
10. Conceptual Design and Sizing Studies 10-1
11. Summary of Results 11-1
12. Vehicle Production Cost Comparison 12-1
13. Technology Development Program Plan. 13-1

Volume II

Appendix

A. Hybrid Vehicle Performance Evaluation Computer Program A-1
B. Heat Engine Exhaust Emissions Collation and Analysis B-1
C. Vehicle Exhaust Emissions Test Program C-1
D. Vehicle Characteristics Over Emission Driving Cycle D-1
E. Heat Engine Data Compilation E-1
F. Acknowledgments to Sources of Subsystems/Component Data F-1

APPENDIX A

HYBRID VEHICLE PERFORMANCE EVALUATION COMPUTER PROGRAM: HEVPEC

CONTENTS

A. HYBRID VEHICLE PERFORMANCE EVALUATION COMPUTER PROGRAM: HEVPEC A-1

- A.1 Introduction A-1
- A.2 HEVPEC Input List A-1
- A.3 Flow Charts A-5
- A.4 HEVPEC Output List A-12
- A.5 Sample Output A-14
- A.6 Nomenclature for HEVPEC Flow Charts A-19

FIGURES

A-1. HEVPEC-S Flow Chart A-6
A-2. HEVPEC-P Flow Chart A-10
A-3. Generator Output Current (IG) Versus Time A-15
A-4. Electric Drive Motor Input Current (IM) Versus Time. . A-16
A-5. Battery State of Charge (S) Versus Time A-17
A-6. Battery Cell Voltage (VBD) Versus Time A-18

APPENDIX A

HYBRID VEHICLE PERFORMANCE EVALUATION COMPUTER PROGRAM: HEVPEC

A.1 INTRODUCTION

This appendix illustrates the logical structures of the series and parallel versions of the HYBRID Program (HEVPEC) along with the necessary input list and a sample of the output format. The series and parallel programs will henceforth be referred to as HEVPEC-S and HEVPEC-P.

A.2 HEVPEC INPUT LIST

Both the series and parallel versions of HEVPEC use FORTRAN IV NAMELIST input format. The following symbols and abbreviations are a list and description of the input variables.

(S)	Indicates variable used in HEVPEC-S only
(P)	Indicates variable used in HEVPEC-P only

A	Vehicle frontal area
C	Air resistance coefficient
COIN	Battery capacity at beginning of driving cycle
CR	Rated capacity battery (C_r)
DELTAT	Interval between consecutive time points of driving profile (Δt)
ETA	Battery charge efficiency (η)
ETAG	Generator efficiency (η_G)
ETARB	Regenerative braking conversion efficiency (η_{RB})
ETAM	Average electric motor efficiency (η_m)

EOF	Flag specifying last case: EOF = 0 not the last case EOF = 1 the last case
G	Gear ratio between electric drive motor and wheels
IG$^{(S)}$	Generator current. If generator current is calculated in the program (i. e., IGFLAG=2), then this variable will not be input.
IGFLAG$^{(S)}$	IGFLAG=1 I_G is an input constant IGFLAG=2 I_G is calculated internally
IGMIN$^{(S)}$	Minimum allowable value of IG (See nomenclature Section A. 6)
IHDR	IHDR=1 80 character BCD description read in after NAMELIST data and printed out at the bottom of each case
IMIN$^{(P)}$	Minimum allowable value of IG$_2$ (See nomenclature Section A. 6)
INK835	INK835 = 1 No plots requested INK835 = 2 Plots produced on Cal Comp pen plotters INK835 = 3 Plots produced on 835 film
IPROF	IPROF = 1 for DHEW driving profile IPROF = 2 for design driving profile
IREGEN	Flag specifying regenerative braking option: IREGEN = 1 (not included) IREGEN = 2 (included)
ITORQUE$^{(S)}$	ITORQUE = 1 Determine motor torque from TIN table ITORQUE = 2 Calculate motor torque from equation (Refer to HEVPEC-S flowchart)
LASTLIN	LASTLIN = 1 Print out every NPRINT time step LASTLIN = 2 Print out last time point only
KBAR	Electric drive motor torque constant ($\overline{K}$)

NPOINT	An integer ≥ 1 if plots are requested to indicate that every NPOINT time point will be plotted
NPROF	Number of prints in driving profile
NPRM$^{(S)}$	Number of entries in RPM table
NCURR$^{(S)}$	Number of I values in TIN array
P	Tire pressure
PAUX	Accessory equipment power
PER	Rated heat engine output (P_{er})
PROFILE	A tabular driving profile (velocity-time points)
PVSEHC	An emission index table for unburned hydrocarbons (e_{HC})
PVSECO	An emission index table for carbon monoxide (e_{CO})
PVSENO	An emission index table for nitric oxide (e_{NO_2})
R	Rolling radius of wheels
RPM$^{(S)}$	Table of values of motor speed corresponding to torques in TIN array
SVSIBC	A table of S versus IMBC (refer to nomenclature Section A. 6 for definition
THETA	Grade angle of road (θ)[*]
TIMEUN	Number of seconds per inch for the time scale (X axis) to be used for the plots
TIN$^{(S)}$	Table of T_m versus I_m for given values of motor speed (N_m)
TMVSTH	A table of time versus sin θ to be used whenever a design driving cycle is used. If the particular design driving cycle does not require grades, then this table need not be input.

---

[*] Symbols in ( ) are used in flow charts presented in Section A. 3.

VB	Voltage of electric drive motor (V_B)
VG	Generator output voltage (V_G)
VIBDS	Table of normalized maximum available battery discharge current [I_{BMAX}/C_r] versus state of charge
VMA	Maximum allowable cell voltage
VMC	Minimum allowable cell voltage
WI	Gross vehicle weight (W_I)
XI	Mechanical linkage loss factor (ξ)

A. 3 FLOW CHARTS

The HEVPEC-S and HEVPEC-P Flow Charts are shown in Figure A-1 and Figure A-2, respectively.

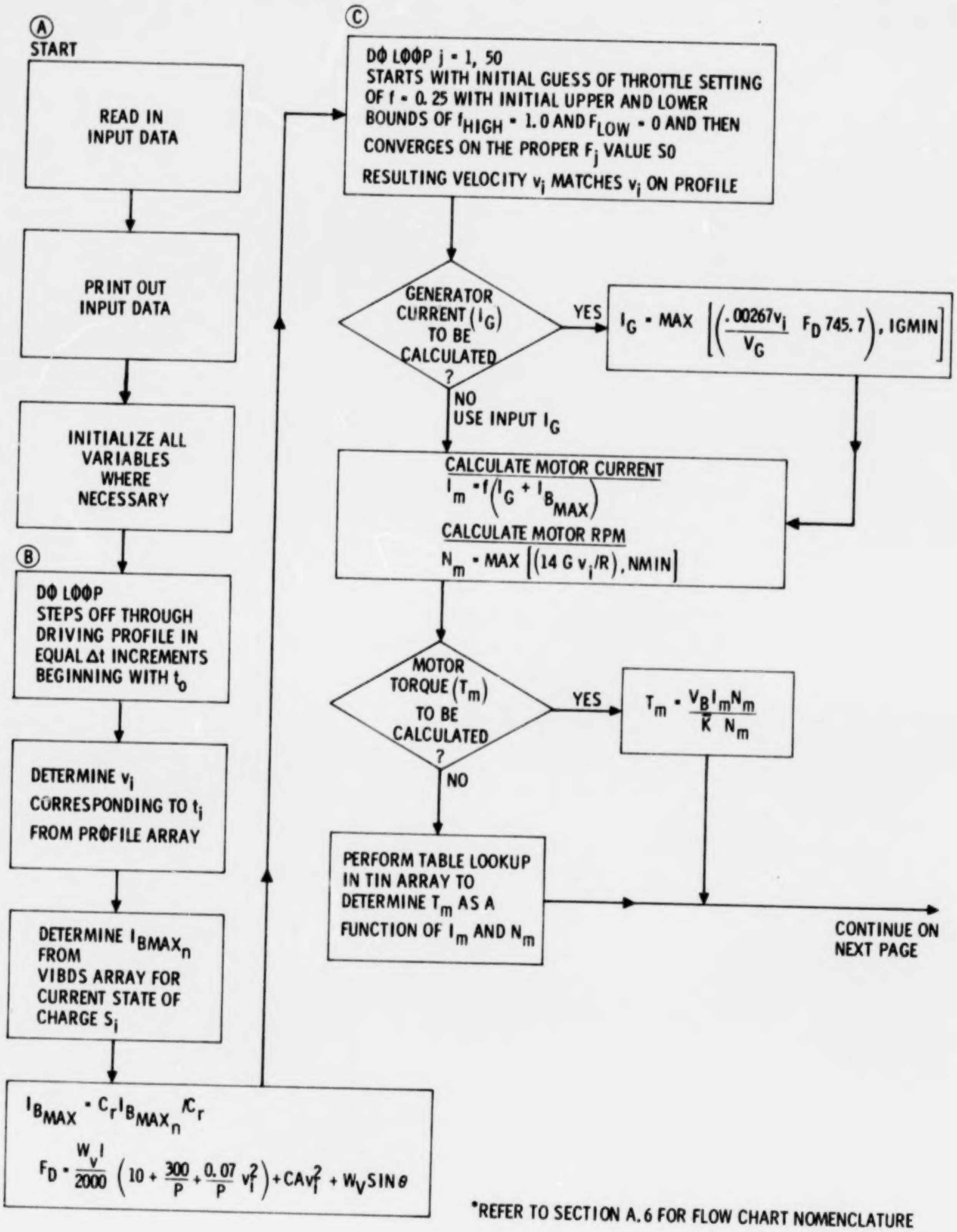
Ⓐ
START
READ IN INPUT DATA
PRINT OUT INPUT DATA
INITIALIZE ALL VARIABLES WHERE NECESSARY
Ⓑ
DØ LØØP
STEPS OFF THROUGH DRIVING PROFILE IN EQUAL Δt INCREMENTS BEGINNING WITH t_0
DETERMINE v_i CORRESPONDING TO t_i FROM PRØFILE ARRAY
DETERMINE I_{BMAX_n} FROM VIBDS ARRAY FOR CURRENT STATE OF CHARGE S_i
$I_{B_{MAX}} = C_r I_{B_{MAX_n}} / C_r$
$F_D = \frac{W_v I}{2000}\left(10 + \frac{300}{P} + \frac{0.07}{P} v_i^2\right) + CAv_i^2 + W_V \mathrm{SIN}\,\theta$
Ⓒ
DØ LØØP j = 1, 50
STARTS WITH INITIAL GUESS OF THROTTLE SETTING OF f = 0.25 WITH INITIAL UPPER AND LOWER BOUNDS OF f_{HIGH} = 1.0 AND F_{LOW} = 0 AND THEN CONVERGES ON THE PROPER F_j VALUE SO RESULTING VELOCITY v_i MATCHES v_i ON PROFILE
GENERATOR CURRENT (i_G) TO BE CALCULATED ?
YES
$I_G = \mathrm{MAX}\left[\left(\frac{.00267 v_i}{V_G} F_D\, 745.7\right), \mathrm{IGMIN}\right]$
NO
USE INPUT I_G
CALCULATE MOTOR CURRENT
$I_m = f\left(I_G + I_{B_{MAX}}\right)$
CALCULATE MOTOR RPM
$N_m = \mathrm{MAX}\left[\left(14\, G\, v_i / R\right), \mathrm{NMIN}\right]$
MOTOR TORQUE (T_m) TO BE CALCULATED ?
YES
$T_m = \frac{V_B I_m N_m}{K\ N_m}$
NO
PERFORM TABLE LOOKUP IN TIN ARRAY TO DETERMINE T_m AS A FUNCTION OF I_m AND N_m
CONTINUE ON NEXT PAGE

*REFER TO SECTION A.6 FOR FLOW CHART NOMENCLATURE

Figure A-1. HEVPEC-S Flow Chart*

---

*Refer to Section A.6 for flow chart nomenclature.

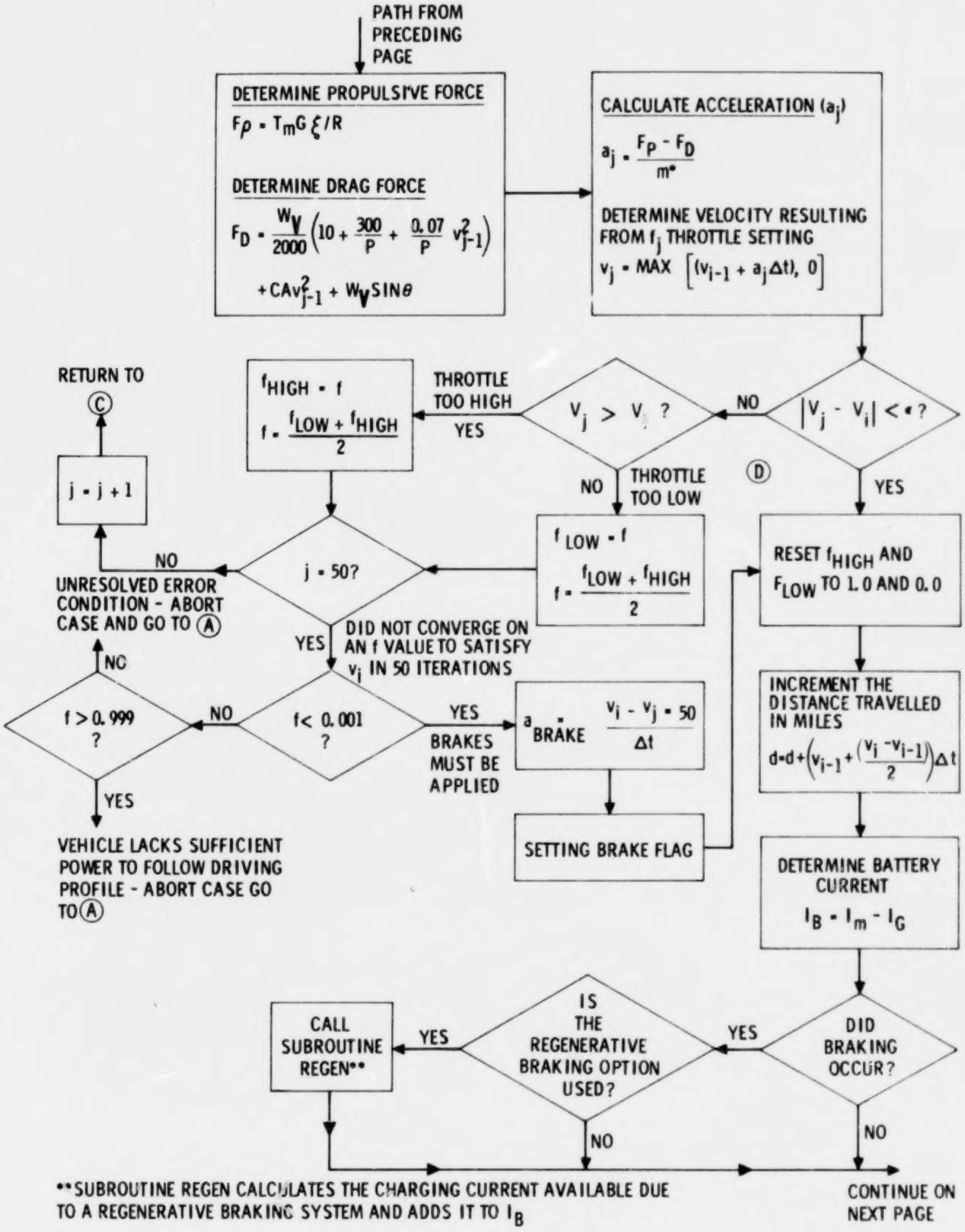
PATH FROM PRECEDING PAGE
DETERMINE PROPULSIVE FORCE
$F_P = T_m G \xi / R$
DETERMINE DRAG FORCE
$F_D = \frac{W_V}{2000}\left(10 + \frac{300}{P} + \frac{0.07}{P} v_{j-1}^2\right) + CAv_{j-1}^2 + W_V \sin\theta$
CALCULATE ACCELERATION (a_j)
$a_j = \frac{F_P - F_D}{m^*}$
DETERMINE VELOCITY RESULTING FROM f_j THROTTLE SETTING
$v_j = \mathrm{MAX}\left[(v_{i-1} + a_j \Delta t), 0\right]$
$|V_j - V_i| < \epsilon$?
NO
YES
$V_j > V_i$?
THROTTLE TOO HIGH
YES
$f_{HIGH} = f$
$f = \frac{f_{LOW} + f_{HIGH}}{2}$
NO
THROTTLE TOO LOW
D
$f_{LOW} = f$
$f = \frac{f_{LOW} + f_{HIGH}}{2}$
RETURN TO C
$j = j + 1$
$j = 50$?
NO
UNRESOLVED ERROR CONDITION - ABORT CASE AND GO TO A
YES
DID NOT CONVERGE ON AN f VALUE TO SATISFY v_i IN 50 ITERATIONS
$f < 0.001$?
NO
$f > 0.999$?
NO
YES
VEHICLE LACKS SUFFICIENT POWER TO FOLLOW DRIVING PROFILE - ABORT CASE GO TO A
YES
BRAKES MUST BE APPLIED
$a_{BRAKE} = \frac{v_i - v_{j=50}}{\Delta t}$
SETTING BRAKE FLAG
RESET f_{HIGH} AND F_{LOW} TO 1.0 AND 0.0
INCREMENT THE DISTANCE TRAVELLED IN MILES
$d = d + \left(v_{i-1} + \left(\frac{v_i - v_{i-1}}{2}\right)\right)\Delta t$
DETERMINE BATTERY CURRENT
$I_B = I_m - I_G$
DID BRAKING OCCUR?
YES
NO
IS THE REGENERATIVE BRAKING OPTION USED?
YES
NO
CALL SUBROUTINE REGEN**
CONTINUE ON NEXT PAGE

**SUBROUTINE REGEN CALCULATES THE CHARGING CURRENT AVAILABLE DUE TO A REGENERATIVE BRAKING SYSTEM AND ADDS IT TO I_B

Figure A-1. HEVPEC-S Flow Chart (Continued)

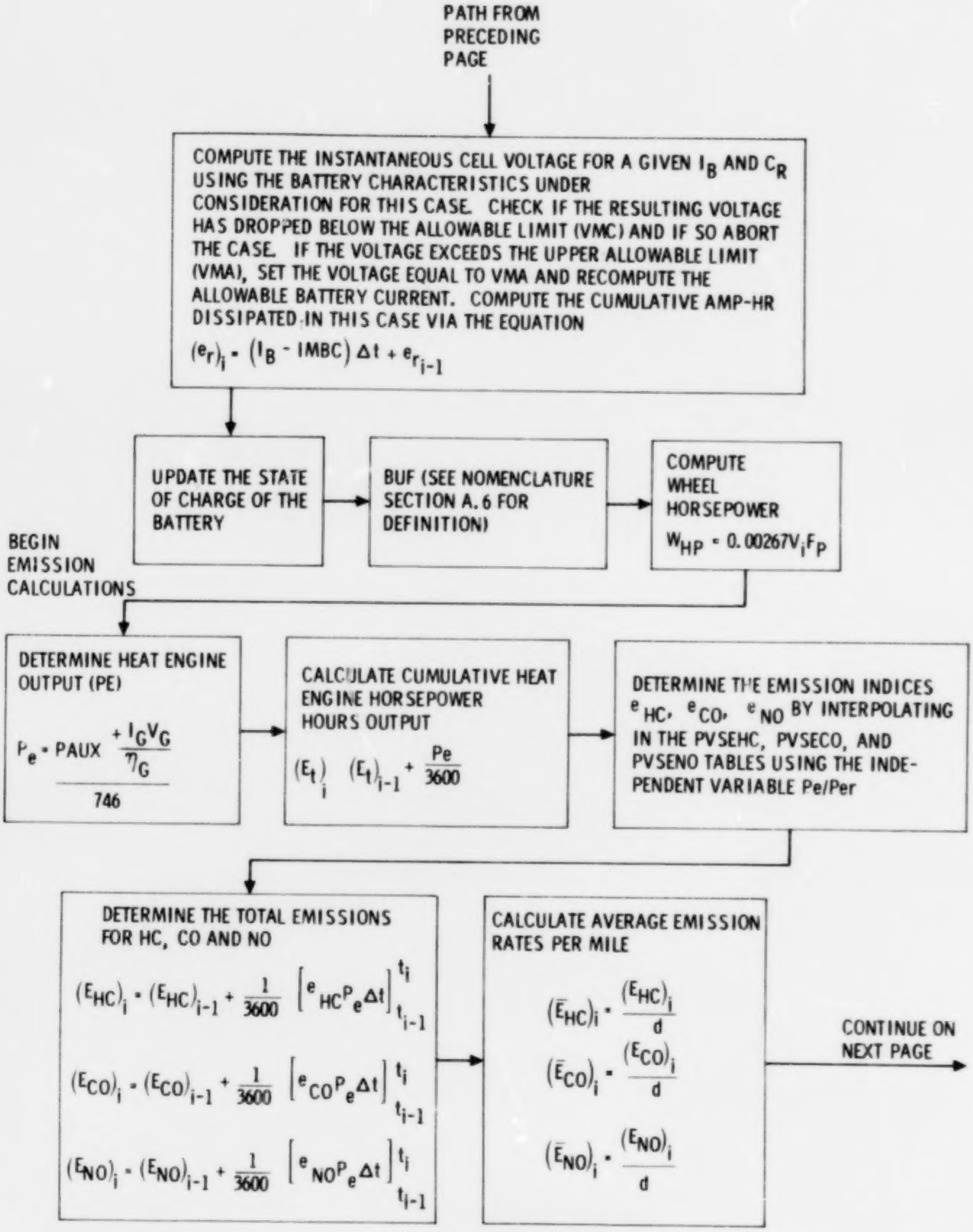
PATH FROM PRECEDING PAGE
COMPUTE THE INSTANTANEOUS CELL VOLTAGE FOR A GIVEN I_B AND C_R USING THE BATTERY CHARACTERISTICS UNDER CONSIDERATION FOR THIS CASE. CHECK IF THE RESULTING VOLTAGE HAS DROPPED BELOW THE ALLOWABLE LIMIT (VMC) AND IF SO ABORT THE CASE. IF THE VOLTAGE EXCEEDS THE UPPER ALLOWABLE LIMIT (VMA), SET THE VOLTAGE EQUAL TO VMA AND RECOMPUTE THE ALLOWABLE BATTERY CURRENT. COMPUTE THE CUMULATIVE AMP-HR DISSIPATED IN THIS CASE VIA THE EQUATION
$(e_r)_i = \left(I_B - IMBC\right)\Delta t + e_{r_{i-1}}$
UPDATE THE STATE OF CHARGE OF THE BATTERY
BUF (SEE NOMENCLATURE SECTION A.6 FOR DEFINITION)
COMPUTE WHEEL HORSEPOWER
$W_{HP} = 0.00267 V_i F_P$
BEGIN EMISSION CALCULATIONS
DETERMINE HEAT ENGINE OUTPUT (PE)
$P_e = \frac{PAUX + \frac{I_G V_G}{\eta_G}}{746}$
CALCULATE CUMULATIVE HEAT ENGINE HORSEPOWER HOURS OUTPUT
$(E_t)_i \quad (E_t)_{i-1} + \frac{Pe}{3600}$
DETERMINE THE EMISSION INDICES e_{HC}, e_{CO}, e_{NO} BY INTERPOLATING IN THE PVSEHC, PVSECO, AND PVSENO TABLES USING THE INDEPENDENT VARIABLE Pe/Per
DETERMINE THE TOTAL EMISSIONS FOR HC, CO AND NO
$(E_{HC})_i = (E_{HC})_{i-1} + \frac{1}{3600}\left[e_{HC} P_e \Delta t\right]_{t_{i-1}}^{t_i}$
$(E_{CO})_i = (E_{CO})_{i-1} + \frac{1}{3600}\left[e_{CO} P_e \Delta t\right]_{t_{i-1}}^{t_i}$
$(E_{NO})_i = (E_{NO})_{i-1} + \frac{1}{3600}\left[e_{NO} P_e \Delta t\right]_{t_{i-1}}^{t_i}$
CALCULATE AVERAGE EMISSION RATES PER MILE
$(\bar{E}_{HC})_i = \frac{(E_{HC})_i}{d}$
$(\bar{E}_{CO})_i = \frac{(E_{CO})_i}{d}$
$(\bar{E}_{NO})_i = \frac{(E_{NO})_i}{d}$
CONTINUE ON NEXT PAGE

Figure A-1. HEVPEC-S Flow Chart (Continued)

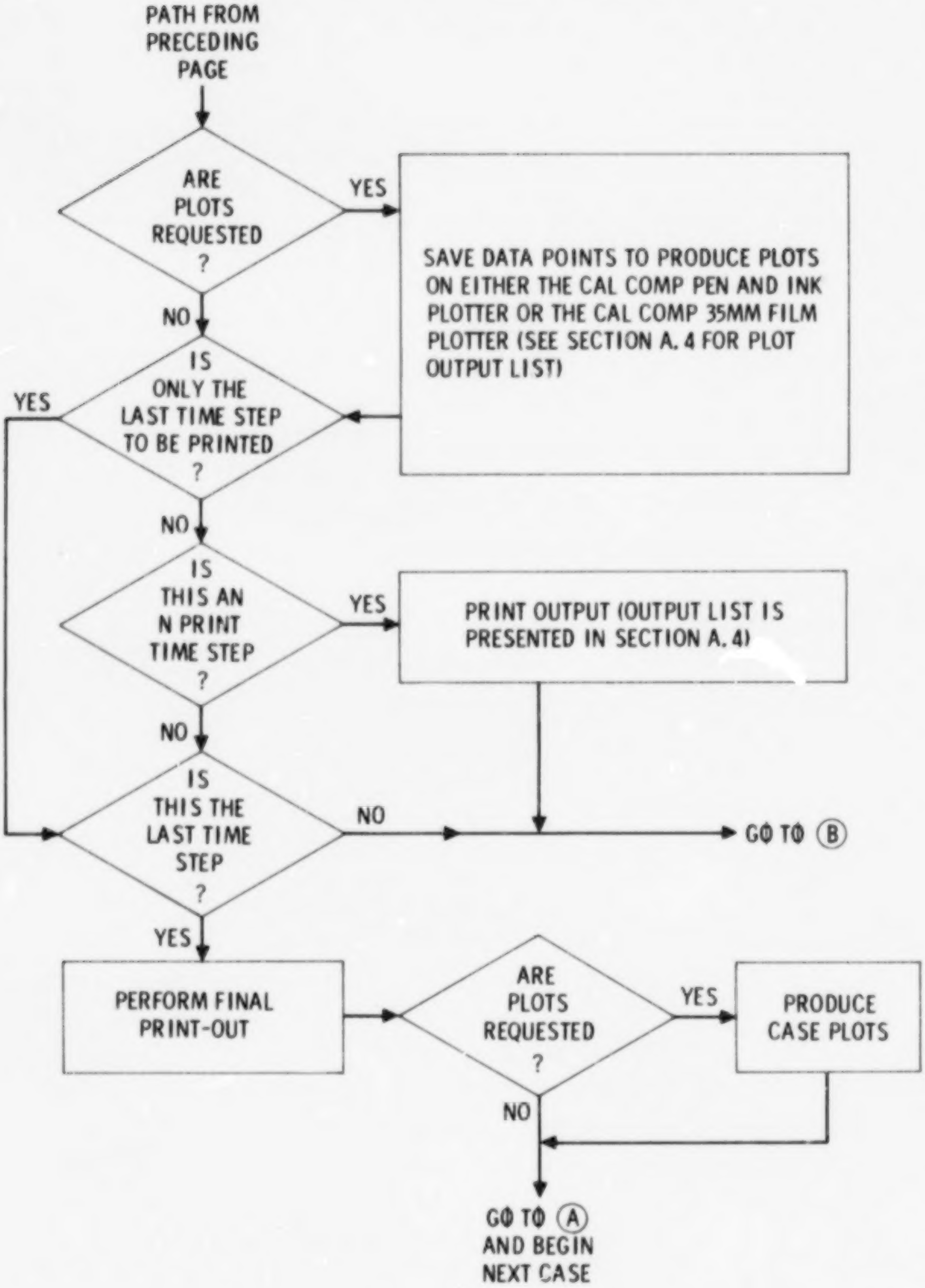
PATH FROM
PRECEDING
PAGE
ARE
PLOTS
REQUESTED
?
YES
SAVE DATA POINTS TO PRODUCE PLOTS ON EITHER THE CAL COMP PEN AND INK PLOTTER OR THE CAL COMP 35MM FILM PLOTTER (SEE SECTION A. 4 FOR PLOT OUTPUT LIST)
NO
IS
ONLY THE
LAST TIME STEP
TO BE PRINTED
?
YES
NO
IS
THIS AN
N PRINT
TIME STEP
?
YES
PRINT OUTPUT (OUTPUT LIST IS PRESENTED IN SECTION A. 4)
NO
IS
THIS THE
LAST TIME
STEP
?
NO
GO TO Ⓑ
YES
PERFORM FINAL
PRINT-OUT
ARE
PLOTS
REQUESTED
?
YES
PRODUCE
CASE PLOTS
NO
GO TO Ⓐ
AND BEGIN
NEXT CASE

Figure A-1. HEVPEC-S Flow Chart (Concluded)

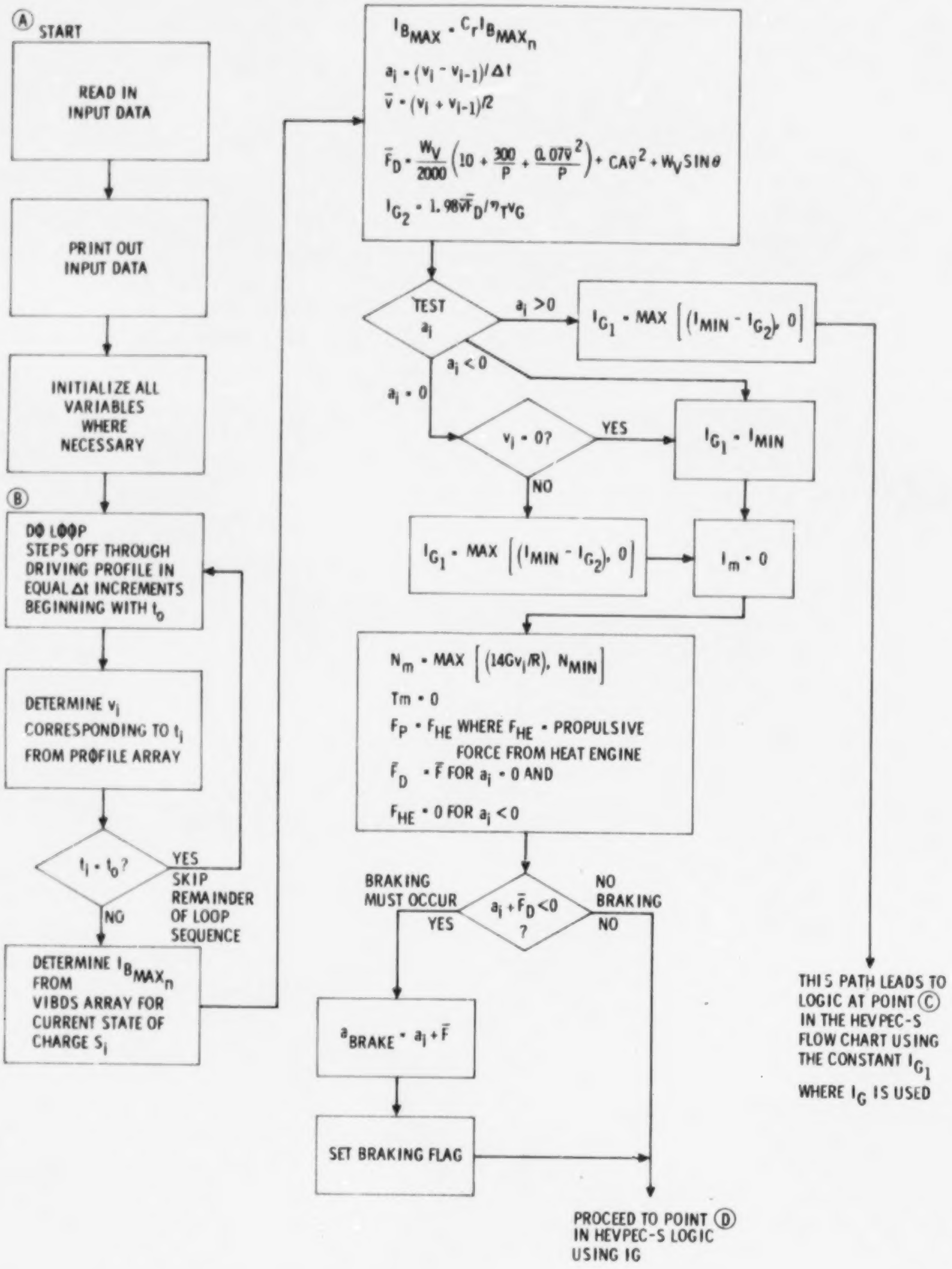
Ⓐ START
READ IN INPUT DATA
PRINT OUT INPUT DATA
INITIALIZE ALL VARIABLES WHERE NECESSARY
Ⓑ
DO LOOP STEPS OFF THROUGH DRIVING PROFILE IN EQUAL Δt INCREMENTS BEGINNING WITH t_0
DETERMINE v_i CORRESPONDING TO t_i FROM PROFILE ARRAY
$t_i = t_0$?
YES
SKIP REMAINDER OF LOOP SEQUENCE
NO
DETERMINE $I_{B_{MAX_n}}$ FROM VIBDS ARRAY FOR CURRENT STATE OF CHARGE S_i
$I_{B_{MAX}} = C_r I_{B_{MAX_n}}$
$a_i = (v_i - v_{i-1})/\Delta t$
$\bar{v} = (v_i + v_{i-1})/2$
$\bar{F}_D = \frac{W_V}{2000}\left(10 + \frac{300}{P} + \frac{0.07\bar{v}^2}{P}\right) + CA\bar{v}^2 + W_V \sin\theta$
$I_{G_2} = 1.98\bar{v}\bar{F}_D/\eta_T v_G$
TEST a_i
$a_i > 0$
$I_{G_1} = MAX\left[(I_{MIN} - I_{G_2}), 0\right]$
$a_i < 0$
$a_i = 0$
$v_i = 0$?
YES
$I_{G_1} = I_{MIN}$
NO
$I_{G_1} = MAX\left[(I_{MIN} - I_{G_2}), 0\right]$
$I_m = 0$
$N_m = MAX\left[(14Gv_i/R), N_{MIN}\right]$
$Tm = 0$
$F_P = F_{HE}$ WHERE F_{HE} = PROPULSIVE FORCE FROM HEAT ENGINE
$\bar{F}_D = \bar{F}$ FOR $a_i = 0$ AND
$F_{HE} = 0$ FOR $a_i < 0$
BRAKING MUST OCCUR
YES
$a_i + \bar{F}_D < 0$?
NO BRAKING
NO
$a_{BRAKE} = a_i + \bar{F}$
SET BRAKING FLAG
PROCEED TO POINT Ⓓ IN HEVPEC-S LOGIC USING IG
THIS PATH LEADS TO LOGIC AT POINT Ⓒ IN THE HEVPEC-S FLOW CHART USING THE CONSTANT I_{G_1} WHERE I_G IS USED

Figure A-2. HEVPEC-P Flow Chart

The remainder of the procedure for HYBRID-P is the same as that for HYBRID-S with the following exceptions:

$$Pe = \frac{1}{746}\left[P_{aux} + \frac{V_G I_{G1}}{\eta_G}\right] + \frac{\bar{v}\,\bar{F}_D}{375(\eta_T)} \quad \text{for} \quad \begin{matrix} a_i = 0 \\ v_i \neq 0 \end{matrix} \quad \text{or} \quad \begin{matrix} a_i > 0 \\ v_i \neq 0 \end{matrix}$$

or

$$Pe = \frac{1}{746}\left[P_{aux} + \frac{V_G I_{min}}{\eta_G}\right] \quad \text{for} \quad \begin{matrix} a_i < 0 \\ v_i \neq 0 \end{matrix} \quad \text{or} \quad \begin{matrix} a_i = 0 \\ v_i = 0 \end{matrix}$$

A.4 HEVPEC OUTPUT LIST

The following symbols and abbreviations are a list of HEVPEC-S and HEVPEC-P output variables and plots.

ACC	Acceleration, mph/sec
BUF	Battery utilization factor (see nomenclature list)
CO	Emission rate of CO, gm/mi
CYCLES	Cumulative number of battery charge-discharge cycles
D	Cumulative distance traveled, mi
DELTAC	Change in battery capacity, amp-hr
ECO	Cumulative amount of CO emitted, gm
EHC	Cumulative amount of HC emitted, gm
ENO	Cumulative amount of NO_2 emitted, gm
ER	Cumulative energy dissipated in resistive load, amp-hr
F	Throttle setting
FD	Total road resistance force, lb
FP	Propulsive force, lb
HC	Emission rate of HC, gm/mi
IBC	Maximum current available for battery charging, amps
IBD	Battery discharge current, amps
IBMAX	Maximum battery discharge current, amps
IG	Generator output current, amps
IG1	Input current to electric drive motor
IG2	Electric current analogue of mechanical power delivered by heat engine directly to wheels, amps

IM	Electric drive motor input current, amps
IMBC	Battery charging current, amps
NM	Electric drive motor speed, rpm
NO	Emission rate of NO_2, gm/mi
PE	Power output of heat engine, hp
S	Battery state of charge, percent
TIME	Profile time, sec
TM	Electric drive motor output torque, ft-lb
V	Vehicle speed, mph
VBD	Cell voltage, volts
WHP	Net output power at wheels, hp

Plots:

S vs Time
VBD vs Time
IBC vs Time
IBD vs Time
IG vs Time
IG2 vs Time
IM vs Time

A. 5 SAMPLE OUTPUT

The following computer printouts are samples from the HYBRID-S and HYBRID-P programs where

DELTAT = 1
NPRINT = 1
LASTLIN = 1

1. HEVPEC - S

```
TIME=  978   IBMAX= 240   IM=  4.8  NM=3564   TM=   2   FP=  14   FD= 31     F= .0185
         DELTAC=-.00238 ACC= -.20   V=28.00   D= 6.07   S= 97.980 IAC= 17.232 IBD=  0.000
             IG= 17.0 VBD=2.21 IMBC=  0.000 ER=  .0033 BUF= 7.84984117E-01   WHP=  1.07
            PE=  8.0 EHC= 2.09082E+00     ECO= 3.13623E+00     ENO= 1.25443E+01             C/C
                      HC= 3.46682E-01     CO= 5.20023E-01      NO= 2.08003E+00       CYCLES = 112
```

2. HEVPEC - P

```
TIME=  631   IBMAX= 750   IM=  0.0  NM=1200   TM=   0   FP=   0   FD= 31     F= .0135
         DELTAC=-.00972 ACC= 0.00   V=  .20   D= 4.05   S=100.000 IAC= 50.000 IBD=  0.000
           IG1= 50.00  IG2=  0.00 VBD=2.40 IMBC= 12.000 ER= 4.4501 BUF= 5.00310770E-02   WHP=  0.00
            PE= 18.6 EHC= 2.51630E-01     ECO= 1.35262E+00     ENO= 8.78228E+00           C/C
                      HC= 6.20615E-02     CO= 3.33607E-01      NO= 2.16604E+00      CYCLES =  38
```

Sample plots of several HEVPEC-S output variables are shown in Figures A-3, A-4, A-5, and A-6.

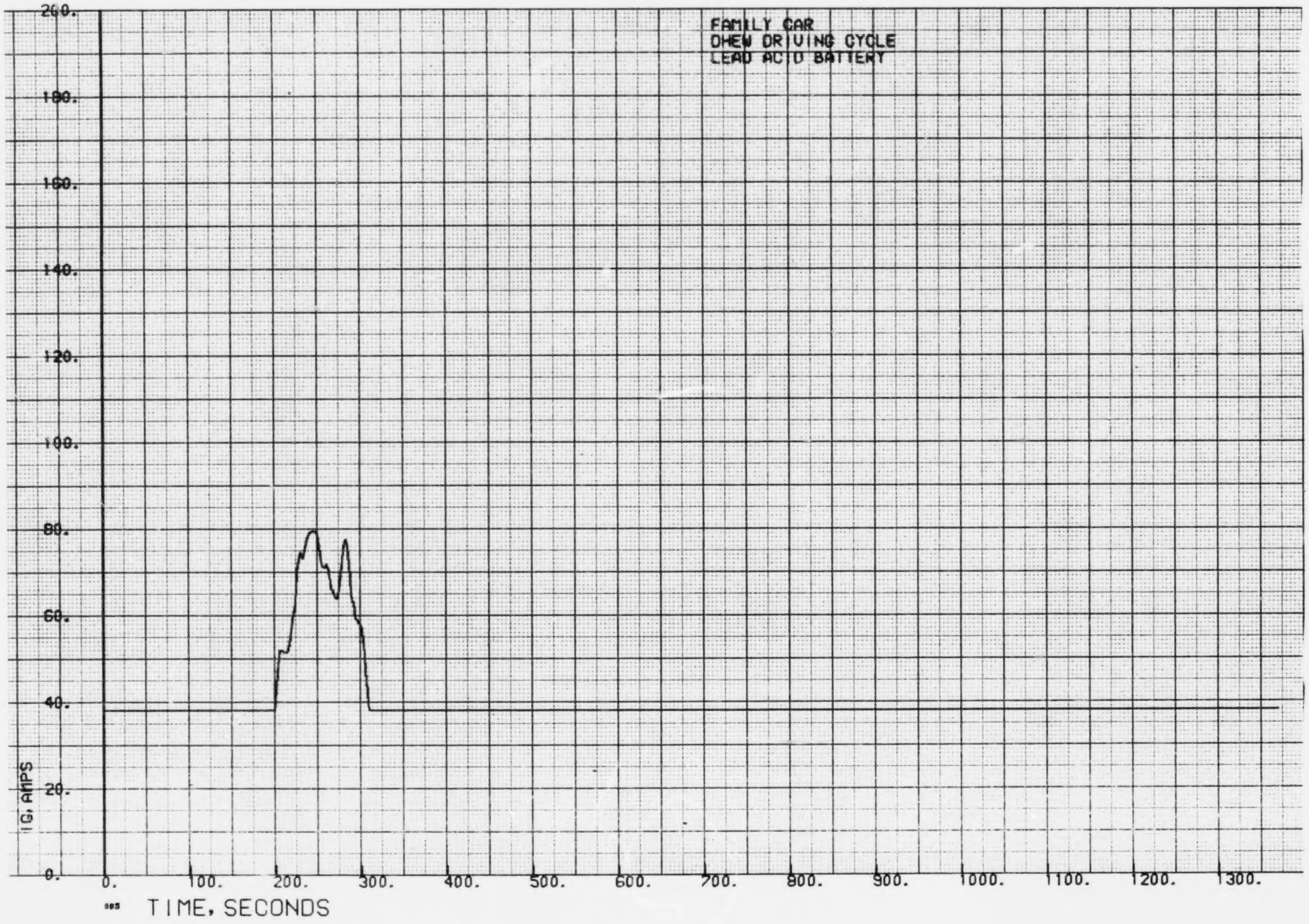

Figure A-3. Generator Output Current (IG) Versus Time

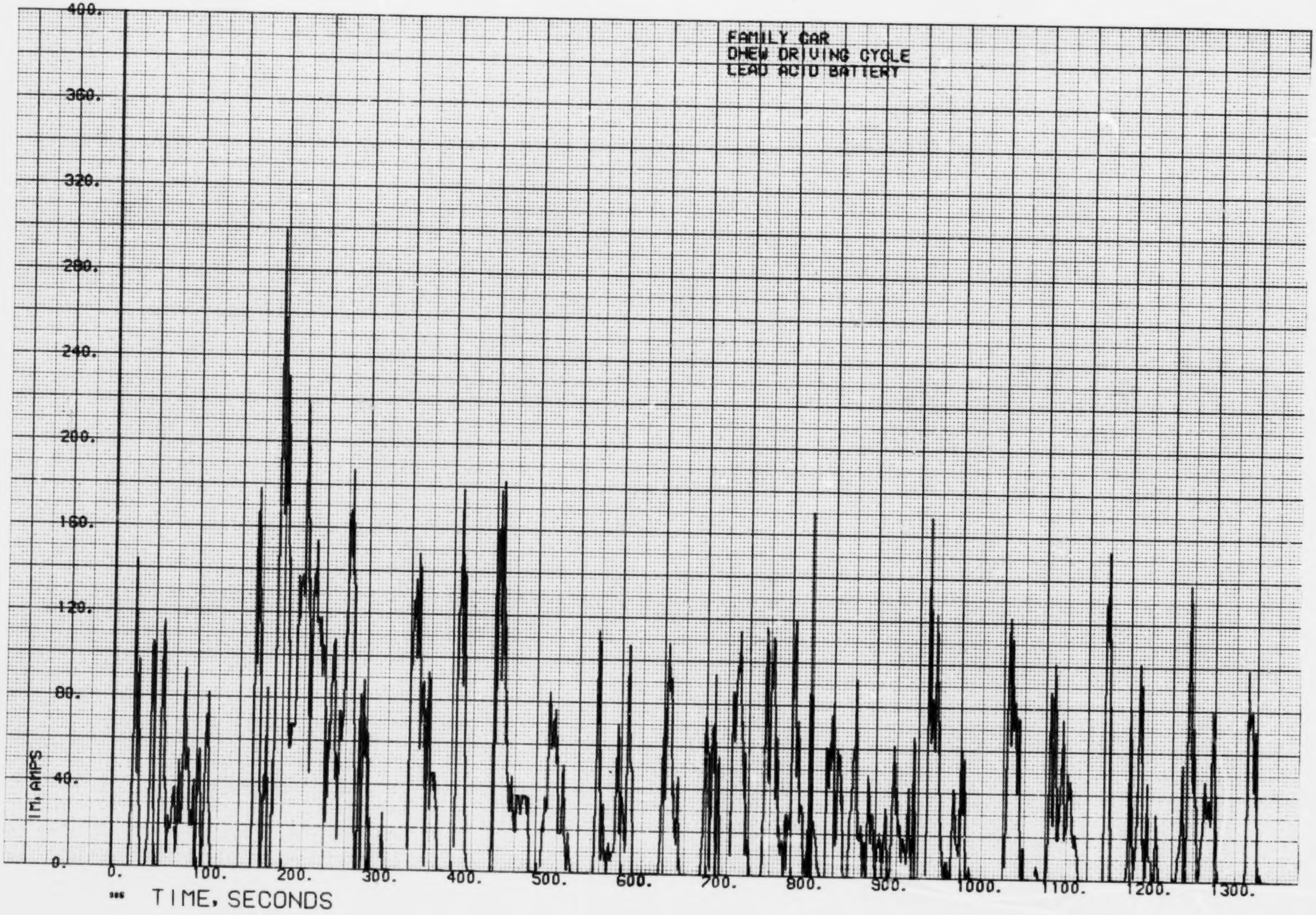

Figure A-4. Electric Drive Motor Input Current (IM) Versus Time

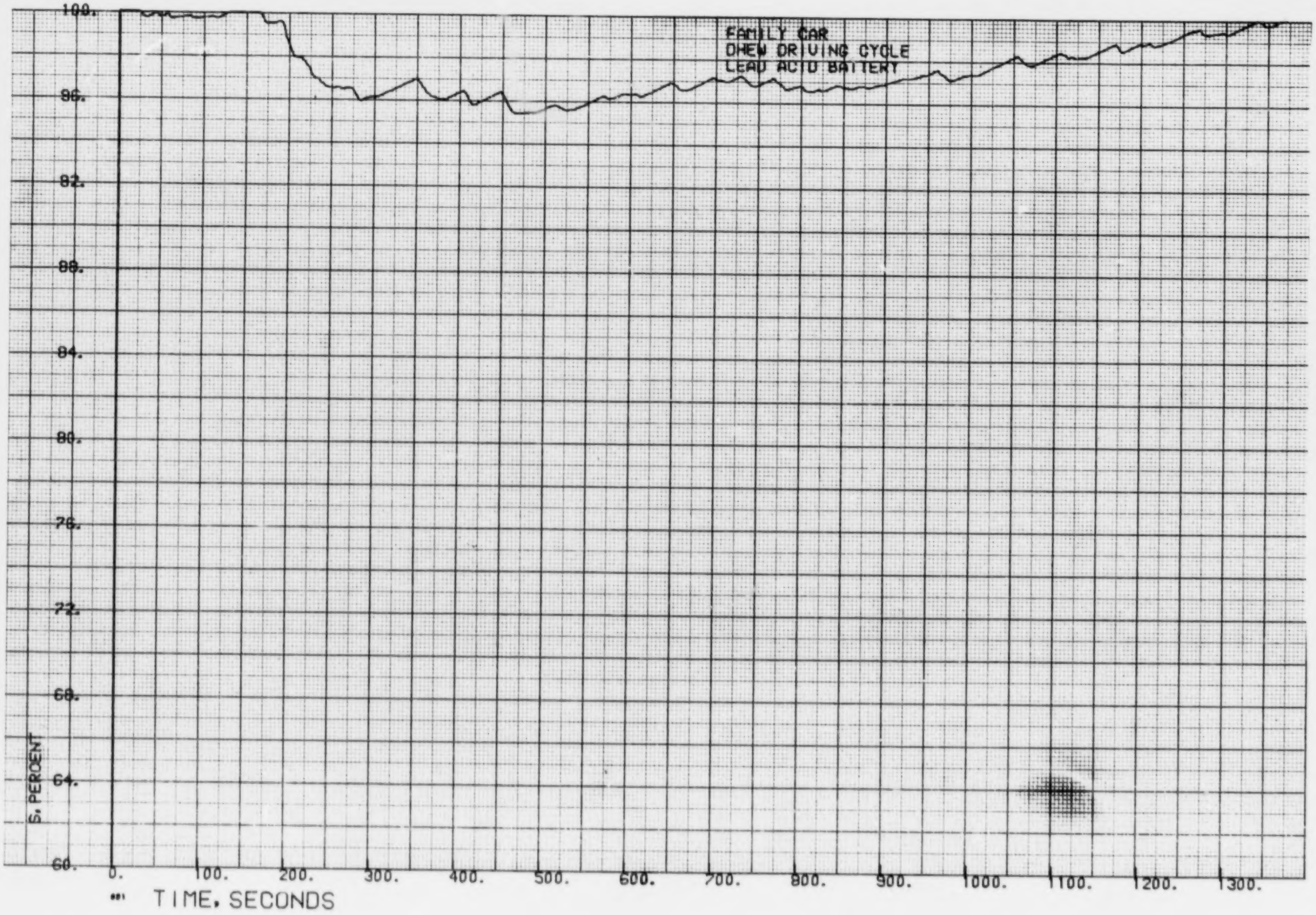

Figure A-5. Battery State of Charge (S) Versus Time

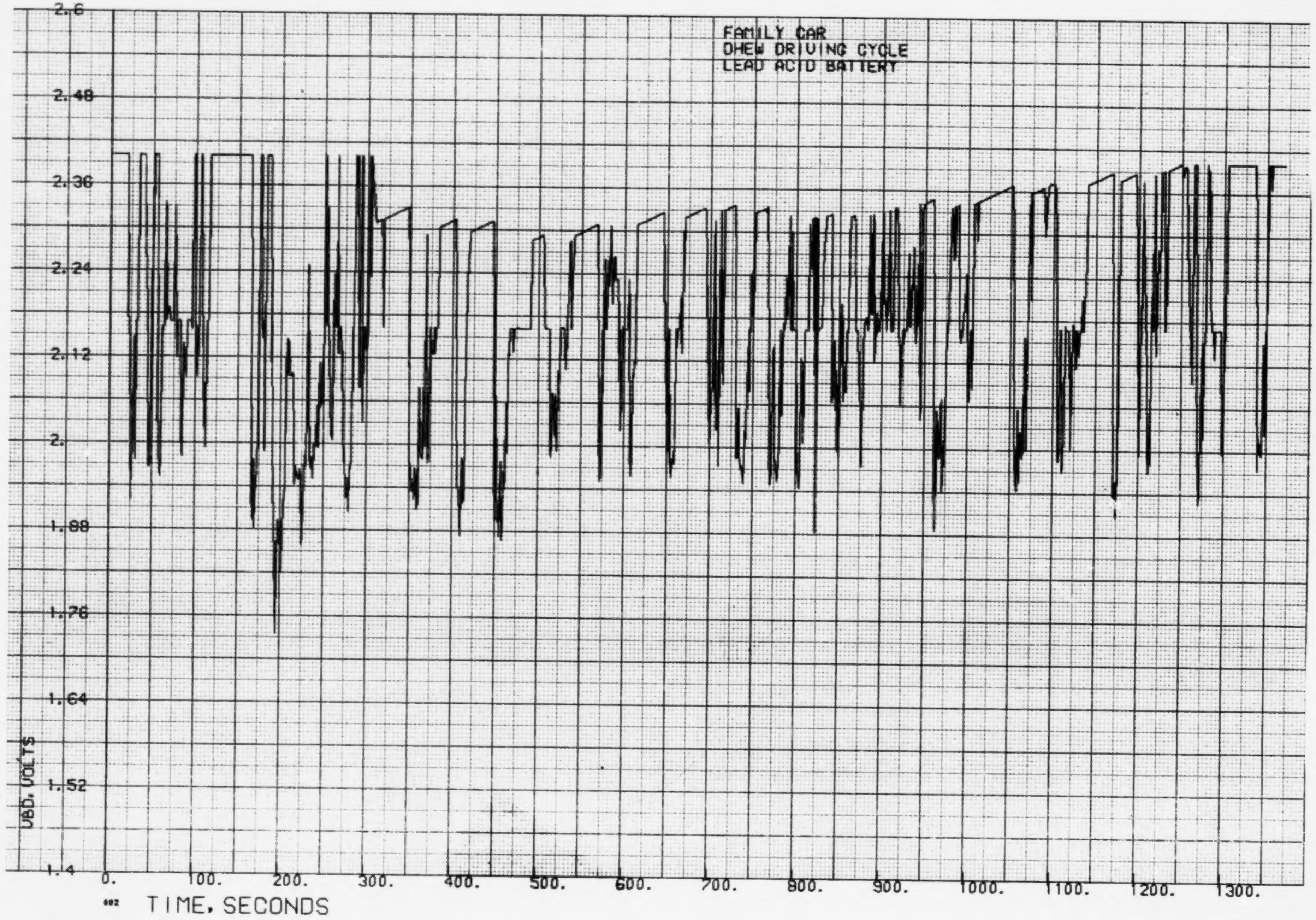

Figure A-6. Battery Cell Voltage (VBD) Versus Time

A. 6 NOMENCLATURE FOR HEVPEC FLOW CHARTS

A	Frontal area of vehicle, ft^2
a_i	Acceleration based on profile velocity, mph/sec
a_j	Acceleration based on net force at wheels, mph/sec
BUF	Battery utilization factor = (cumulative energy drained from battery/cumulative charging energy available)
C	Air resistance coefficient = $0.002558\ C_d$, $lb/(ft\text{-}mph)^2$
C_d	Aerodynamic drag coefficient
C_r	Rated capacity of battery, amp-hr
d	Cumulative distance traveled, mi
$(e_r)_i$	Cumulative energy dissipated in parasitic load, amp-hr
$(E_{HC})_i$, $(E_{CO})_i$, $(E_{NO_2})_i$	Cumulative amount of unburned Hydrocarbons (HC), Carbon Monoxide (CO), and Nitric Oxide (NO_2) emitted, grams
$(\overline{E}_{HC})_i$, $(\overline{E}_{CO})_i$, $(\overline{E}_{NO_2})_i$	Specific emission rate of HC, CO, and NO_2, grams/mi
f	Throttle setting
$(E_t)_i$	Cumulative energy output of heat engine, hp-hr
F_D	Total drag force (rolling resistance plus aerodynamic drag), lb
F_p	Propulsive force at wheels, lb
G	Gear ratio

I_G	Generator output current (HEPVEC-S only)
IG_1	Generator output current (HPEVEC-P only)
I_m	Input current to electric drive motor, amps
I_B	Battery current, amps
IMBC	Maximum allowable battery charge current, amps
$I_{B_{MAX}}$	Maximum allowable battery discharge current, amps
IGMIN	Minimum value of I_G, amps
IMIN	Minimum value of IG_2, amps
IG_2	Electric current analogue of mechanical power output of heat engine directed to wheels, amps
$\overline{K}$	Motor torque constant, volt-amp/rpm-ft-lb
m^*	Effective vehicle mass (includes rotational inertia effects) (lb-sec)/mph = 1.1 m
m	Vehicle mass, (lb-sec)/mph
N_m	Speed of electric drive motor, rpm
NMIN	Minimum value of N_m, rpm
P_e	Power output of heat engine, hp
P_{er}	Rated power output of heat engine, hp
P	Tire pressure, psi
P_{aux}	Accessory power requirement, watts
R	Rolling radius of tire, ft
Δt	$t_i - t_{i-1}$, sec
T_m	Output torque of electric drive motor, ft-lb
TIN	Input array (see input list, Section A.2)

t_i	i^{th} time step in driving cycle (velocity profile), sec
V_B	Battery voltage (input constant), volts
V_G	Generator output voltage (input constant), volts
V_i	i^{th} speed step in velocity profile, mph
V_j	Computed speed, mph
VIBS	Input array (see input list, Section A.2)
W_V	Vehicle weight, lb
θ	Road grade
ξ	Mechanical linkage loss factor (series), percent
η_m	Average efficiency of electric drive motor, percent
η	Battery recharge efficiency, percent
η_G	Average efficiency of generator, percent
η_T	Transmission efficiency (parallel), percent

Indices

i	driving cycle (speed-time profile) index
j	internal program iteration index

APPENDIX B

HEAT ENGINE EXHAUST EMISSIONS

CONTENTS

B. HEAT ENGINE EXHAUST EMISSIONS B-1

B. 1 General B-1

B. 1. 1 Introduction B-1

B. 1. 2 Pollutants B-1

B. 1. 2. 1 Hydrocarbons. B-1

B. 1. 2. 2 Carbon Monoxide B-2

B. 1. 2. 3 Nitric Oxide B-2

B. 1. 2. 4 Sulfur Dioxide B-2

B. 1. 2. 5 Aldehydes B-2

B. 1. 2. 6 Particulates B-2

B. 1. 3 Exhaust Emission Data Format B-3

B. 2 Spark Ignition Engine Emissions B-4

B. 2. 1 General B-7

B. 2. 2 Combustion and Emission Characteristics . . . B-7

B. 2. 3 Methods to Reduce Emissions B-9

B. 2. 3. 1 Air/Fuel Ratio B-10

B. 2. 3. 2 Spark Timing B-10

B. 2. 3. 3 Design Modifications B-11

B. 2. 3. 4 Catalytic Converters B-11

B. 2. 3. 5 Exhaust Gas Recirculation B-12

B. 2. 3. 6 Water Injection B-12

B. 2. 3. 7 Exhaust Manifold Reactors B-14

B. 2. 4 Other Engine and Fuel Types B-14

B. 2. 4. 1 Wankel Rotary Engine B-15

B. 2. 4. 2 Stratified Charge Engine B-15

B. 2. 4. 3 Liquified Petroleum Gas B-15

B. 2. 5 Parametric Engine Emission Data B-16

CONTENTS (Continued)

B.2.6 Design Load Emissions B-21

B.2.6.1 State-of-the-Art Technology B-21

B.2.6.2 Projected Technology B-29

B.2.7 Part-Load Emission Characteristics. B-31

B.2.8 Cold Start Emissions B-33

B.2.9 Instrumentation B-36

B.2.10 Other Pollutants B-37

B.3 Diesel Engine Emissions B-37

B.3.1 General B-37

B.3.2 Combustion and Emission Characteristics . . B-41

B.3.3 Design Load Emissions B-44

B.3.3.1 State-of-the-Art Technology B-44

B.3.3.2 Projected Technology B-49

B.3.4 Part-Load Emissions Characteristics B-51

B.3.4.1 Actual Engine Part-Load Emissions B-51

B.3.4.2 Selected Part-Load Emissions. . . B-86

B.3.5 Cold Start Emissions B-99

B.3.6 Instrumentation B-100

B.3.7 Other Pollutants. B-100

B.4 Gas Turbines B-101

B.4.1 General B-101

B.4.2 Design Load Emission Characteristics. B-101

B.4.2.1 State-of-the-Art Technology B-101

B.4.2.2 Projected Technology B-106

B.4.3 Part-Load Emissions Characteristics B-108

B.4.4 Cold Start Emissions B-112

B.4.5 Effect of Fuel on Gas Turbine Emissions . . . B-114

B.4.6 Instrumentation B-114

B.4.7 Other Pollutants. B-114

CONTENTS (Continued)

B. 5 Rankine Engine Emissions B-115

  B. 5. 1 General B-115

  B. 5. 2 Engine and Test Description B-116

  B. 5. 3 Combustion and Exhaust Emission Characteristics B-118

  B. 5. 4 Design Load Emissions B-130

    B. 5. 4. 1 State-of-the-Art Technology B-130

    B. 5. 4. 2 Projected Technology B-136

  B. 5. 5 Part-Load Emissions B-137

  B. 5. 6 Cold Start Emissions B-137

  B. 5. 7 Instrumentation B-139

  B. 5. 8 Other Pollutants. B-139

B. 6 Stirling Engine Emissions B-140

  B. 6. 1 General B-140

  B. 6. 2 Design Load Emissions B-140

    B. 6. 2. 1 State-of-the-Art Technology B-140

    B. 6. 2. 2 Projected Technology B-145

  B. 6. 3 Part-Load Emissions B-149

  B. 6. 4 Cold Start Emissions B-150

  B. 6. 5 Instrumentation B-150

  B. 6. 6 Other Pollutants. B-152

B. 7 References B-153

TABLES

B-1. Spark Ignition Engines (Gasoline) and Design Load Specific Mass Emissions B-6

B-2. Four-Cycle, Naturally-Aspirated, Direct-Injection Diesel Engines and Design Load Specific Mass Emissions B-38

B-3. Four-Cycle, Turbocharged, Direct-Injection Diesel Engines and Design Load Specific Mass Emissions B-39

B-4. Four-Cycle, Turbocharged, Prechamber Diesel Engines and Design Load Specific Mass Emissions B-39

B-5. Two-Cycle, Direct-Injection Diesel Engines and Design Point Specific Mass Emissions B-40

B-6. Gas Turbine Engines B-102

B-7. Rankine Engine A - General Motors SE-101 Burner Emissions B-122

B-8. Rankine Engine Automobile Emissions, DHEW Driving Cycle, Hot Start B-122

B-9. Rankine Engine B - Williams Steam Car Emissions . . . B-122

B-10. Rankine Engine C - Marquardt Burner Emissions, Vaporized, Premixed Injection TMH Fuel, 50 Percent Design Flow B-128

B-11. Rankine Engine D - Thermo Electron Corporation Burner Emissions B-128

B-12. Rankine Engine E - Bessler Boiler Emission Data B-131

B-13. Rankine Engine Automobile Cold Start Emissions B-131

B-14. General Motors Research 10 hp Stirling Engine Emissions B-142

B-15. Philips 80 hp Stirling Engine Emissions B-144

FIGURES

B-1. Typical Spark Ignition Engine Exhaust Emissions Versus Air/Fuel Ratio (Gasoline) B-8

B-2. Effect of Exhaust Gas Recirculation on NO Emissions and Performance - Spark Ignition Engines B-13

B-3. Toyota 115.7 CID Engine Hydrocarbon Emissions B-17

B-4. Toyota 115.7 CID Engine Carbon Monoxide Emissions . . B-18

B-5. Toyota 115.7 CID Engine Nitric Oxide Emissions. B-19

B-6. Toyota 115.7 CID Engine Air/Fuel Ratio Versus Brake Horsepower B-20

B-7. CFR Engine - Emission Test Data (1000 rpm; Gasoline) . B-22

B-8. CFR Engine - Power Output Versus Air/Fuel Ratio. . . . B-23

B-9. Spark Ignition Engines - Hydrocarbon Emission, Steady State Design Load (Gasoline). B-24

B-10. Spark Ignition Engines - Carbon Monoxide Emission, Steady State Design Load (Gasoline). B-25

B-11. Spark Ignition Engines - Nitric Oxide Emission, Steady State Design Load (Gasoline). B-26

B-12. Spark Ignition Engines - HC, CO, NO, Emissions, Steady State Part-Load, Air/Fuel = 15-16 . . . . B-32

B-13. Ratio of Cold Start Emissions to Hot Start Emissions, DHEW Cycle. B-34

B-14. Typical Diesel Engine Exhaust Emissions Versus Air/Fuel Ratio B-42

B-15. Diesel Engines - Hydrocarbon Emission, Steady State Design Load B-45

B-16. Diesel Engines - Carbon Monoxide Emission, Steady State Design Load B-46

FIGURES (Continued)

B-17. Diesel Engines - Nitric Oxide Emission, Steady State Design Load B-47

B-18. Four-Cycle, Naturally-Aspirated Direct-Injection Diesel - Engine A - Part-Load Hydrocarbon Emissions B-52

B-19. Four-Cycle, Naturally-Aspirated Direct-Injection Diesel - Engine A - Part-Load Carbon Monoxide Emissions B-53

B-20. Four-Cycle, Naturally-Aspirated Direct-Injection Diesels - Engine A - Part-Load Nitric Oxide Emissions B-54

B-21. Four-Cycle, Naturally-Aspirated Direct-Injection Diesel - Engine B - Part-Load Hydrocarbon Emissions B-55

B-22. Four-Cycle, Naturally-Aspirated Direct-Injection Diesel - Engine B - Part-Load Carbon Monoxide Emissions B-56

B-23. Four-Cycle, Naturally-Aspirated Direct-Injection Diesel - Engine B - Part-Load Nitric Oxide Emissions B-57

B-24. Four-Cycle, Naturally-Aspirated Direct-Injection Diesel - Engine C - Part-Load Hydrocarbon Emissions B-58

B-25. Four-Cycle, Naturally-Aspirated Direct-Injection Diesel - Engine C - Part-Load Carbon Monoxide Emissions B-59

B-26. Four-Cycle, Naturally-Aspirated Direct-Injection Diesel - Engine C - Part-Load Nitric Oxide Emissions B-60

B-27. Four-Cycle, Naturally-Aspirated Direct-Injection Diesel - Engine D - Part-Load Hydrocarbon Emissions B-61

FIGURES (Continued)

B-28. Four-Cycle, Naturally-Aspirated Direct-Injection Diesel - Engine D - Part-Load Carbon Monoxide Emissions B-62

B-29. Four-Cycle, Naturally-Aspirated Direct-Injection Diesel - Engine D - Part-Load Nitric Oxide Emissions B-63

B-30. Four-Cycle, Naturally-Aspirated Direct-Injection Diesel - Engine E - Part-Load Carbon Monoxide Emissions B-64

B-31. Four-Cycle, Naturally-Aspirated Direct-Injection Diesel - Engine E - Part-Load Nitric Oxide Emissions B-65

B-32. Four-Cycle, Naturally-Aspirated Direct-Injection Diesel - Engine F - Part-Load Hydrocarbon Emissions B-66

B-33. Four-Cycle, Naturally-Aspirated Direct-Injection Diesel - Engine F - Part-Load Carbon Monoxide Emissions B-67

B-34. Four-Cycle, Naturally-Aspirated Direct-Injection Diesel - Engine F - Part-Load Nitric Oxide Emissions B-68

B-35. Four-Cycle, Turbocharged Direct-Injection Diesel - Engine I - Part-Load Hydrocarbon Emissions B-69

B-36. Four-Cycle, Turbocharged Direct-Injection Diesel - Engine I - Part-Load Carbon Monoxide Emissions B-70

B-37. Four-Cycle, Turbocharged Direct-Injection Diesel - Engine I - Part-Load Nitric Oxide Emissions B-71

B-38. Four-Cycle, Turbocharged Direct-Injection Diesel - Engine J - Part-Load Hydrocarbon Emissions B-72

B-39. Four-Cycle, Turbocharged Direct-Injection Diesel - Engine J - Part-Load Carbon Monoxide Emissions. B-73

FIGURES (Continued)

B-40. Four-Cycle, Turbocharged Direct-Injection Diesel - Engine J - Part-Load Nitric Oxide Emissions B-74

B-41. Four-Cycle, Turbocharged Direct-Injection Diesel - Engine K - Part-Load Carbon Monoxide Emissions. . . . B-75

B-42. Four-Cycle, Turbocharged Direct-Injection Diesel - Engine K - Part-Load Nitric Oxide Emissions B-76

B-43. Four-Cycle, Turbocharged Prechamber Diesel - Engine L - Part-Load Hydrocarbon Emissions B-77

B-44. Four-Cycle, Turbocharged Prechamber Diesel - Engine L - Part-Load Carbon Monoxide Emissions . . . B-78

B-45. Four-Cycle, Turbocharged Prechamber Diesel - Engine L - Part-Load Nitric Oxide Emissions B-79

B-46. Four-Cycle, Turbocharged Prechamber Diesel - Engine M - Part-Load Hydrocarbon Emissions B-80

B-47. Four-Cycle, Turbocharged Prechamber Diesel - Engine M - Part-Load Carbon Monoxide Emissions. . . . B-81

B-48. Four-Cycle, Turbocharged Prechamber Diesel - Engine M - Part-Load Nitric Oxide Emissions B-82

B-49. Four-Cycle, Turbocharged Prechamber Diesel - Engine N - Part-Load Hydrocarbon Emissions B-83

B-50. Four-Cycle, Turbocharged Prechamber Diesel - Engine N - Part-Load Carbon Monoxide Emissions. . . . B-84

B-51. Four-Cycle, Turbocharged Prechamber Diesel - Engine N - Part-Load Nitric Oxide Emissions B-85

B-52. Two-Cycle, Direct-Injection Diesel - Engine P - Part-Load Hydrocarbon Emissions B-87

B-53. Two-Cycle, Direct-Injection Diesel - Engine P - Part-Load Carbon Monoxide Emissions B-88

B-54. Two-Cycle, Direct-Injection Diesel - Engine P - Part-Load Nitric Oxide Emissions B-89

FIGURES (Continued)

B-55. Two-Cycle, Direct-Injection Diesel - Engine Q - Part-Load Hydrocarbon Emissions B-90

B-56. Two-Cycle, Direct-Injection Diesel - Engine Q - Part-Load Carbon Monoxide Emissions B-91

B-57. Two-Cycle, Direct-Injection Diesel - Engine Q - Part-Load Nitric Oxide Emissions B-92

B-58. Four-Cycle Diesel Engines - Hydrocarbon Emission, Steady State Part-Load, Rated Speed B-93

B-59. Four-Cycle Diesel Engines - Carbon Monoxide Emission, Steady State Part-Load, Rated Speed B-94

B-60. Four-Cycle Diesel Engines - Nitric Oxide Emission, Steady State Part-Load, Rated Speed B-95

B-61. Four-Cycle Diesel Engines - Hydrocarbon Emission, Steady State Part-Load, Variable Speed B-96

B-62. Four-Cycle Diesel Engines - Carbon Monoxide Emission, Steady State Part-Load, Variable Speed B-97

B-63. Four-Cycle Diesel Engines - Nitric Oxide Emission, Steady State Part-Load, Variable Speed B-98

B-64. Gas Turbines-Hydrocarbon Emission, Steady State Design Load B-103

B-65. Gas Turbines-Carbon Monoxide Emission, Steady State Design Load B-104

B-66. Gas Turbines-Nitric Oxide Emission, Steady State Design Load B-105

B-67. Gas Turbine-Test Data Part-Load Emissions B-109

B-68. Gas Turbine-Test Data Part-Load Emissions B-110

B-69. Gas Turbine-Test Data Part-Load Emissions B-111

FIGURES (Continued)

B-70. Gas Turbines - HC, CO, NO, Emissions, Steady State Part-Load B-113

B-71. Rankine Engines - General Motors Research SE-101 Burner Emissions (60 Percent Design Air Flow) B-119

B-72. Rankine Engines - General Motors Research SE-101 Burner Emissions (Air/Fuel Ratio = 25) B-120

B-73. Rankine Engines - Marquardt Burner A Emissions (Vaporized, Premixed Injection TNH Fuel, 50 Percent Design Flow) B-124

B-74. Rankine Engines - Marquardt SUE Burner Emissions (Vaporized TMH Fuel, 50 Percent Design Flow) B-125

B-75. Rankine Engines - Marquardt Burner A Emissions (TMH Fuel) B-126

B-76. Rankine Engines - Thermo Electron Corporation Burner Emissions B-129

B-77. Rankine Engines - Bessler Boiler Emission Data B-132

B-78. Rankine Engines - Hydrocarbon Emission, Steady State, Design Load B-133

B-79. Rankine Engines - Carbon Monoxide Emission, Steady State Design Load B-134

B-80. Rankine Engines - Nitric Oxide Emission, Steady State Design Load B-135

B-81. Rankine Engines - HC, CO, NO, Emissions, Steady State Part-Load B-138

B-82. Stirling Engines - Hydrocarbon Emission, Steady State Design Load B-146

B-83. Stirling Engines - Carbon Monoxide Emission, Steady State Design Load B-147

B-84. Stirling Engines - Nitric Oxide Emission, Steady State Design Load B-148

B-85. Stirling Engines - HC, CO, NO, Emissions, Steady State Part-Load B-151

APPENDIX B

HEAT ENGINE EXHAUST EMISSIONS

B.1 GENERAL

B.1.1 Introduction

Engine exhaust emission characteristics were established for the following five types of heat engines considered in the Hybrid Heat Engine/Electric Vehicle Systems Study:

Spark Ignition Engine (Otto Cycle)
Compression Ignition Engine (Diesel Cycle)
Gas Turbine Engine (Brayton Cycle)
Rankine Cycle Engine (Steam)
Stirling Cycle Engine

The main pollutants emitted from heat engines are hydrocarbons, carbon monoxide, oxides of nitrogen, oxides of sulfur, aldehydes, and particulates. This study was limited to the hydrocarbons, carbon monoxide, and nitric oxide emissions primarily due to a lack of available quantitative information on other pollutants. Evaporative hydrocarbon emissions were not considered in the study since methods have been developed which essentially eliminate this problem. To provide a better understanding of the problems associated with engine exhaust emissions the following section presents a brief discussion of the various pollutants.

B.1.2 Pollutants

B.1.2.1 Hydrocarbons

Although not toxic, the hydrocarbons participate in the chemical smog formation process in the atmosphere. Theoretically, the hydrocarbon (HC) concentration in combustion gases decreases with increasing air/fuel ratio and becomes essentially zero for stoichiometric air/fuel ratios. However, an actual engine will always have some HC emissions as a result of incomplete combustion in the wall zone of the chamber.

B. 1. 2. 2 Carbon Monoxide

Carbon monoxide (CO) is a toxic substance. Its concentration in the exhaust of heat engines is determined primarily by air/fuel ratio and quench effects in the combustion chamber.

B. 1. 2. 3 Nitric Oxide

Nitric oxide (NO) emitted from heat engines is converted to nitrogen dioxide (NO_2) in the atmosphere. The NO_2 is rather toxic and is one of the species involved in the photochemical smog formation process. Formation of NO in the combustion chamber is kinetically controlled and is a function of the combustion temperature. The NO concentrations in the exhaust of heat engines are generally lower than the equilibrium concentrations computed for the combustion chamber, but higher than those computed for the exhaust temperature. Initially, the exhaust NO_2 concentration is very low, generally less than five percent of NO.

B. 1. 2. 4 Sulfur Dioxide

The sulfur dioxide (SO_2) concentration is directly related to the sulfur content in the fuel. Thus, SO_2 control is accomplished by limiting the amount of sulfur in the fuel.

B. 1. 2. 5 Aldehydes

Aldehyde concentration is related to combustion in lean air/fuel ratio zones. Also, combustor design and temperature-time history of the combustion products affect aldehyde formation. Odor and aldehydes are related, and odor generally tends to be more severe in gas turbines and diesels than in spark ignition engines.

B. 1. 2. 6 Particulates

Particulate matter can potentially be emitted as a result of impurities and additives contained in the fuel. Frequently carbon particles (smoke) are found in the exhaust. Formation of carbon is related to combustion in fuel rich zones in the chamber.

B.1.3 Exhaust Emission Data Format

The heat engine exhaust emission data for HC, CO, and NO are presented in terms of specific mass emissions, grams/bhp-hr. Selection of this term was based on the conclusion that the emissions of the various heat engines have to be compared on a mass basis rather than a concentration basis. The specific mass emissions were computed from the measured specie concentrations by the following equations:

Hydrocarbon:

$$HC = \frac{14 \times 10^{-6} \times 454 \times W_e \times C_{HC}}{MW_e \times bhp}, \text{ grams/bhp-hr}$$

Carbon Monoxide:

$$CO = \frac{28 \times 10^{-6} \times 454 \times W_e \times C_{CO}}{MW_e \times bhp}, \text{ grams/bhp-hr}$$

Nitric Oxide:

$$NO = \frac{30 \times 10^{-6} \times 454 \times W_e \times C_{NO}}{MW_e \times bhp}, \text{ grams/bhp-hr}$$

where

C_{HC} = Hydrocarbon concentration, ppm C

C_{CO} = Carbon monoxide concentration, ppm

C_{NO} = Nitric oxide concentration, ppm

W_e = Exhaust flow rate, lb/hr

MW_e = Molecular weight of exhaust gases

bhp = Engine brake horsepower

Steady state design load and part-load emission characteristics for both current state-of-the-art and projected technologies were established for each of the five engine types. The emissions of the three pollutants at engine design load are presented in terms of specific mass emission versus engine design brake horsepower. The part-load emissions are characterized by part-load emission factors, defined as the ratio of part-load specific mass emission to design load specific mass emission versus percent design load. Except for the state-of-the-art technology diesel engines, there was not sufficient data available to correlate exhaust emissions and engine speed.

No attempt was made to characterize the emissions for transient operation of the heat engines under changing load conditions. In the case of the hybrid system, the energy required for vehicle acceleration above that provided by the heat engine is supplied by the battery/electric motor system. Heat engine cold start emissions have been considered where data was available; however, additional work is required before a complete assessment can be made of cold start emission characteristics.

Whereas the emission characteristics presented in this report have been derived from the most accurate data available, additional efforts are necessary to establish a more comprehensive and reliable data base for heat engine emissions.

B.2 SPARK IGNITION ENGINE EMISSIONS

During the past several years, much has been accomplished in the effort to characterize and minimize the emissions from spark ignition engines. In spite of this achievement and the wealth of information gathered by many investigators, it still was not possible to acquire a sufficiently large data sample for use in this study, and, as a result, a number of assumptions had to be made. Although some of the required information is undoubtedly available at various organizations, additional work is needed to determine the emission characteristics of spark ignition engines as a function of air/fuel ratio, speed, load, and design modifications.

Most of the published spark ignition engine emission data are concerned with the emissions over the seven-mode and Department of Health, Education and Welfare (DHEW) driving cycles. Since the engine operating conditions are continuously changing during these cycles, it is very difficult to accurately convert these emission data to the specific mass emission numbers required for this study. Another difficulty arises from the fact that the air/fuel ratio of current spark ignition engines varies with operating point and from engine to engine between approximately 11 and 16. This results in very large variations in HC, CO, and NO emissions.

The HC, CO, and NO emission data from automotive spark ignition engines were made available by the Toyota Motor Company (Refs. B-1 and B-2) and another engine manufacturer (Ref. B-3). More recently, additional part-load data were provided informally by General Motors Corporation (Ref. B-4), and TRW Systems (Ref. B-5). Unfortunately, these data were not received in time to be fully incorporated into this study. However, a brief comparison of this latter data with the part-load emissions derived from the Toyota and the engine manufacturer's data indicates reasonable agreement in the trends. Emission data from single-cylinder engines were obtained from R. Hurn (Ref. B-6) and H. Newhall and El-Messiri (Ref. B-7). Hurn has tested a Cooperative Fuel Research (CFR) engine over a wide range of air/fuel ratios using gasoline, methane, and propane as the fuel. The engine used by Newhall had a prechamber and was also tested over a wide range of air/fuel ratios using gasoline as fuel. These data were used primarily to characterize the emissions in the "ultra lean" operating regime (air/fuel ratio > 20).

Performance data were gathered on a number of devices and techniques aimed at reducing the emissions from spark ignition engines. These include catalytic converters, exhaust manifold reactors, exhaust gas recirculation, and water injection. All these systems were considered for potential application in spark ignition engines and provided the basis for establishing the projected emission levels of these engines.

The engines considered in this study are listed in Table B-1.

Table B-1. Spark Ignition Engines (Gasoline) and Design Load Specific Mass Emissions

Engine Identification	A	B	C	D	E
Engine	Toyota	NA	CFR	CFR	Prechamber
Rated HP	NA**	191	NA	NA	NA
Rated Speed	NA	3200	NA	NA	NA
Compression Ratio	8:1	8:1	NA	NA	NA
Displacement	115.7	400	NA	NA	NA
Air/Fuel Ratio	15*	16*	15	22	25
HC, grams/bhp-hr	0.68	0.30	NA	NA	0.7
CO, grams/bhp-hr	8.0	3.0	3.0	2.1	16
NO, grams/bhp-hr	12.5	13.0	18.0	1.00	0.7
Reference	B-1	B-3	B-6	B-6	B-7

*At selected operating points, not at rated condition

**Not available

B.2.1 General

The exhaust emissions from spark ignition engines are affected primarily by air/fuel ratio. Other factors affecting emissions include spark timing, chamber and induction system design, mixture ratio non-uniformity, and fuel atomization.

The effect of air/fuel ratio on exhaust emission is illustrated in Fig. B-1 which shows HC, CO, and NO emission concentrations versus air/fuel ratio. Below stoichiometric, not enough oxygen is available and, as a result, considerable amounts of HC and CO are emitted. Both HC and CO concentrations decrease rapidly with increasing air/fuel ratio. The HC concentration decreases to minimum for air/fuel ratios between approximately 15 and 18 and then increases again as a result of quench effects. The point of minimum HC concentration is a function of many parameters, including degree of mixture ratio non-uniformity and combustion chamber design. The CO concentration remains essentially constant for air/fuel ratios above 16. However, it is also conceivable that the CO concentration might increase again at ultra high air/fuel ratios as a result of quenching of the chemical reactions by the additional air.

The NO concentration is rather low for air/fuel ratios much below stoichiometric, however, it increases sharply as air/fuel ratio increases. This increase is primarily due to a higher combustion chamber temperature. The maximum concentration is obtained at an air/fuel ratio approximately 10 percent greater than stoichiometric as a result of the combined effects of combustion temperature and oxygen concentration. Beyond that point NO decreases rather rapidly due to the reduction in combustion temperature.

B.2.2 Combustion and Emission Characteristics

As reported by Daniel (Refs. B-8 and B-9), the hydrocarbons emitted from spark ignition engines are partly the result of quench effects in the boundary layer adjacent to the cylinder walls. In addition, some of the larger fuel droplets may not be completely vaporized or combusted within the time

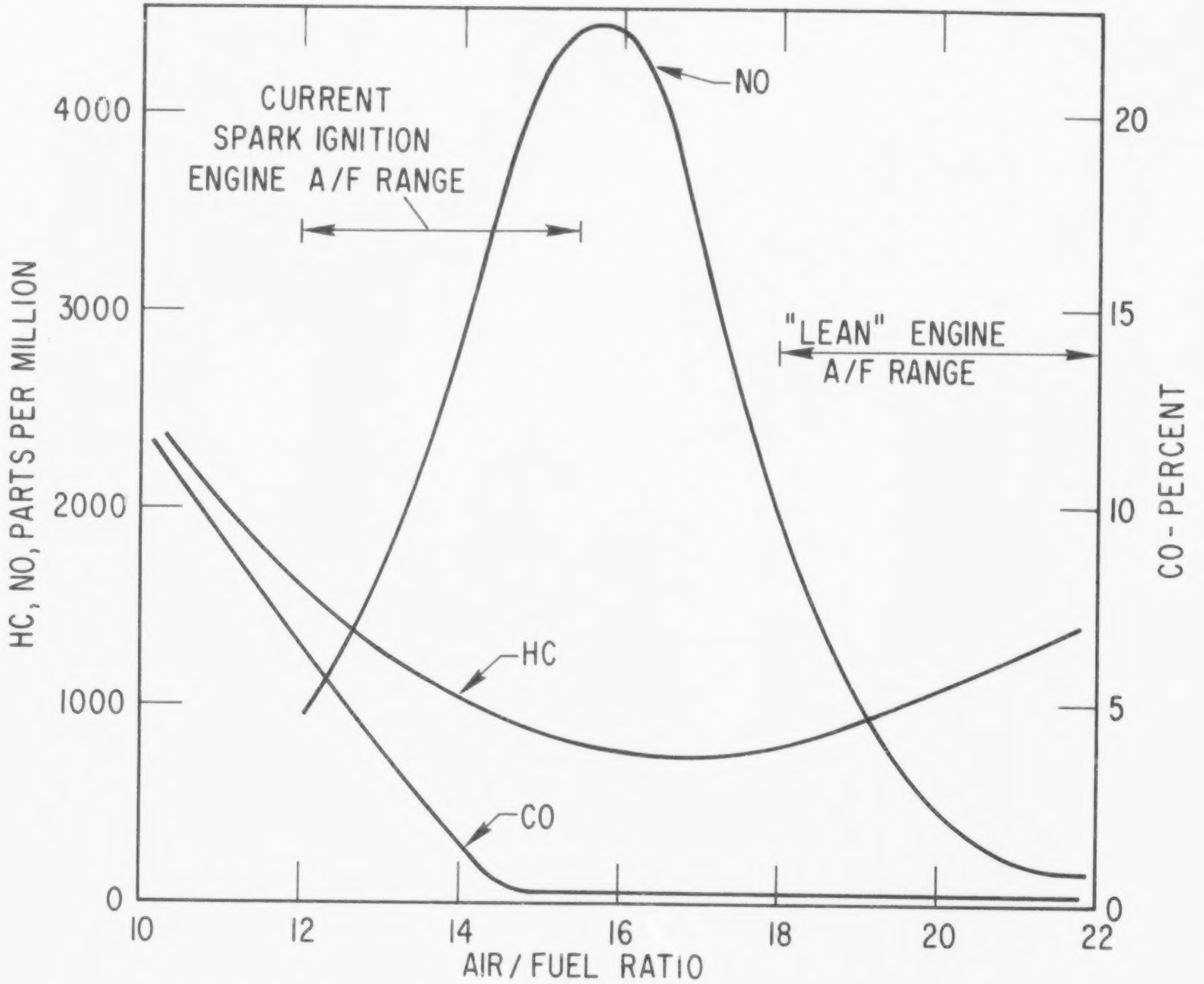

Figure B-1. Typical Spark Ignition Engine Exhaust Emissions Versus Air/Fuel Ratio (Gasoline) frame typical of spark ignition engines. The molecular structure of the emitted HC is generally quite different from that of the fuel used in the engine (Ref. B-10).

Starkman (Ref. B-11) has shown that the CO exhaust concentration of spark ignition engines is generally lower than the calculated equilibrium value in the chamber. However, the CO concentration in the exhaust is much higher than the equilibrium value corresponding to the exhaust temperature, particularly in the lean regime. This points out that the CO reactions are too slow to remain in equilibrium during the expansion of the gases in the cylinder. Sawyer (Ref. B-12) has predicted similar trends for gas turbines.

Much experimental and theoretical work has been undertaken in an effort to provide a basic understanding of the formation processes of nitric oxide. Newhall and Shahed (Ref. B-13) have determined the formation of NO experimentally and have concluded that NO is formed primarily in the post flame gases. Eyzat and Guibet (Ref. B-14) and Lavoie, Heywood and Keck (Ref. B-15) have shown theoretically that the NO formation in internal combustion engines is kinetically controlled. The predicted NO concentrations in the chamber are generally much lower than the equilibrium values, particularly in the lean regime because the reactions are too slow. As the gases expand in the cylinder the temperature decreases rapidly and, as a result, the NO reactions freeze at a level which is much higher than the equilibrium value computed for the exhaust temperature. This has been verified experimentally by Newhall and Starkman (Ref. B-16). Caretto et al (Ref. B-17) have theoretically analyzed the effect of engine speed on NO emission and have obtained results which are in reasonable agrement with experiments. As speed decreases, the NO concentration decreases.

B.2.3 Methods to Reduce Emissions

In addition to air/fuel ratio, there are many other factors affecting emissions, including variation of spark timing, chamber and induction system design, mixture preparation, and manifold pressure. Also, exhaust gas recirculation, water injection, and catalytic converters affect engine emissions. These factors were considered in estimating the projected engine emission characteristics and are briefly discussed in the following paragraphs.

B.2.3.1 Air/Fuel Ratio

As indicated in Fig. B-1, the emissions of HC, CO, and NO can be reduced simultaneously by increasing the air/fuel ratio beyond stoichiometric. However, driveability of the engine generally deteriorates at high air/fuel ratios, particularly when the mixture ratio distribution is not uniform. Operation in the fuel rich regime results in low NO emissions. However, the corresponding HC and CO emissions are high and would have to be controlled externally by other means, such as thermal or catalytic devices. At an air/fuel ratio of approximately 13 there are equal mole fractions of NO and CO. Thus the reaction, $2\ CO + 2\ NO = 2CO_2 + N_2$, is theoretically feasible. This reaction, however, is too slow unless a catalyst is added in the exhaust line.

B.2.3.2 Spark Timing

Huls and Nickol (Ref. B-18), Hagen and Holiday (Ref. B-19), Jackson et al (Ref. B-20), Fagley et al (Ref. B-21), Freeman and Stahman (Ref. B-22), and Hittler and Hamkins (Ref. B-23) have demonstrated the effects of spark timing on HC and NO emissions. When retarding the spark, ignition of the air/fuel mixture in the cylinder is delayed. This results in lower chamber temperatures and less NO. Also combustion of part of the mixture then occurs during the expansion stroke. Thus higher exhaust gas temperatures are obtained and additional oxidation of HC can occur in the exhaust system provided, of course, that oxygen is available. Eltinge et al (Ref. B-24) have shown that HC can be further reduced by insulating the exhaust manifold. No effect of spark ignition timing on CO has been reported. It should be mentioned that engine power and fuel consumption are adversely affected by spark retardation.

B.2.3.3 Design Modifications

Modification of the conventional air/fuel induction system can potentially result in lower HC and CO emissions. Jones and Gagliardi (Ref. B-25), Bartholomew (Ref. B-26), Trayser and Creswick (Ref. B-27), and others have shown experimentally that smaller mixture ratio excursions and lower HC and CO emissions can be obtained when using a preheated and premixed air/fuel charge. Similar effects might be realized by using optimized carburetor intake manifold configurations or fuel injections.

As previously mentioned, part of the HC emission from internal combustion engines results from quench effects occurring in the film zone adjacent to the cylinder walls. Thus, a reduction of the cylinder surface area to volume ratio should be effective in minimizing HC emissions.

Huls, Myers, and Uyehara (Ref. B-28) have shown that reduction of engine compression ratio can result in lower HC emissions. As compression ratio decreases the exhaust gas temperature increases and this promotes additional HC reactions in the exhaust system.

B.2.3.4 Catalytic Converters

The potential effectiveness of catalytic converters has been previously stated. Schwochert (Ref. B-29) has conducted experiments with non-leaded gasoline and a precious metal catalyst on two automobiles. When warm, the HC and CO conversion efficiencies of the catalyst were initially 88 percent and 91 percent, respectively. After 50,000 miles of driving over the modified American Manufacturers Association (AMA) cycle, the HC conversion efficiency of the catalyst was reduced to approximately 74 percent while the CO efficiency remained unchanged. For a cold start, the HC and CO efficiencies were 70 percent when new and decreased to 55 percent after 50,000 miles. Osterhaut et al (Ref. B-30) have published similar results.

It was recently reported that a base metal catalyst manufactured by Universal Oil Products (UOP) is very effective in simultaneously reducing HC, CO, and NO emissions so long as the air/fuel ratio is maintained between approximately 13.5 and 16.5. In that case HC, CO, and NO effectiveness values are approximately 75 percent, 90 percent, and 80 percent, respectively. No information is available on the cold start characteristics of the UOP catalyst.

B.2.3.5 Exhaust Gas Recirculation

Exhaust gas recirculation has been shown to be one of the more effective methods for reducing NO emissions. Kopa (Ref. B-31) has demonstrated that significantly lower NO can be obtained by adding exhaust gas recirculation which results in lower combustion temperatures. This is illustrated in Fig. B-2, where the NO reduction efficiency obtained by Kopa is shown as a function of percent exhaust recirculated. Also shown in the figure are SFC and engine power. For 15-percent recirculation, the NO concentration was reduced by approximately 80 percent with a 15-percent loss in power and a 10-percent increase in fuel consumption. According to Kopa, HC and CO emission were not adversely affected by recirculation. Newhall (Ref. B-32) has conducted a theoretical study of exhaust gas recirculation and his analysis supports the data measured by Kopa. The study by Newhall indicates that the maximum amount of recirculation possible might be lower in the lean regime. Benson (Ref. B-33) has reported NO emission reduction efficiencies of approximately 80 percent when combining exhaust gas recirculation and spark retardation. W. Glass et al (Ref. B-34) have tested two automobiles with exhaust gas recirculation. Reductions in NO of approximately 60 percent were achieved with approximately 12.5 percent recycle flow rate with little change in HC and CO emissions.

B.2.3.6 Water Injection

Nicholls et al (Ref. B-35) have presented test data showing the effects on NO emissions of water injection into the intake manifold. At water flow to fuel flow rates of 1.0, the NO reduction efficiency is approximately 60 percent and increases for air/fuel ratios below stoichiometric. It appears that water injection becomes less effective above stoichiometric. Water injection has very little effect on engine power and fuel consumption.

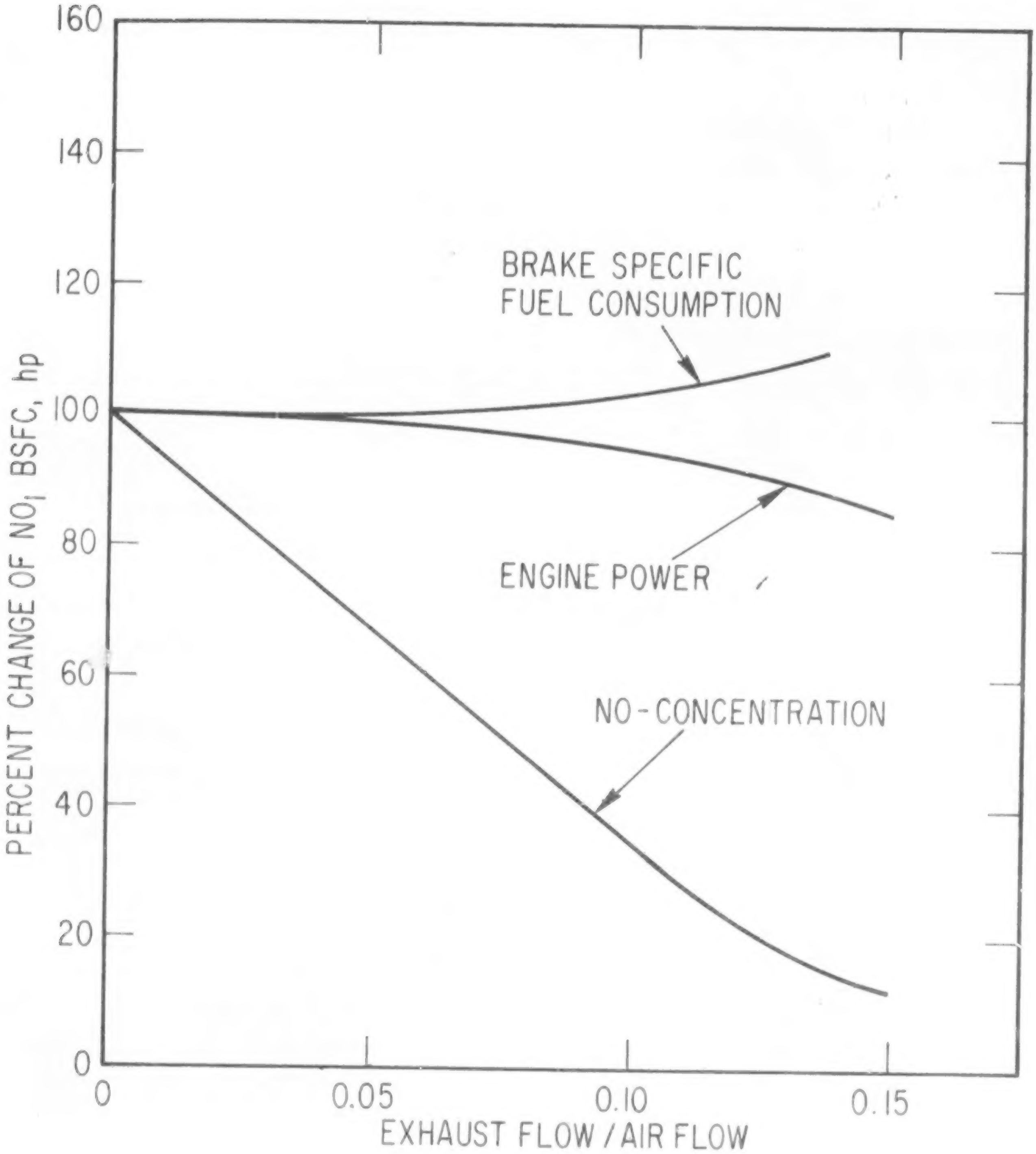

Figure B-2. Effect of Exhaust Gas Recirculation on NO Emissions and Performance - Spark Ignition Engines

B.2.3.7 Exhaust Manifold Reactors

Exhaust manifold reactors provide a high temperature zone in the engine exhaust system to promote further oxidation of the HC and CO. Secondary air is provided when the engine is operated below stoichiometric. Mikita et al (Ref. B-36) have tested such a device on two cars and have demonstrated HC, CO, and NO emission levels below the 1975 standards. Although basically feasible, the system presently has a number of disadvantages such as large volume and high cost.

Cantwell et al (Ref. B-37) have presented emission data for cold and hot starts using this device. Based on test data from the seven-mode driving cycle, the HC and CO emissions for a cold start test are 1.65 and 1.35 times those obtained with a hot start. These factors are comparable to those of standard engines. This is further discussed in Section B.2.8.

Glass et al (Ref. B-38) have reported on a synchrothermal reactor concept which is designed to operate at air/fuel ratios below stoichiometric in order to minimize NO emissions. Small amounts of recirculation are used to further promote NO reduction. Secondary air is injected into the exhaust manifold of each cylinder, and, in order to maximize temperature, the air injection is synchronized with the valve opening. For the seven-mode cycle, the reported exhaust concentrations are 10 ppm HC, 0.3 percent CO, and 150 ppm NO. At 50 mph, the concentrations are higher.

B.2.4 Other Engine and Fuel Types

In addition to the standard spark ignition engines, two advanced spark ignition engines show some promise with respect to the hybrid application. These are the Wankel rotary engine and the Stratified Charge engine. Also, consideration has been given to conventional spark ignition engines using natural gas or liquefied petroleum gas (LPG) as fuel.

B.2.4.1 Wankel Rotary Engine

Owing to its light weight and small volume the Wankel engine warrants further consideration. While the emission characteristics of the Wankel engine with an exhaust manifold reactor are similar to standard spark ignition engines, it appears that those emissions might be further reduced by design modifications and additional development work. Although some emission data have been reported by Cole and Jones (Ref. B-39), the scope of this study and the lack of a comprehensive data sample did not permit further examination of the Wankel engines and its emission characteristics.

B.2.4.2 Stratified Charge Engine

Mitchell et al (Ref. B-40) have presented a description of a Stratified Charge engine originally designed for low SFC and multifuel capability. The engine has an air swirl chamber, fuel injection, and spark ignition and is designed to operate at air/fuel ratios above 20. The engine has demonstrated low fuel consumption characteristics and the HC and CO emissions are reasonably low. Since an adequate emission data sample is not available at this time, no attempt was made to characterize the emissions of this engine for use in the hybrid study.

B.2.4.3 Liquified Petroleum Gas

McJones and Corbell (Ref. B-41) have reported emission data from a spark ignition engine operated with natural gas. The engine used in the program was operated with approximately 25 percent excess air and with retarded spark. The principal HC constituent found in the exhaust was methane which is considerably less reactive than the HC species normally present in the exhaust of spark ignition engines. The HC, CO, and NO emissions were lower for natural gas and LPG, primarily because the air/fuel ratio was increased compared to operation on gasoline. Engine power output was reduced by approximately 15 percent. Driveability was excellent over a wide range of operating conditions. Baxter et al (Ref. B-42) have reported some emission data gathered from a spark ignition engine operated on LPG.

The reactivity of the hydrocarbon in the exhaust was approximately 30 percent of the reactivity of typical gasoline engine exhaust.

B.2.5 Parametric Engine Emission Data

Steady-state mass emission data for the Toyota engine are presented in Figs. B-3 through B-5 in terms of specific mass emissions versus engine brake horsepower. These data were computed from the specie concentration data presented by Matsumoto et al (Ref. B-1) and the engine air flow data subsequently provided by Toyota upon Aerospace request (Ref. B-2). The HC data presented by Matsumoto were measured by nondispersive infrared (NDIR) instrumentation. To account for sensitivity differences between NDIR and flame ionization detector (FID), the HC concentrations were multiplied by a factor of 2 before conversion to specific mass emissions. Tyree and Springer (Ref. B-43) have shown that this value is reasonable. However, there are indications that the factor varies with varying operating conditions as a result of a shift in molecular structure of the emitted hydrocarbons. As indicated in Fig. B-3, the HC specific mass emissions increase with decreasing speed and rise sharply at very low power levels. This trend is the direct result of the air/fuel ratio variations of the Toyota engine presented in Fig. B-6. As expected, the CO mass emissions show similar trends. Also, the NO emission plotted in Fig. B-5 is as expected, considering the air/fuel ratio schedule depicted in Fig. B-6.

The data plotted in Figs. B-3 through B-5 were used to determine the design load specific mass emissions for operation of the engine at air/fuel ratios between 15 and 16. It should be mentioned that the highest power output of the engine at an air/fuel ratio of 15 was approximately 75 percent of design horsepower. The emissions at that load point were then considered full-load points for the purpose of this study. The data obtained from another engine manufacturer (Ref. B-3) were analyzed accordingly. That engine was operated at air/fuel ratios of approximately 16 over a wide range of load

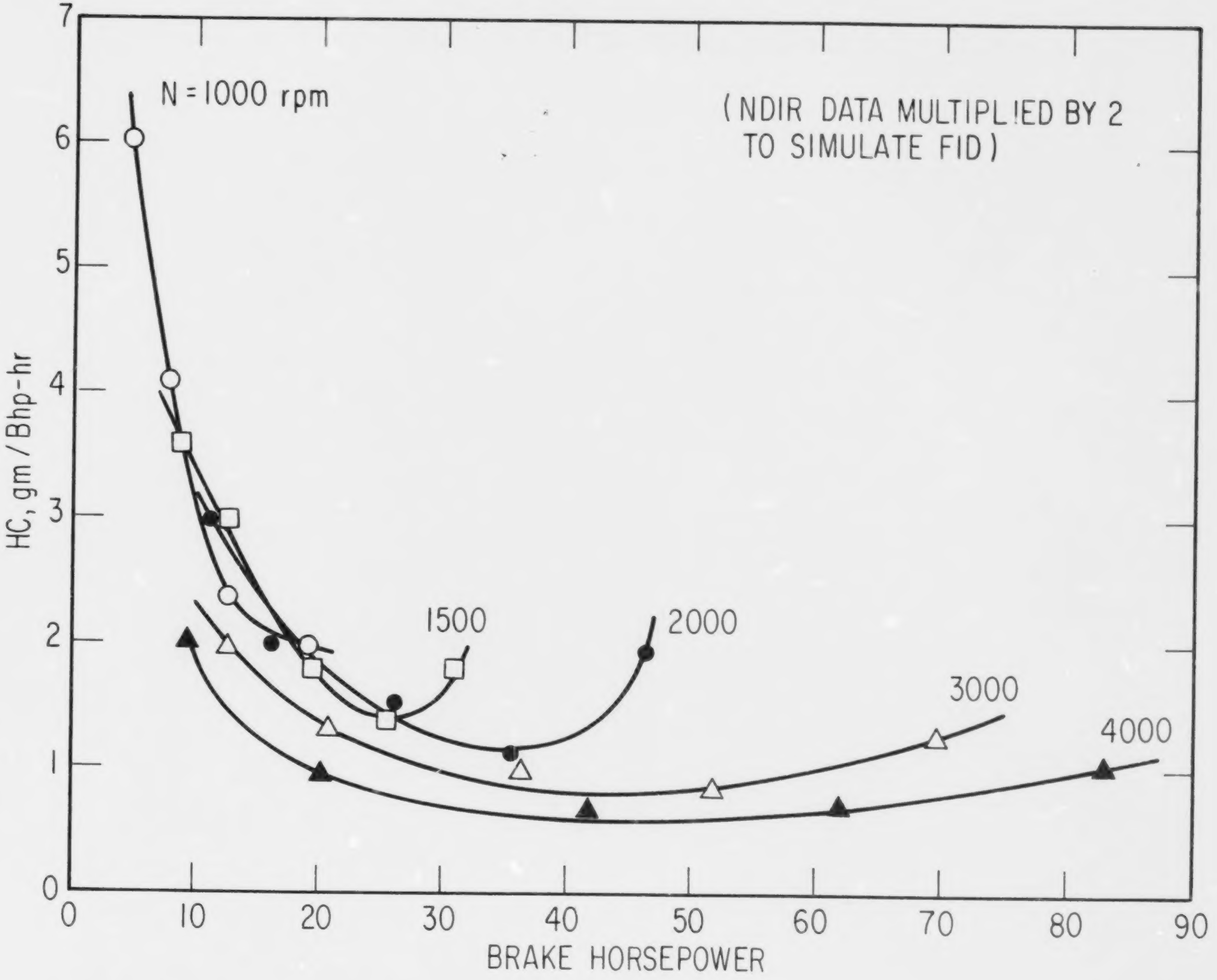

Figure B-3. Toyota 115.7 CID Engine Hydrocarbon Emissions

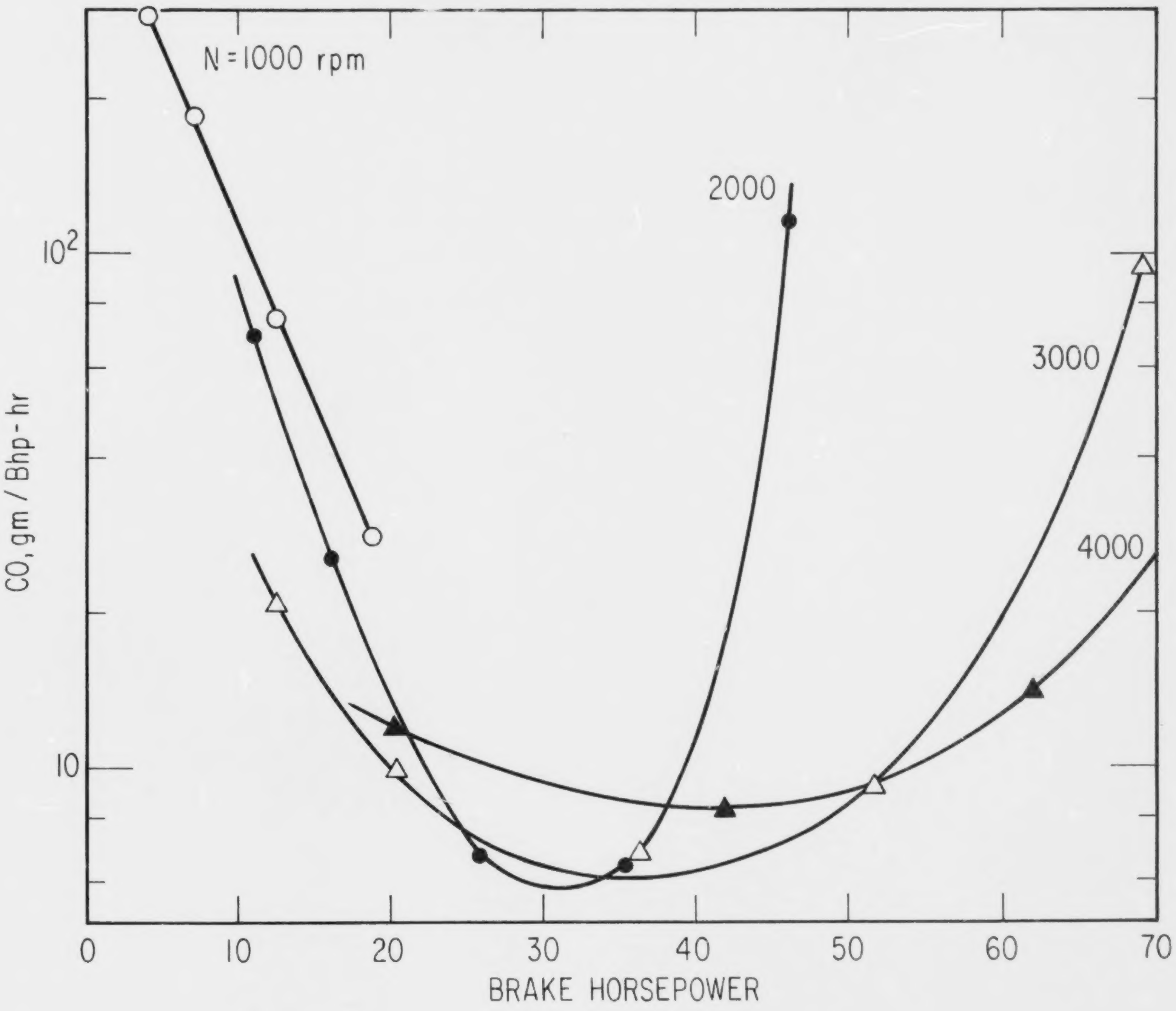

Figure B-4. Toyota 115.7 CID Engine Carbon Monoxide Emissions

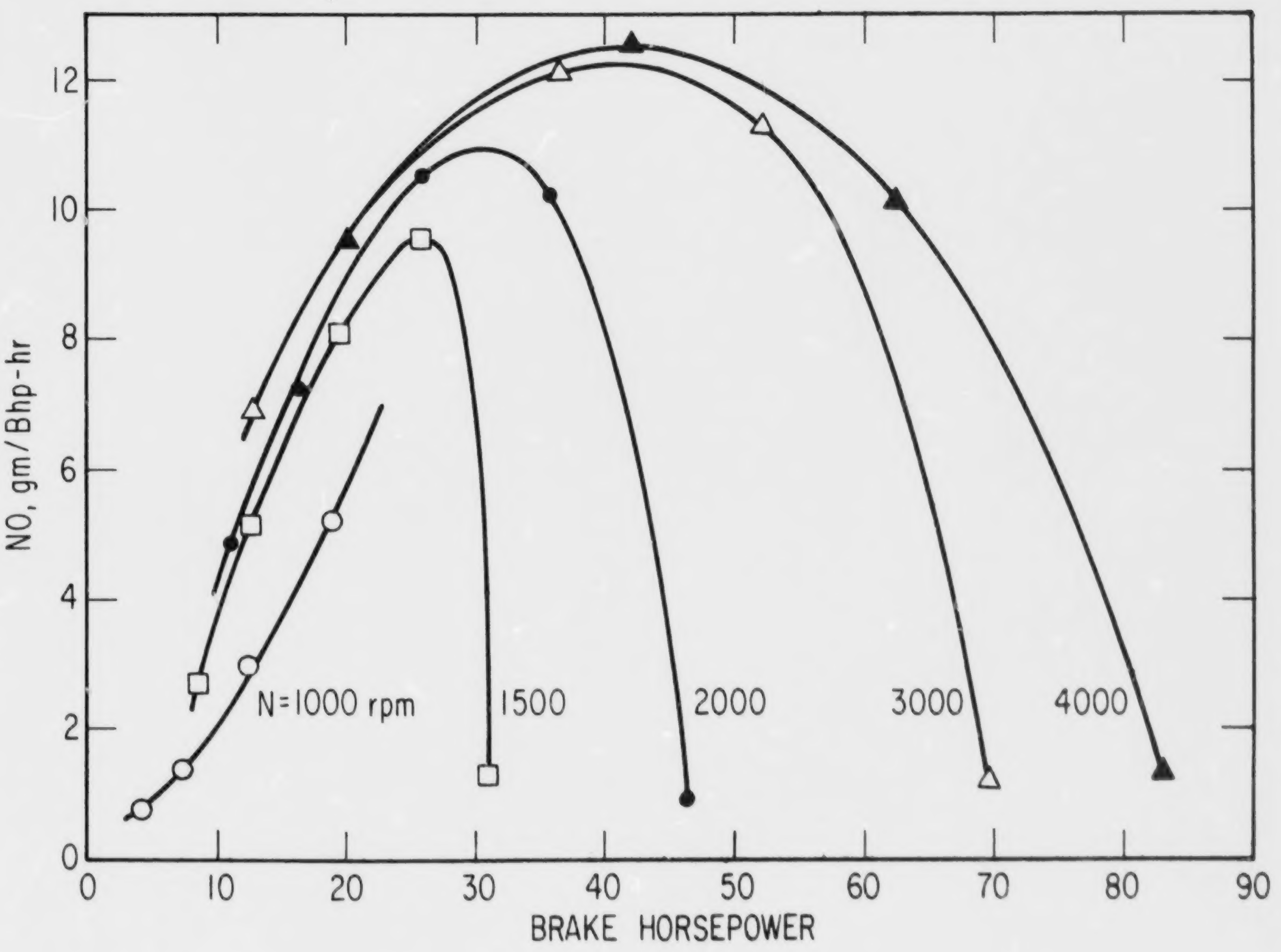

Figure B-5. Toyota 115.7 CID Engine Nitric Oxide Emissions

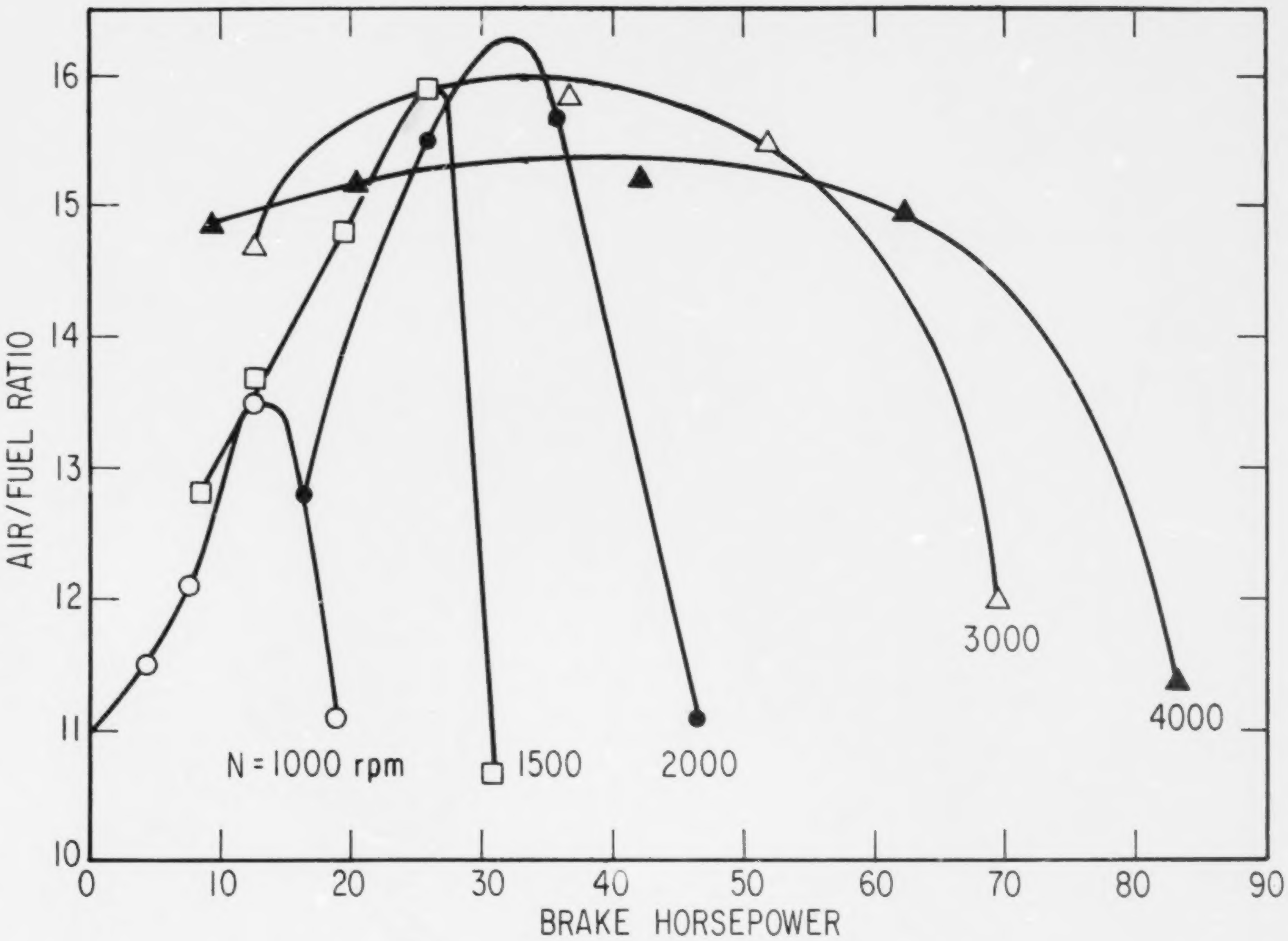

Figure B-6. Toyota 115.7 CID Engine Air/Fuel Ratio Versus Brake Horsepower conditions. Again, the HC emissions were measured by NDIR, and, for the purpose of this study, the data were increased by a factor of 2 to account for sensitivity differences between the NDIR and FID instrumentation. The design load specific mass emissions of these engines are also listed in Table B-1.

The CO and NO specific mass emissions for a single-cylinder CFR engine operated at 1000 rpm with gasoline are presented in Fig. B-7. These data were computed from concentration, flow rate, and indicated horsepower data informally obtained from R. Hurn (Ref. B-6). The test data shown in the figure are for two flow conditions: 50 percent and 86 percent of maximum flow. The dashed NO curve was drawn to represent a flow rate of approximately 60 to 70 percent. This curve was used as the basis for estimating the NO specific mass emissions of engines operated at air/fuel ratios of 19 and 22. The air/fuel ratio of 19 was considered a maximum value for the present state-of-the-art technology, while 22:1 is a projection. It should be pointed out that a considerable penalty in engine horsepower output occurs when operating at these very high air/fuel ratios. This is shown in Fig. B-8 where the ratio of engine power to maximum engine power is plotted as a function of air/fuel ratio. This power loss must be considered in engine weight and volume calculations for current hybrid applications, but it is anticipated that this power loss can be circumvented in future engine designs (viz., stratified charge) and, hence, was not included in calculations of engine weight and volume. In addition, there is some loss in fuel economy. Newhall and El-Messiri (Ref. B-7) have published data from their prechamber work over a range of air/fuel ratios. A set of HC, CO, and NO specific mass emissions selected from that data for an air/fuel ratio of 25:1 is listed in Table B-1. As indicated, this device has rather low HC and NO emissions. However, the CO specific mass emission appears to be on the high side.

B. 2. 6 Design Load Emissions

B. 2. 6. 1 State-of-the-Art Technology

The design load specific mass emission points listed in Table B-1 are plotted in Figs. B-9 through B-11. These data points provided the basis for the

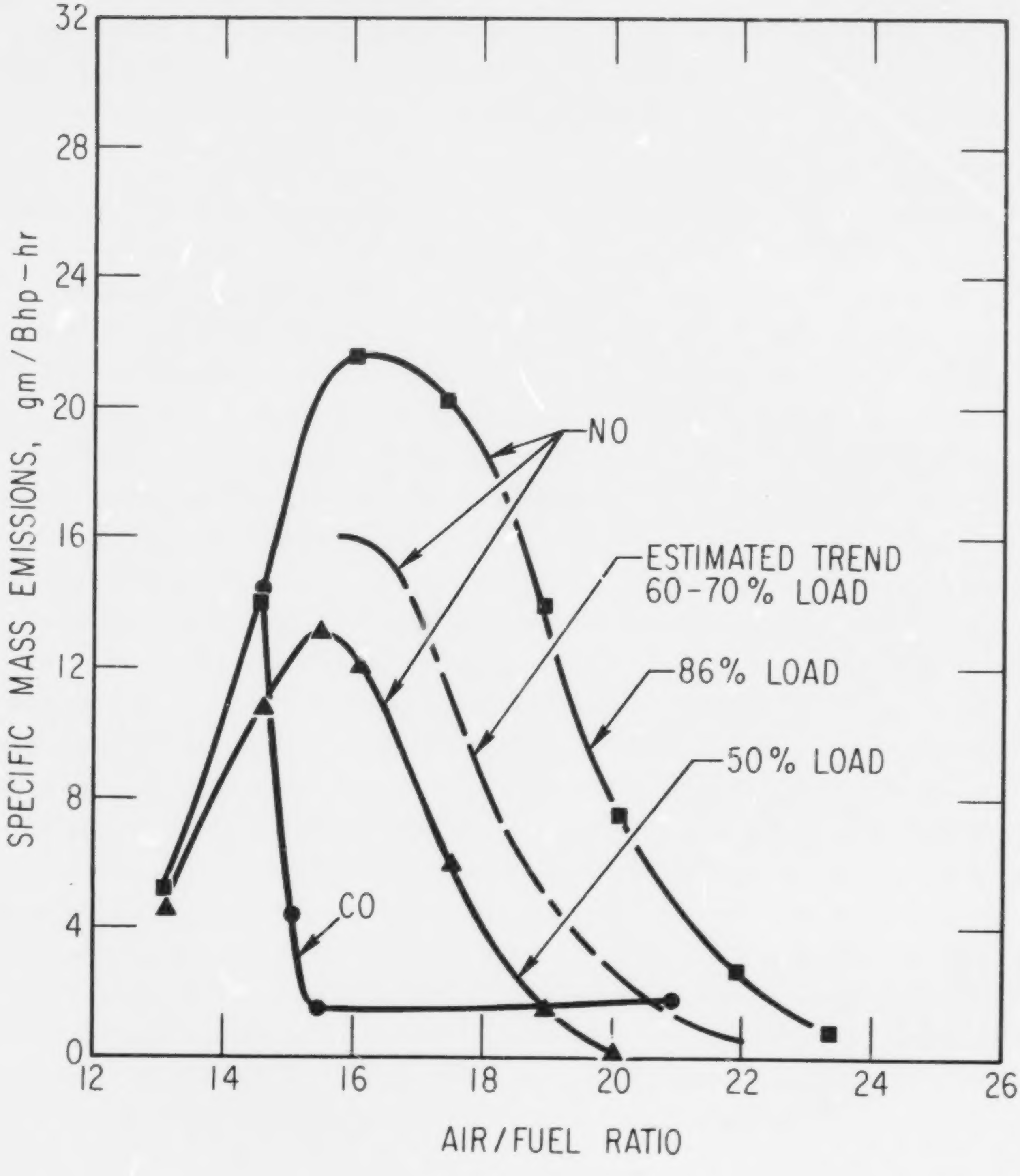

Figure B-7. CFR Engine - Emission Test Data
(1000 rpm; Gasoline)

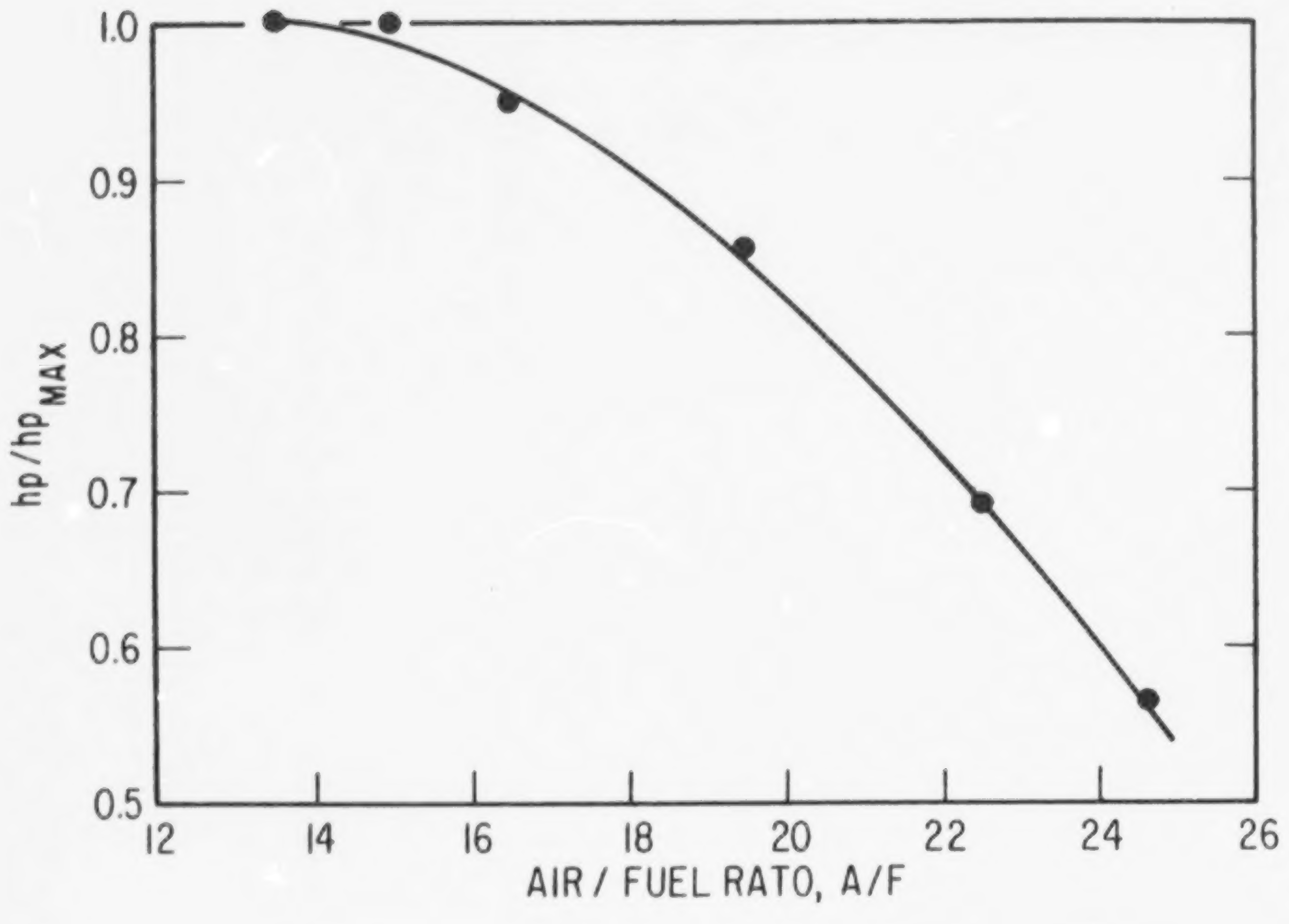

Figure B-8. CFR Engine - Power Output Versus Air/Fuel Ratio

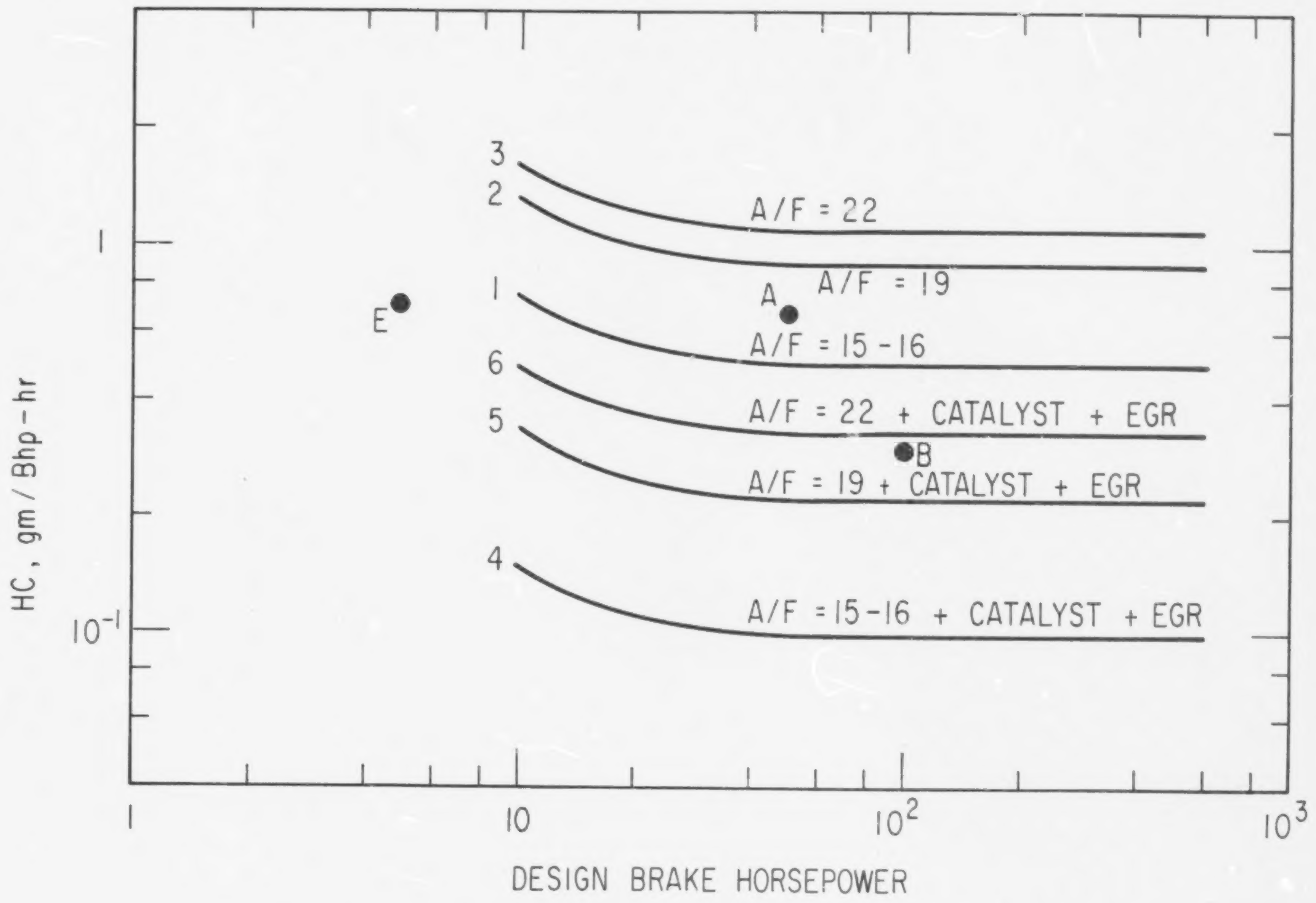

Figure B-9. Spark Ignition Engines - Hydrocarbon Emission, Steady State Design Load (Gasoline)

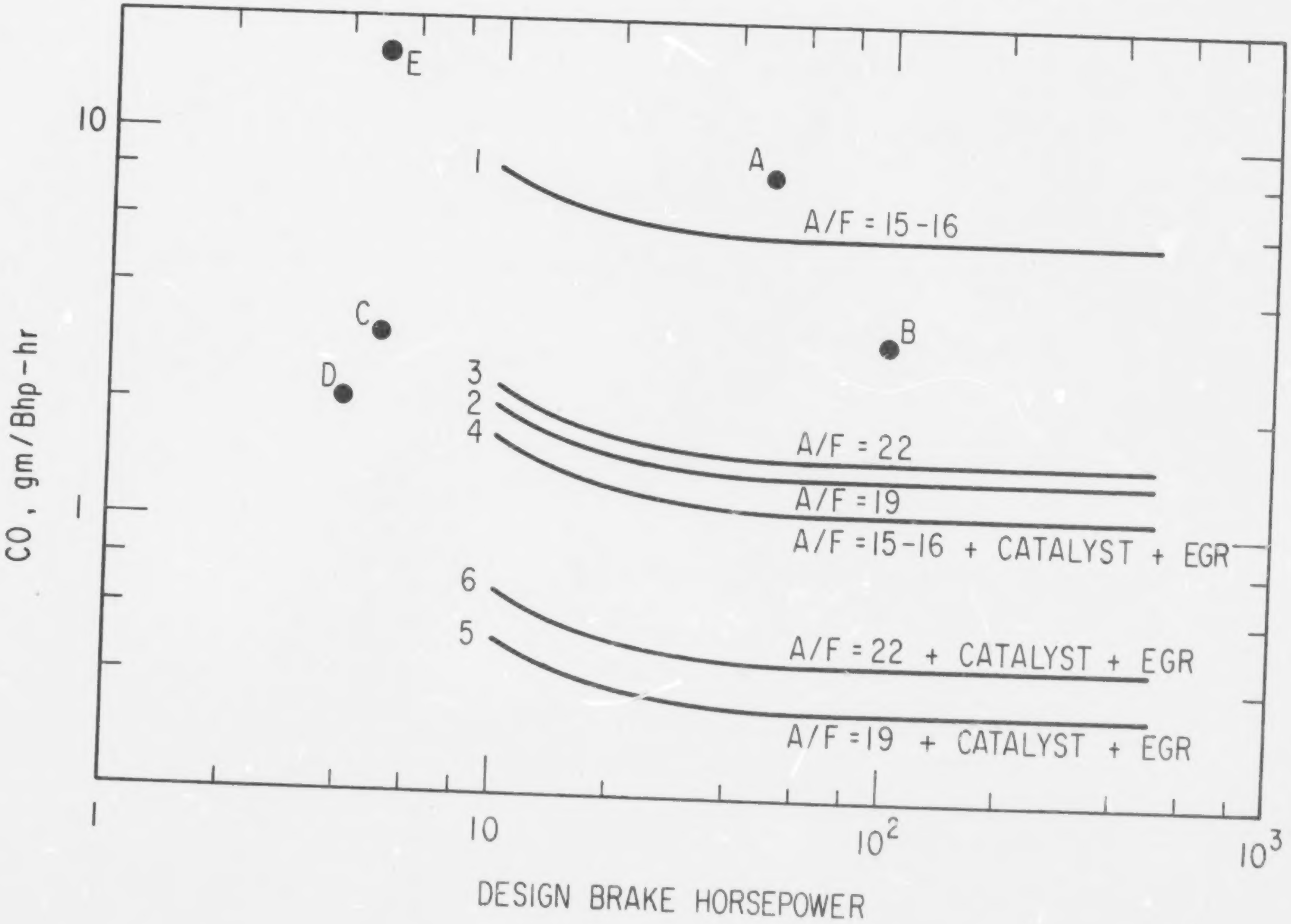

Figure B-10. Spark Ignition Engines - Carbon Monoxide Emission, Steady State Design Load (Gasoline)

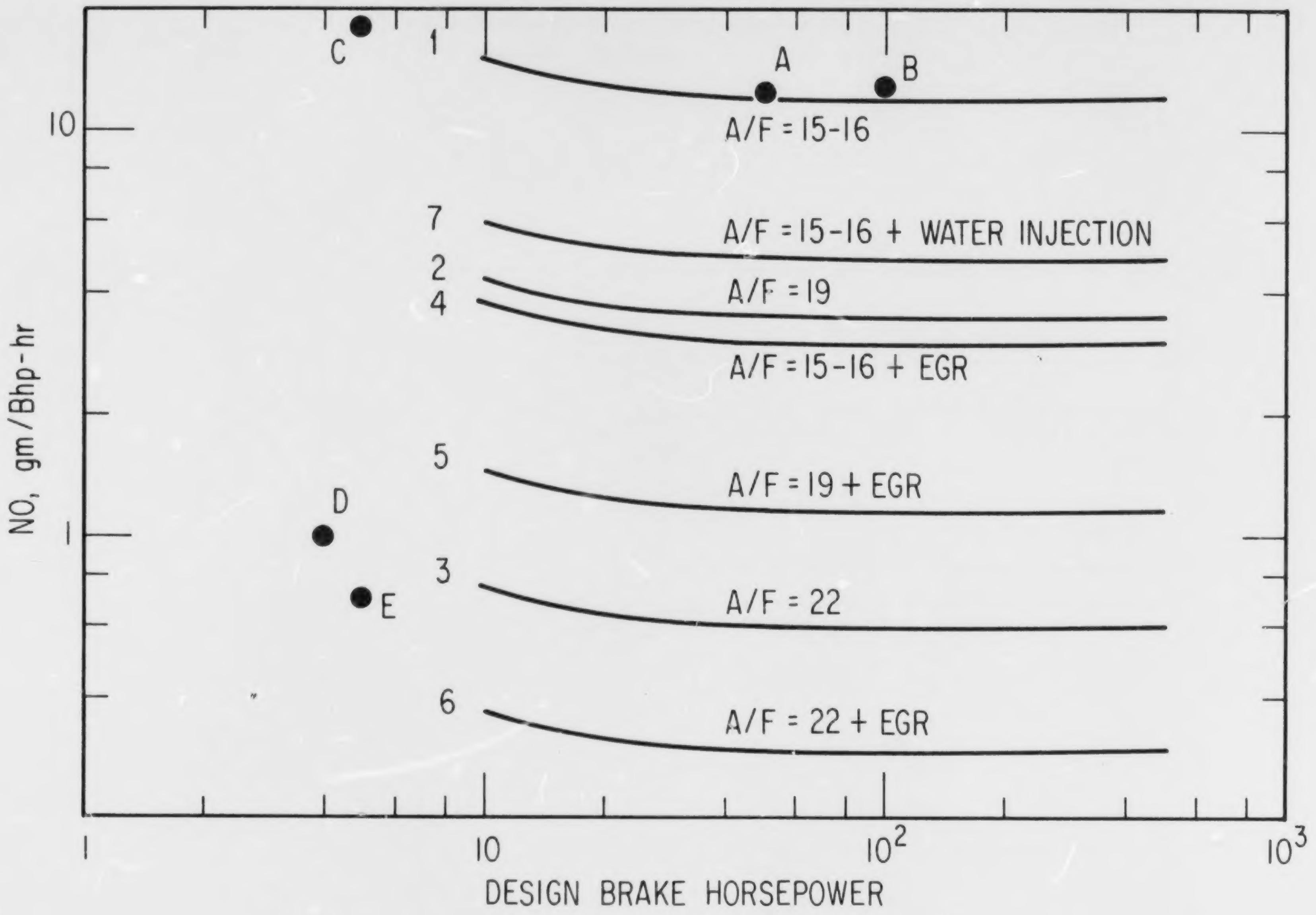

Figure B-11. Spark Ignition Engines - Nitric Oxide Emission, Steady State Design Load (Gasoline) emission characteristics selected for the various spark ignition engine configurations and operating conditions considered in this study. Obviously, the data available are hardly sufficient to draw very accurate conclusions. However, all efforts to obtain additional test data were unsuccessful. This attests to the need for a comprehensive spark ignition engine emission test program covering primarily the high air/fuel ratio regime.

Curves No. 1 in Figs. B-9 through B-11 were drawn between multicylinder engine points A and B and are for air/fuel ratios between approximately 15 and 16. Curves No. 2 represent an air/fuel ratio of 19. Based on discussions with R. Hurn (Ref. B-6) and D. Cole (Ref. B-44), an air/fuel ratio of approximately 18 to 19 is considered a maximum for the present state-of-the-art technology of multicylinder engines. However, the problems normally associated with lean engine operation should be minimized for a hybrid vehicle because the engine can be designed for operation at a single point or for a relatively small range of operating conditions. Also, operation under transient conditions can be minimized in the hybrid. These factors, however, cannot be fully evaluated at this time. The assumed increase of the HC specific mass emissions at air/fuel ratio of 19 compared to air/fuel ratio of 15-16 is due to the combined effects of power loss and increasing quench effects (Fig. B-9).

As previously mentioned, the CO concentrations in the exhaust of spark ignition engines are very low. This is reflected in Curve No. 2 of Fig. B-10 which represents an air/fuel ratio of 19.

The NO specific mass emissions of engines A and B are in excellent agreement, indicating again that air/fuel ratio is the principal parameter affecting NO emissions in current engines. Curve No. 2, representing an air/fuel ratio of 19, is based primarily on the data obtained from R. Hurn and includes spark timing adjustments to minimize NO emissions. It should be noted that the data by Hurn are for a small single-cylinder engine; large multicylinder engines may show different emissions.

The effect of catalytic converters in the exhaust system and exhaust gas recirculation (EGR) on emissions is illustrated by Curves No. 4 to No. 6. Curve No. 4, representing an air/fuel ratio of 15-16,was obtained from Curve No. 1 by using an HC and CO conversion efficiency of 80 percent and an NO effectiveness of 75 percent. The assumed catalyst effectiveness is conservative by comparison with the data published by Schwochert and by Universal Oil Products. However, the catalytic converter effectiveness is lower during engine warmup. Also, addition of EGR tends to increase HC and CO. Identical conversion efficiencies were used for CO and HC. This assumption may be somewhat conservative since CO conversion efficiencies tend to be higher than HC efficiencies, at least over the range of air/fuel ratios presently used in spark ignition engines. Since the CO mass emissions are already very low at air/fuel ratios above approximately 15, the assumption of a more conservative CO conversion effectiveness is not that critical. This is even more apparent when considering a cold start. In that case, a large portion of the total CO emitted over a driving cycle is generated during the engine/catalyst warmup period.

The selected exhaust gas recirculation effectiveness is based upon the previously discussed test data using a recirculation rate of approximately 15 percent.

Catalytic converters were not considered as a means to reduce NO, primarily because of insufficient data. Although NO conversion efficiencies of approximately 75 percent were reported by Universal Oil Products for air/fuel ratios of 15-16, it appears that NO effectiveness decreases very rapidly at lean air/fuel ratios. Combining NO catalysts and EGR might be feasible for operation at stoichiometric or slightly higher air/fuel ratios and very low NO emissions might be achieved with that approach. This concept should be further investigated.

Curves No. 5, representing an air/fuel ratio of 19, were obtained from Curves No. 2 by assessing a HC and CO conversion efficiency of 75 percent and an EGR efficiency of 67 percent. Reduced efficiencies were used to account for the lower combustion chamber and exhaust gas temperatures. The assumed reduction in catalytic converter efficiency may be conservative in view of a number of possible catalyst design modifications. For instance, the catalyst could be electrically heated thereby improving its effectiveness. In a hybrid/electric engine system there is always an adequate supply of stored electrical energy.

The effect of water injection into the intake manifold of the engine on NO emissions is illustrated by Curve No. 7 of Fig. B-11 for an air/fuel ratio of approximately 15-16 and a water flow to fuel flow rate ratio of 1.0. In accordance with the data by Nicholls et al (Ref. B-35), an NO reduction efficiency of 60 percent was used. In view of the relatively low effectiveness of water injection on NO, it appears that this approach may not be attractive due to the added complexity of such a system.

The HC, CO, and NO specific mass emissions are assumed to be constant for engine design power levels above approximately 50 hp. Below that point, the HC emissions are assumed to increase due to decreasing engine efficiency and increasing quench effects.

B.2.6.2 Projected Technology

The design load specific mass emissions for the projected technology are presented by Curves No. 3 and No. 6 of Figs. B-9 through B-11. Curves No. 6 are for air/fuel ratio of 22 and Curves No. 7 for air/fuel ratios of 22 plus catalytic converter and exhaust gas recirculation. The selected air/fuel ratio of 22 is considered the practical limit for spark ignition engines. However, this value should not be taken too literally but merely as an indication of an ultra lean operation. Further studies are required to determine the optimum ultra lean air/fuel ratio by considering emissions as well as engine performance aspects.

As shown by Curve No. 3 of Fig. B-9, the HC emissions at an air/fuel ratio of 22 are somewhat higher than at an air/fuel ratio of 19. This small increase is the result of a number of opposing effects. Generally, for very lean mixtures, the HC specific mass emissions tend to increase due to lower engine power output for a given air flow rate and increased quench effects. However, the HC emissions might be further reduced by means of additional chamber and induction system design optimization.

The CO specific mass emissions at an air/fuel ratio of 22 are slightly higher than those at an air/fuel ratio of 19 due to a loss in engine power at the higher ratio.

The NO specific mass emissions at an air/fuel ratio of 22 are considerably lower than at an air/fuel ratio of 19. The assumed reduction is based on single-cylinder data by Hurn and by Newhall, with the assumption of optimized spark timing.

The effects of catalytic converters and exhaust gas recirculation on emissions at an air/fuel ratio of 22 are shown by Curves No. 6. An even lower HC and CO conversion efficiency of 70 percent was assumed to account for the lower exhaust temperatures. A recirculation efficiency of 50 percent was used to construct the NO Curve in Fig. B-11. This trend reflects to some degree the observations made by Newhall (Ref. B-32) and Matsumoto et al (Ref. B-1).

Again, the HC, CO, and NO specific mass emissions are constant for engine design horsepower output levels of 50 and above. Below that point, the NO specific mass emissions increase somewhat to reflect decreasing engine efficiency and increasing wall quenching effects.

Since HC and CO emissions can be effectively controlled by means of a catalytic converter and engine component design modifications (at least under hot start conditions), the principal problem remaining is NO emissions. Since EGR and spark timing changes are not sufficiently effective, it appears that a leaner mixture is required to meet future NO emission goals. Additional efforts should be directed towards this approach which theoretically looks very interesting, but may develop practical problems such as poor driveability, reduced power output, and increased fuel consumption.

However, these potential problems are believed to be less severe in the case of a hybrid engine configuration. More work in that area is needed to resolve these questions.

B.2.7 Part-Load Emission Characteristics

The part-load emission characteristics of spark ignition engines operating at air/fuel ratios of 15-16 are presented in Fig. B-12 in terms of the ratio of species specific mass emission at part-load to species specific mass emission at design load versus percent design load. These curves were derived for constant engine speed from the very limited data sample provided by Toyota and another engine manufacturer. The two engines show somewhat different part-load emission characteristics and the curves presented in Fig. B-12 are averages from the two engines. Part-load emission data for CO and NO recently received from General Motors (Ref. B-4) and TRW Systems (Ref. B-5) indicate similar trends. The part-load specific mass emissions at an air/fuel ratio of approximately 15 are obtained by multiplying the part-load emission factors from Fig. B-12 and the design load specific mass emissions presented in Figs. B-9 through B-11.

It is realized that engine exhaust emissions are also a function of engine speed. As a result, lower part-load emission factors might be obtained by varying speed as load is varied. The optimum speed versus load schedule must be determined for each hybrid system application by considering heat engine emissions as well as other parameters which affect the operation of engine system components, such as generator, motor, and controls. Presently, there is a serious lack of applicable engine data, and thus speed could not be used as an emission correlation parameter in this study. More work is required in that area before these questions can be adequately answered.

For the purpose of this study, HC, CO, and NO part-load specific mass emission factors of 1.0 were used for air/fuel ratios of 19 and 22. This choice was made primarily because of the lack of applicable test data.

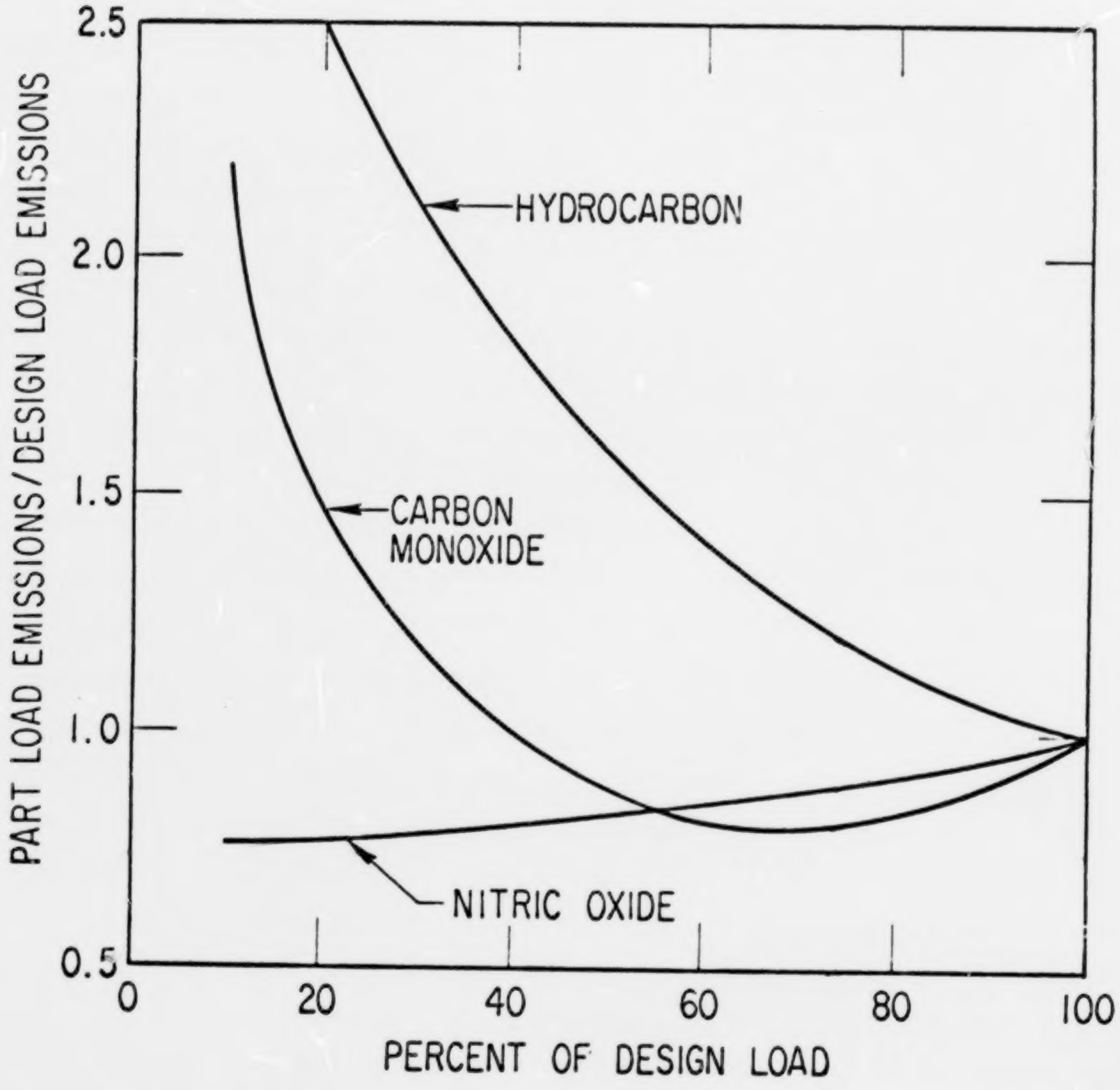

Figure B-12. Spark Ignition Engines - HC, CO, NO, Emissions, Steady State Part-Load, Air/Fuel = 15-16

Also, it appears that changes in spark timing and engine design modifications and the addition of catalytic converters and EGR can have a significant effect on the engine part-load emission characteristics. Currently, these changes cannot be anticipated and systematic research and development programs are required to resolve these questions.

B.2.8 Cold Start Emissions

For light-duty vehicles, Federal test procedures specify that the vehicle be kept at ambient temperature for 12 hr prior to the DHEW and seven-mode cycle tests. The vehicle exhaust emissions obtained over the DHEW driving cycle are determined by the constant volume bag sampling technique, and therefore reflect all the emissions generated during the warmup period of the engine from the moment the key is turned on. Thus it is necessary to ascertain the effect on emissions of this cold start period, which can be considerable, depending on engine operating conditions. In the case of an engine equipped with a catalytic reactor, there is an additional degradation of emission during the period that the catalyst is cold and relatively inactive. Since the engine exhaust emission data compiled for this study were based on steady-state, hot engine data, it was necessary to ascertain the influence of both engine and/or catalyst warmup on emission. Data obtained during the latter part of the study which give some feel for the magnitude of cold start emissions are discussed in the following paragraphs.

A cold start emission correction factor was derived that could be applied to the vehicle emissions which were calculated on the basis of steady-state, hot engine data in grams/mi over the DHEW cycle. This factor is defined as the ratio of cold start cycle emissions to hot start cycle emissions. At the onset of the study, very little information was available on cold start emission characteristics. Data was obtained, however, from several sources by various techniques which are summarized in Fig. B-13.

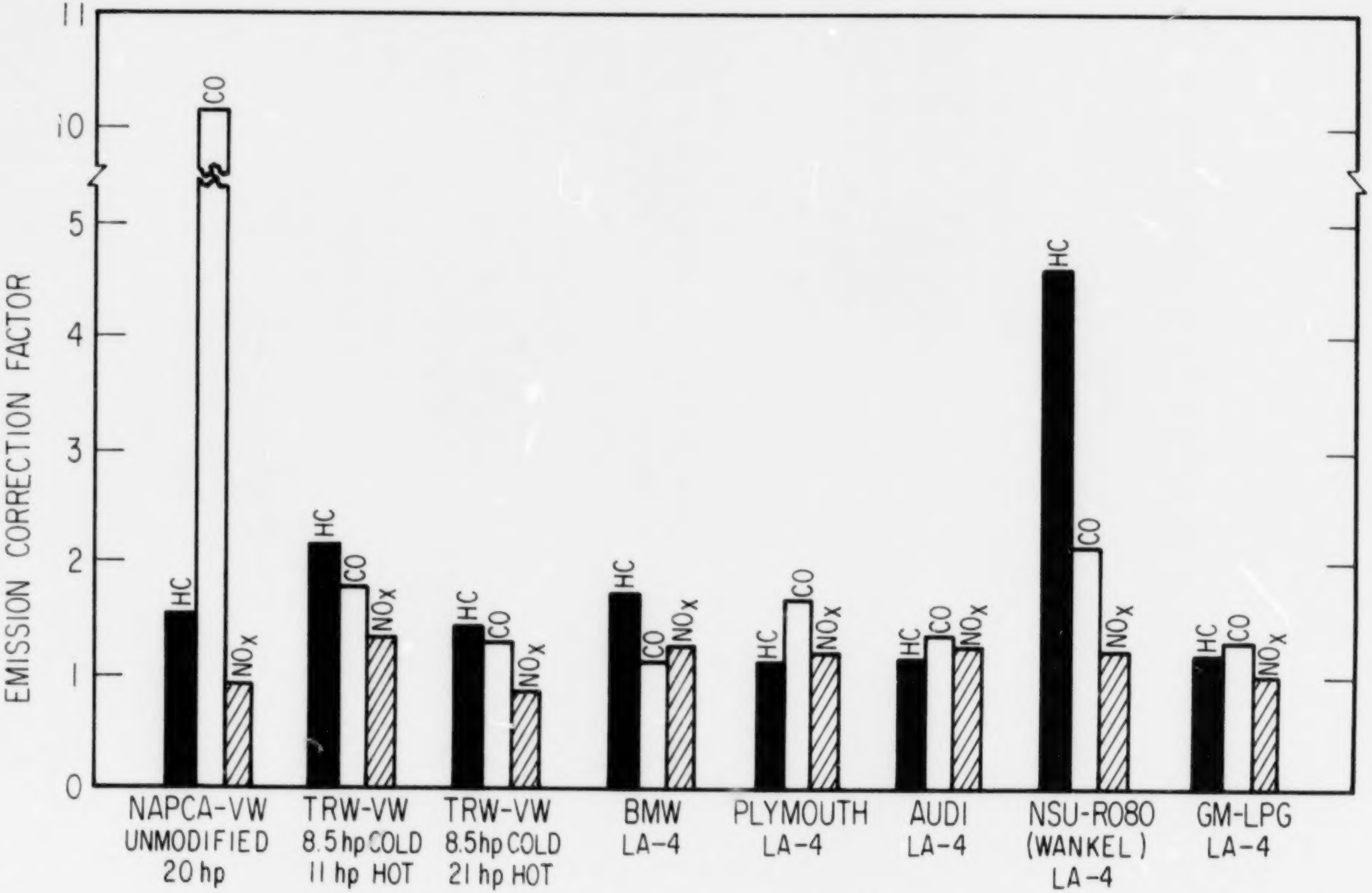

Figure B-13. Ratio of Cold Start Emissions to Hot Start Emissions, DHEW Cycle

Information was obtained from APCO (Ref. B-45) for vehicles tested over the DHEW (or LA-4) cycle, comparing the emissions generated during the normal test procedure with a 12-hr soak to that of a test initiated when the engine was hot. The emission correction factors shown in Fig. B-13 for the BMW, Plymouth, Audi, and NSU-R080 were derived from these test data. The NO_x correction factor for these tests seem suspect, since all other data indicate a lower NO_x emission level during engine warmup.

During the latter portion of the study period, engine tests were conducted by TRW Systems (Ref. B-46) to derive cold start emission characteristics for an engine operating over the hybrid mode of operation; that is, steady-state conditions. The TRW System tests were conducted with the objective of determining what changes could be made to minimize cold start emission in the hybrid mode of operation. To complement this activity, tests were run at APCO to derive the cold start characteristics of an unmodified VW engine. In order to approximate the hybrid system engine operation, the vehicle was tested on a chassis dynamometer with the engine being started as rapidly as possible to 2000 rpm and running steady-state at approximately 20 shaft horsepower. Both the TRW and APCO tests were conducted with two bags. In the APCO test, one bag was used to collect the emissions generated over the first two minutes, and the second bag was used to collect the hot engine emissions over a hot two-minute period. The TRW tests were based on three-minute bag samples.

Preliminary results from the TRW tests indicate that by modifying the choke operation and spark advance, and also by ramping the engine power output, the cold start emissions can be reduced from that indicated by an unmodified engine. Emission correction factors derived from these tests are shown in Fig. B-13. The factors derived from the TRW tests are for the hybrid mode of engine operation with 8.5 hp output during the first three minutes followed by the indicated power levels for the remainder of the DHEW cycle.

Also shown in Fig. B-13 are correction factors derived from General Motors vehicle test data (Ref. B-47). The General Motors test was conducted with LPG fuel over the DHEW cycle. The engine had some spark advance control and was operated at an air/fuel ratio of approximately 17.5. It had a catalyst and EGR. A bag sample was taken of the total emissions over the cycle, and a separate bag was used to collect the emissions generated during the first 124 sec of the cycle.

From these data it can be seen that a wide range of correction factors can result which are influenced by engine design and operation. Much work remains to be done to minimize cold start emissions.

Based on the data presented in Fig. B-13, the following cold start correction factors were selected to represent the spark ignition engines.

Pollutants	Cold Start Correction Factors	
	State-of-the-Art Technology	Projected Technology
HC	1.3	1.2
CO	1.3	1.2
NO	0.95	0.95

B.2.9 Instrumentation

The HC concentrations of Engines A and B were measured by means of NDIR instrumentation. To account for the different sensitivities of NDIR and FID instruments, the HC concentrations were multiplied by a factor of 2 before conversion to specific mass emissions. The data obtained from Hurn and from Newhall are FID data. In all cases, NDIR was used to measure CO and NO. Generally, NO_2 was ignored. Since the NO_2 concentration in the exhaust of spark ignition engines is less than five percent of the total oxides of nitrogen, the error is negligible.

B.2.10 Other Pollutants

No quantitative data on other pollutants are available for spark ignition engines. Sulfur and lead oxides can be controlled by limiting the sulfur and lead content in the fuel. Smoke is generally not a problem in spark ignition engines except in poorly maintained engines.

B.3 DIESEL ENGINE EMISSIONS

B.3.1 General

Emission test data from a large number of automotive diesel engines were extracted from the literature or were obtained directly from the manufacturers. The engines considered in this study and some of the important specifications and operating parameters are listed in Tables B-2 through B-5. Also presented in those tables are the design load specific mass emissions of hydrocarbon, carbon monoxide, and nitric oxide. The engine speeds are the maximum speeds used in the various tests which, in some instances, are slightly different from the rated speeds quoted by the manufacturers. The listed output power is the maximum value observed at the highest engine speed. All engines were tested without fan, but with fuel pump and a simulated air cleaner pressure drop.

The four-cycle, naturally-aspirated, direct-injection diesels of domestic and foreign origin are listed in Table B-2. The four-cycle, turbocharged, direct-injection engines manufactured by Mack and by another manufacturer are shown in Table B-3. Turbocharged, prechamber engine data from two Caterpillar 1674 engines are presented in Table B-4. Engine points M and N are the same engine tested by two different laboratories. Data from three domestic two-cycle direct-injection engines are presented in Table B-5. Engine P had been run in a bus for approximately 190,000 mi before testing. That engine was retested after installation of the General Motors Environmental Improvement Package.

Table B-2. Four-Cycle, Naturally-Aspirated, Direct-Injection Diesel Engines and Design Load Specific Mass Emissions

Engine Identification	A	B	C	D	E	F	G	H
Manufacturer	Perkins	General Motors	Mack	Caterpillar		Cummins	M. A. N	Mercedes Benz
Displacement, $in.^3$	354	478	673	573	707	495	913	347
No. of Cylinders	6	6	6	6	8	4	8	4
Compression Ratio	---	17.5	16.6	17	16.5	---	---	17.0
Maximum Power, bhp	112	155	180	186	230	113	274	118
Maximum Speed, rpm	2800	3200	2100	3000	2600	1800	2200	2800
HC, grams/bhp-hr	0.6	2.05	1.26	0.81	----	0.67	----	----
CO, grams/bhp-hr	14.9	5.71	5.29	4.26	4.76	9.42	4.95	----
NO, grams/bhp-hr	5.45	3.24	10.9	5.41	6.11	3.03	9.31	5.89
Reference	B-48	B-48	B-48	B-48	B-49	B-48	B-49	B-49

Table B-3. Four-Cycle, Turbocharged, Direct-Injection Diesel Engines and Design Load Specific Mass Emissions

Engine Identification	I	J	K
Manufacturer	Mack	Mack	Another Manufacturer
Displacement, in.^{3}	673	673	950
No. of Cylinders	6	6	8
Compression Ratio	16.6	16.6	15.5
Maximum Power, bhp	232	250	400
Maximum Speed, rpm	2100	2100	2500
HC, grams/bhp-hr	2.94	1.55	----
CO, grams/bhp-hr	5.16	4.14	3.52
NO, grams/bhp-hr	7.97	6.99	7.46
Reference	B-48	B-48	B-49

Table B-4. Four-Cycle Turbocharged, Prechamber Diesel Engines and Design Load Specific Mass Emissions

Engine Identification	L	M	N
Manufacturer	Caterpillar	Caterpillar	Caterpillar
Displacement, in.^{3}	638	638	638
No. of Cylinders	6	6	6
Compression Ratio	17	17	17
Maximum Power, bhp	285	285	320
Maximum Speed, rpm	2200	2200	2200
HC, grams/bhp-hr	0.19	0.07	0.10
CO, grams/bhp-hr	0.96	0.86	0.96
NO, grams/bhp-hr	3.60	3.10	3.30
Reference	B-48	B-50	B-51

Table B-5. Two-Cycle, Direct-Injection Diesel Engines and Design Point Specific Mass Emissions

Engine Identification	O	P(1)	Q(2)	R(3)
Manufacturer	Detroit Diesel	Detroit Diesel	Detroit Diesel	
Displacement, $in.^3$	284	426	426	45
No. of Cylinders	4	6	6	1
Compression Ratio	17	---	---	
Maximum Power, bhp	127	180	180	45
Maximum Speed, rpm	2100	2100	2100	
HC, grams/bhp-hr	1.41	5.18	0.44	--
CO, grams/bhp-hr	4.09	13.10	5.42	--
NO, grams/bhp-hr	6.85	8.69	7.38	1.5
Reference	B-48	B-53	B-53	B-52

(1) Engine tested as received after 190,000 odometer miles

(2) Same engine after installation of General Motors Environmental Improvement Package

(3) Turbocharged

B.3.2 Combustion and Emission Characteristics

To provide a better understanding of the exhaust emission characteristics of diesel engines, a brief discussion is presented of the combustion processes and exhaust emission trends of various diesel engine types. In direct-injection, naturally-aspirated, and turbocharged diesels, the fuel is injected during the compression stroke and combustion is generally initiated before the piston reaches top dead center, resulting in high peak pressures, temperatures, and NO concentrations in the exhaust. Some reduction in peak temperature and NO emission can be achieved by retarding fuel injection, generally without much deterioration in specific fuel consumption.

In prechamber diesels, all the fuel is injected into the small prechamber and is ignited there. The hot, fuel-rich combustion products are then expanded into the main chamber where combustion is then completed. Generally, injection timing is set such that combustion in the main chamber is initiated just before top dead center. As a result, part of the combustion takes place while the piston moves downward and the peak temperatures and the formation of NO are reduced without adversely affecting the other pollutants and fuel consumption.

The general trend of diesel engine exhaust emissions is illustrated in Fig. B-14, showing HC, CO, and NO concentrations as a function of air/fuel ratio. These data are from a four-stroke, naturally-aspirated, direct-injection diesel engine tested by Yumlu and Carey (Ref. B-54) over a speed range between 50 and 110 percent of rated speed. According to Yumlu and Carey (Ref. B-54), Marshall (Ref. B-48), and Perez and Landen (Ref. B-55), similar trends are obtained for turbocharged and prechamber diesels. However, the magnitude of the emissions is generally different for various engine types. The emission concentrations of diesels are not directly representative of the mass of pollutants emitted, because of the wide variations in air/fuel ratio.

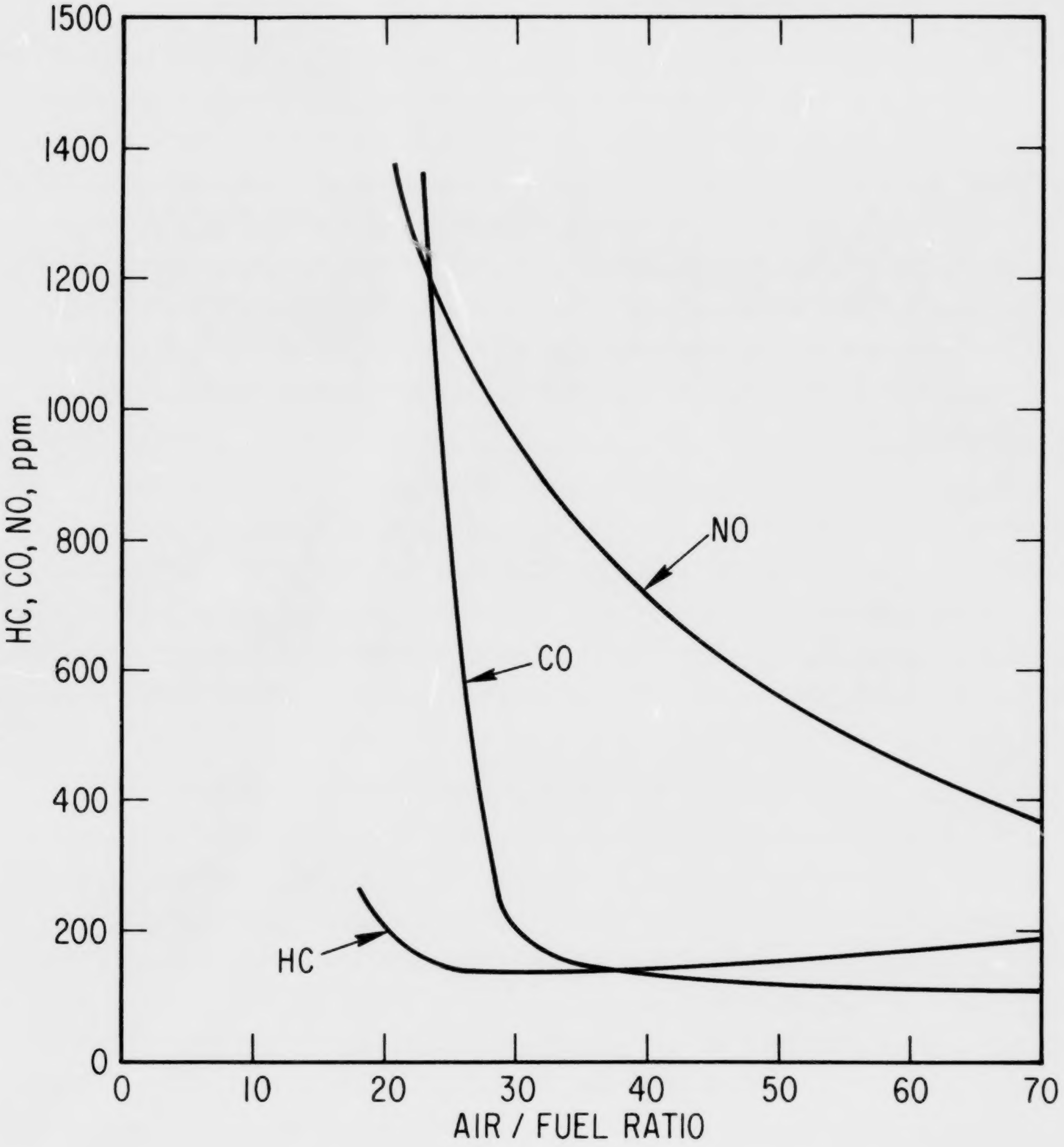

Figure B-14. Typical Diesel Engine Exhaust Emissions Versus Air/Fuel Ratio

The HC concentrations remain essentially constant over a wide range of air/fuel ratios. Although not shown in Fig. B-14, the HC concentration shows some variation with engine speed. This is supported by data from Marshall (Ref. B-48). As expected from theoretical considerations, the HC concentrations tend to increase at very high air/fuel ratios as a result of lower combustion temperatures. As air/fuel ratios approach stoichiometric, the increase is due to the reduction in oxygen concentration.

The CO concentration in the exhaust is primarily a function of the air/fuel ratio of the mixture. It decreases rapidly with increasing air/fuel ratios as a result of the increasing oxygen concentration, and reaches a minimum at air/fuel ratios of approximately 30 to 40. At air/fuel ratios below approximately 60, the CO concentration generally rises again as a result of quench effects. These trends are essentially independent of engine speed and are characteristic of all diesel engine types.

The NO concentration in diesels increases steadily with decreasing air/fuel ratio. This trend agrees with theory and reflects the rise in combustion temperature. For simplicity, only a single NO curve is drawn in Fig. B-14, although the data indicate some speed effect and show decreasing NO concentrations as speed is reduced at constant air/fuel ratio. This may be the combined result of lower residence time of the gases in the chamber and changes in the injection spray characteristics. The data presented by Marshall for engines of different makes show less variation and no clear trend of NO concentration with speed.

Saadawi (Ref. B-56) has observed similar CO and NO trends, but the HC concentration of his engine decreases as engine speed is increased. According to Saadawi this may be the result of higher turbulence and better fuel mixing obtained at the higher speeds. Marshall and Hurn (Ref. B-57) have investigated the effects of engine component design, operational mode, and fuel characteristics on engine emissions. Based upon this work it is concluded that all these parameters have some effect on the emissions.

From the simplified emission concentration curves presented in Fig. B-14, the conclusion is drawn that the emission of CO from diesel engines does not present a problem except perhaps at very high load conditions where the air/fuel ratio becomes relatively low. The principal problem of diesel engines is the emission of NO which, at high load conditions, can reach the levels of spark ignition engines.

It should be pointed out that diesel engine exhaust contains other potentially noxious species including aldehydes and smoke. These problems are generally more serious in diesels than in spark ignition engines.

B. 3. 3 Design Load Emissions

B. 3. 3. 1 State-of-the-Art Technology

The hydrocarbon, carbon monoxide, and nitric oxide design load emissions of diesel engines are listed in Tables B-2 through B-5. These values were computed from the species concentration, flow rate, and engine brake horsepower data presented in the references, using the conversion correlations discussed in Section B. 1. 3. In all cases, an exhaust gas molecular weight of 29. 0 was used, which is a good approximation for the range of air/fuel ratios used in diesels.

As previously mentioned, the highest speed and power settings used in the various test programs are considered the engine design conditions for the purpose of this study. Comparison with the engine rating by the manufacturer has indicated that the differences are small enough to be neglected, especially in view of the normally observed hardware-to-hardware variations in engine performance.

The design load specific mass emissions for the various engines considered are presented in Figs. B-15 through B-17. These data points provided the basis for establishing the present state-of-the-art design load emission characteristics of four-cycle, naturally-aspirated and turbocharged, direct-injection and turbocharged, prechamber diesel engines. Insufficient data

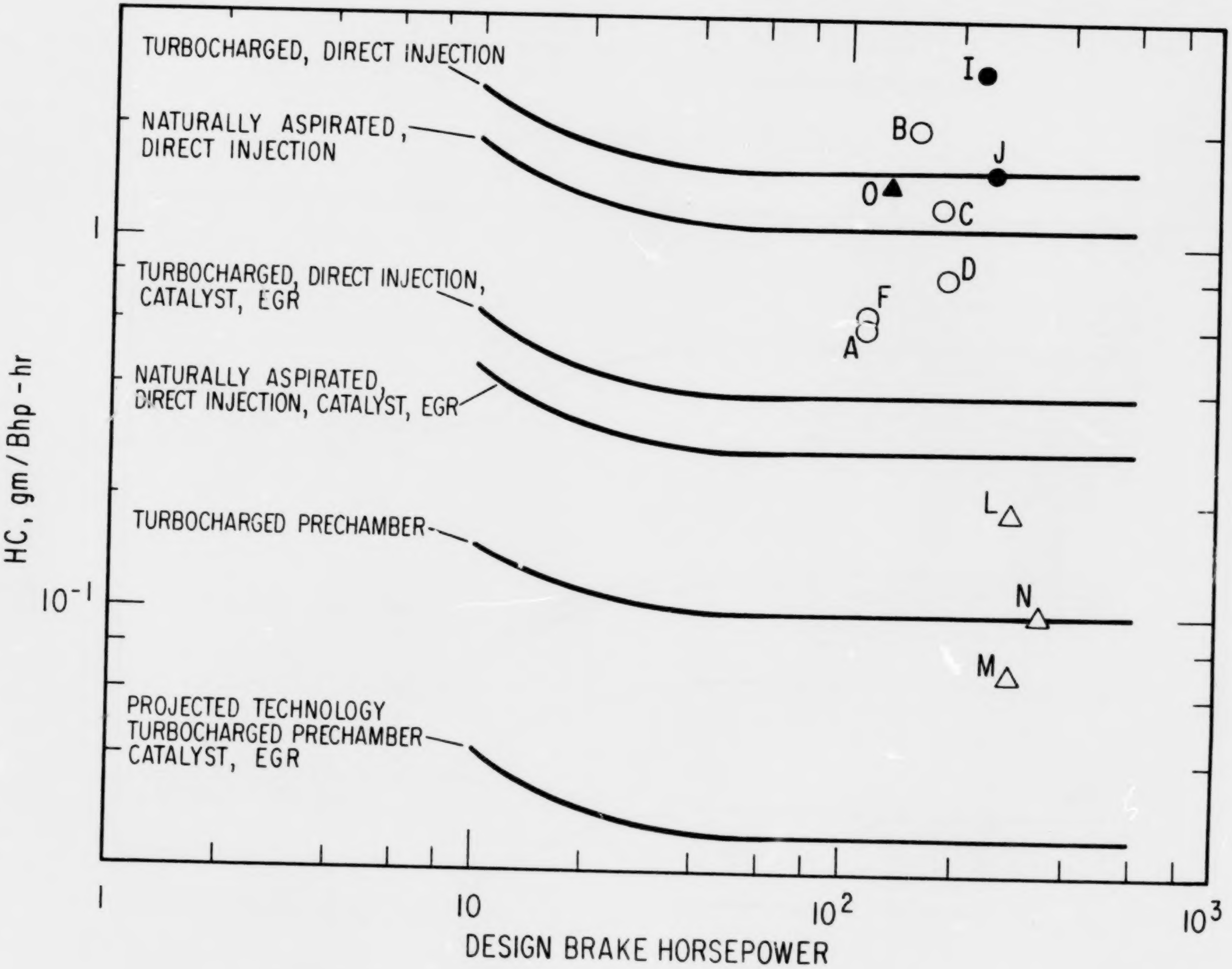

Figure B-15. Diesel Engines - Hydrocarbon Emission, Steady State Design Load

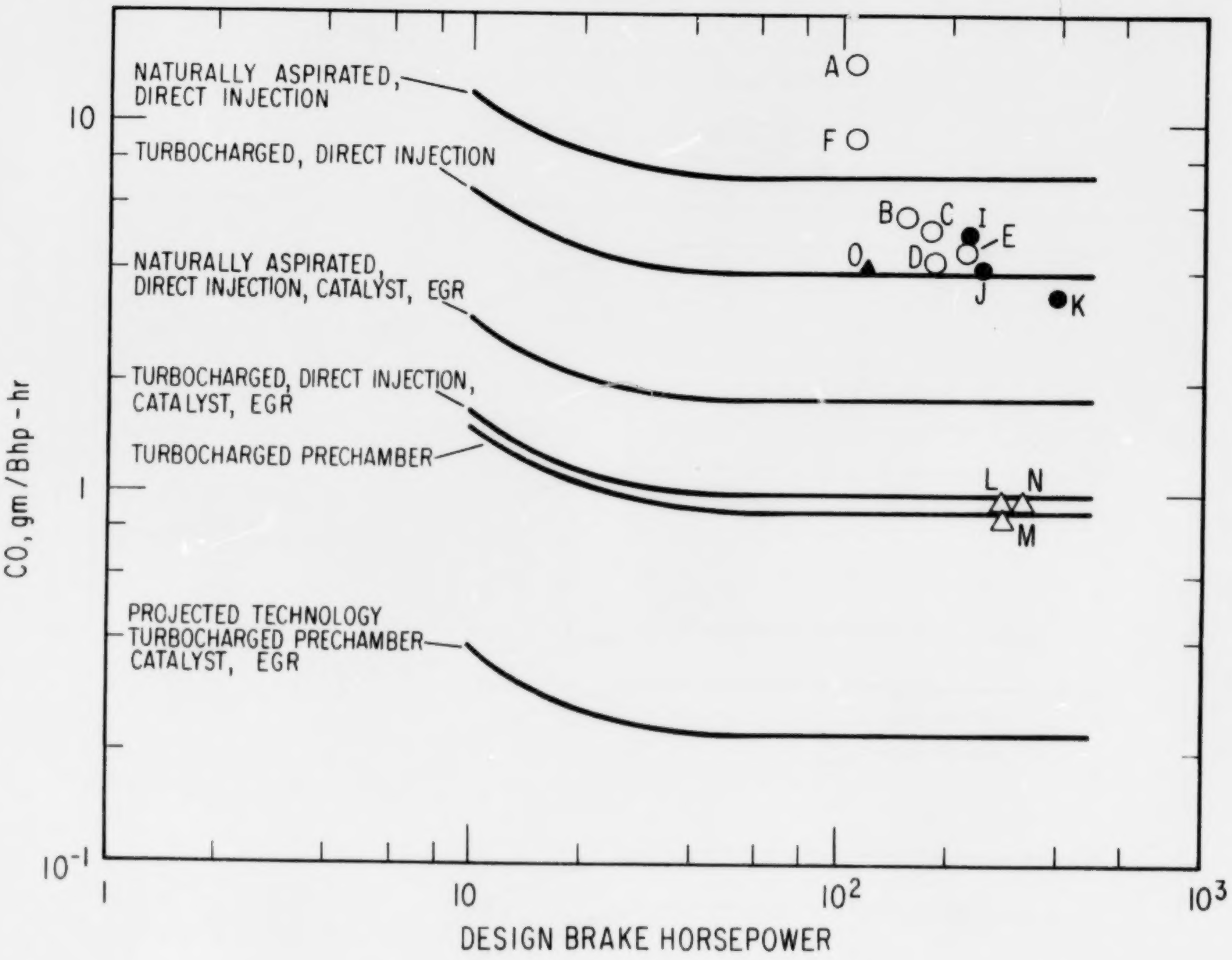

Figure B-16. Diesel Engines - Carbon Monoxide Emission, Steady State Design Load

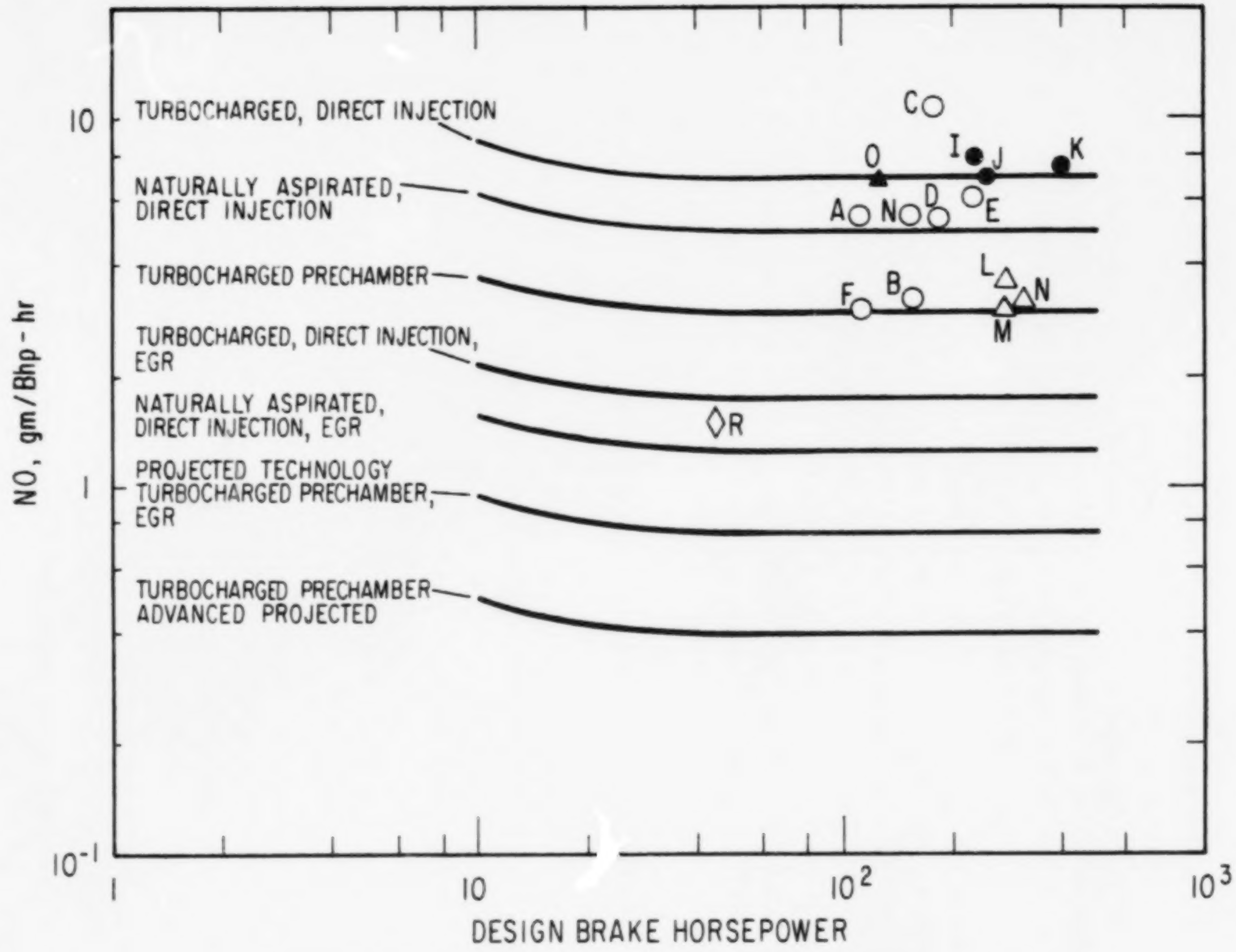

Figure B-17. Diesel Engines - Nitric Oxide Emission, Steady State Design Load were available to classify the two-cycle diesels. As shown, constant specific mass emissions were assumed for each engine type for design power levels above 50 hp. Below that point, the emissions are assumed to increase primarily to reflect the lower engine efficiency and the higher wall quenching effects, resulting from less favorable cylinder surface area-to-volume ratios. The NO increases at a lower rate than the HC and CO.

The HC specific mass emissions of the four-cycle, turbocharged, direct-injection engine are the highest of the three engine types, although theoretically the HC emissions of turbocharged diesels should be lower than those of naturally-aspirated engines. The curve representing this engine type was drawn through the lower of the two points. This points out the need of additional emission data for turbocharged, direct-injection diesels. Very low HC emissions were obtained from the two turbocharged, prechamber diesels manufactured by the Caterpillar Tractor Company. One of the engines was tested both at the Southwest Research Institute (Ref. B-51) and by another Laboratory (Ref. B-50). The other engine was analyzed at the Bureau of Mines (Ref. B-48). The observed differences in the emissions provide some indication of hardware-to-hardware and test-to-test effects. A study of test-to-test variabilities was reported in Ref. B-58. A small, single-cylinder diesel engine was tested successively at 13 different laboratories using different test procedures. The standard deviation in the HC concentration was about 50 percent. Part of this variability is attributed to real differences in the emissions and part to the different techniques and instrumentation used by the various investigators.

The design load emission characteristics of the turbocharged, direct-injection and prechamber diesels were derived from a very limited data sample, and, as a result, the effects of manufacturing tolerances may not be adequately accounted for. This should be considered when using the curves.

As indicated in Fig. B-17, the variations in CO specific mass emissions from the various engines are considerably smaller. This trend was expected since CO concentration is determined primarily by air/fuel ratio. The design load air/fuel ratios of the diesels are quite comparable. In accordance with expectations, the highest CO emissions are obtained with the naturally-aspirated, direct-injection diesels and the lowest emissions with the Caterpillar turbocharged prechamber engines. Data from the two prechamber engines are in excellent agreement.

Nitric oxide represents the major emission problem in diesel engines. As expected, the turbocharged, direct-injection diesel has the highest NO emissions, and these values are comparable to the NO emitted from present spark ignition engines. The naturally-aspirated, direct-injection diesels show somewhat lower NO emissions. The NO emissions of turbocharged prechamber engines are even lower. It is apparent that the NO emission levels of present diesels have to be reduced significantly before future emission goals can be met.

Because of its low specific mass emissions, the turbocharged, prechamber diesel curves were used to represent state-of-the-art technology diesel engines for the vehicle emission comparisons. It should be noted, however, that the specific fuel consumption of prechamber diesel engines is slightly higher than that of direct-injection engines (See Section 8).

In addition to relating specific mass emissions to engine design load, attempts were made to correlate the data with the power output per cylinder. This type of presentation would certainly have merit. However, it was not possible to achieve a better correlation owing to the large variability in the data and the small data sample.

B.3.3.2 Projected Technology

The projected design load emissions are also presented in Figs. B-15 through B-17. For each engine type, the projected emissions are based on an arbitrary reduction by a factor of 4. These improvements are considered reasonable goals that might be achieved with modified injection systems, combustion chambers, injection timing, and the addition of catalytic converters and EGR. The effects of catalytic converters on diesel engine emissions have been investigated by Springer (Ref. B-59) and more recently by Aerospace (See Appendix C). The catalytic devices tested by Springer had been used on a bus for a time period of approximately one month. The effectiveness of these catalysts was generally rather low. The precious metal catalysts showed somewhat higher effectiveness than the base metal devices. A precious metal catalytic converter was used in the Aerospace program on a Daihatsu diesel. High HC and CO conversion efficiencies were obtained but NO remained essentially unchanged. At this time there is no information available to determine the effects of operating time on the effectiveness of that catalyst. In addition to reducing HC and CO, the odor of the exhaust was practically eliminated. A test program is needed to evaluate catalyst performance as affected by operating time.

The projected NO emissions are also plotted in Fig. B-17. The curves shown for the three engine types were reduced by a factor of 4 to reflect the effects of EGR, chamber and injection system modifications, and the possible addition of a catalytic converter for NO. Although presently the prospects for NO catalysts are not optimistic, such a device might become feasible in the future. Since no data are available on diesel engine EGR and its effect on NO emission, the selected factor of 4 is approximate, at best. Research work should be conducted, particularly in the area of EGR to provide the parametric data required for a complete assessment of this concept, including the effects on engine performance and driveability. One equipment manufacturer feels that the projected NO emissions might be further reduced by a factor of approximately 2. Although not supported by data, a factor of 8 was used to construct the lowest NO curve in Fig. B-17 from the state-of-the-art technology curve of the prechamber diesel engine. This curve was not used in the vehicle emission calculations of this study.

Since HC and CO emissions of diesel engines are generally already low, future efforts should be aimed primarily at NO. This becomes even more evident when catalytic converters are utilized for HC and CO control. Again, the specific mass emissions are assumed to be constant for engine design power outputs above 50 hp. At lower design power levels the specific mass emissions increase to reflect the lower engine efficiency and the higher specie concentrations.

B.3.4 Part-Load Emissions Characteristics

B.3.4.1 Actual Engine Part-Load Emissions

The part-load emissions of some of the engines are presented in Figs. B-18 through B-57 in terms of specific mass emissions versus percent design load at rated speed. Figures B-18 through B-34 are for four-cycle, naturally-aspirated, direct-injection engines. For each speed, the HC emissions increase with decreasing load. At constant load, HC decreases with decreasing speed, except for engine F which shows little change for the two speeds considered. The CO part-load emissions of the naturally-aspirated engines show similar trends. As load is reduced at each speed, the specific CO mass emissions decrease initially as a result of increasing air/fuel ratio, and then increase again as load is further reduced. This increase is the result of lower engine efficiency and some increase in the CO concentration. The part-load NO specific mass emissions for these engines show small and somewhat irregular variations with load. It appears that the opposing effects of increasing air/fuel ratio and decreasing engine efficiency obtained with decreasing load (at constant speed) tend to cancel each other.

The part-load specific mass emission characteristics of the four-cycle, turbocharged, direct-injection diesels considered in this study are plotted in Figs. B-35 through B-42. The trends are similar to those of the naturally-aspirated engines. However, the NO emissions of engines J and [illegible] increase with decreasing speed. Engine L shows the opposite trend.

The part-load emissions of the two Caterpillar turbocharged, prechamber diesels are presented in Figs. B-43 through B-51. As for the other two engine types, the HC emissions increase with decreasing load and increasing speed. The CO emissions increase steadily with decreasing load. It is not

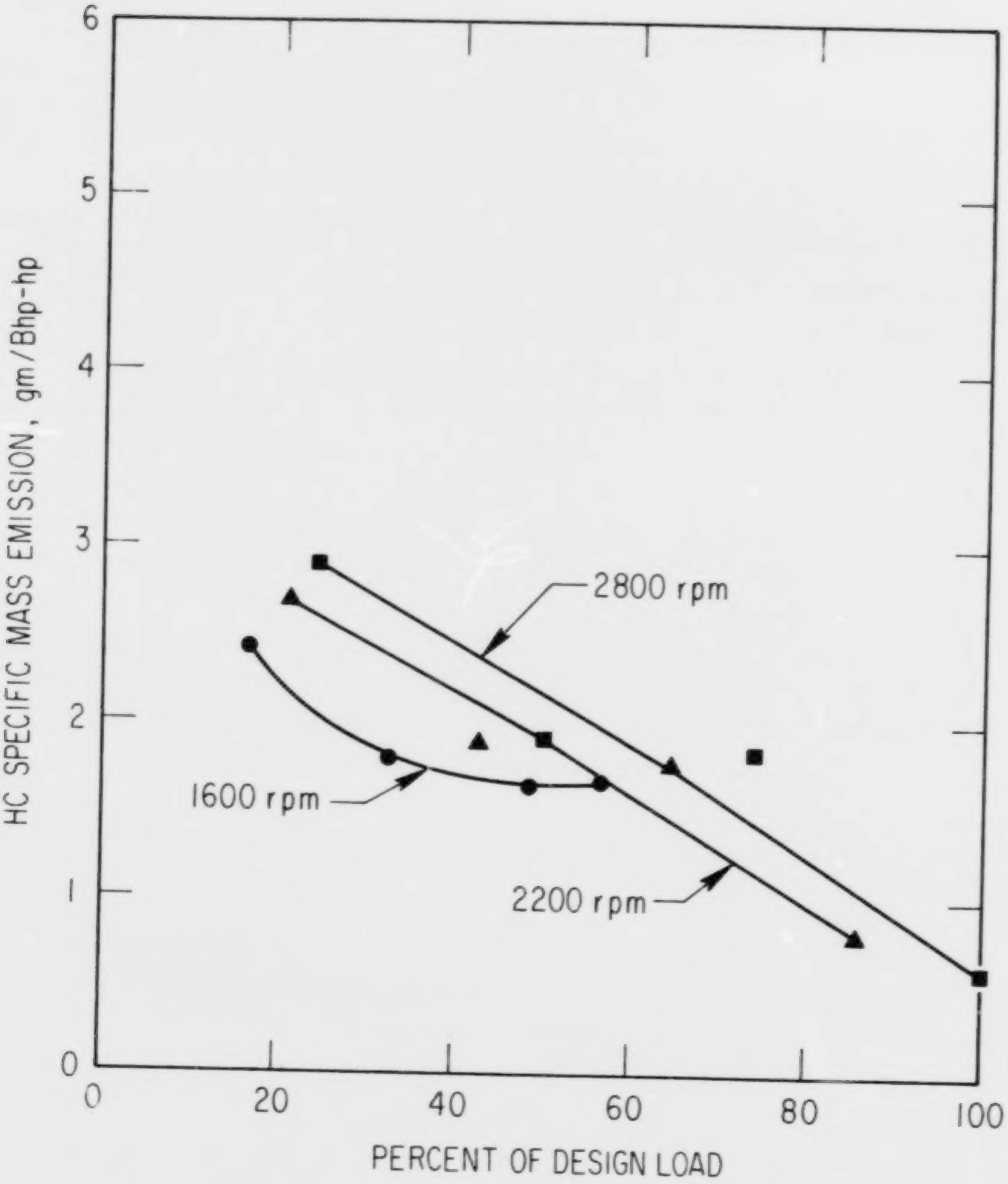

Figure B-18. Four-Cycle, Naturally-Aspirated Direct-Injection Diesel - Engine A - Part-Load Hydrocarbon Emissions

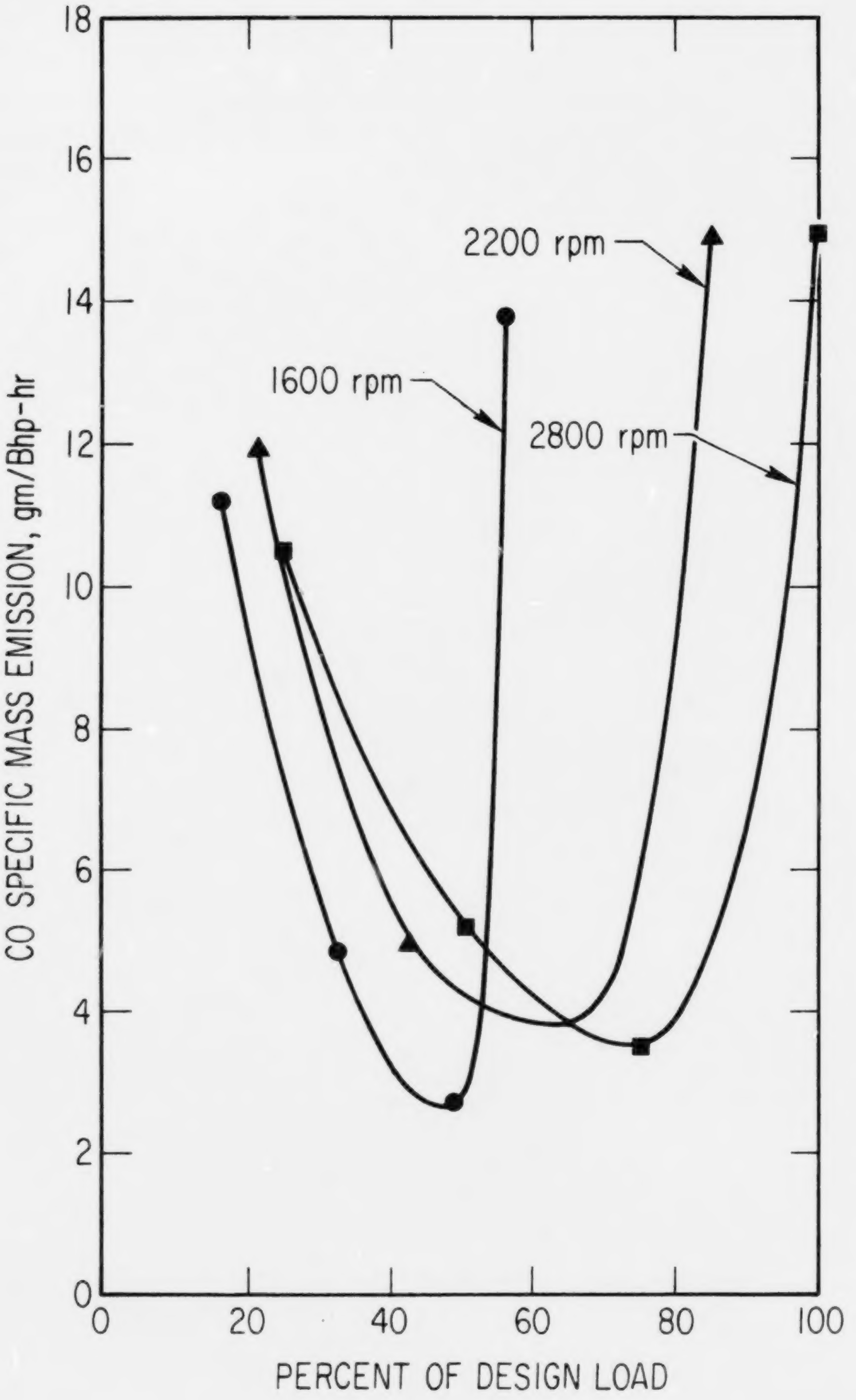

Figure B-19. Four-Cycle, Naturally-Aspirated Direct-Injection Diesel - Engine A - Part-Load Carbon Monoxide Emissions

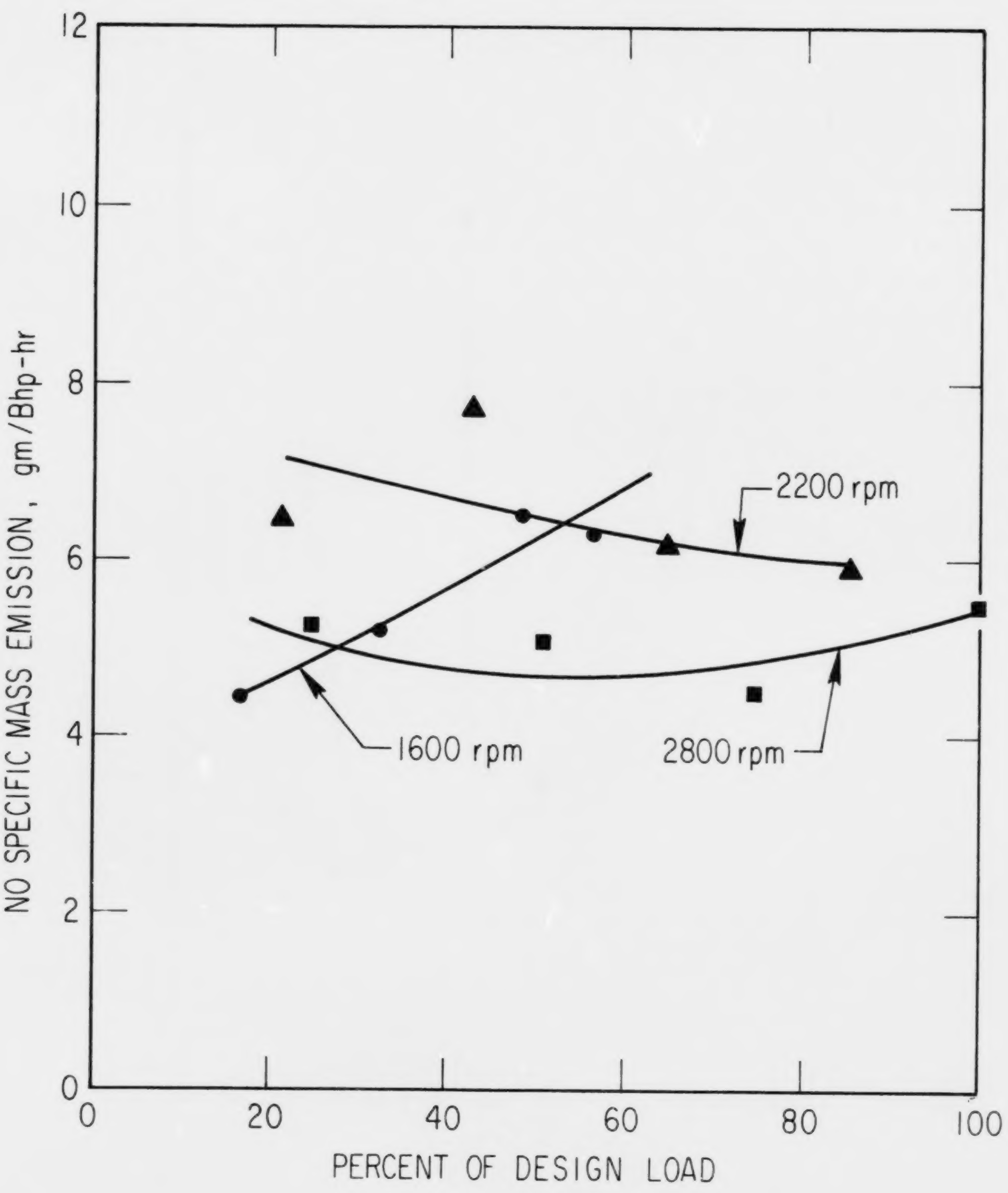

Figure B-20. Four-Cycle, Naturally-Aspirated Direct-Injection Diesels - Engine A - Part-Load Nitric Oxide Emissions

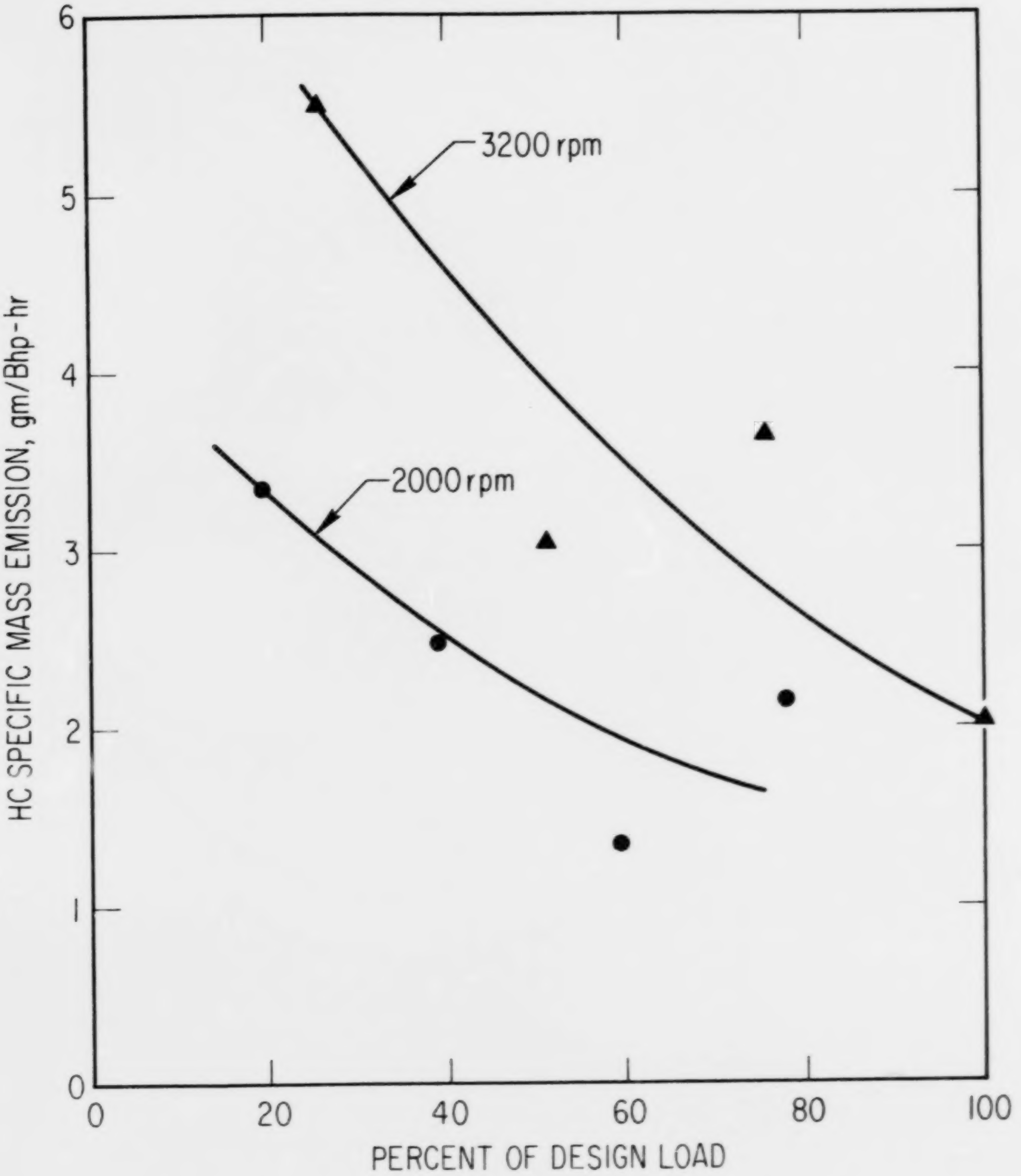

Figure B-21. Four-Cycle, Naturally-Aspirated Direct-Injection Diesel - Engine B - Part-Load Hydrocarbon Emissions

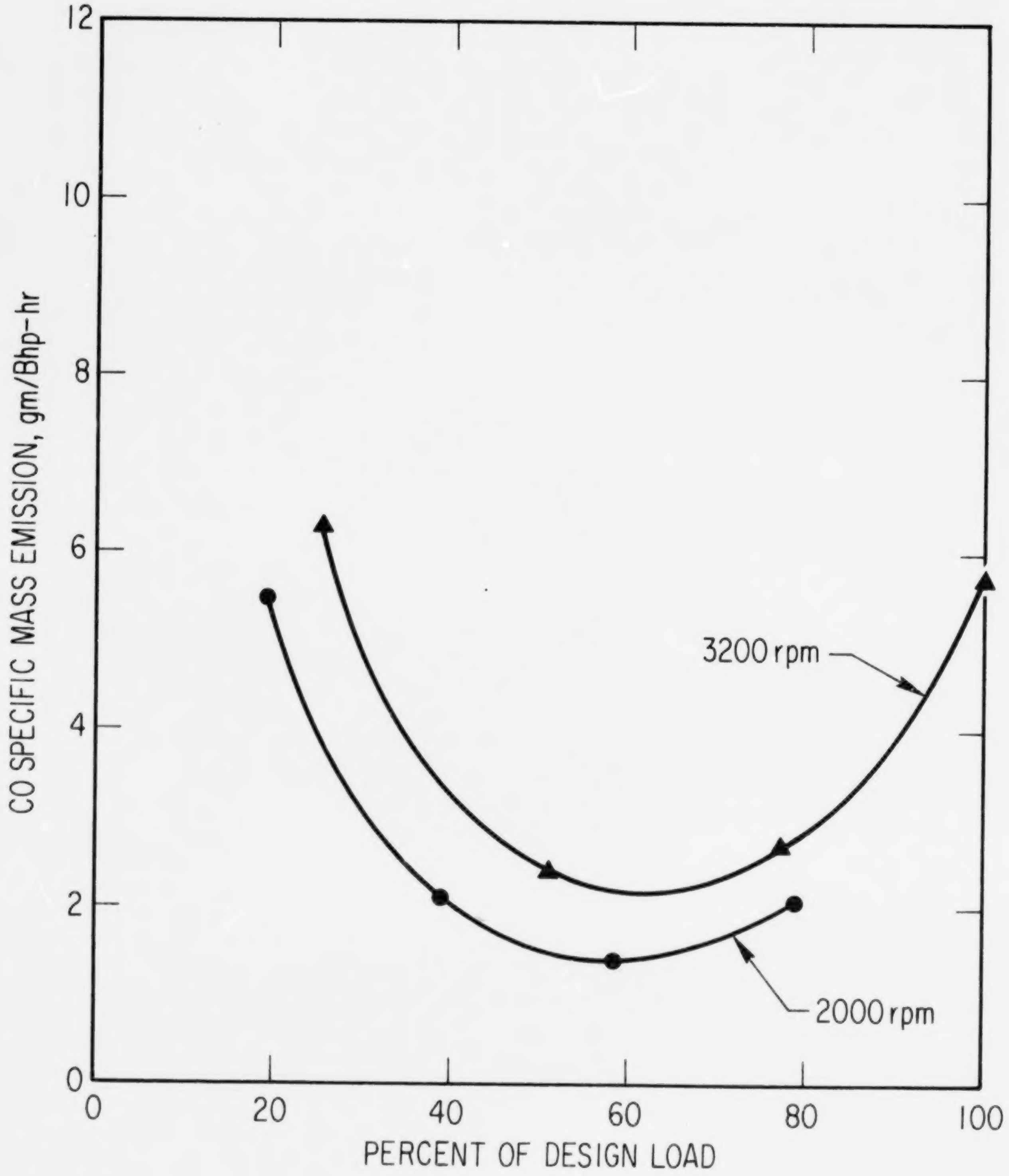

Figure B-22. Four-Cycle, Naturally-Aspirated Direct-Injection Diesel - Engine B - Part-Load Carbon Monoxide Emissions

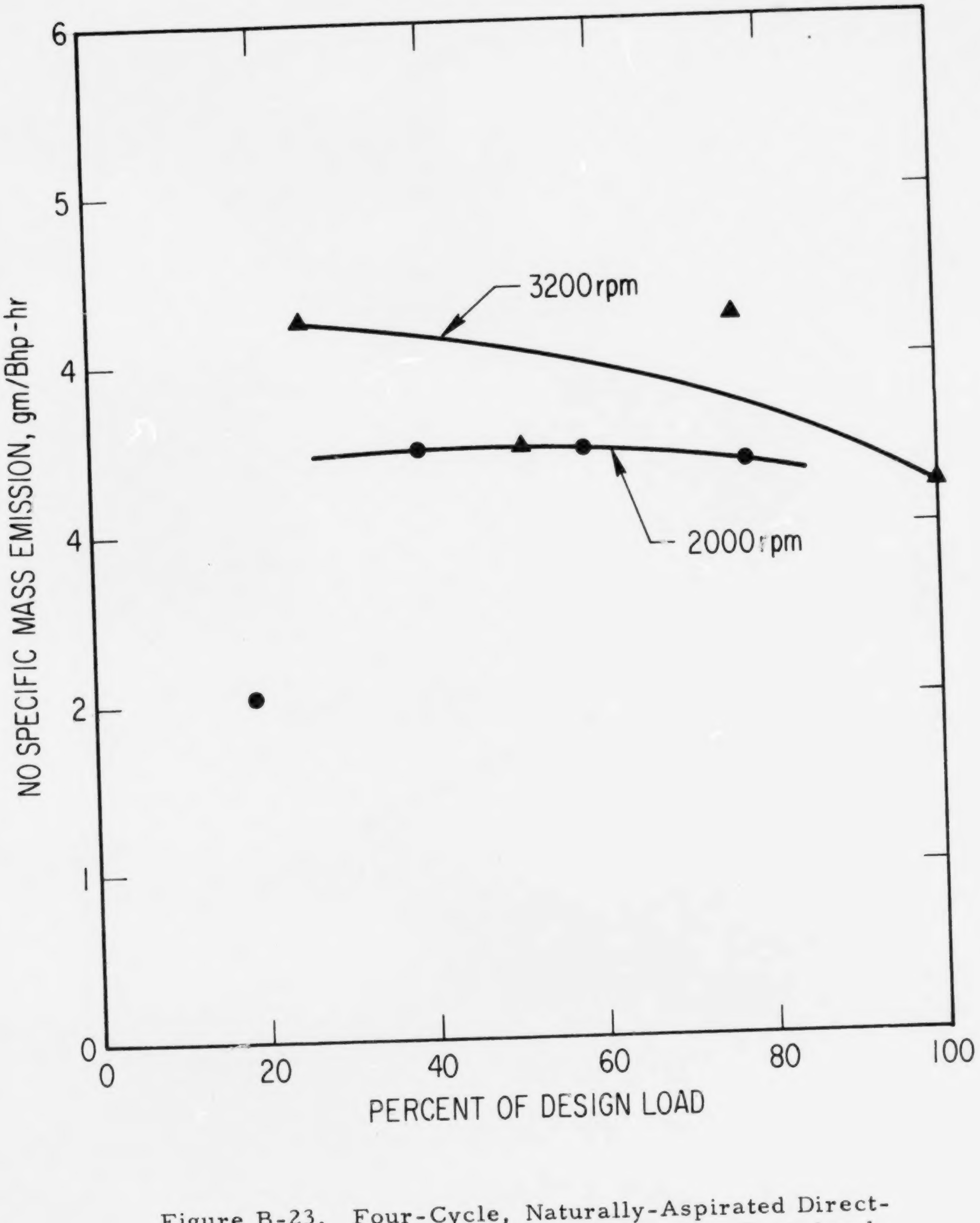

Figure B-23. Four-Cycle, Naturally-Aspirated Direct-Injection Diesel - Engine B - Part-Load Nitric Oxide Emissions

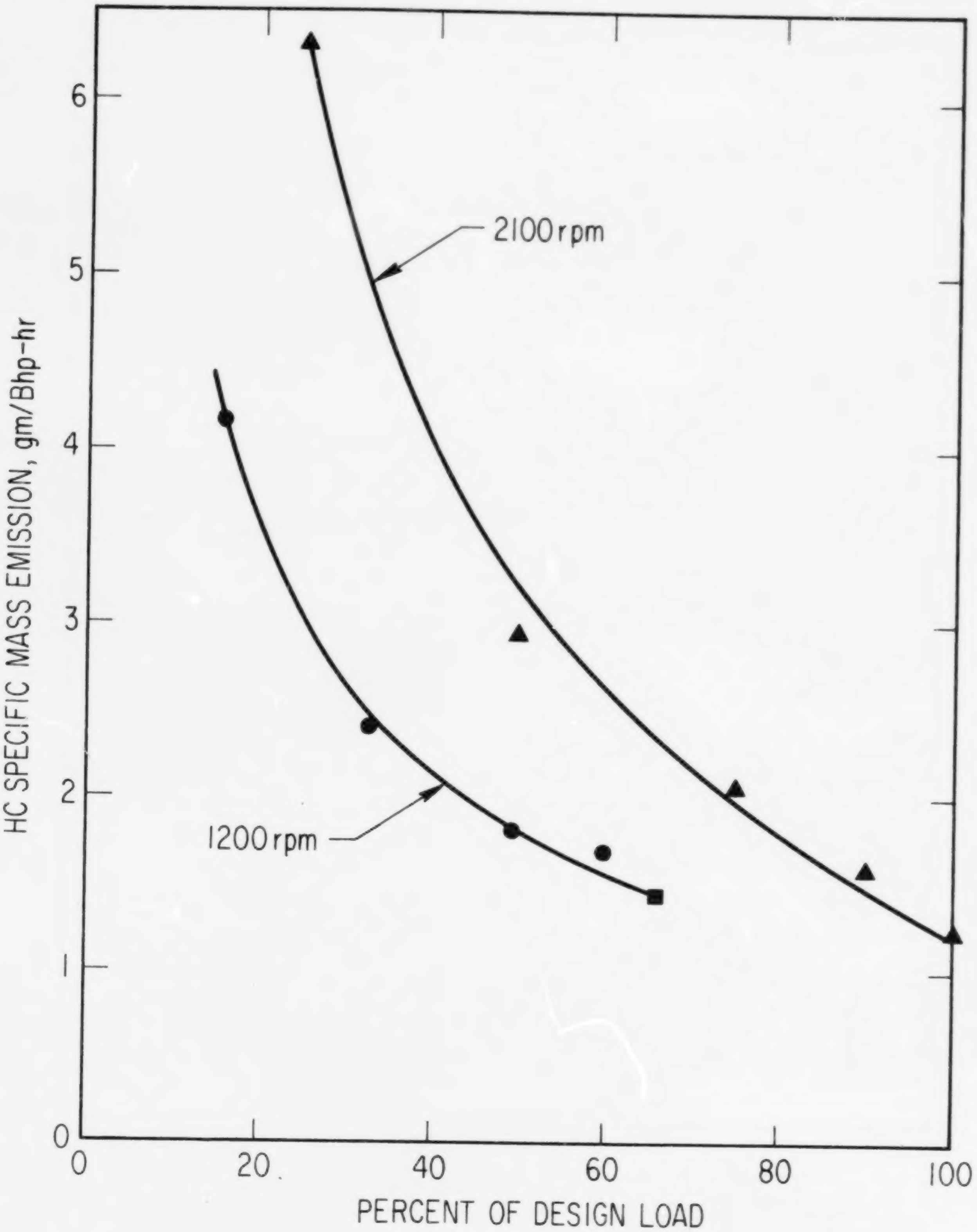

Figure B-24. Four-Cycle, Naturally-Aspirated Direct-Injection Diesel - Engine C - Part-Load Hydrocarbon Emissions

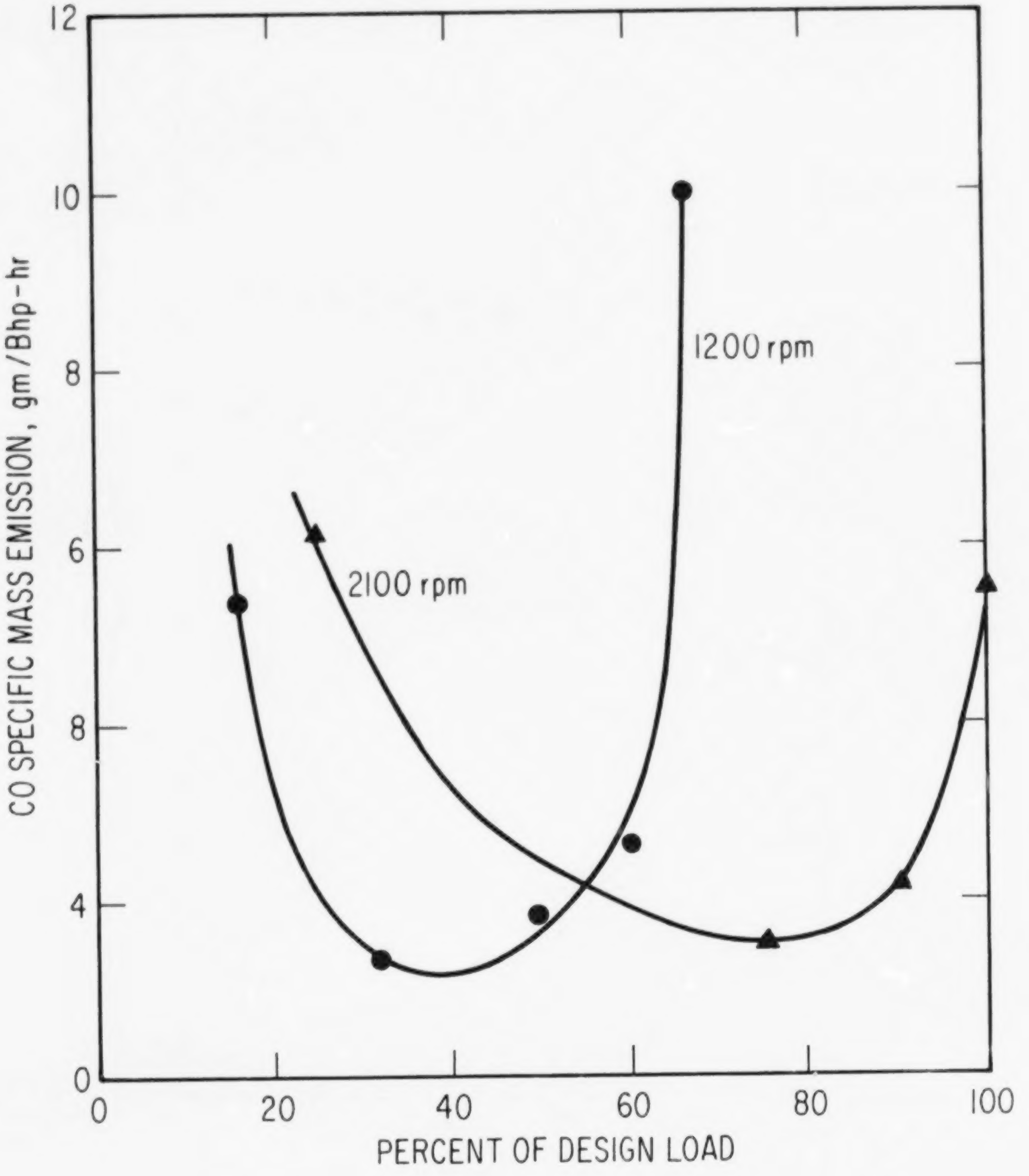

Figure B-25. Four-Cycle, Naturally-Aspirated Direct-Injection Diesel - Engine C - Part-Load Carbon Monoxide Emissions

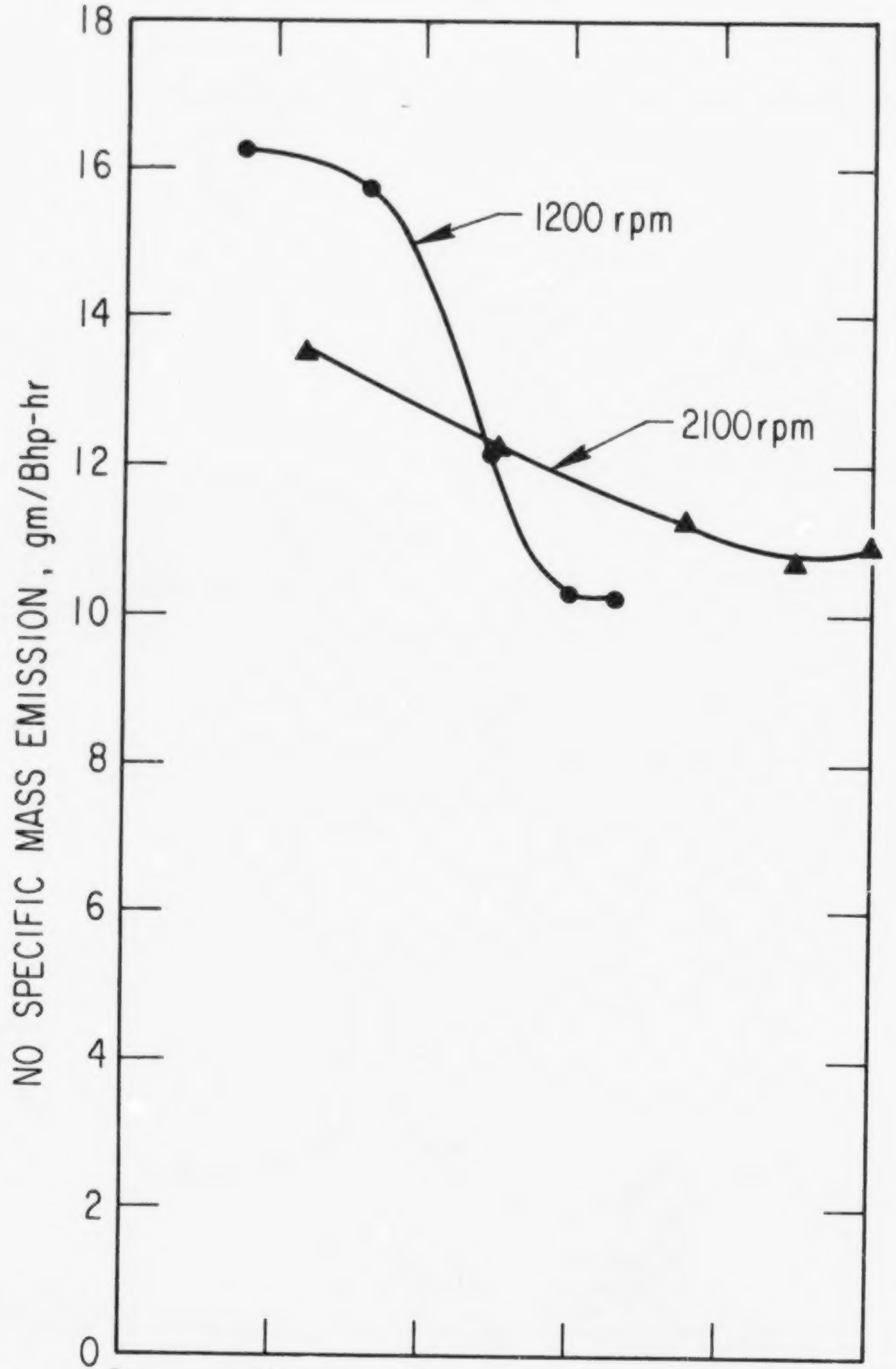

Figure B-26. Four-Cycle, Naturally-Aspirated Direct-Injection Diesel - Engine C - Part-Load Nitric Oxide Emissions

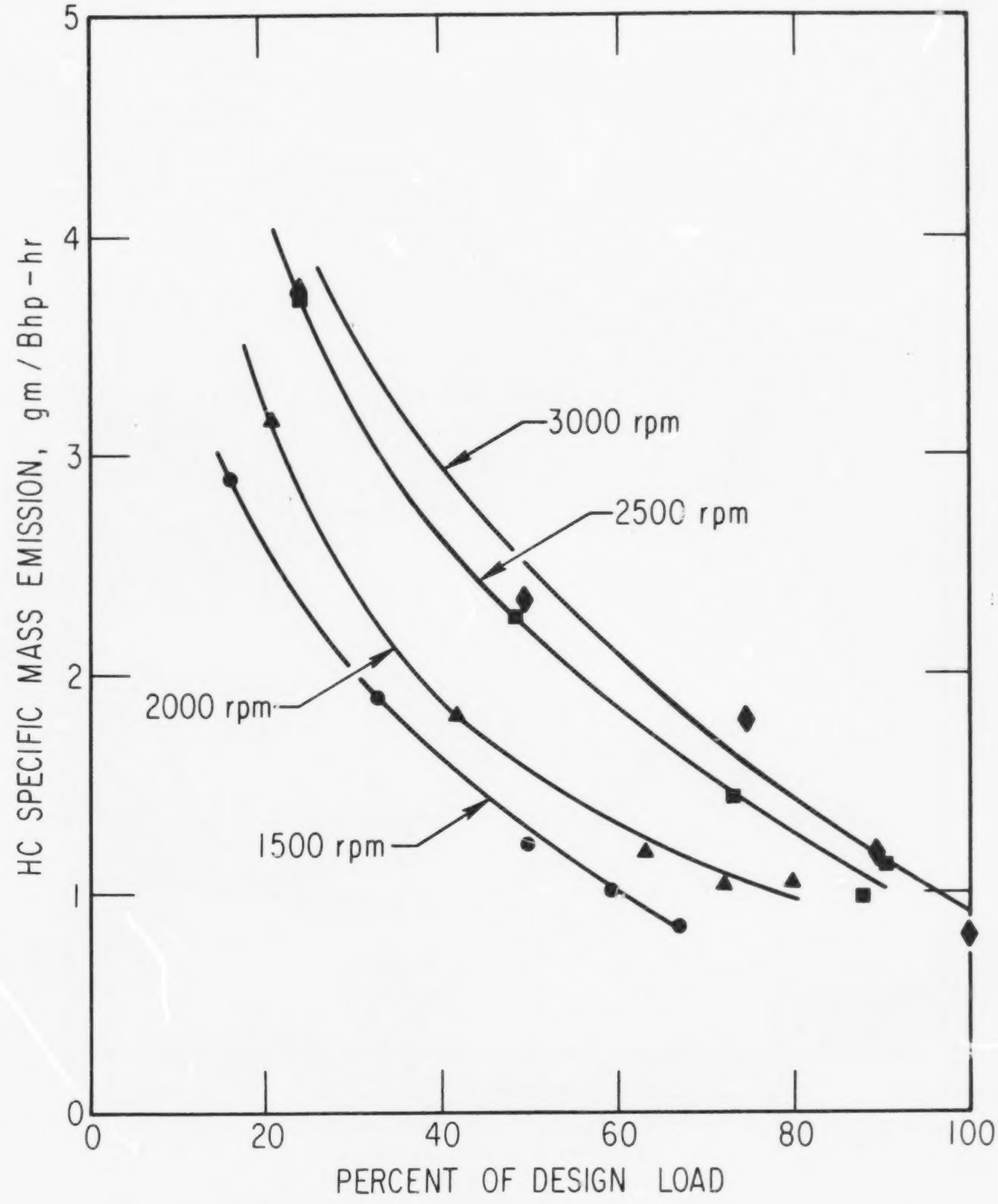

Figure B-27. Four-Cycle, Naturally-Aspirated Direct-Injection Diesel - Engine D - Part-Load Hydrocarbon Emissions

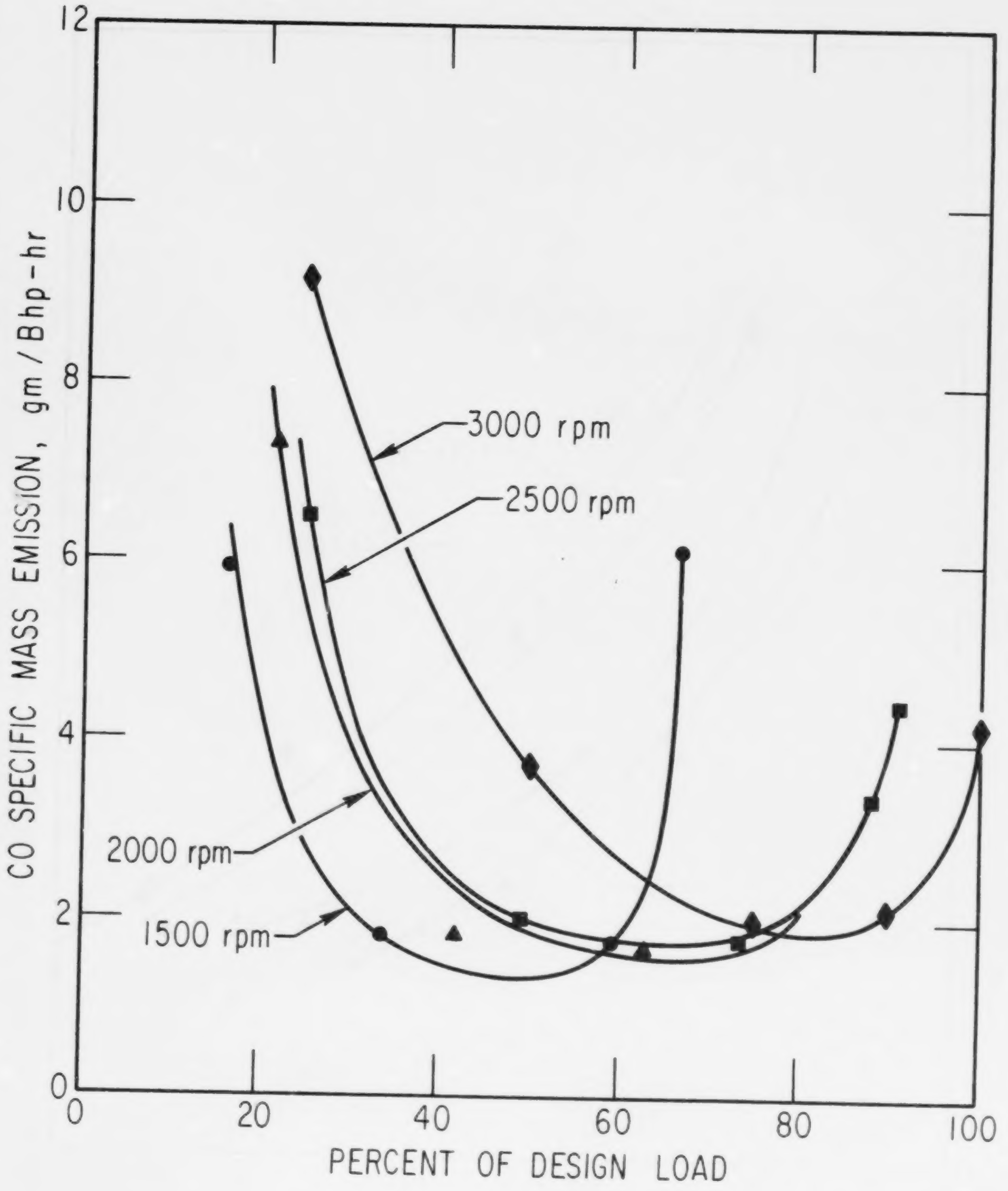

Figure B-28. Four-Cycle, Naturally-Aspirated Direct-Injection Diesel - Engine D - Part-Load Carbon Monoxide Emissions

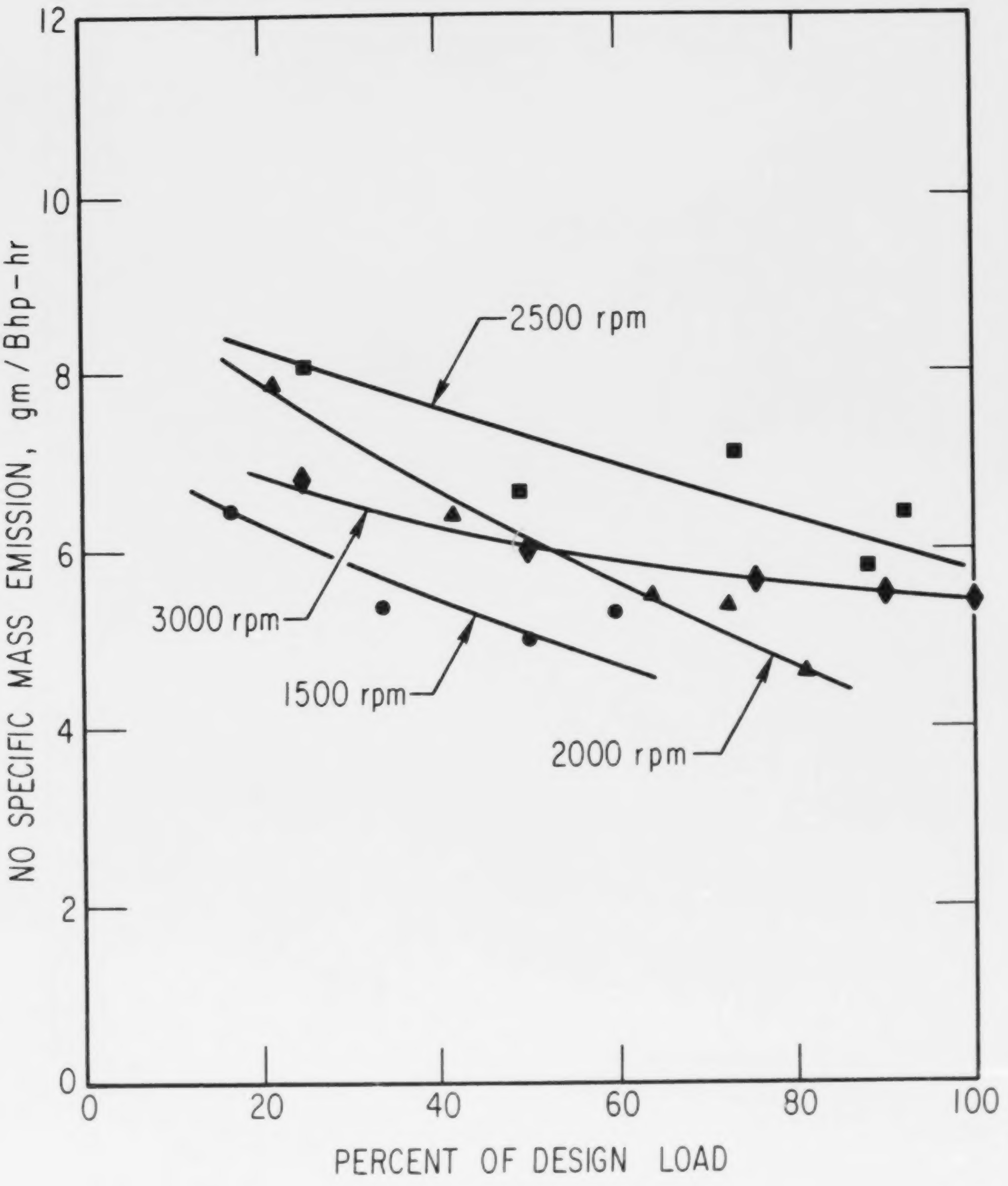

Figure B-29. Four-Cycle, Naturally-Aspirated Direct-Injection Diesel - Engine D - Part-Load Nitric Oxide Emissions

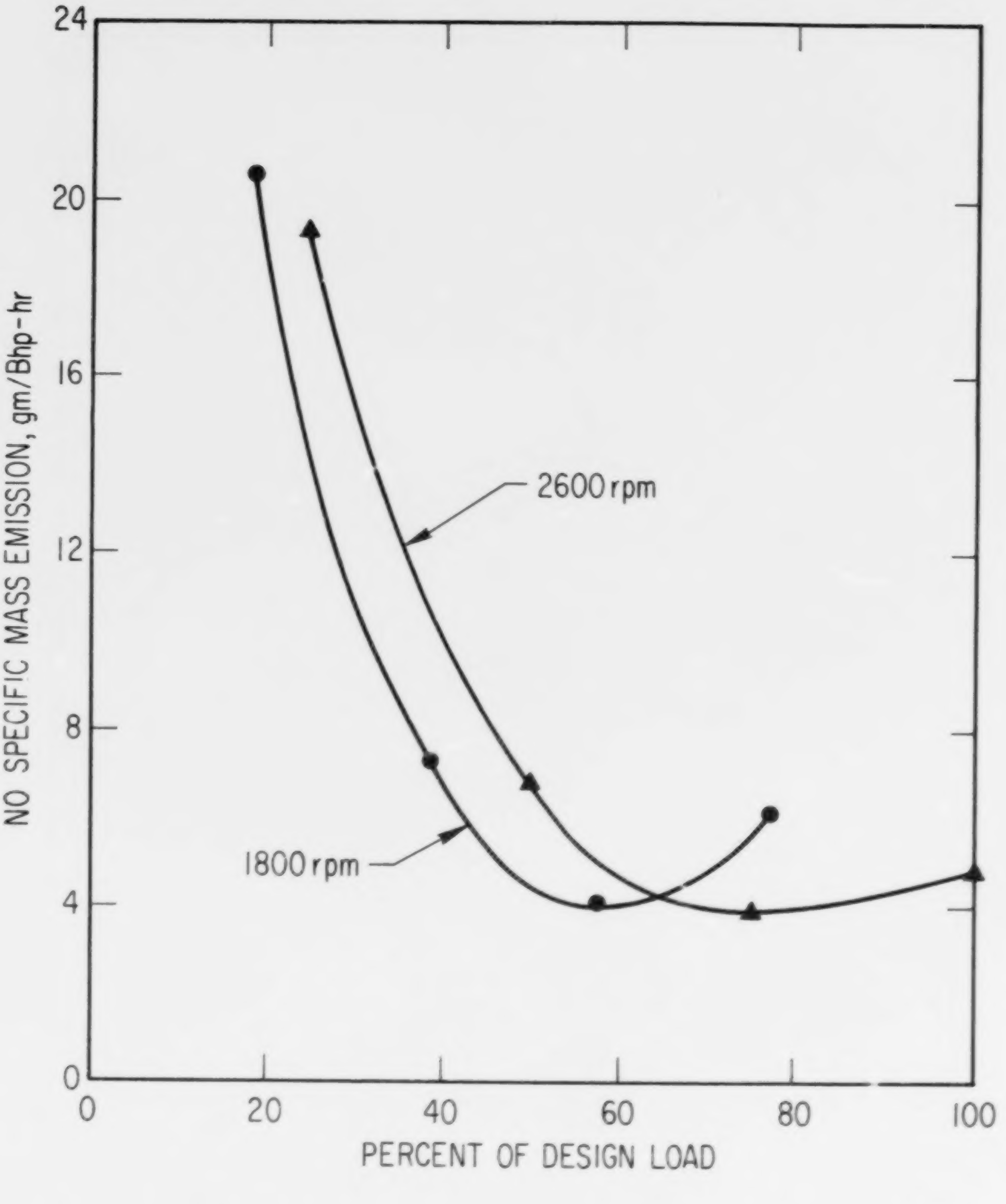

Figure B-30. Four-Cycle, Naturally-Aspirated Direct-Injection Diesel - Engine E - Part-Load Carbon Monoxide Emissions

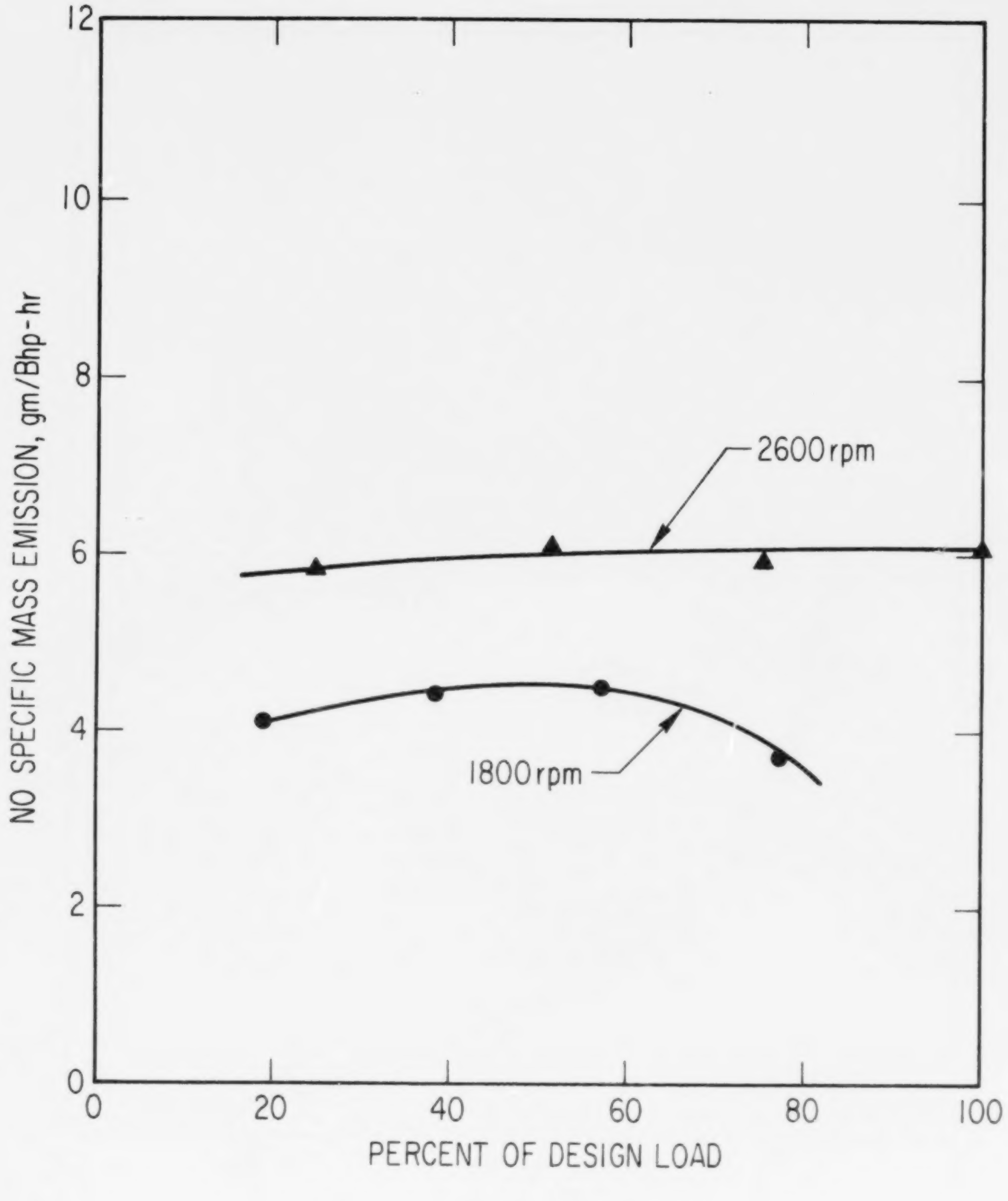

Figure B-31. Four-Cycle, Naturally-Aspirated Direct-Injection Diesel - Engine E - Part-Load Nitric Oxide Emissions

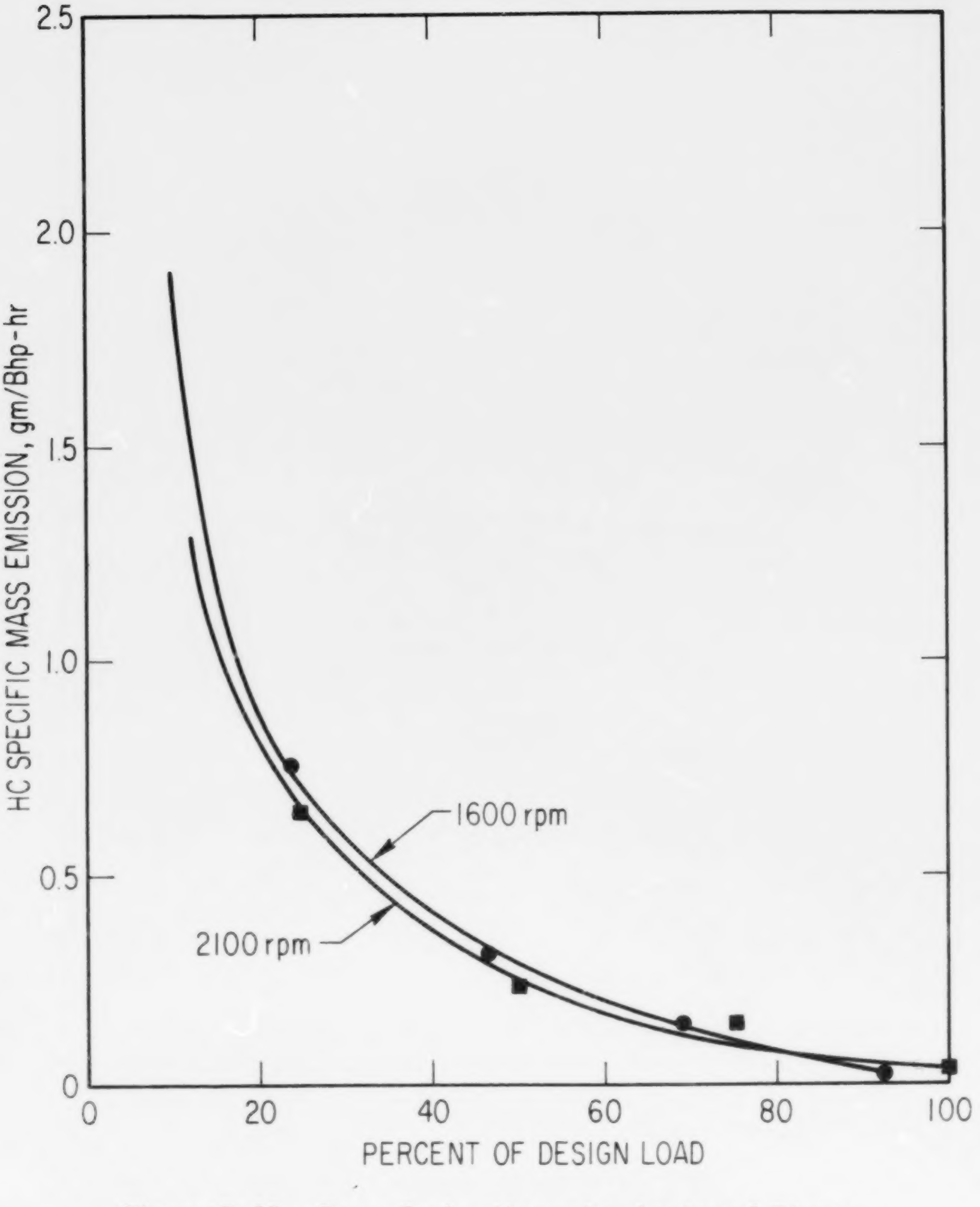

Figure B-32. Four-Cycle, Naturally-Aspirated Direct-Injection Diesel - Engine F - Part-Load Hydrocarbon Emissions

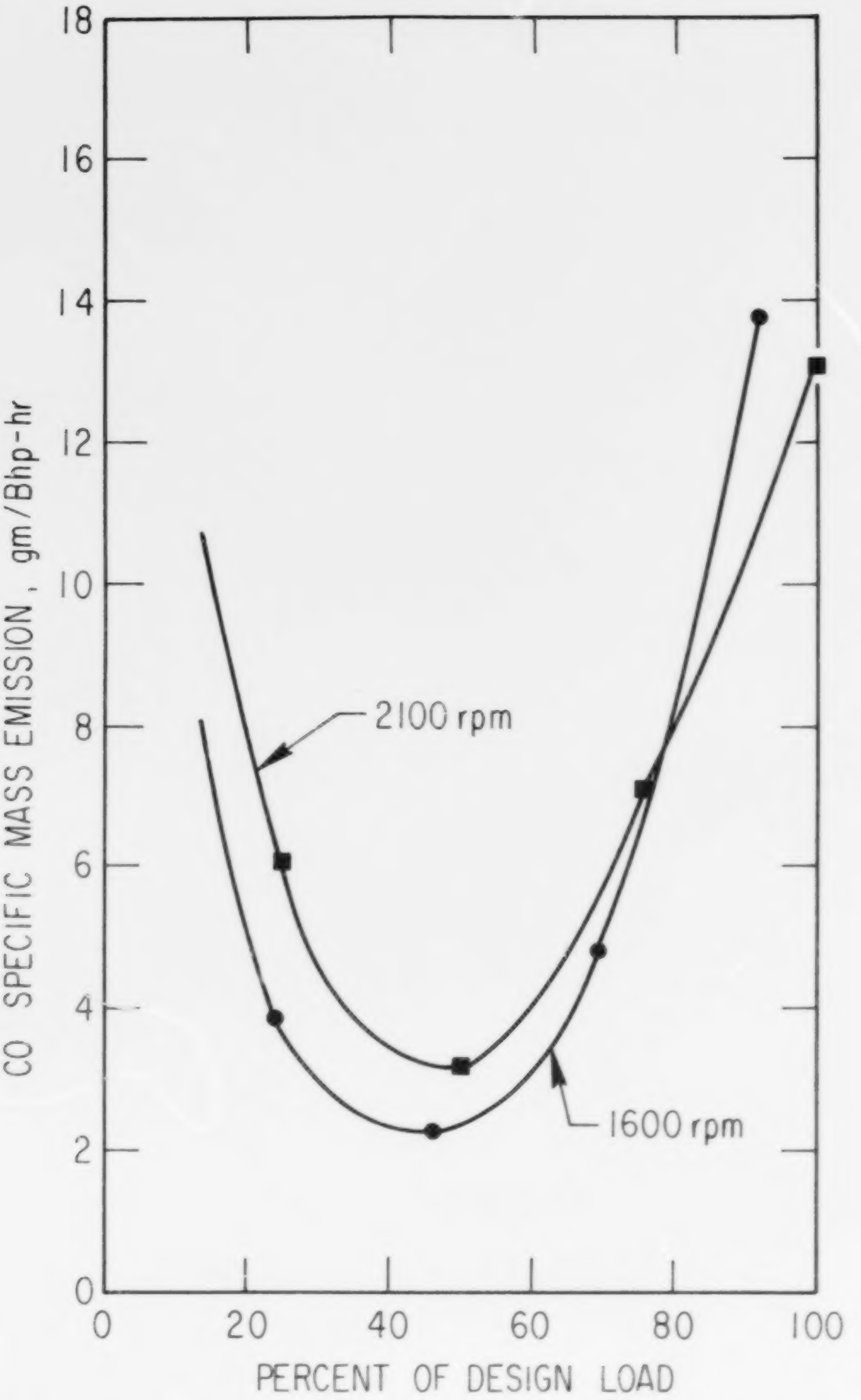

Figure B-33. Four-Cycle, Naturally-Aspirated Direct-Injection Diesel - Engine F - Part-Load Carbon Monoxide Emissions

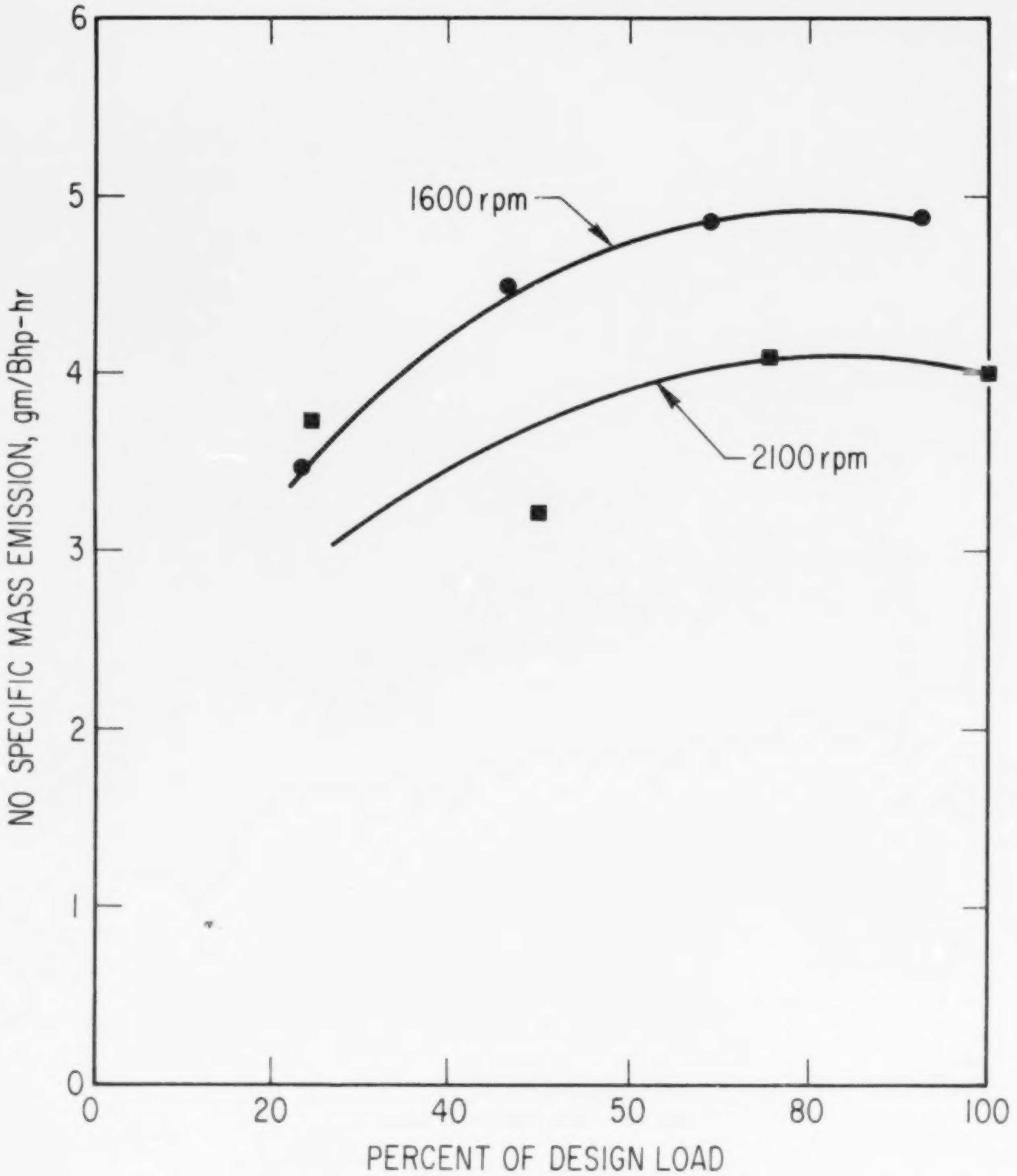

Figure B-34. Four-Cycle, Naturally-Aspirated Direct-Injection Diesel - Engine F - Part-Load Nitric Oxide Emissions

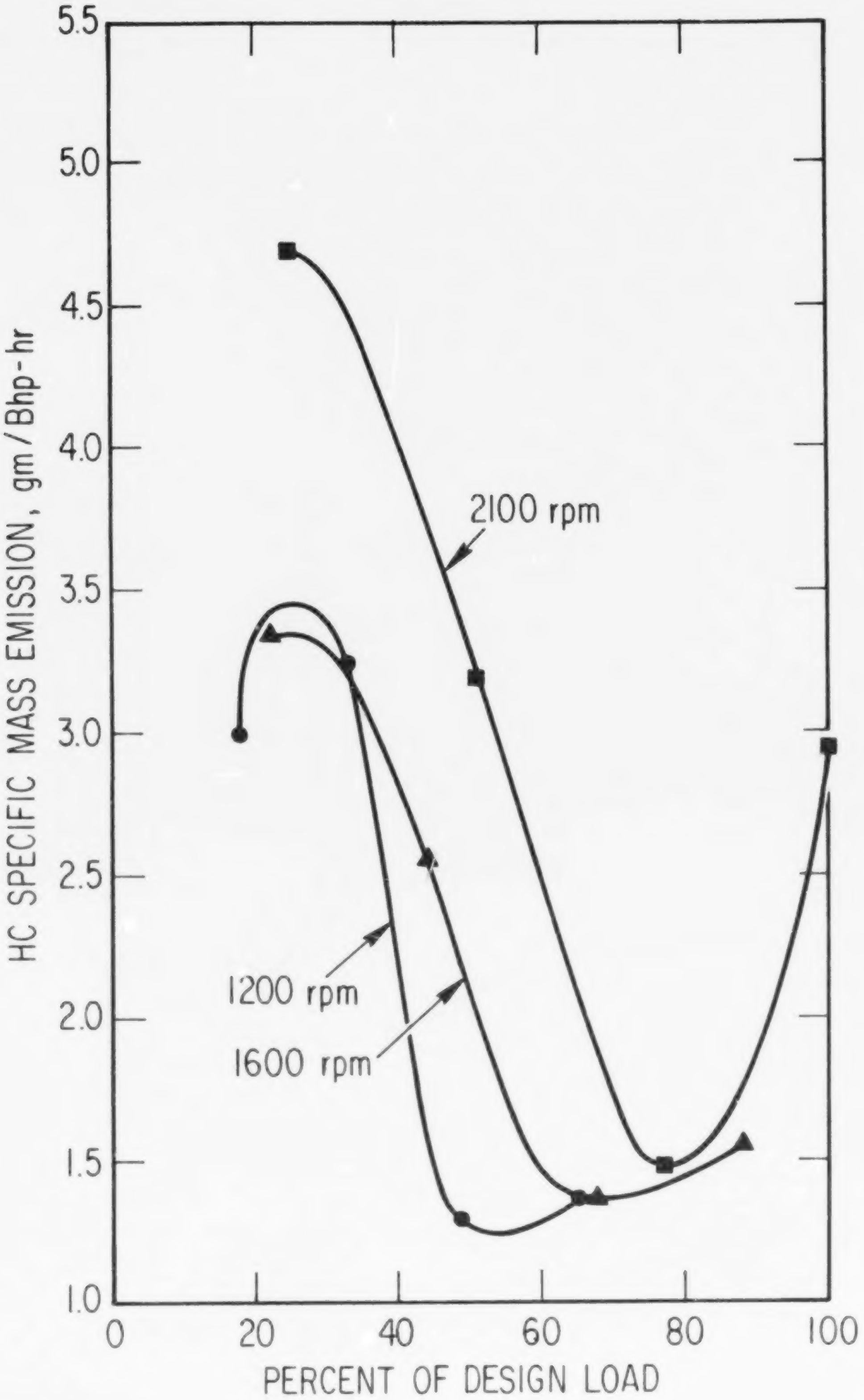

Figure B-35. Four-Cycle, Turbocharged Direct-Injection Diesel - Engine I - Part-Load Hydrocarbon Emissions

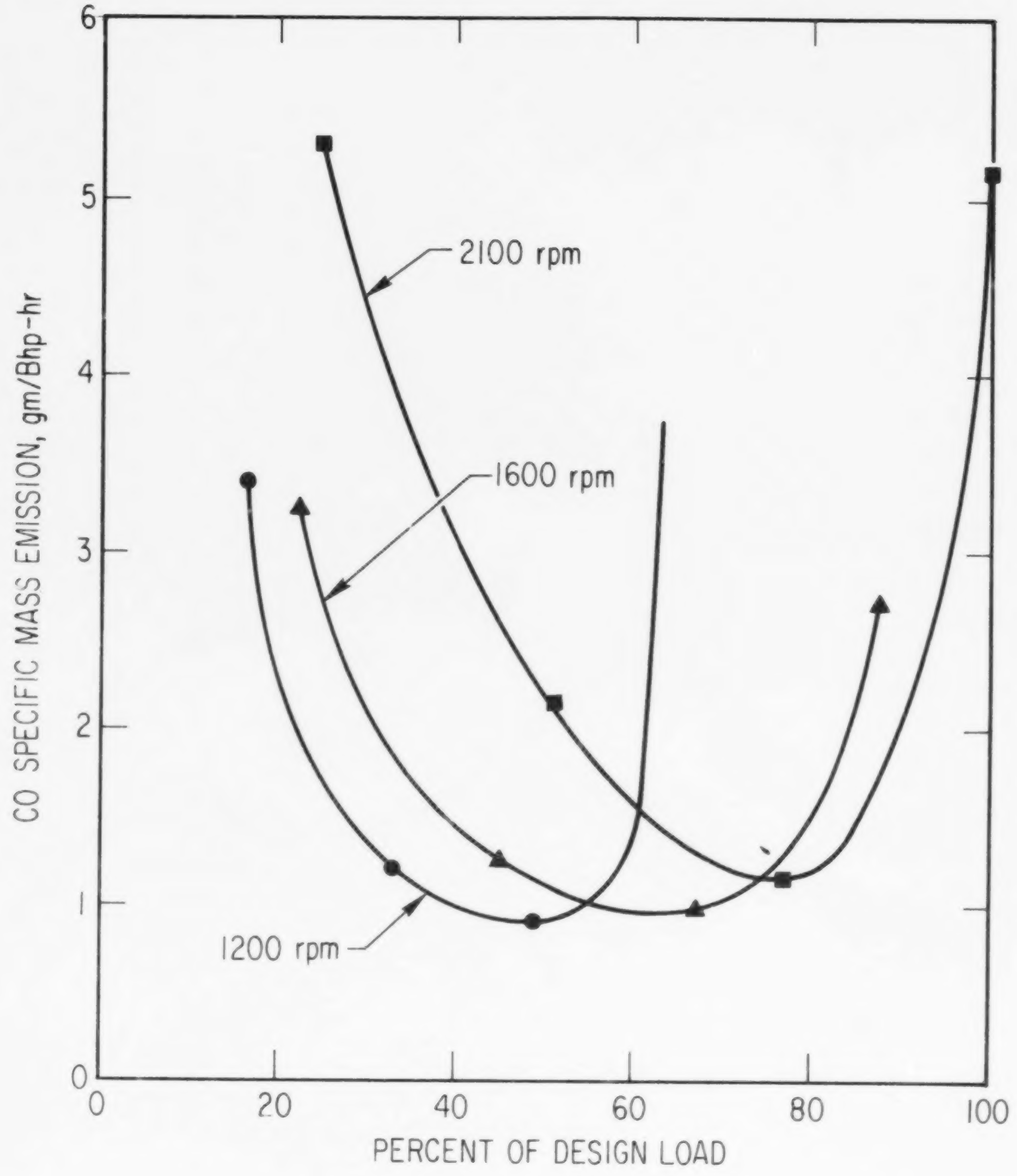

Figure B-36. Four-Cycle, Turbocharged Direct-Injection Diesel - Engine I - Part-Load Carbon Monoxide Emissions

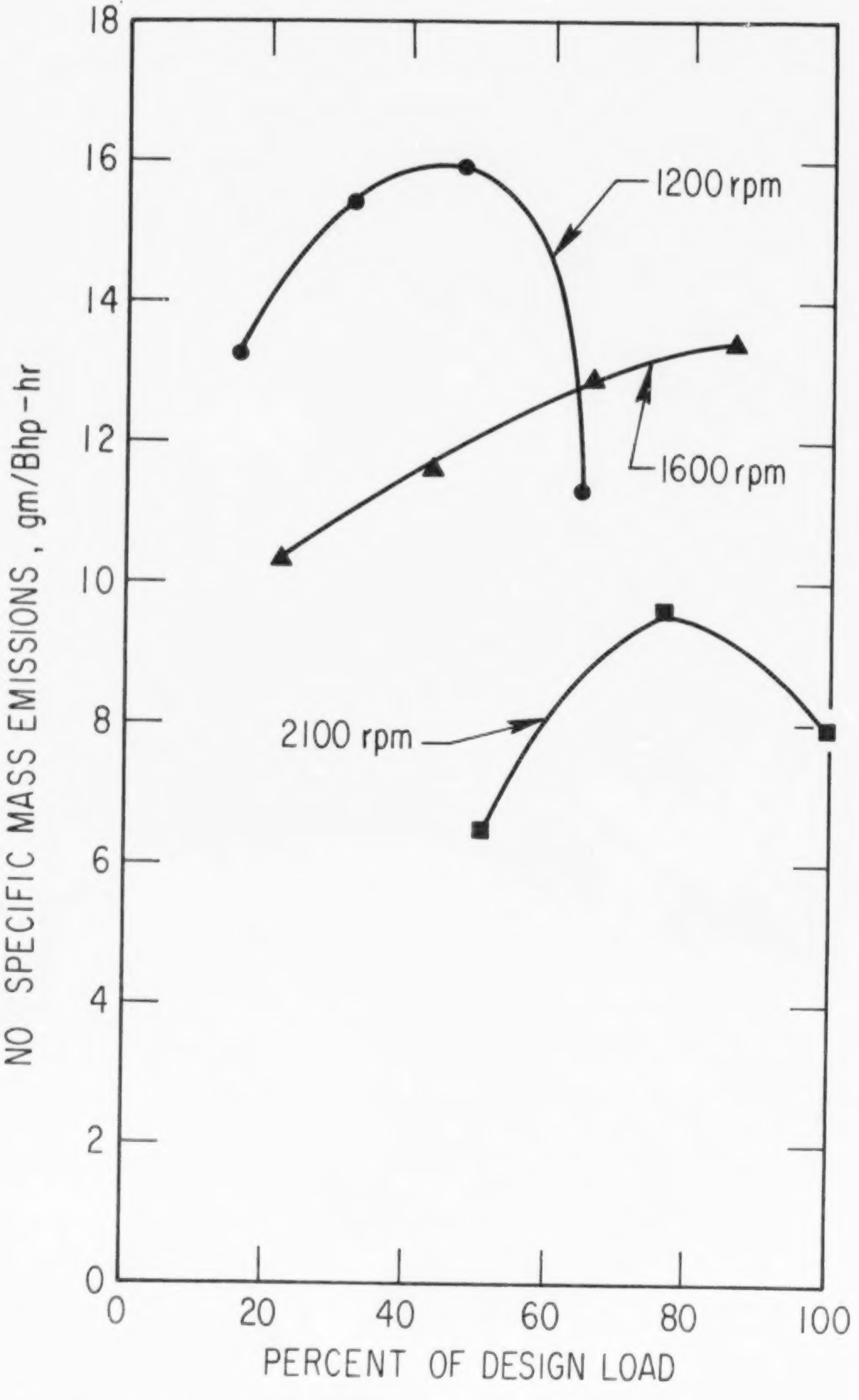

Figure B-37. Four-Cycle, Turbocharged Direct-Injection Diesel - Engine I - Part-Load Nitric Oxide Emissions

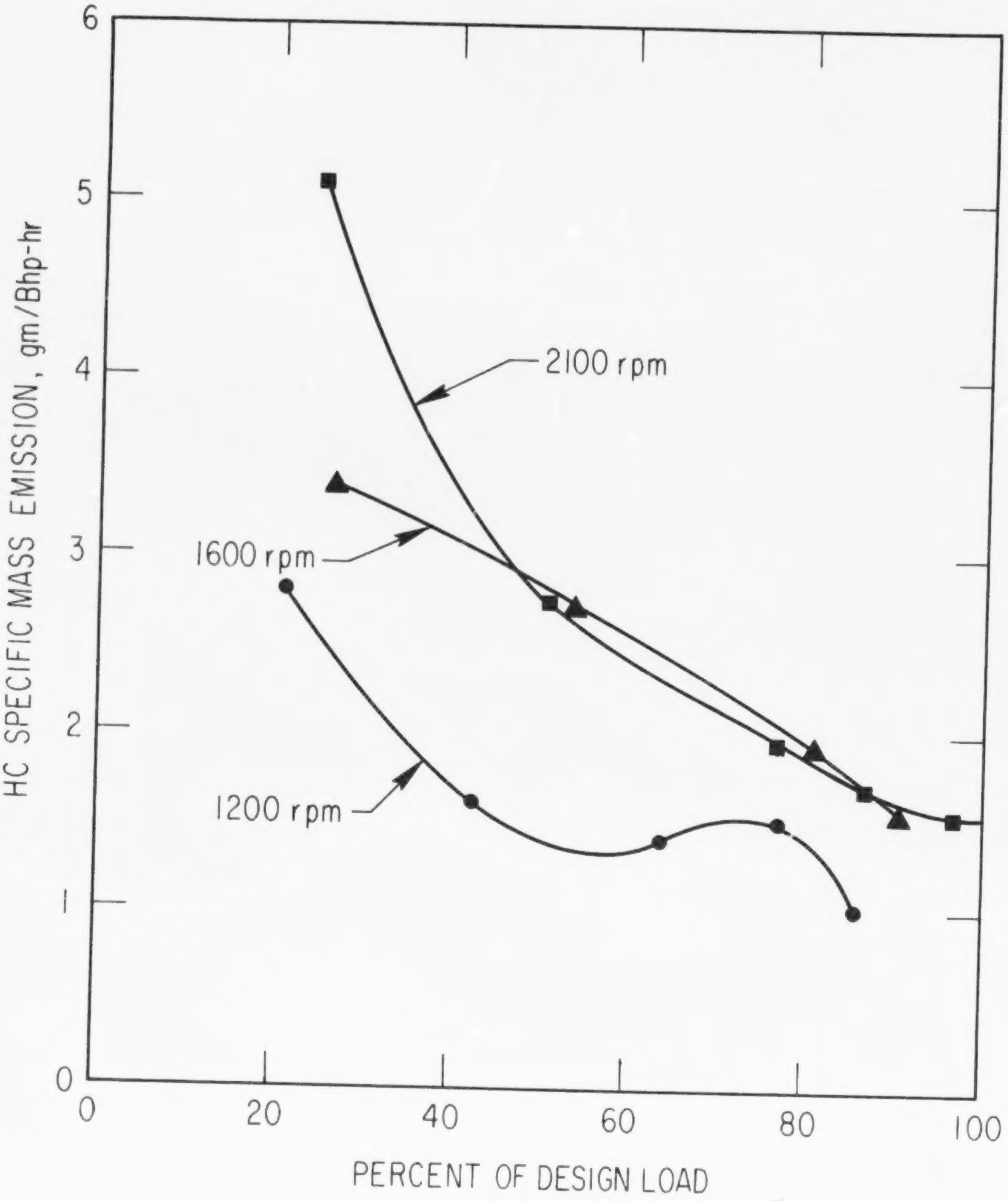

Figure B-38. Four-Cycle, Turbocharged Direct-Injection Diesel - Engine J - Part-Load Hydrocarbon Emissions

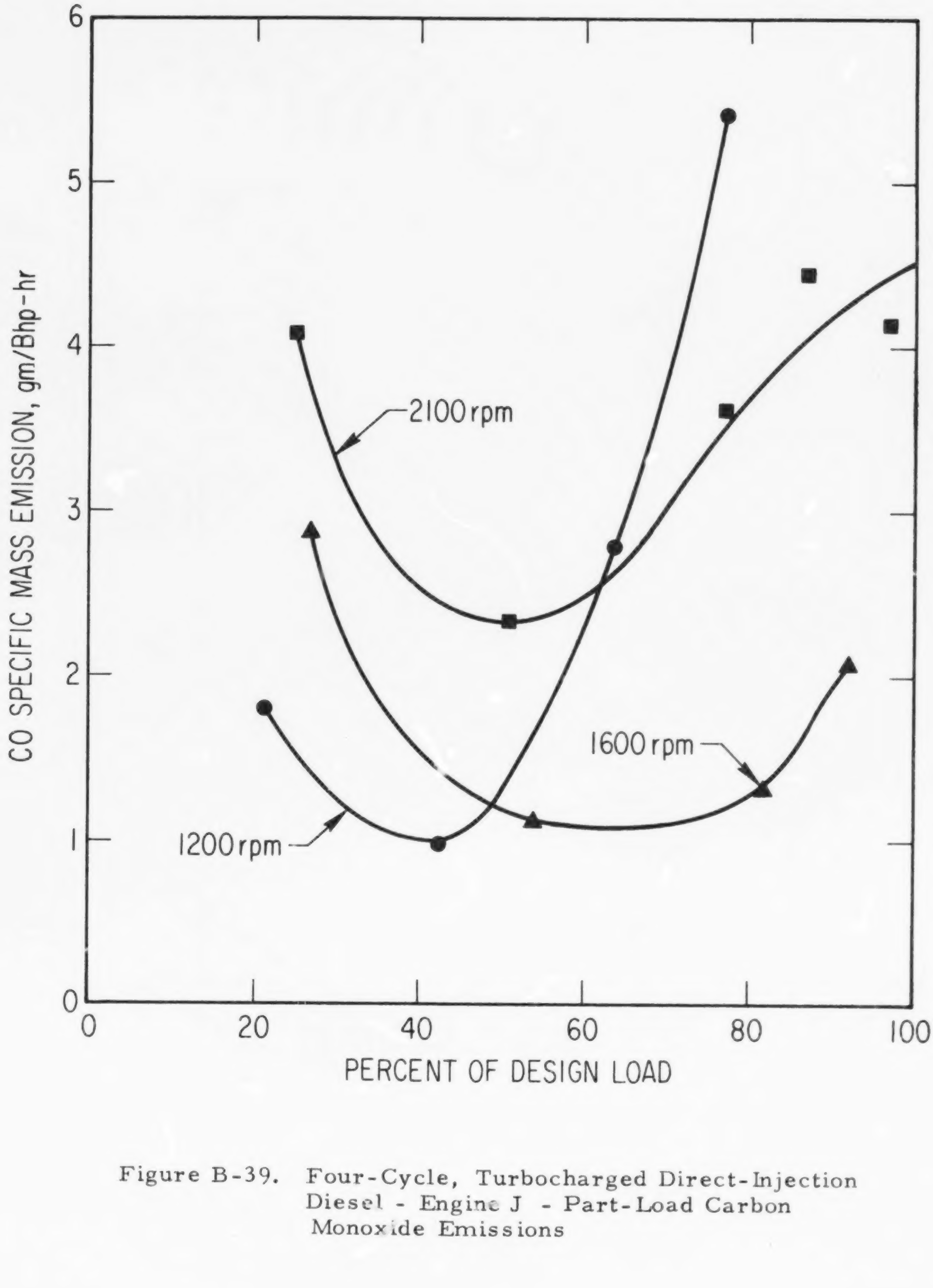

Figure B-39. Four-Cycle, Turbocharged Direct-Injection Diesel - Engine J - Part-Load Carbon Monoxide Emissions

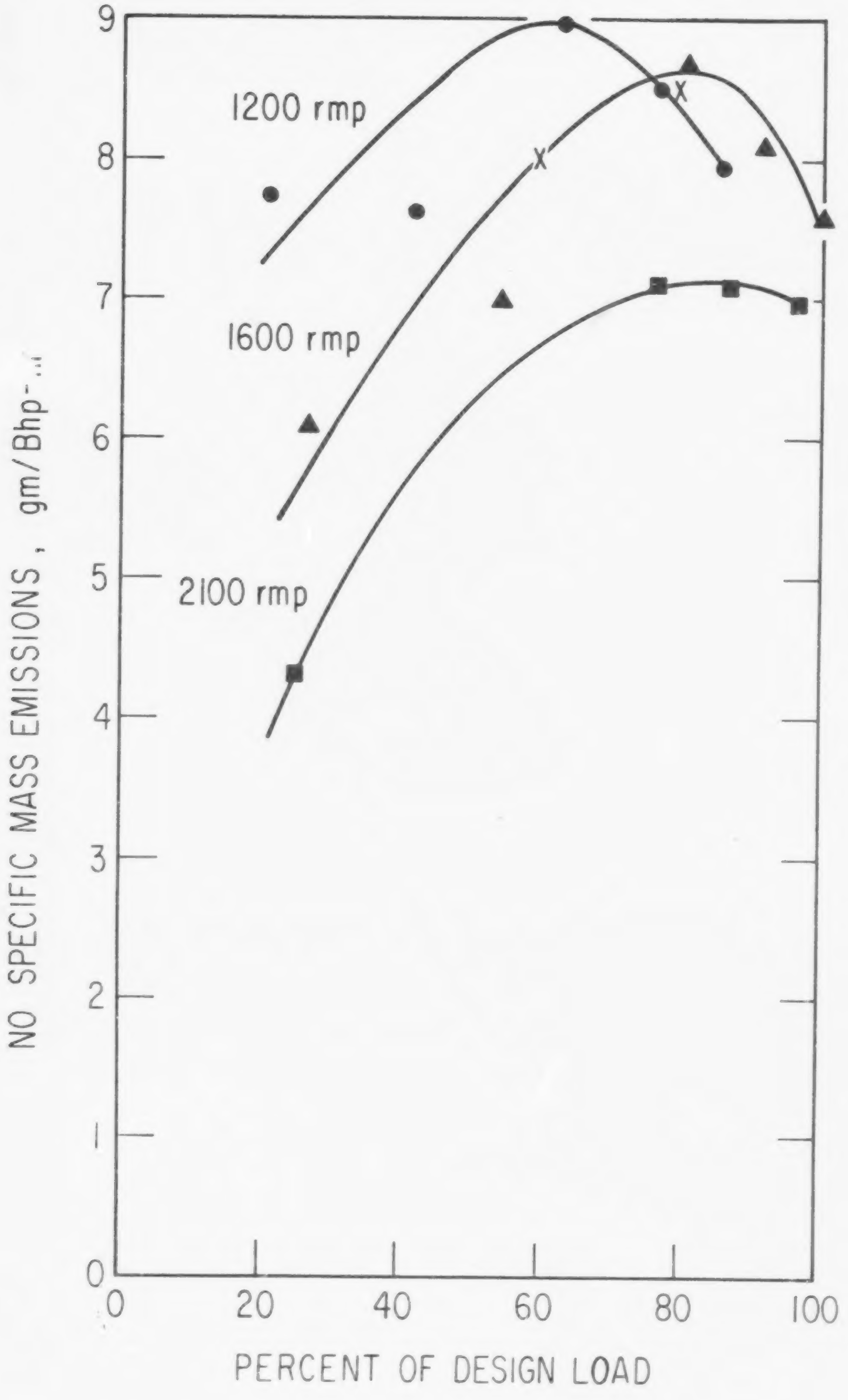

Figure B-40. Four-Cycle, Turbocharged Direct-Injection Diesel - Engine J - Part-Load Nitric Oxide Emissions

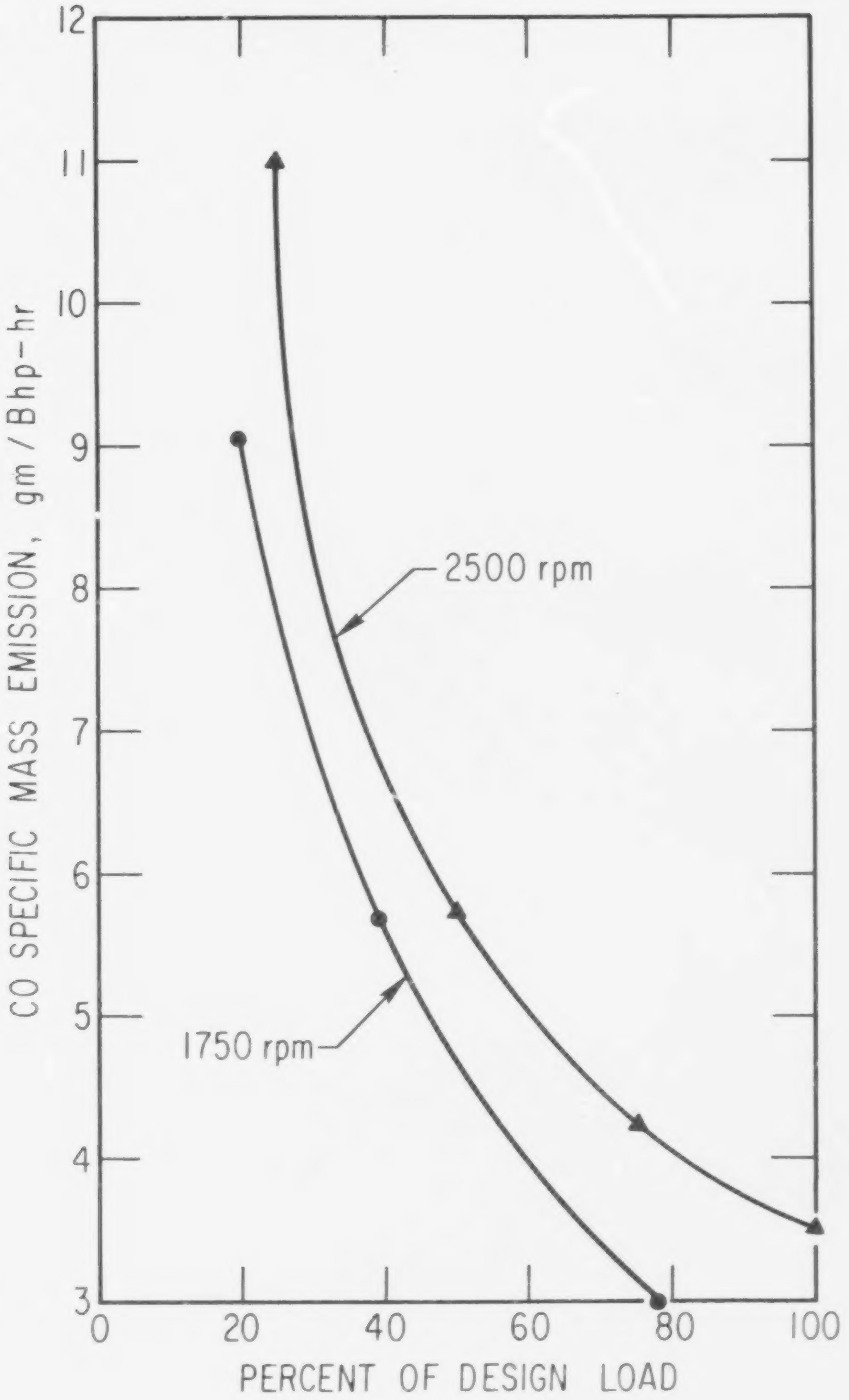

Figure B-41. Four-Cycle, Turbocharged Direct-Injection Diesel - Engine K - Part-Load Carbon Monoxide Emissions

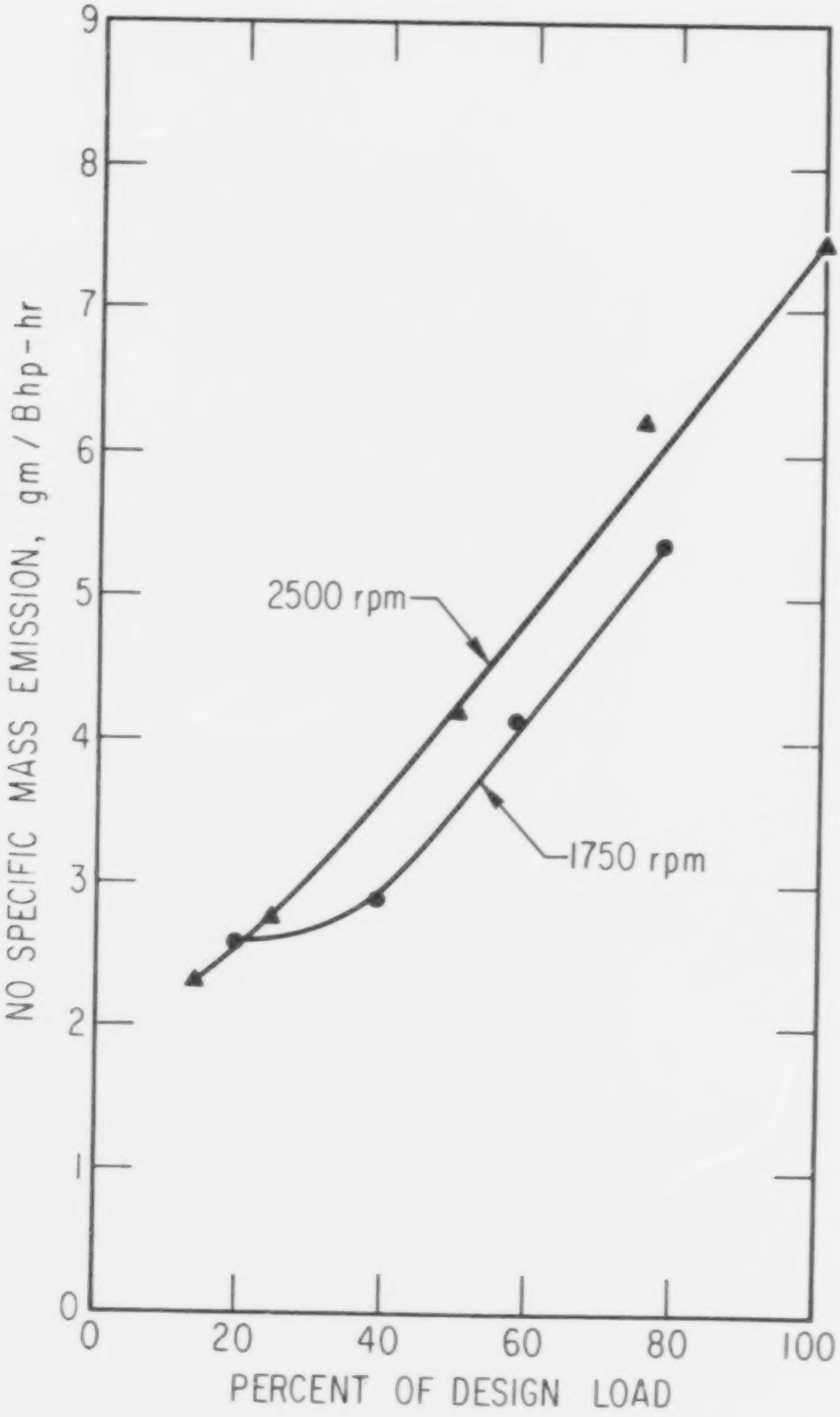

Figure B-42. Four-Cycle, Turbocharged Direct-Injection Diesel - Engine K - Part-Load Nitric Oxide Emissions

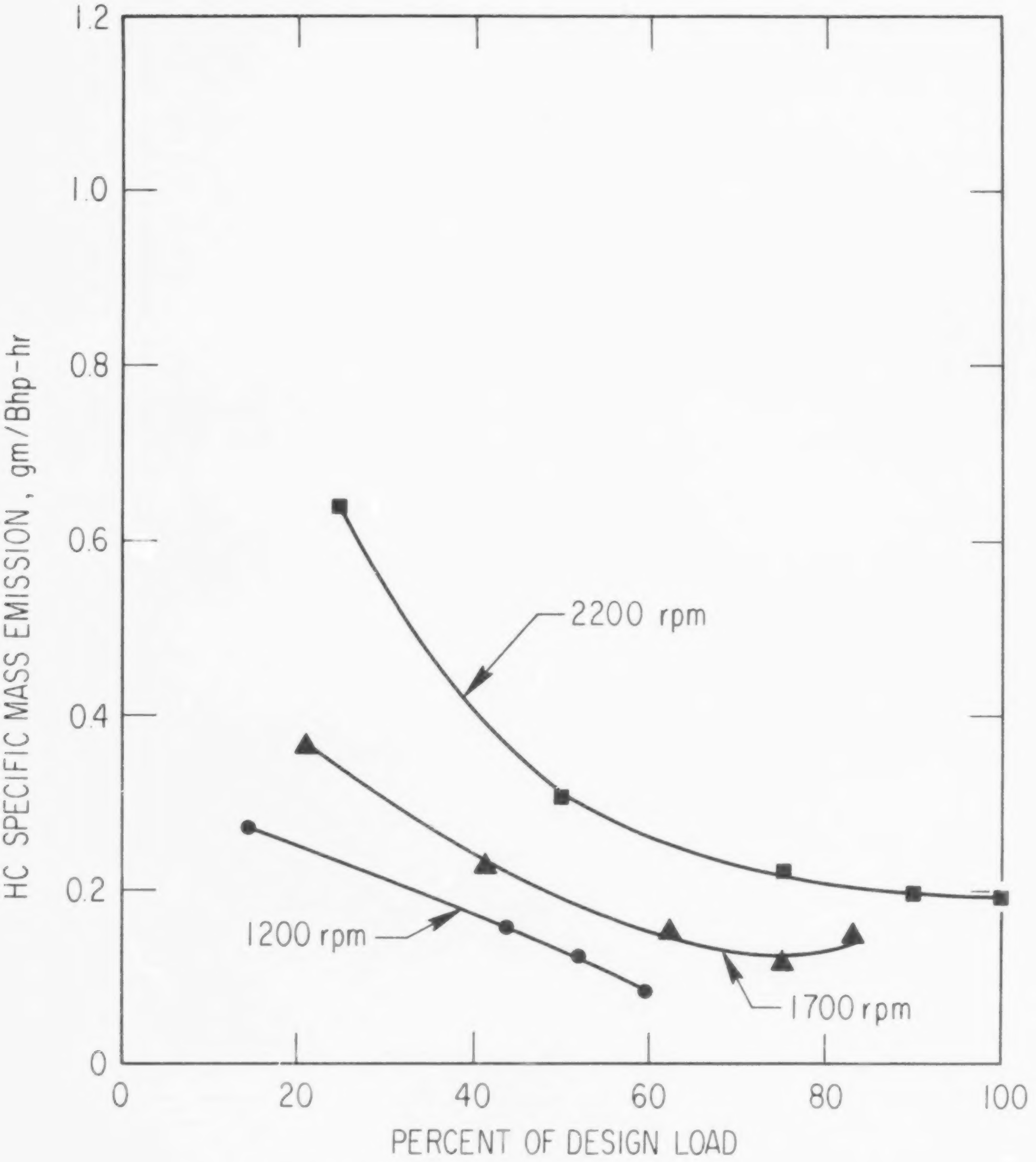

Figure B-43. Four-Cycle, Turbocharged Prechamber Diesel - Engine L - Part-Load Hydrocarbon Emissions

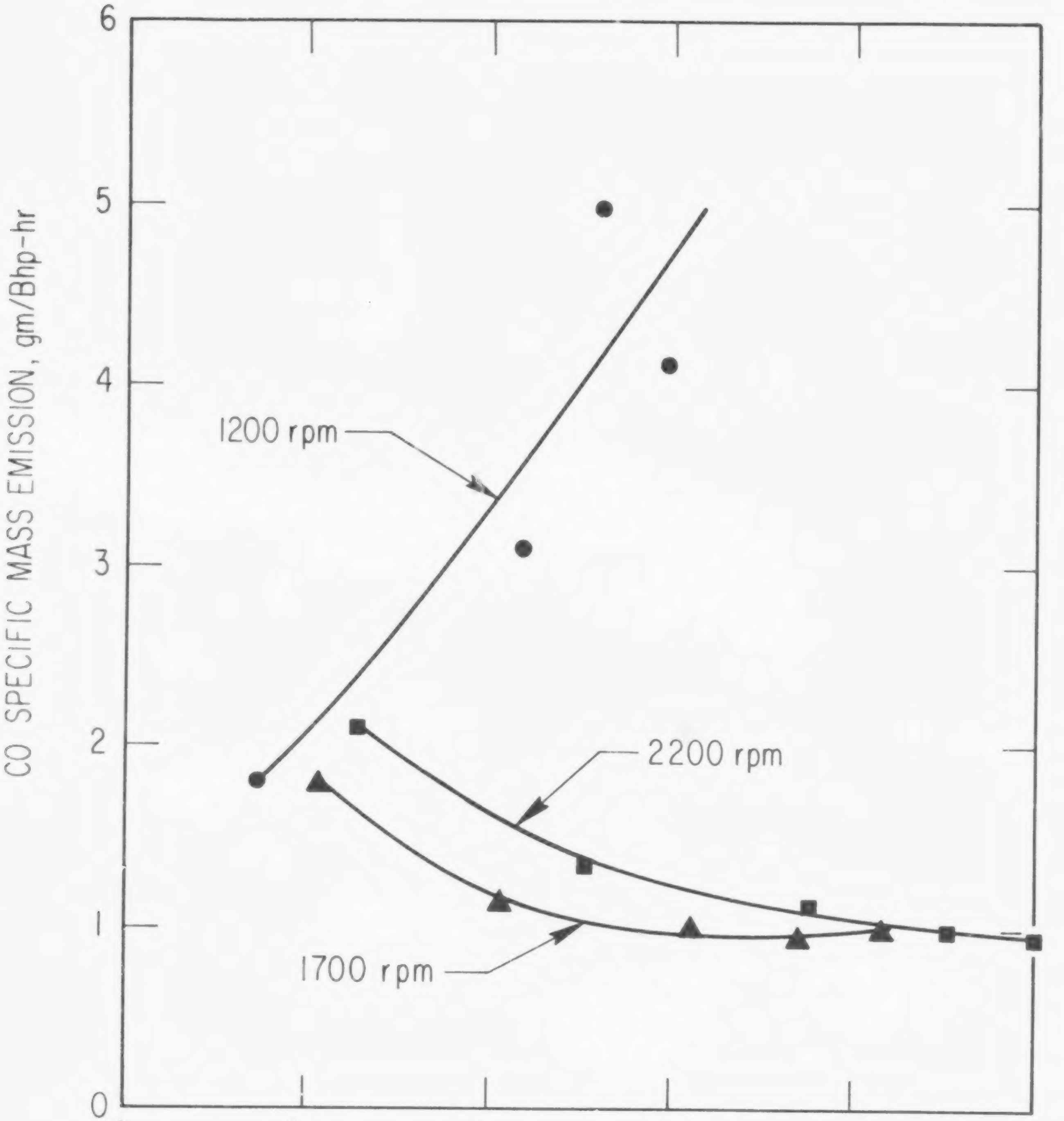

Figure B-44. Four-Cycle, Turbocharged Prechamber Diesel - Engine L - Part-Load Carbon Monoxide Emissions

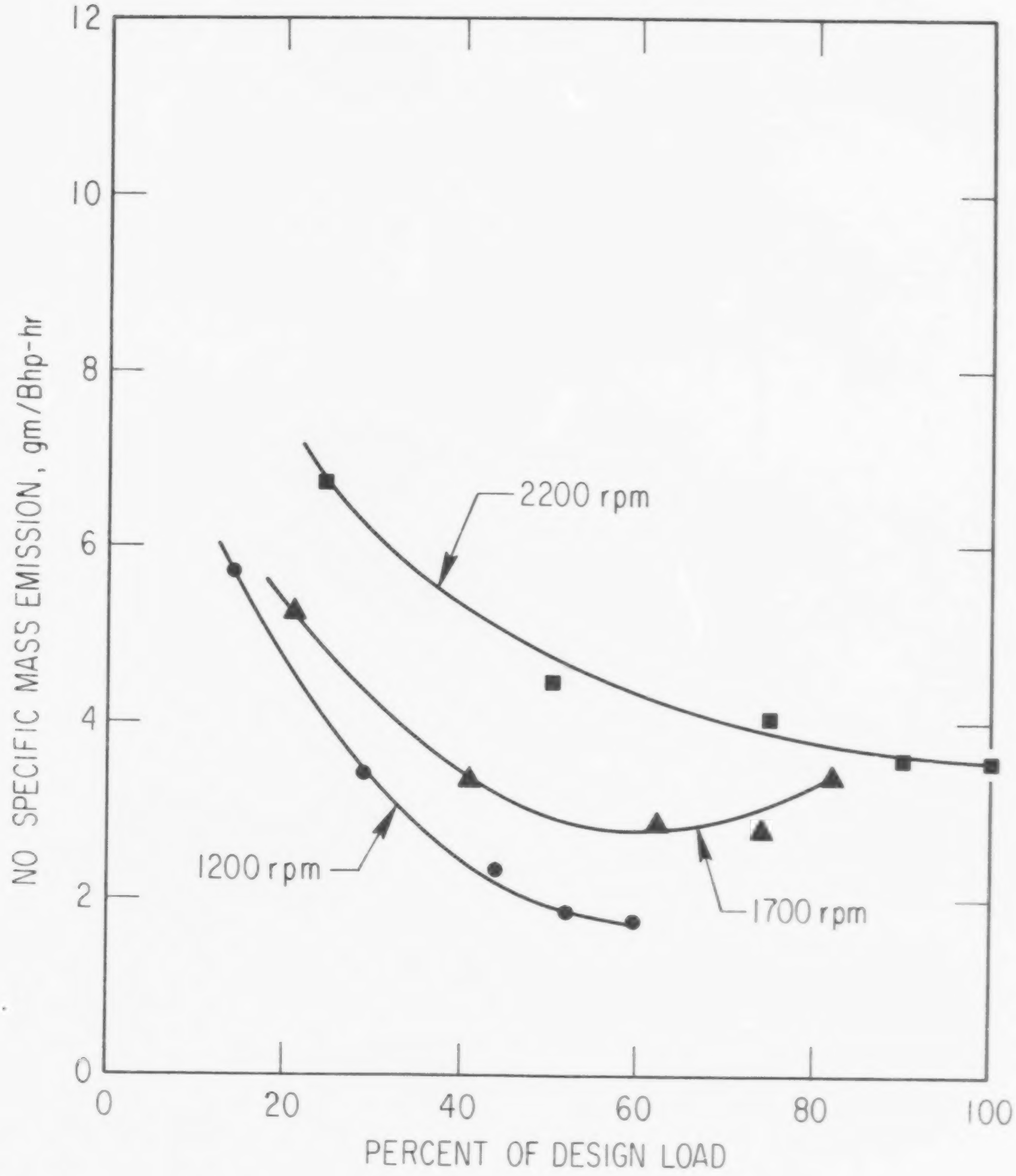

Figure B-45. Four-Cycle, Turbocharged Prechamber Diesel - Engine L - Part-Load Nitric Oxide Emissions

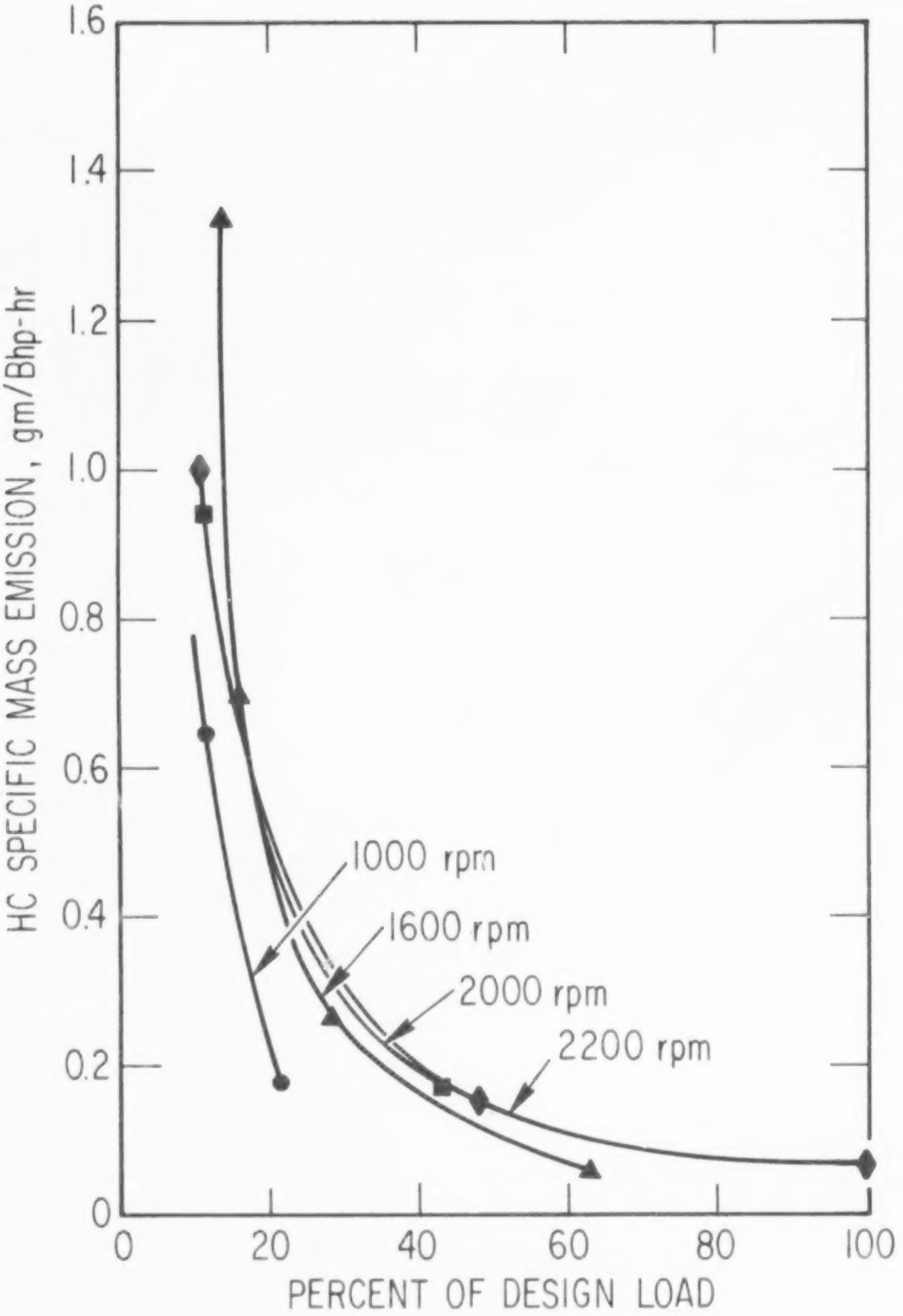

Figure B-46. Four-Cycle, Turbocharged Prechamber Diesel - Engine M - Part-Load Hydrocarbon Emissions

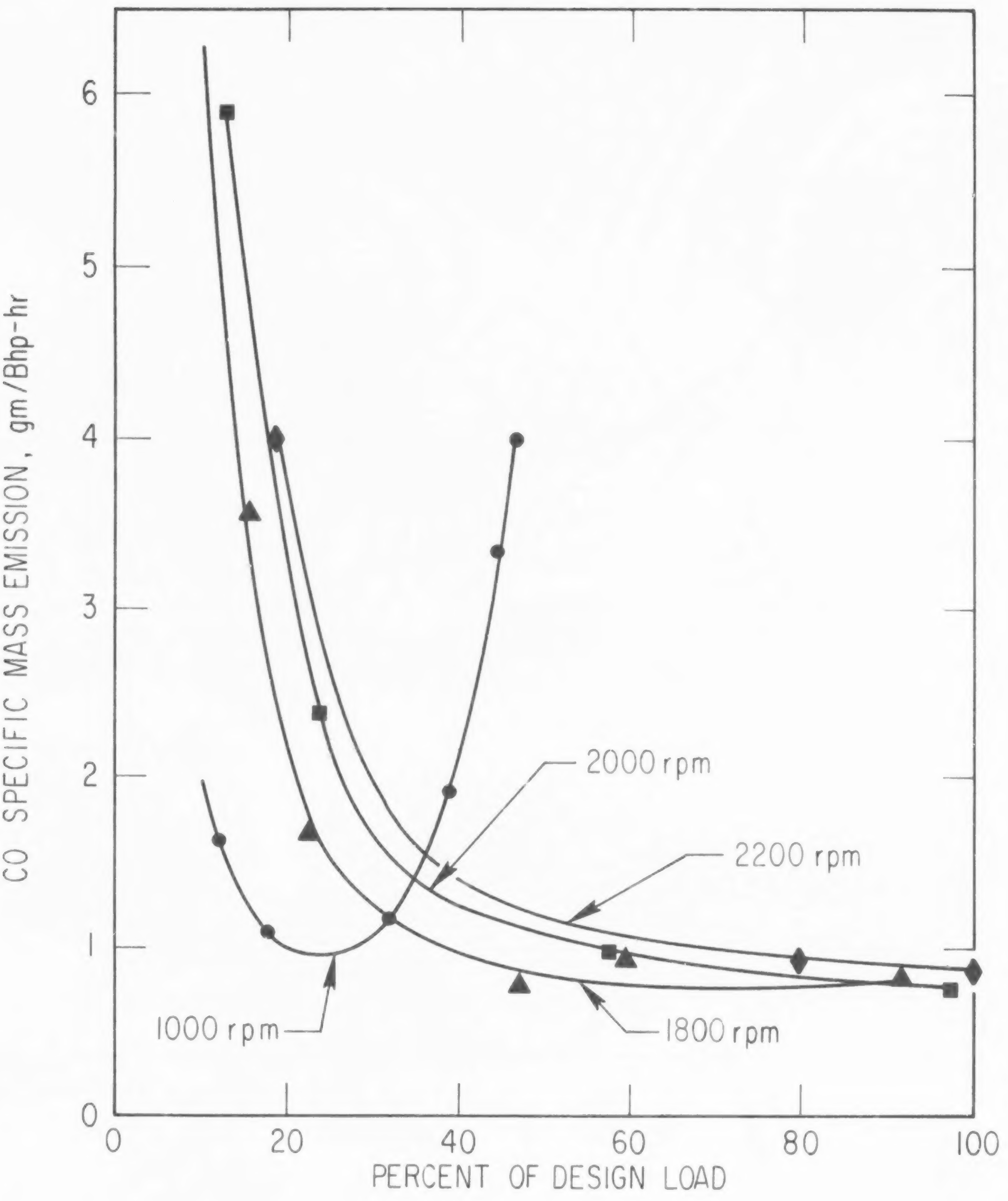

Figure B-47. Four-Cycle, Turbocharged Prechamber Diesel - Engine M - Part-Load Carbon Monoxide Emissions

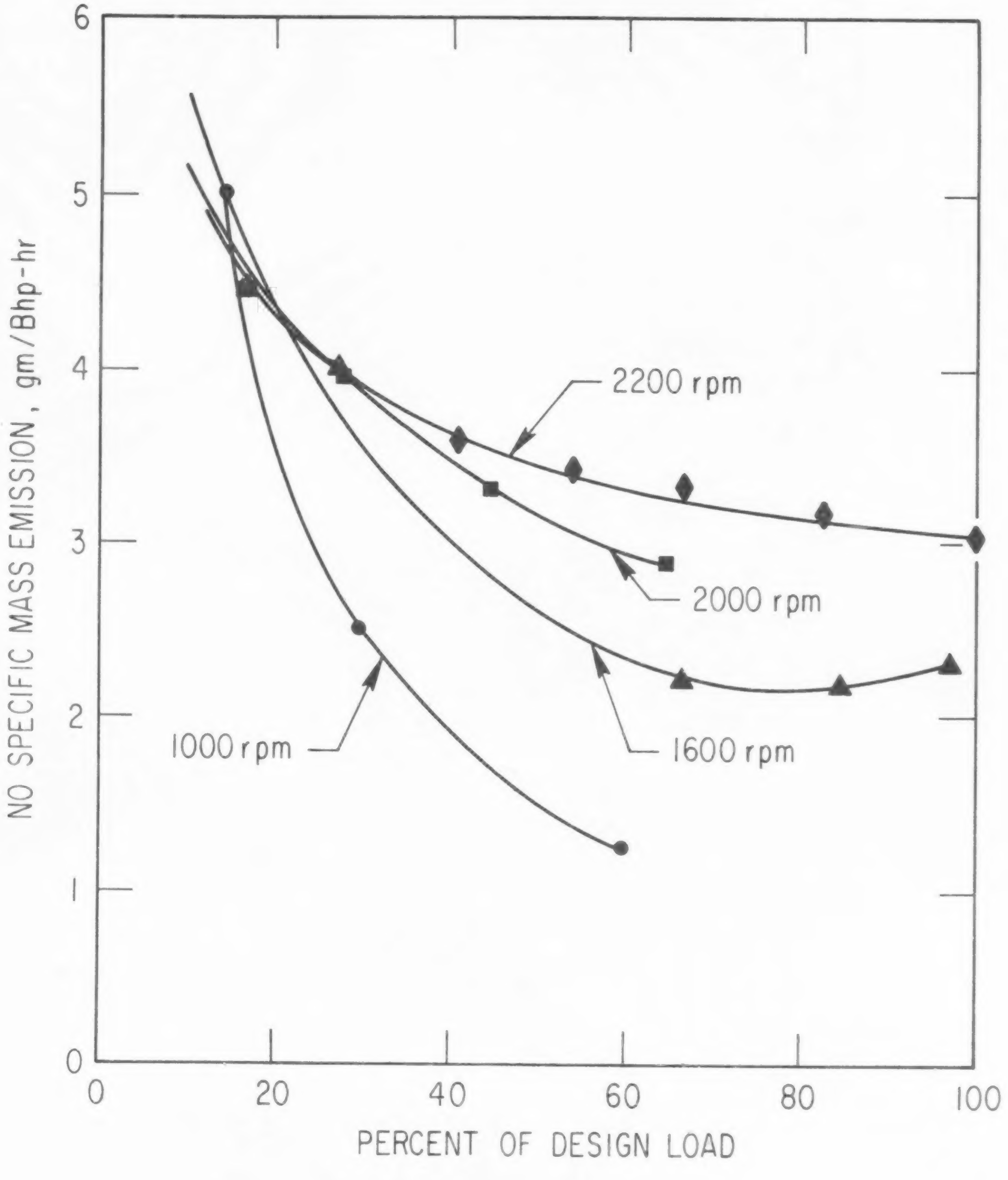

Figure B-48. Four-Cycle, Turbocharged Prechamber Diesel - Engine M - Part-Load Nitric Oxide Emissions

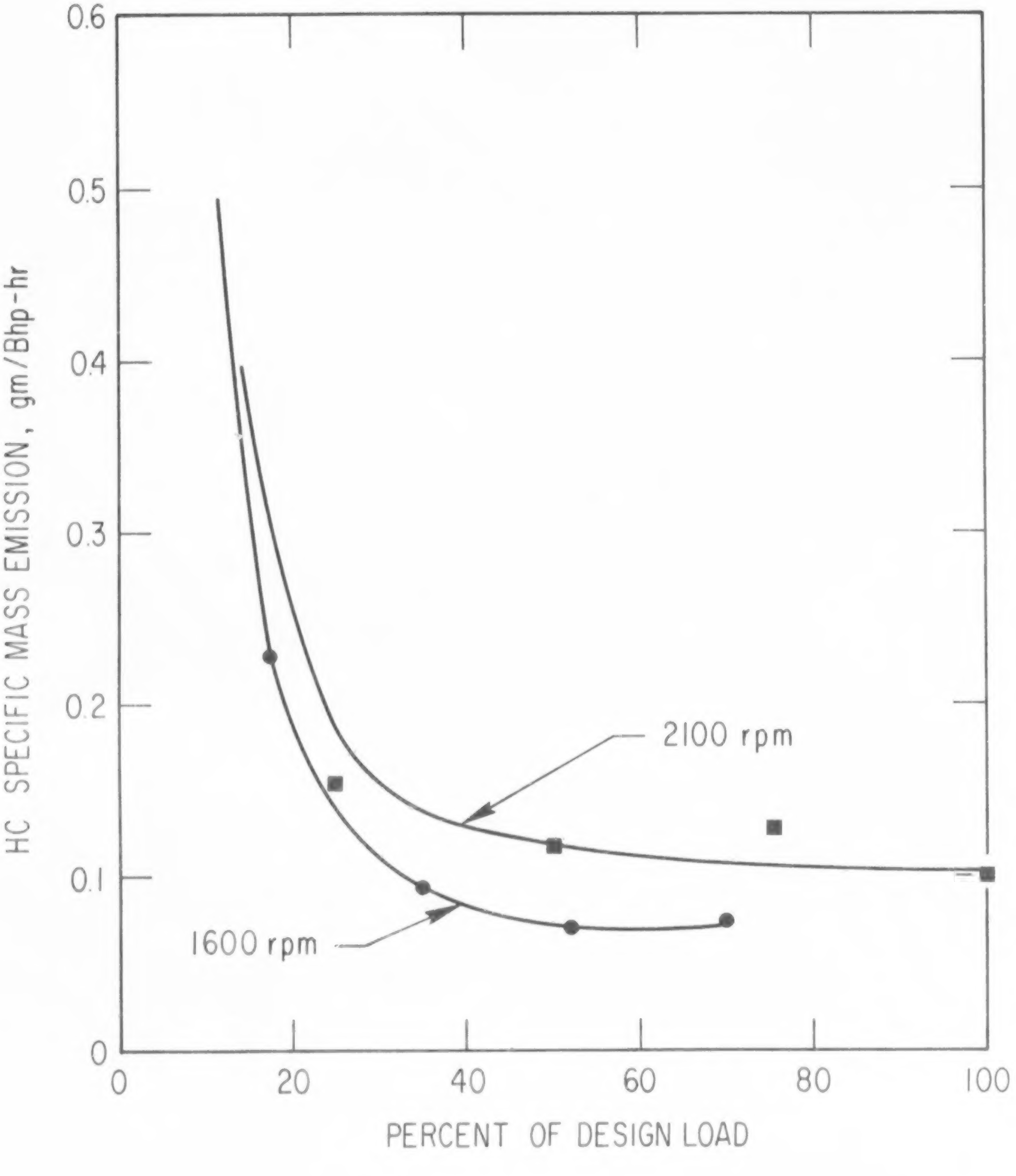

Figure B-49. Four-Cycle, Turbocharged Prechamber Diesel - Engine N - Part-Load Hydrocarbon Emissions

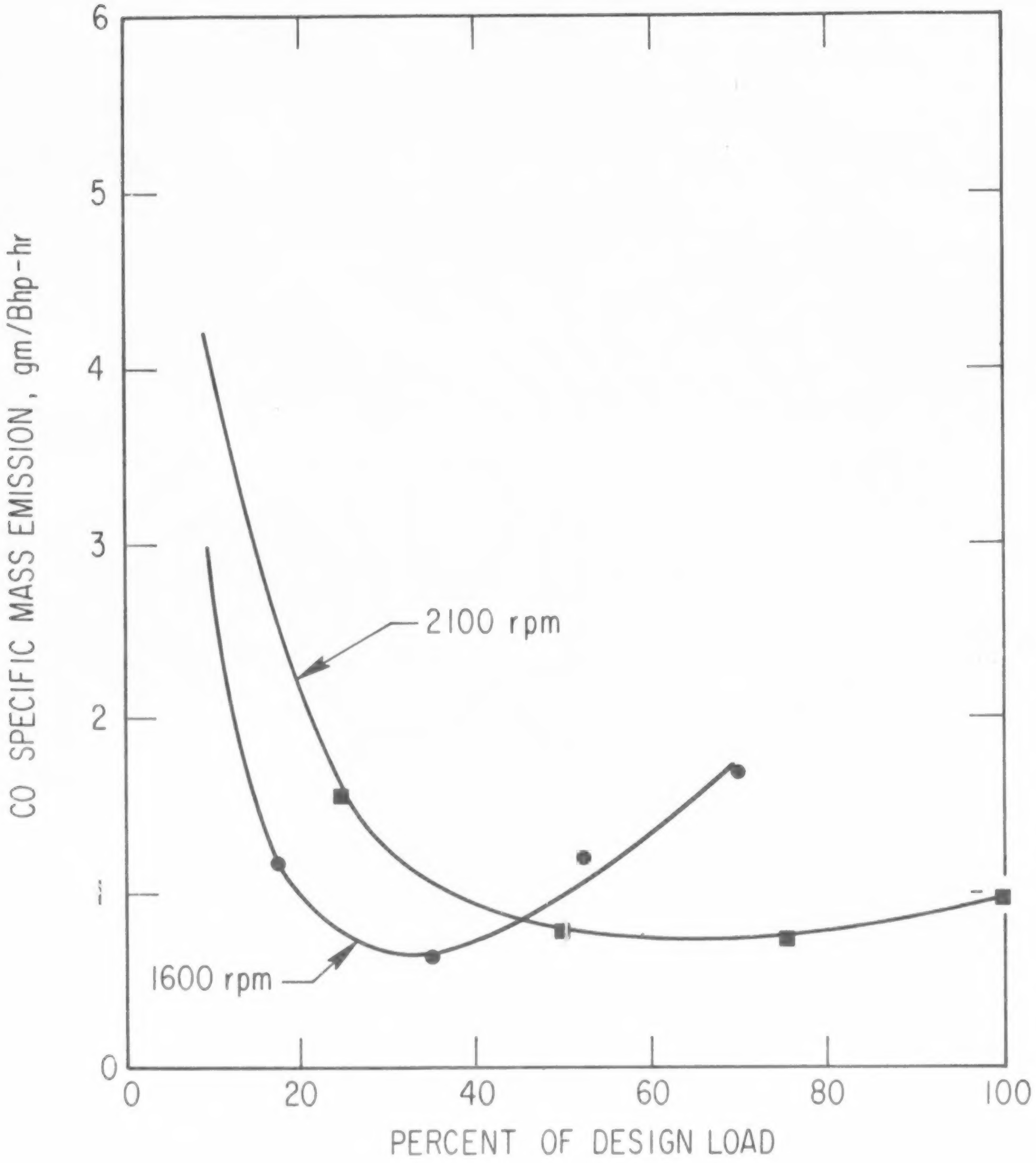

Figure B-50. Four-Cycle, Turbocharged Prechamber Diesel - Engine N - Part-Load Carbon Monoxide Emissions

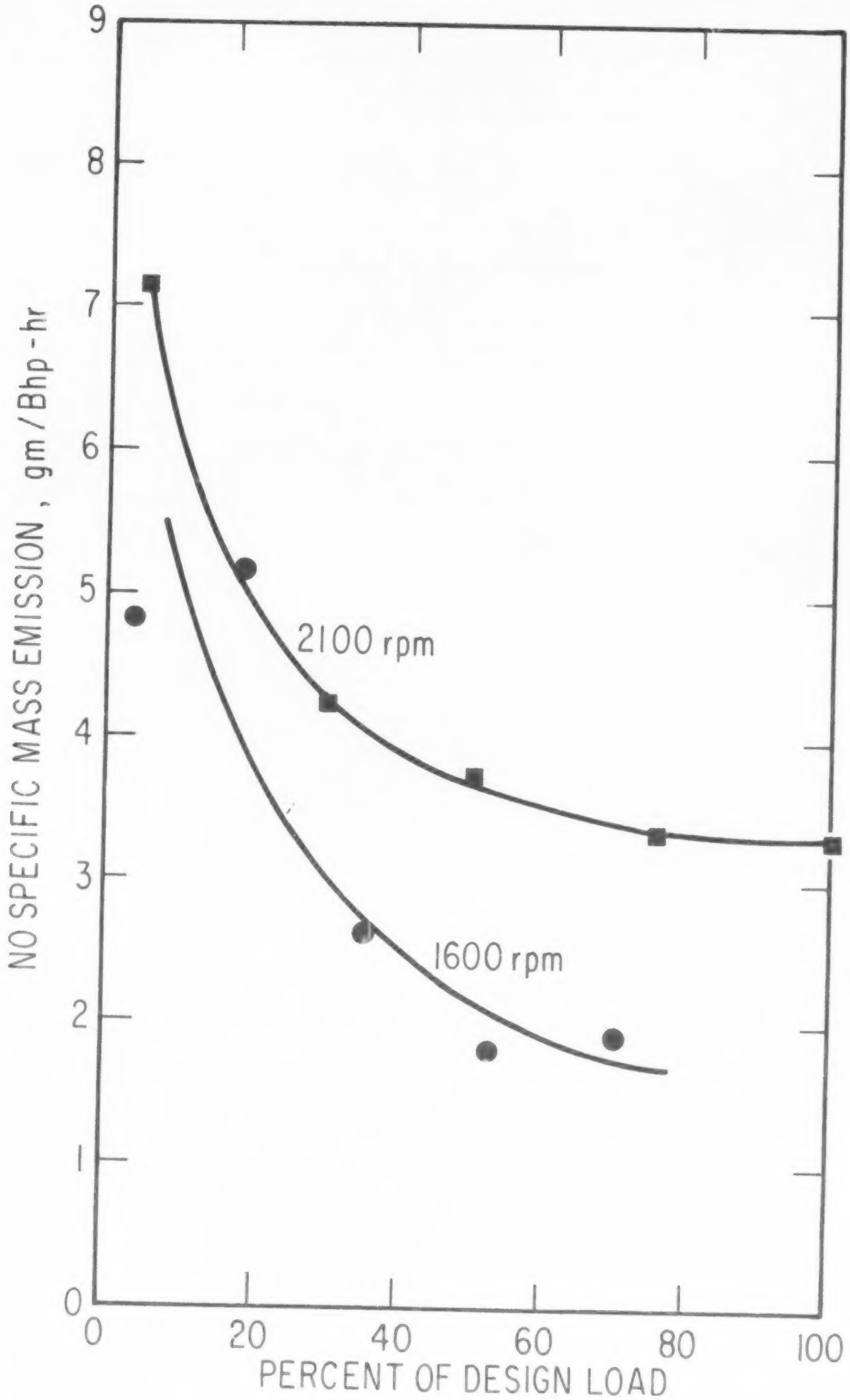

Figure B-51. Four-Cycle, Turbocharged Prechamber Diesel - Engine N - Part-Load Nitric Oxide Emissions clear whether this trend is characteristic of all prechamber engines or only the Caterpillar design. The NO emissions increase with decreasing load and increasing speed.

Insufficient information is available to characterize the part-load emissions of two-cycle diesel engines. The only part-load data were provided by one laboratory (Ref. B-53) for a General Motors 6V-71 engine which had been operated in a city coach for approximately 190,000 odometer miles. This engine was tested as received and after incorporation of the General Motors Environmental Improvement Package (EIP), which consists of a modified injection system having lower dribble volume and a catalytic muffler. The emissions of the non-modified engine are shown in Figs. B-52 through B-54 as a function of percent design load at design speed. The emissions after installation of the EIP are presented in Figs. B-55 through B-57 and show significant reductions in HC and CO. This improvement is primarily due to injection system modifications and, to a lesser degree, the addition of the catalyst. Although not used to characterize the emissions of two-cycle engines, the data are included for general information.

B.3.4.2 Selected Part-Load Emissions

Based on the part-load data presented in Figs. B-18 through B-51, two extreme sets of part-load characteristics were constructed for each of the three engine configurations representing the state-of-the-art technology. The ratio of the part-load specific mass emissions to the full-load emissions at design speed versus percent full load is presented in Figs. B-58 through B-63. These factors and the design load emissions presented in Figs. B-15 through B-17 provide all the information necessary for computation of the specific mass emissions at any part-load operating point.

The first set of part-load emission factors, plotted in Figs. B-58 through B-60, are based on constant engine speed, equal to the rated speed. In the second set, Figs. B-61 through B-63, the engine speed is varied with load to minimize part-load emissions. In general, it is more desirable from an

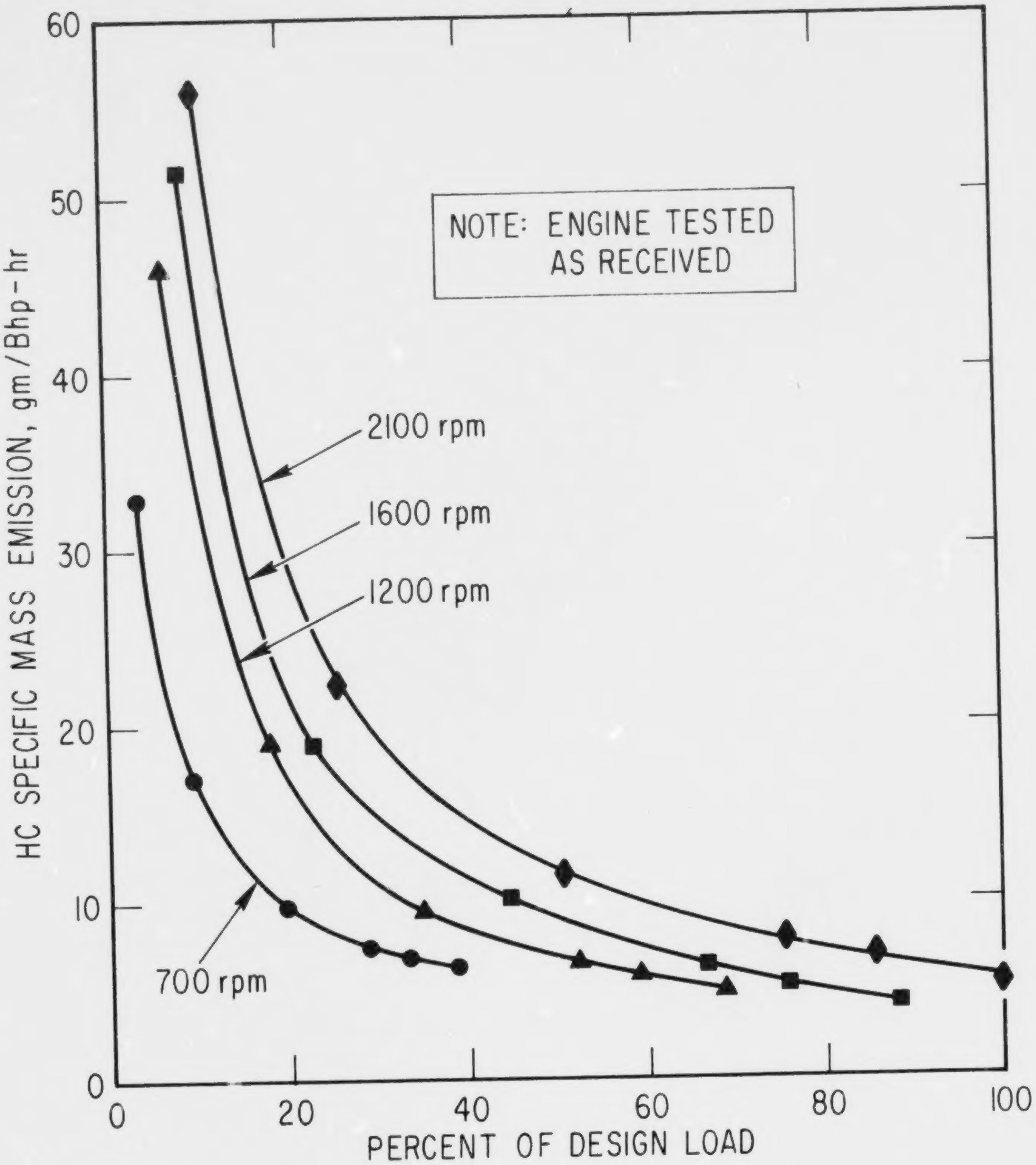

Figure B-52. Two-Cycle, Direct-Injection Diesel-Engine P-Part-Load Hydrocarbon Emissions

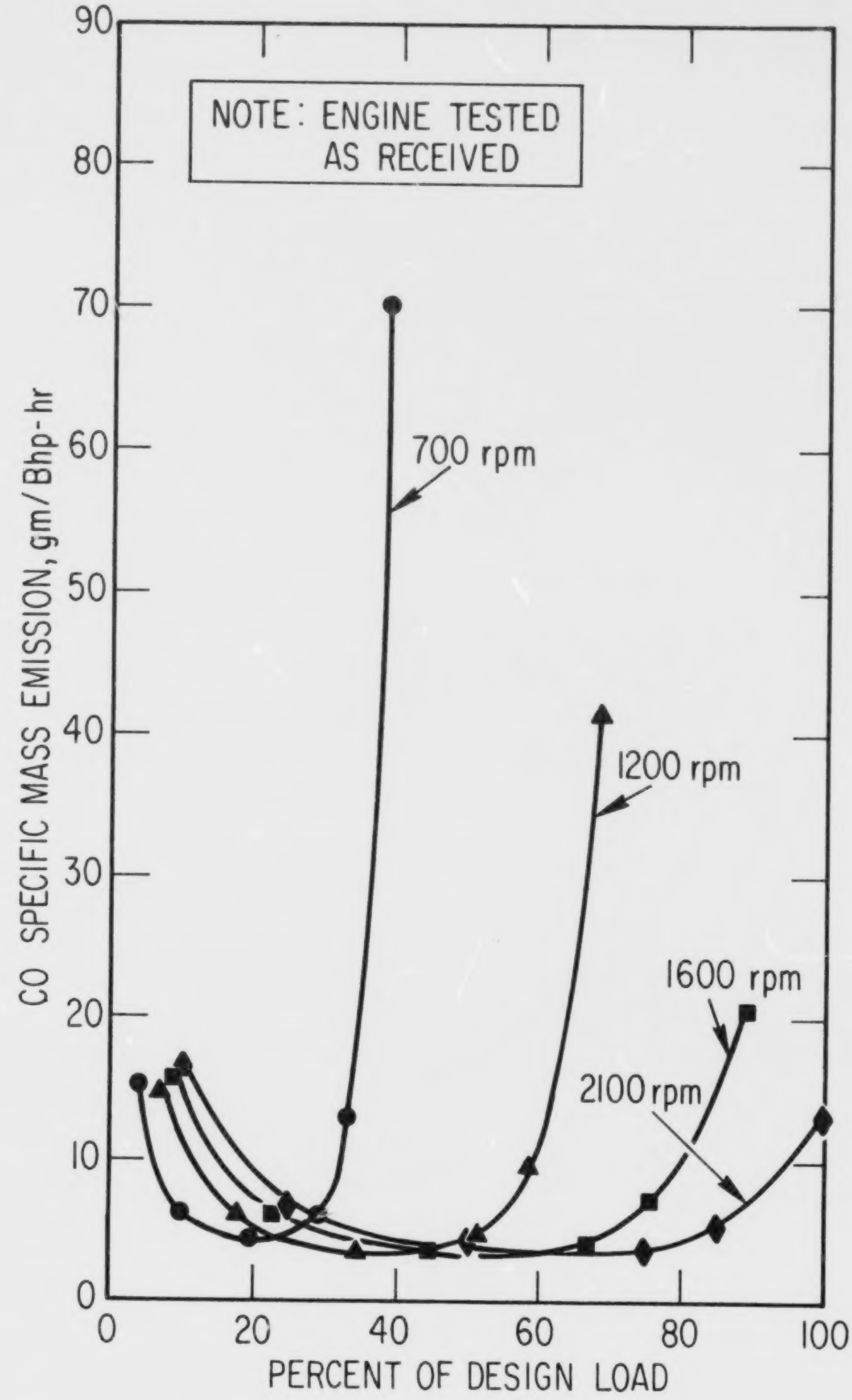

Figure B-53. Two-Cycle, Direct-Injection Diesel - Engine P-Part-Load Carbon Monoxide Emissions

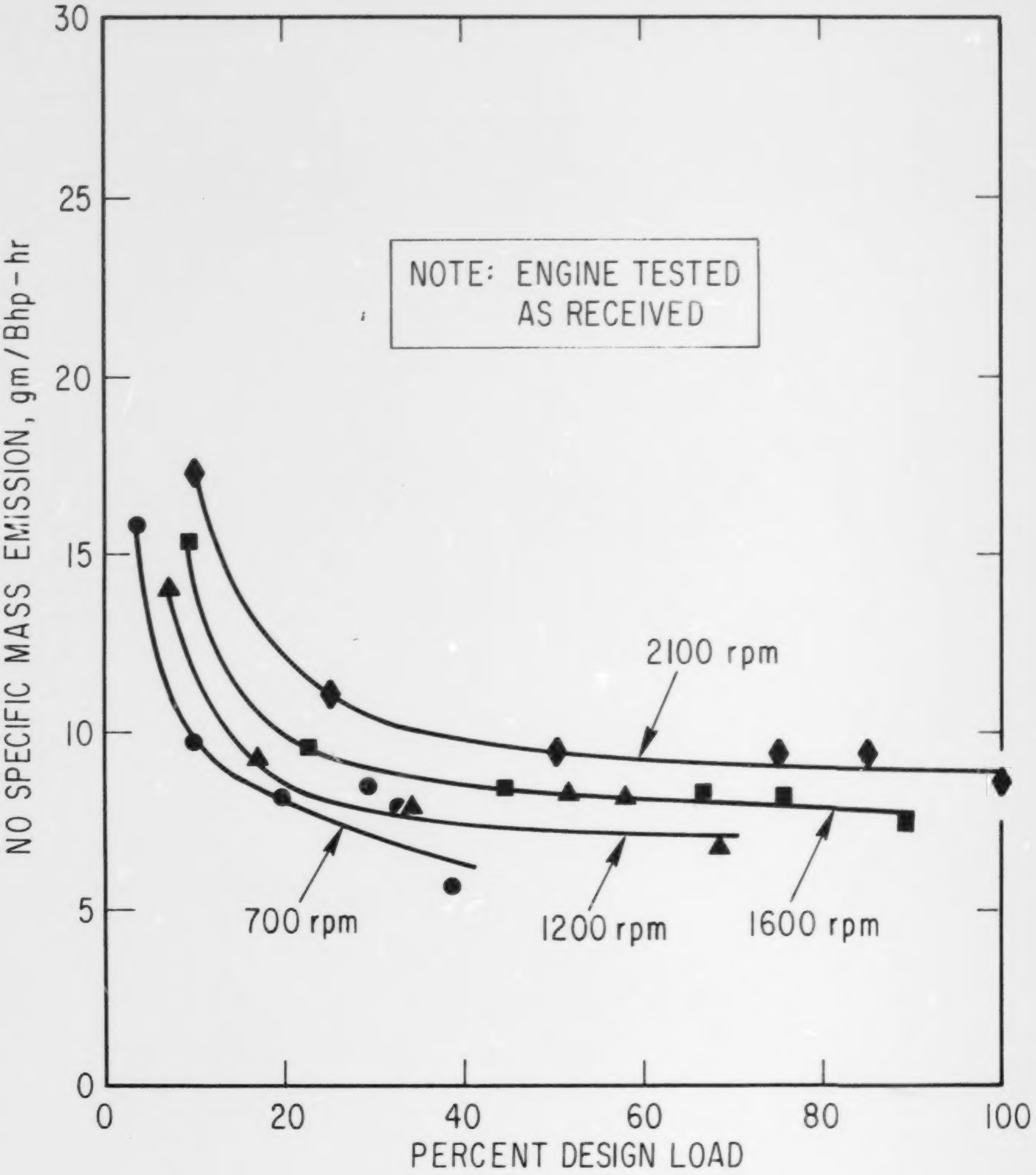

Figure B-54. Two-Cycle, Direct-Injection Diesel - Engine P - Part-Load Nitric Oxide Emissions

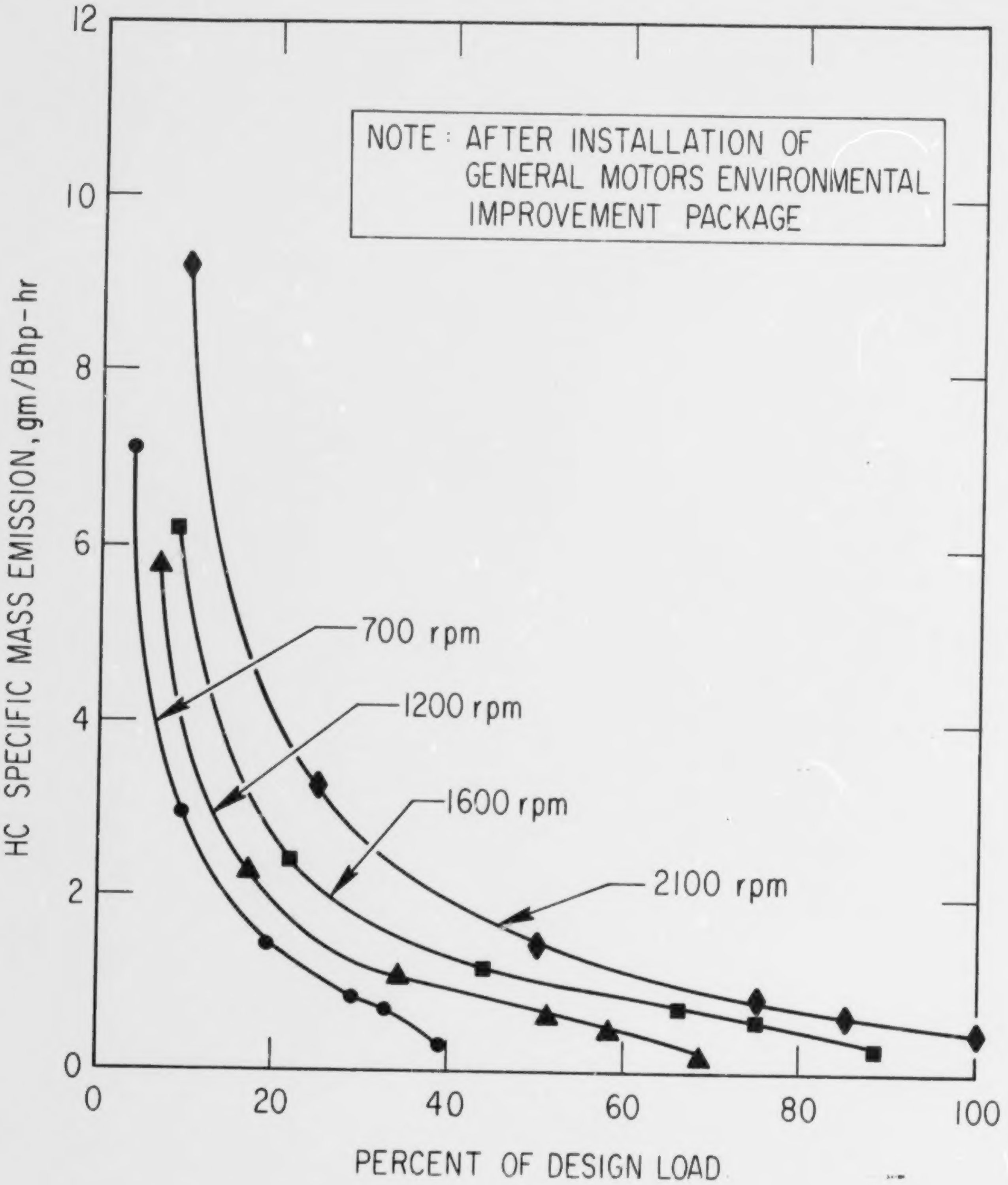

Figure B-55. Two-Cycle, Direct-Injection Diesel - Engine Q - Part-Load Hydrocarbon Emissions

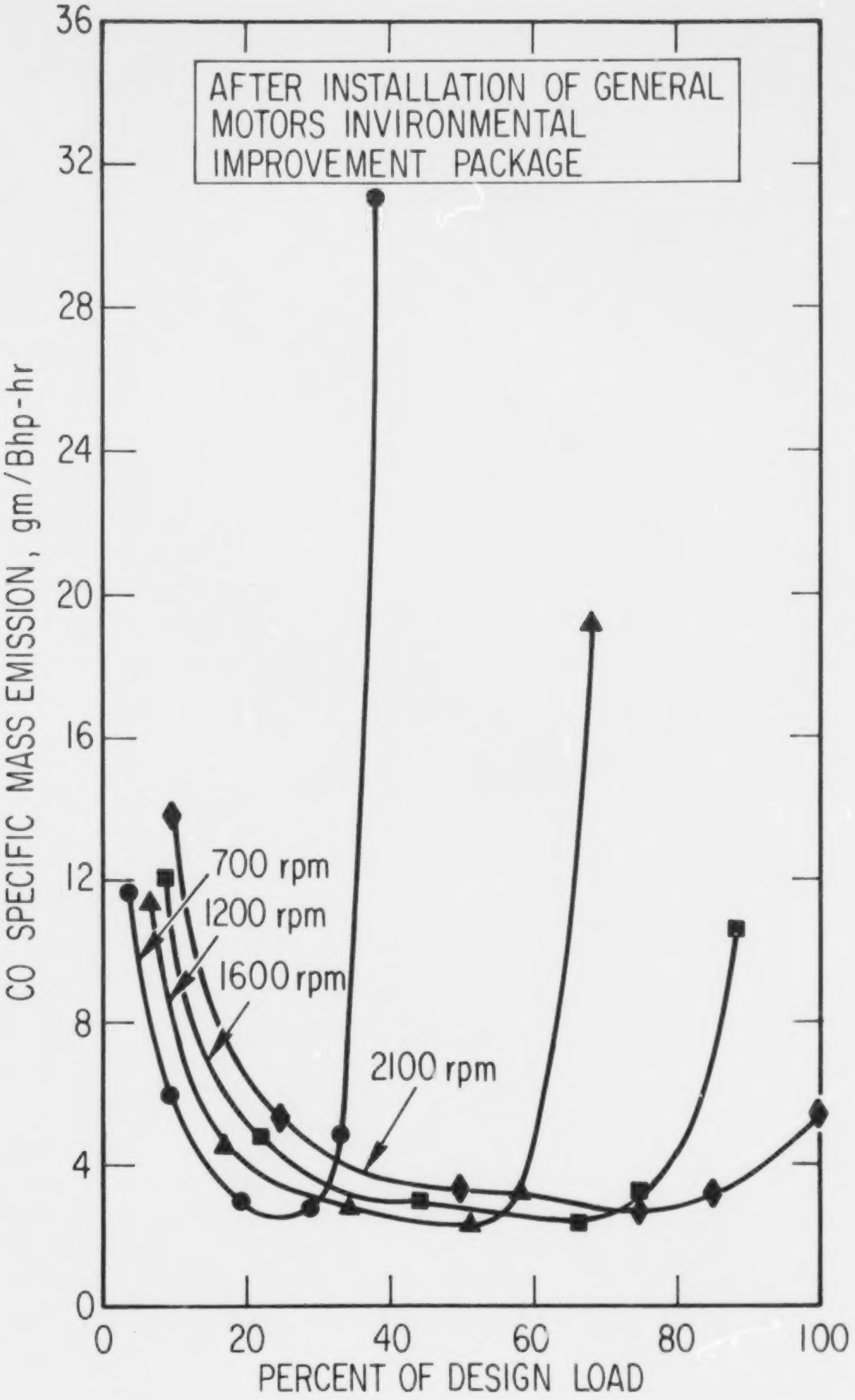

Figure B-56. Two-Cycle, Direct-Injection Diesel - Engine Q - Part-Load Carbon Monoxide Emissions

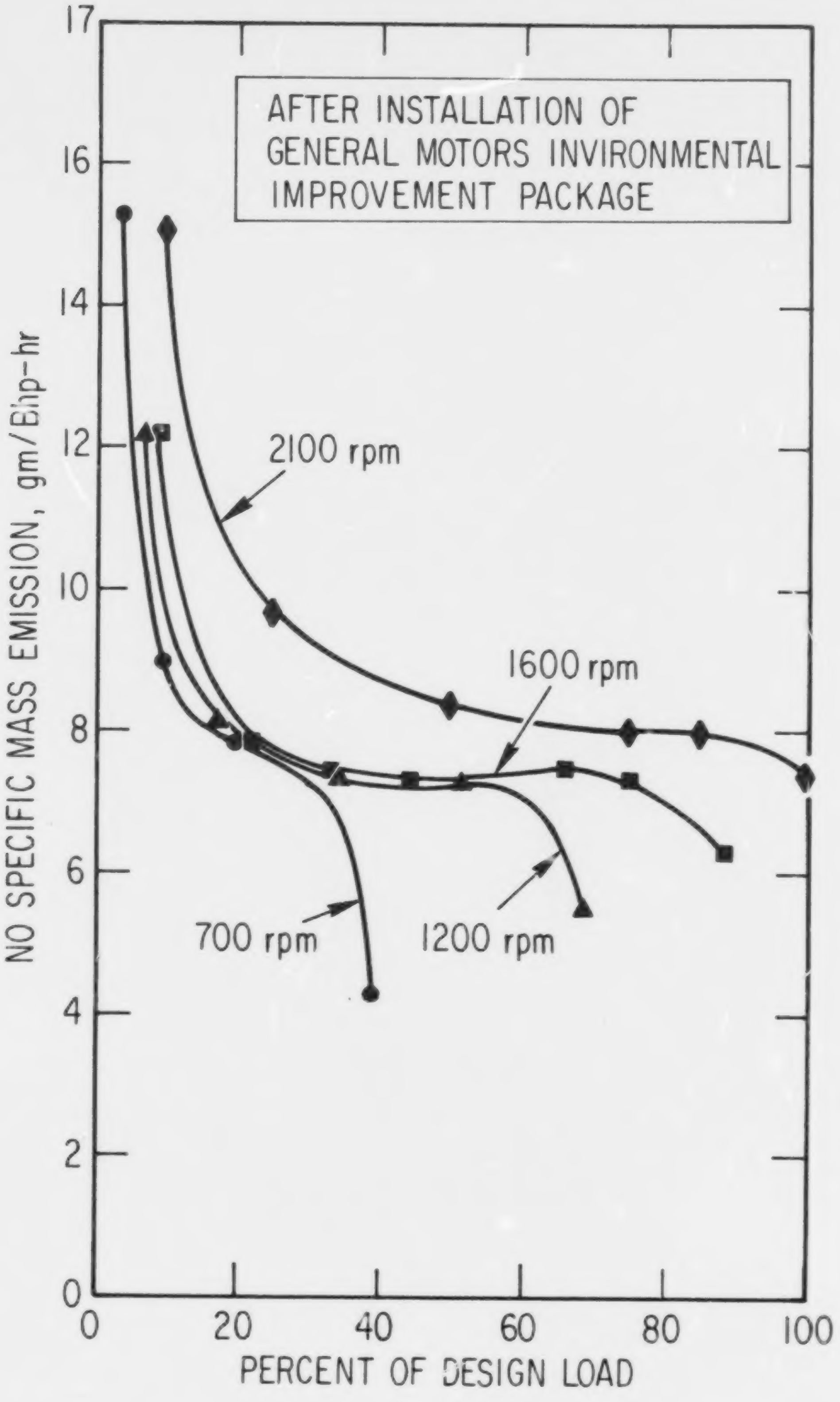

Figure B-57. Two-Cycle, Direct-Injection Diesel - Engine Q - Part-Load Nitric Oxide Emissions

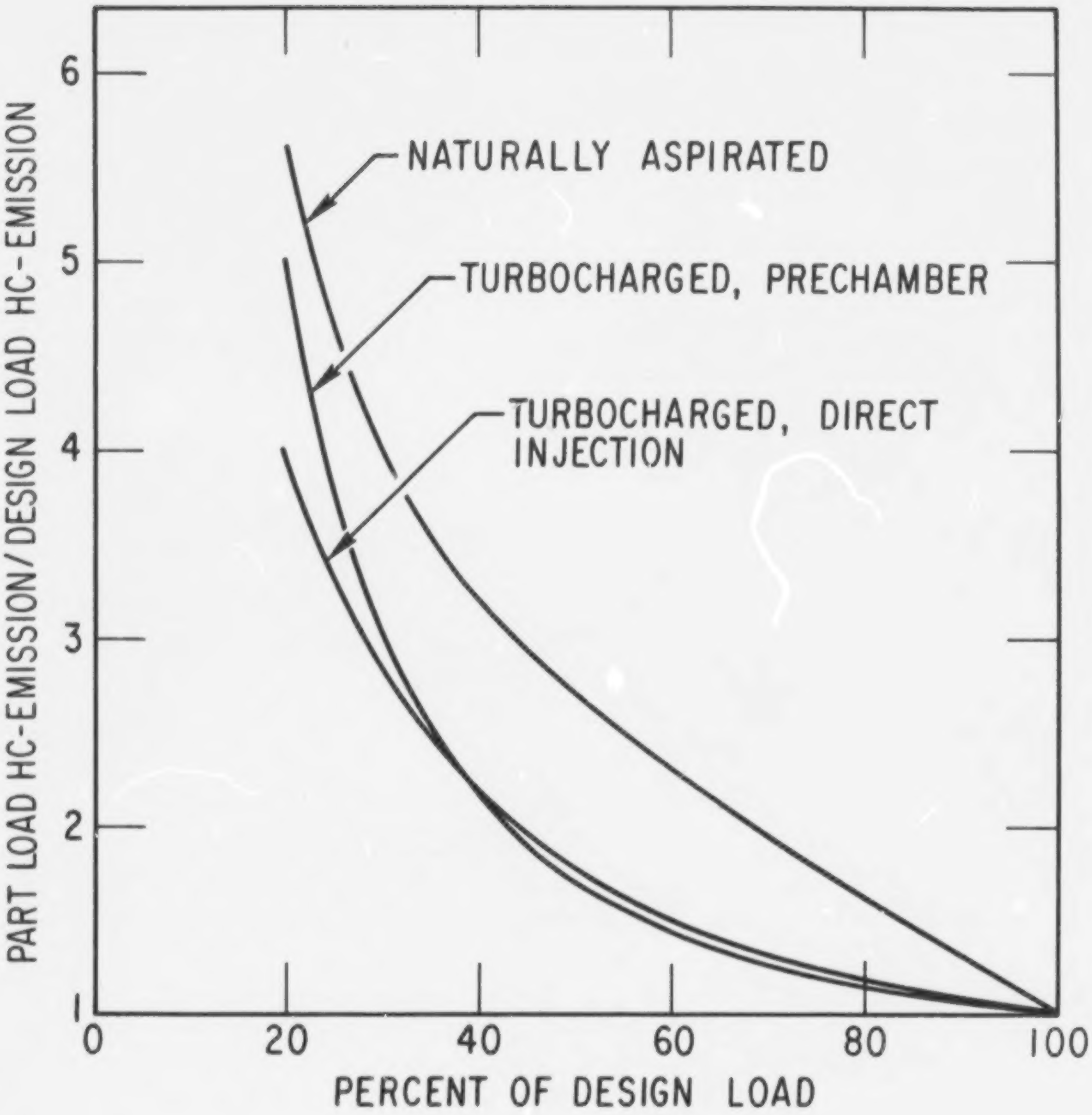

Figure B-58. Four-Cycle Diesel Engines - Hydrocarbon Emission, Steady State Part-Load, Rated Speed

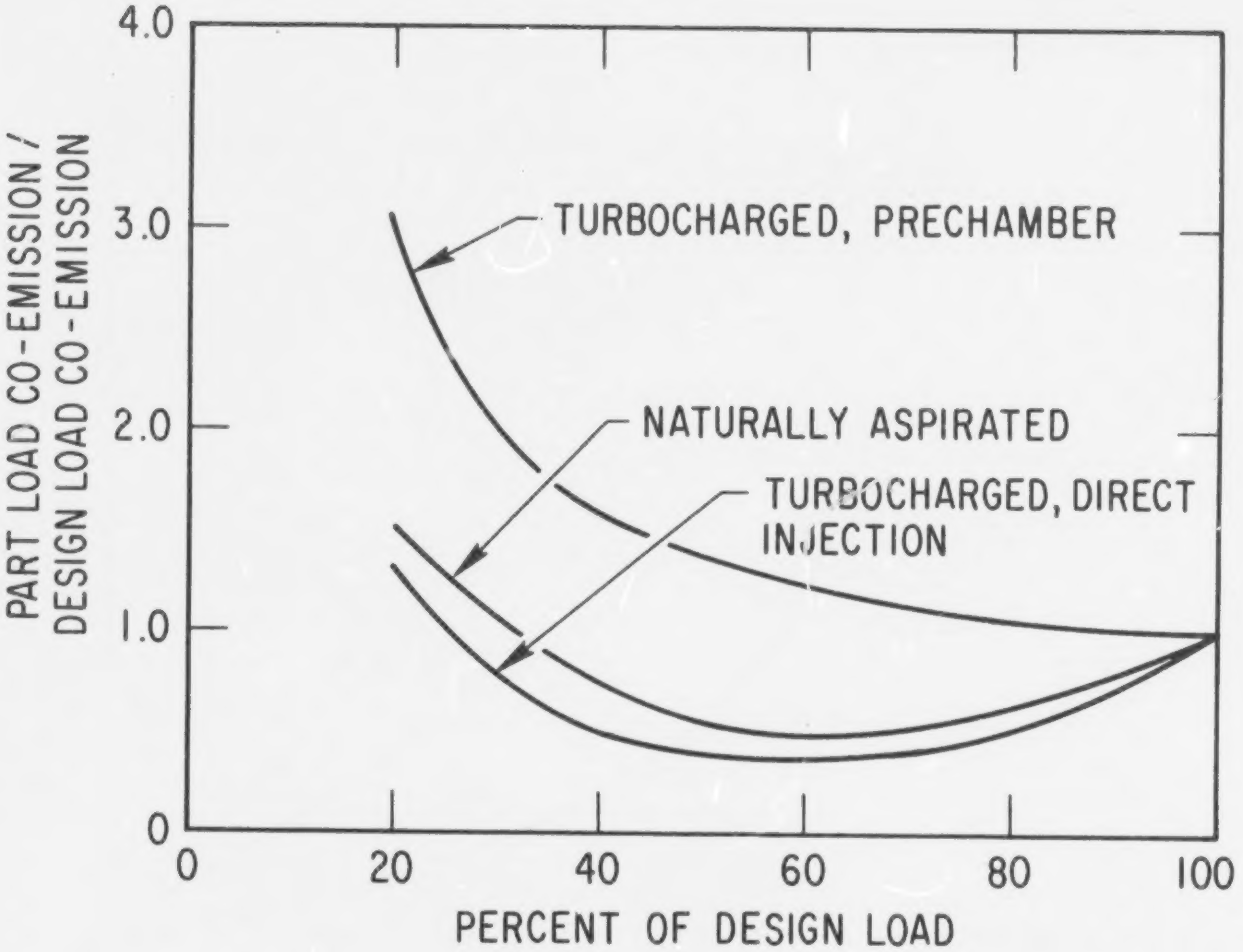

Figure B-59. Four-Cycle Diesel Engines - Carbon Monoxide Emission, Steady State Part-Load, Rated Speed

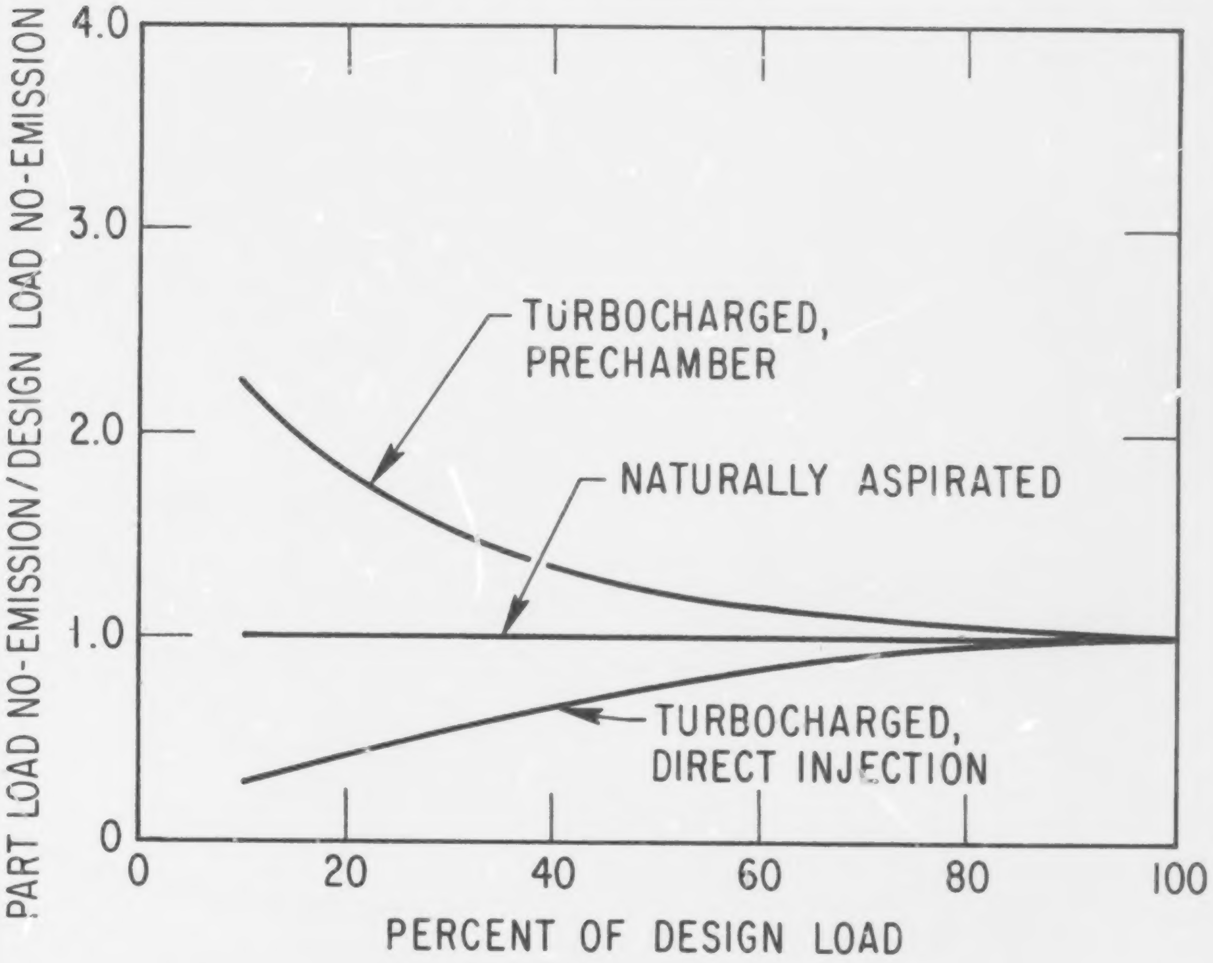

Figure B-60. Four-Cycle Diesel Engines - Nitric Oxide Emission, Steady State Part-Load, Rated Speed

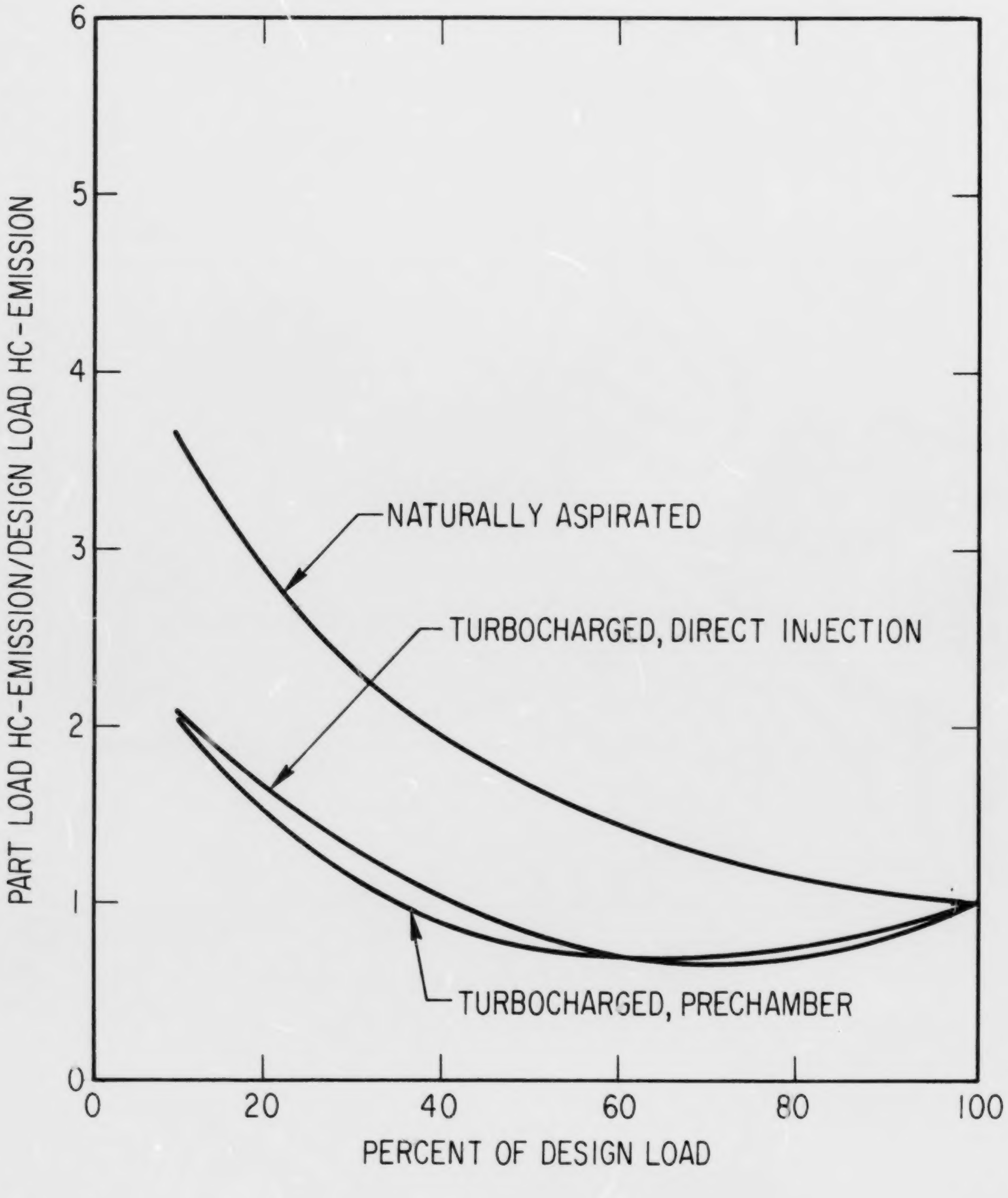

Figure B-61. Four-Cycle Diesel Engines - Hydrocarbon Emission, Steady State Part-Load, Variable Speed

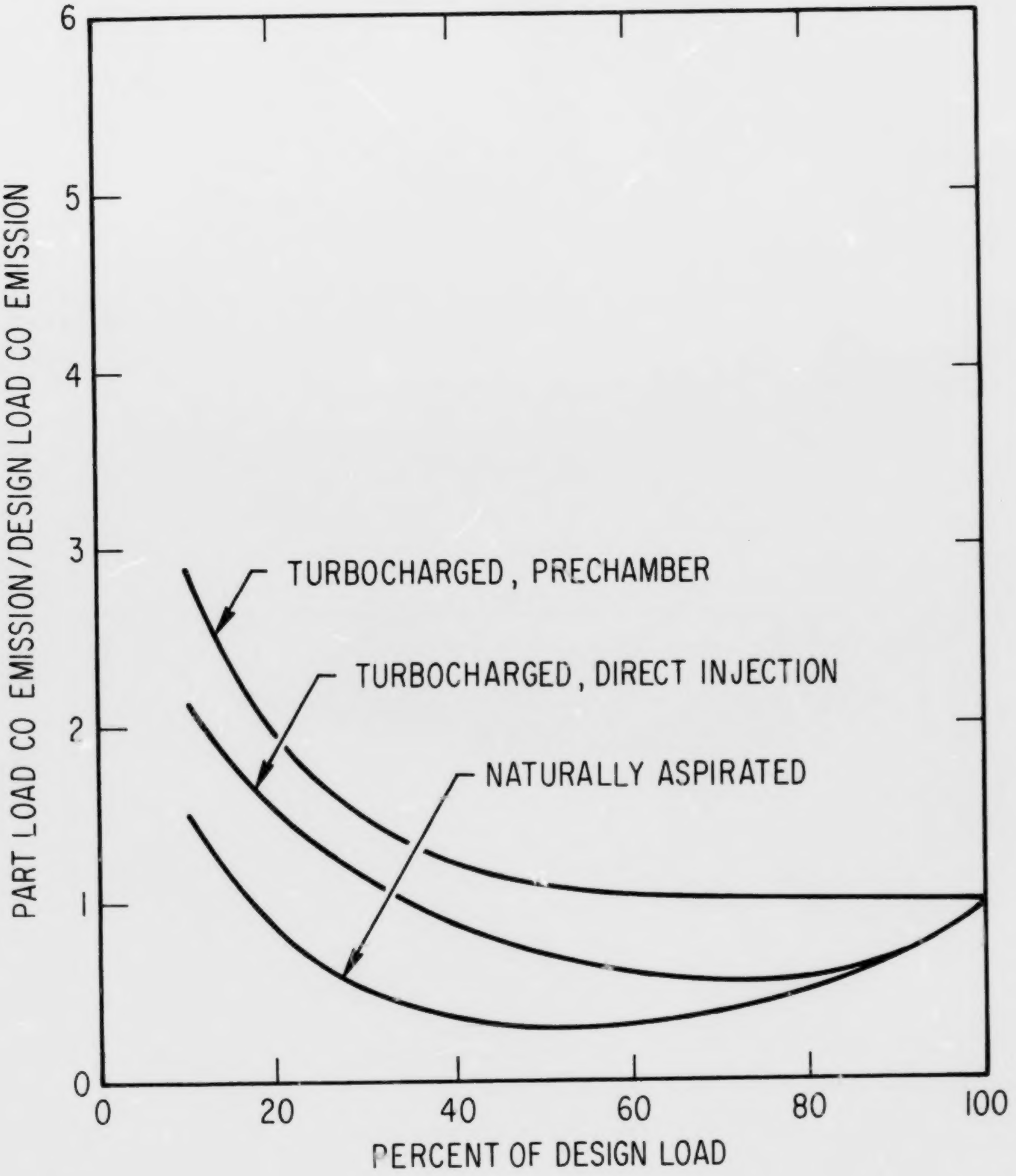

Figure B-62. Four-Cycle Diesel Engines - Carbon Monoxide Emission, Steady State Part-Load, Variable Speed

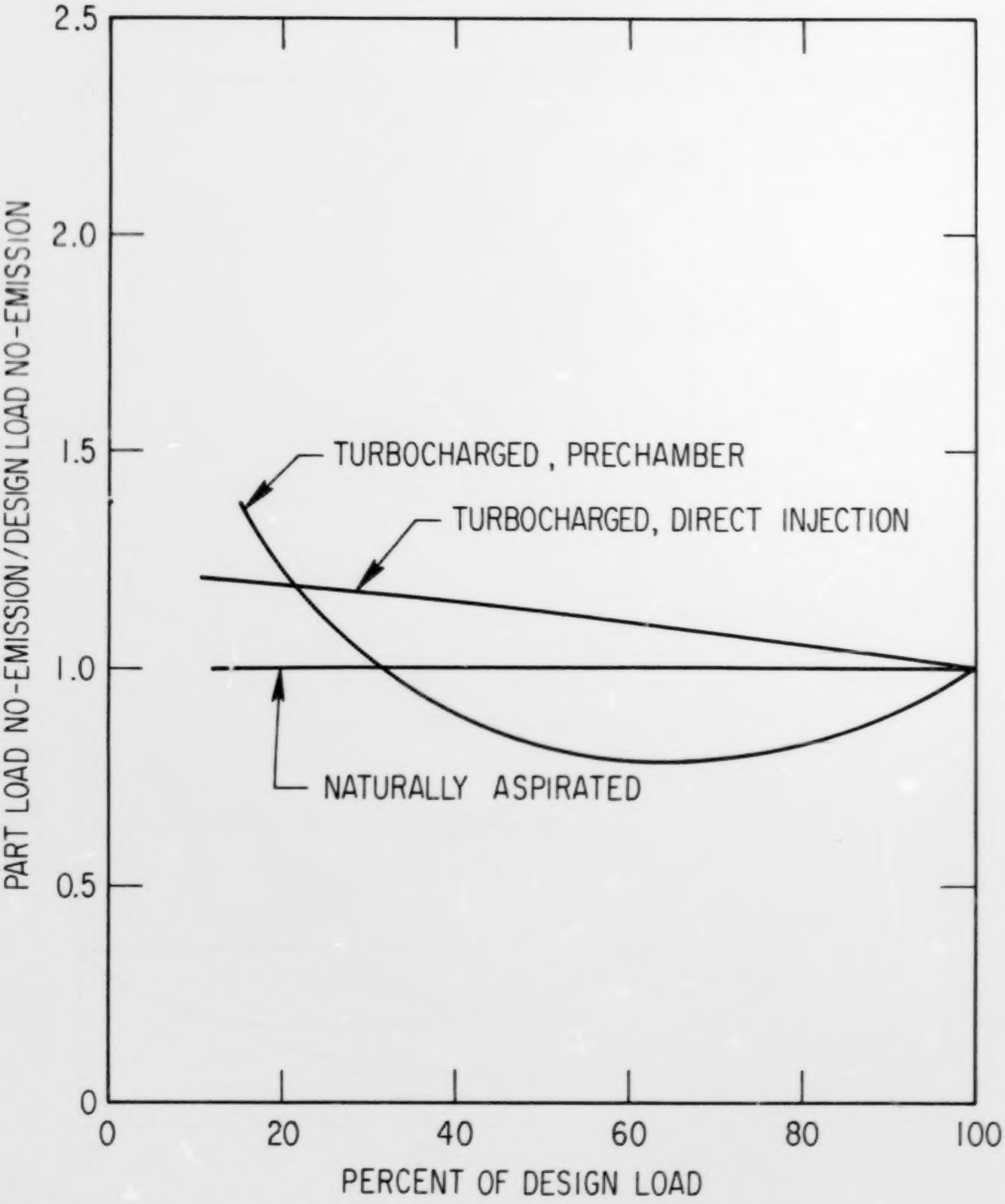

Figure B-63. Four-Cycle Diesel Engines - Nitric Oxide Emission, Steady State Part-Load, Variable Speed emission and SFC point of view to vary engine speed with load. However, in the case of a hybrid, the operating characteristics of the other system components must also be considered in selecting the optimum engine speed schedule.

A comparison of the two sets of part-load emission factors indicates that the HC emissions of the three engine configurations are lower for the variable speed schedule. For example, at 25 percent of design load, the variable speed HC emission factors are approximately half of those obtained with constant speed. In the case of CO, the differences are somewhat smaller. At 25 percent of design load, the variable speed emissions are approximately 75 percent of the constant speed values. The NO part-load emission factors of the turbocharged, prechamber diesels are lower when the speed is varied. For the naturally-aspirated, direct-injection engines, the factors are essentially independent of speed. However, the NO part-load emission factors of the turbocharged, direct-injection diesels are higher when the speed is varied. It is emphasized again that these trends were established by averaging available test data. In the case of the turbocharged, direct-injection and prechamber engines, only three sets of data each were considered and, as a result, the selected trends may not be truly representative of this engine type.

No attempt was made to establish part-load emission factors for two-cycle engines owing to a lack of available data.

The part-load emission characteristics in Figs. B-58 through B-63 are representative of the present state-of-the-art technology. Flat part-load characteristics were used in the vehicle emission calculations for the projected technology. This choice was made because of a lack of test data from engines designed for minimum emissions.

B.3.5 Cold Start Emissions

The only cold start emission data available for diesel engines are from the tests conducted by The Aerospace Corporation as a part of this study. The details of this program are contained in Appendix C of this report. Multiple bag vehicular tests indicate that there is no change in CO emissions from cold to hot conditions. HC emissions also appear to be the same for both cold and hot conditions, based on comparison of seven-mode data calculated from hot FID concentration data. The NO emissions are somewhat lower for a cold start.

B.3.6 Instrumentation

All the HC data used in this study were recorded by means of continuous hot FID instrumentation. As discussed by Hurn and Marshall (Ref. B-59), Pearsall (Ref. B-60), and Johnson et al (Ref. B-61), heating of the sample line to approximately 400°F is mandatory to prevent condensation of the heavier HC constituents contained in the exhaust of diesel engines.

Continuous NDIR instrumentation was used exclusively to measure the CO and NO concentrations. In some instances, NO_2 was measured by nondispersive, ultraviolet (NDUV) instruments, but in the majority of the tests the NO_2 was ignored. This introduces a small error, less than 10 percent. In view of the uncertainties in the concentration, flow rate, and power output data, this error is negligible for this study.

B.3.7 Other Pollutants

The diesel engine can emit other pollutants, primarily odor and smoke. Much work has been conducted in the past to study the odor characteristics of diesels (Refs. B-62 through B-64) and it is generally concluded that a relationship exists between odor and aldehydes. However, further study is required before this problem is completely understood. There are indications that the odor/aldehyde emissions from prechamber diesels are lower than those from naturally-aspirated engines. Odor from diesel engines might be reduced by fuel injection system modification. Some reduction in odor was also achieved by using a catalytic converter in the exhaust (Ref. B-62).

Smoke is largely dependent upon engine air/fuel ratio and load, however, it is also affected by combustion chamber and injection system design, type of fuel used, and engine maintenance (Refs. B-63, B-65, and B-66). Formation of smoke has been reduced by using barium additives in the fuel (Refs. B-63 and B-67).

B.4 GAS TURBINES

B.4.1 General

This section presents a detailed discussion of the exhaust emission data used to characterize the full load and part-load emissions of gas turbines. The data were acquired from both the manufacturer and the available literature. The gas turbines considered in this study and important engine design parameters are listed in Table B-6. Additional information on these engines may be obtained from the references listed.

B.4.2 Design Load Emission Characteristics

B.4.2.1 State-of-the-Art Technology

The design load specific mass emissions are presented in Figs. B-64 through B-66. The data were computed from engine flow rates and species concentrations, using the equations presented in Section B.1.3. The specific mass emissions of engines B, C, and D were obtained from the manufacturer.

A comparison of the specific mass emission data indicates large variations in unburned hydrocarbon and carbon monoxide due, to some extent, to the degree of sophistication used in the design of the combustion system. Since minimization of exhaust emissions was not a design consideration on engines A, B, C, E, and F, the relatively high HC and CO emissions, although low by comparison to uncontrolled internal combustion engines, are not representative of modern automotive gas turbines. These data are presented primarily to indicate trends. The variations in the NO emissions are considerably smaller. Engines E and F showed the lowest NO emissions of the group. However, their HC and CO emissions are among the highest, possibly indicating that rapid quenching of the chemical reactions in both primary and secondary zones of the combustor is occurring in these engines.

Table B-6. Gas Turbine Engines

Engine Identification	A	B	C	D	E	F	G	H
Manufacturer		Williams Research Corp.			Solar		General Motors Research	
Design hp	540	440	65	75	1100	350	275	275
Engine Designation	400 kw	131 L	WR 9-7	131 Q	Saturn	Spartan	GT 309	GT 309 Mod. Comb.
Compressor	2-stage, radial	1-stage, radial	1-stage, radial	-----	8-stage, axial	single-stage radial	------	--------
Turbine	------	1-stage, axial	2-stage, axial	-----	3-stage, axial	single-stage radial	------	--------
Regenerator	Yes	No	No	Yes	No	No	Yes	Yes
Pressure Ratio	8.2	5.1	4.0	3.8	6.5	3.5	------	--------
Turbine Inlet Temp., °F	1600	1600	1980	1700	1500	1500	1700	1700
Number of Shafts	1	1	1	1	1	1	2	2
References	B-68	B-69 and B-70			B-71		B-72, B-73, B-74	

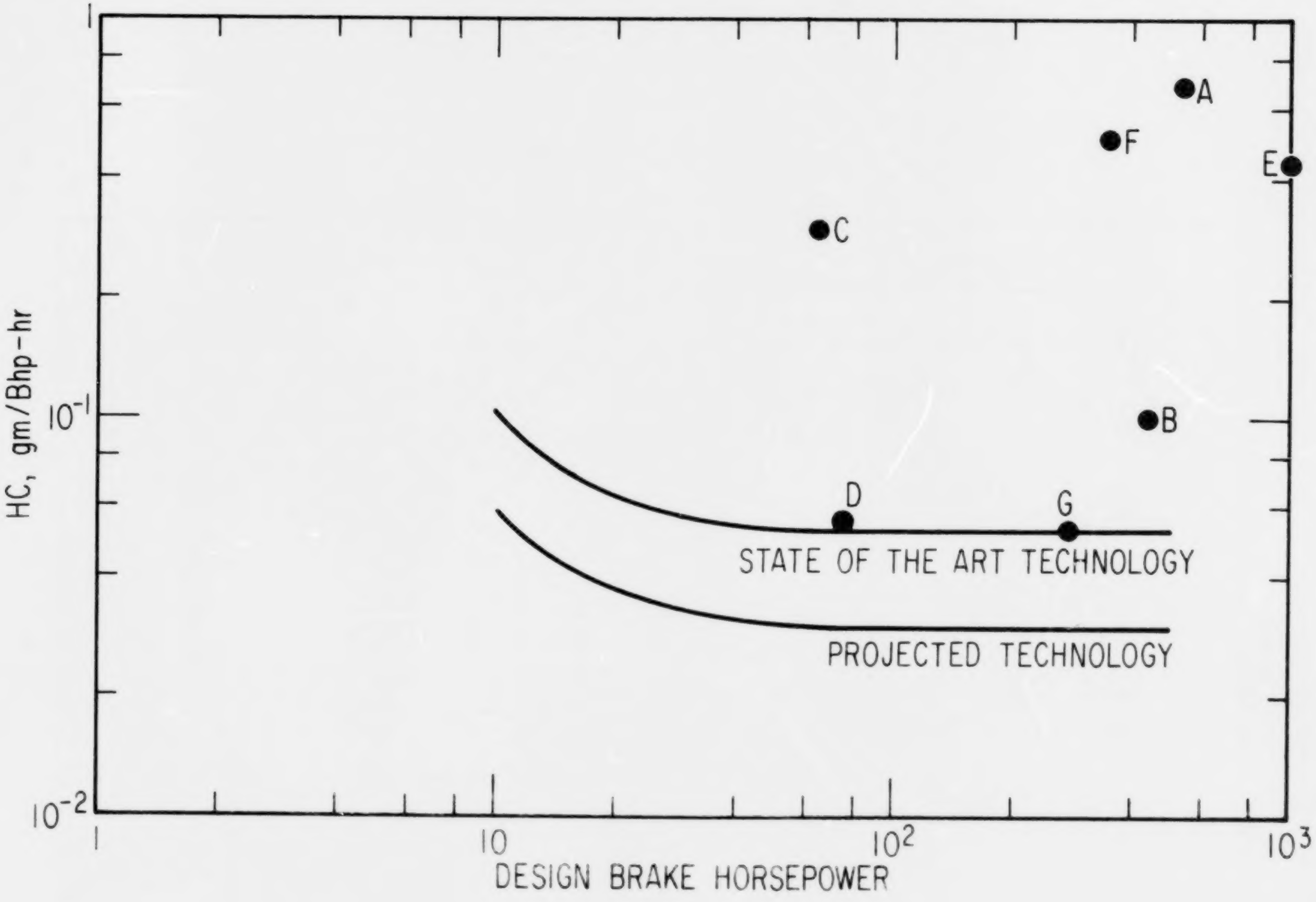

Figure B-64. Gas Turbines-Hydrocarbon Emission, Steady State Design Load

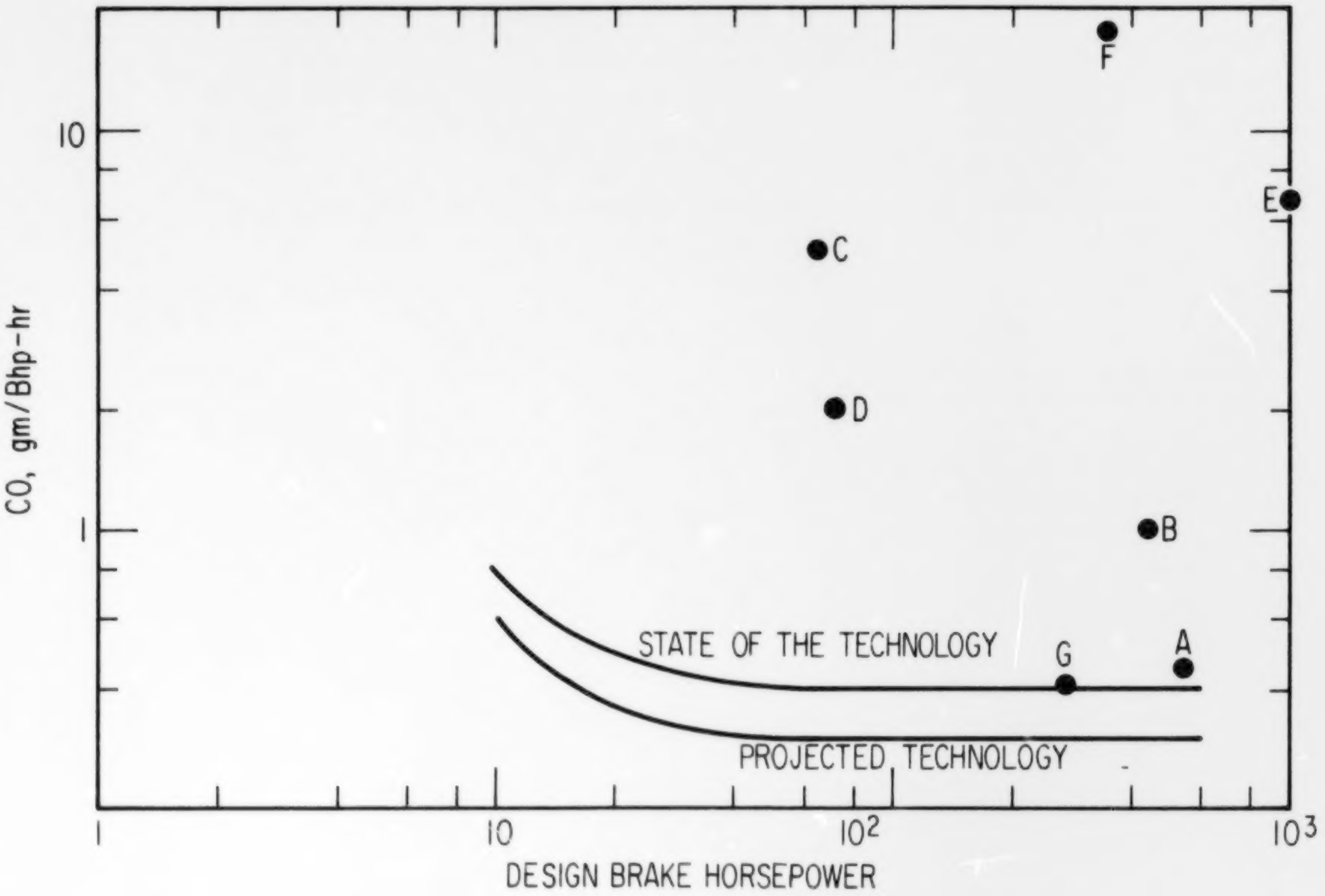

Figure B-65. Gas-Turbines-Carbon Monoxide Emission,
Steady State Design Load

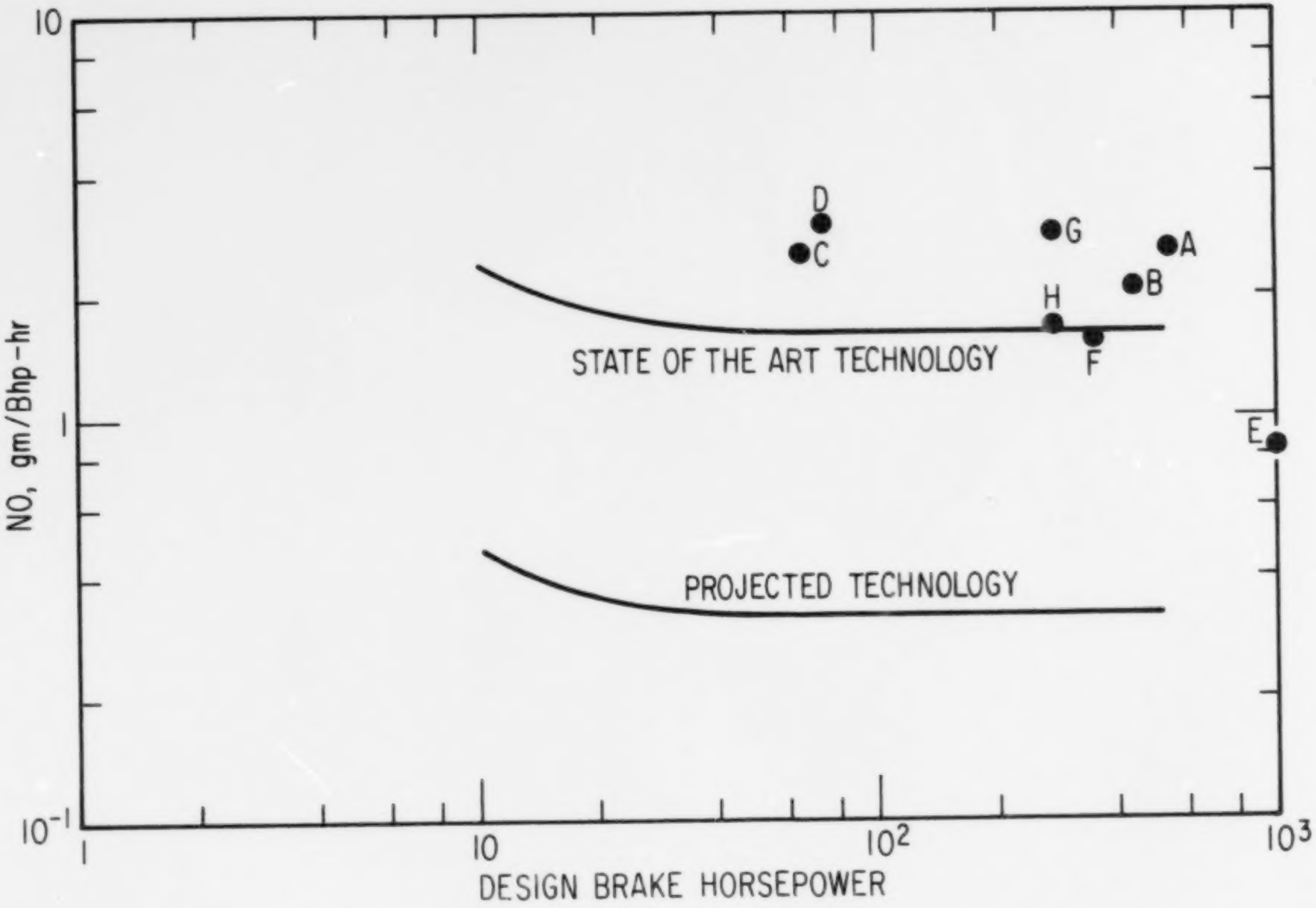

Figure B-66. Gas Turbines-Nitric Oxide Emission, Steady State Design Load

The design load specific mass emission correlations representing present state-of-the-art technology were drawn through points G and H, Figs. B-64 through B-66. Engine G is the General Motors Research gas turbine which was designed for automotive applications. The so-called standard burner is used on this engine (Refs. B-73 and B-74). Engine H is basically the same GT-309 gas turbine as engine G, with the exception of a modified burner designed for minimum NO (Ref. B-74). A more detailed discussion of the effects of burner design on emissions is presented below. Although there is some indication that the hydrocarbon and carbon monoxide emissions of engine H are actually somewhat higher than for engine G, the G levels are considered as representative of present state-of-the-art technology.

The design load emission correlations shown in Figs. B-64 through B-66 are flat for engine design loads above 50 hp. Below that point, the specific mass emissions are assumed to increase as a result of lower turbomachinery efficiencies. In addition, wall quench effects may become increasingly important, resulting in higher HC and CO concentrations. The HC and CO specific mass emissions are assumed to increase similarly, while NO increases less.

B.4.2.2 Projected Technology

A comparison of the specific mass emission data presented in Figs. B-64 through B-66 indicates that nitric oxide poses the most serious emission problem in gas turbines, and significant improvements must be made before the future emission goals can be met.

Studies performed by Cornelius and Wade (Ref. B-74), Sawyer et al (Refs. B-75 through B-78), have pointed the way towards lower nitric oxide emissions. The formation of nitric oxide is kinetically controlled and is rather slow by comparison to the other chemical reactions in the burner. The most direct approach towards NO control is to reduce the maximum local temperature in the combustion chamber. The use of a lean primary zone is a promising method of reducing that temperature. Another approach of NO control is the quenching of the NO formation reactions immediately downstream of the primary zone of the burner. This is accomplished by adding secondary air further upstream in the burner, thereby reducing the residence time of the combustion gases in the primary zone. A similar approach has been used by Bell (Ref. B-79) in stationary gas and steam turbine burners. Although this method has been shown to be effective in reducing nitric oxide (Ref. B-74), it may actually result in higher HC and CO emissions because of thermal quenching of the HC and CO reactions. As shown by Sawyer (Ref. B-78), the CO concentrations in the primary zone of the burner are initially very high. At the relatively low temperatures in the secondary zone, the HC and CO reactions are progressing at a slower rate, and generally the stay time is not sufficiently long to reach completion of these reactions.

In addition to primary zone quenching, General Motors Research has also investigated the effect of primary zone equivalence ratio variations on nitric oxide emissions (Ref. B-74). Results from that program indicate that the nitric oxide emissions were reduced by a factor of approximately 2 without adversely affecting engine and burner operation and the emissions of hydrocarbon and carbon monoxide. Further improvements are believed to be possible through additional work on the burner, including optimization of primary and secondary zones, inlet air temperature, mixture and mass flow distribution, and addition of EGR. Based on these considerations, a reduction of the NO emissions by a factor of 5, compared to present state-of-the-art values appears to be feasible. This factor was used to draw the projected NO curve in Fig. B-66. The projected HC and CO emissions are reduced by a factor of 2.

Again, constant specific mass emissions were assumed for design power levels above 50 hp. At lower design powers the emissions are assumed to increase.

B.4.3 Part-Load Emissions Characteristics

The part-load emission characteristics of engines A, B, C, D, G, and H are depicted in Figs. B-67 through B-69. No part-load data were available from engines E and F. The information is presented as the ratio of part-load emission to design load emission versus percent of design load. The specific mass emission factors for engine configurations G and H were computed from species concentration and flow rate data (Refs. B-73 and B-74) and engine HP versus gasifier speed curves (Ref. B-72). According to discussions with General Motors (Ref. B-80), this approach is acceptable. However, there is some uncertainty in the specific mass emission data of engines G and H below approximately 25 percent of design load because of uncertainties in the corresponding power output values taken from Ref. B-73.

The HC and CO specific mass emissions increase with decreasing load (Figs. B-67 and B-68). Engines C, D, and G have comparable hydrocarbon and carbon monoxide emission characteristics, while engines A and B show greater increases with decreasing load. In all cases, this increasing trend is due largely to a reduction of turbomachinery efficiency. In addition, cycle efficiency decreases with decreasing load as a result of decreasing turbine inlet temperature, except for engine G which operates at constant turbine inlet temperature down to approximately 35 percent of design load.

There are basic differences in the part-load nitric oxide emission characteristics of the turbines considered in this study. According to Fig. B-69, the nitric oxide specific mass emissions of engines A, B, and C increase with decreasing load. The increase is primarily the result of lower thermodynamic cycle efficiency at part-load. This is a typical characteristic of simple gas turbines. Initially, the part-load nitric oxide emissions of engines G and H increase with decreasing load primarily as a result of increasing burner inlet air temperature. As the degree of power transfer is reduced, both burner and turbine inlet temperature decrease rapidly, resulting in lower specific mass emissions of nitric oxide. At very low

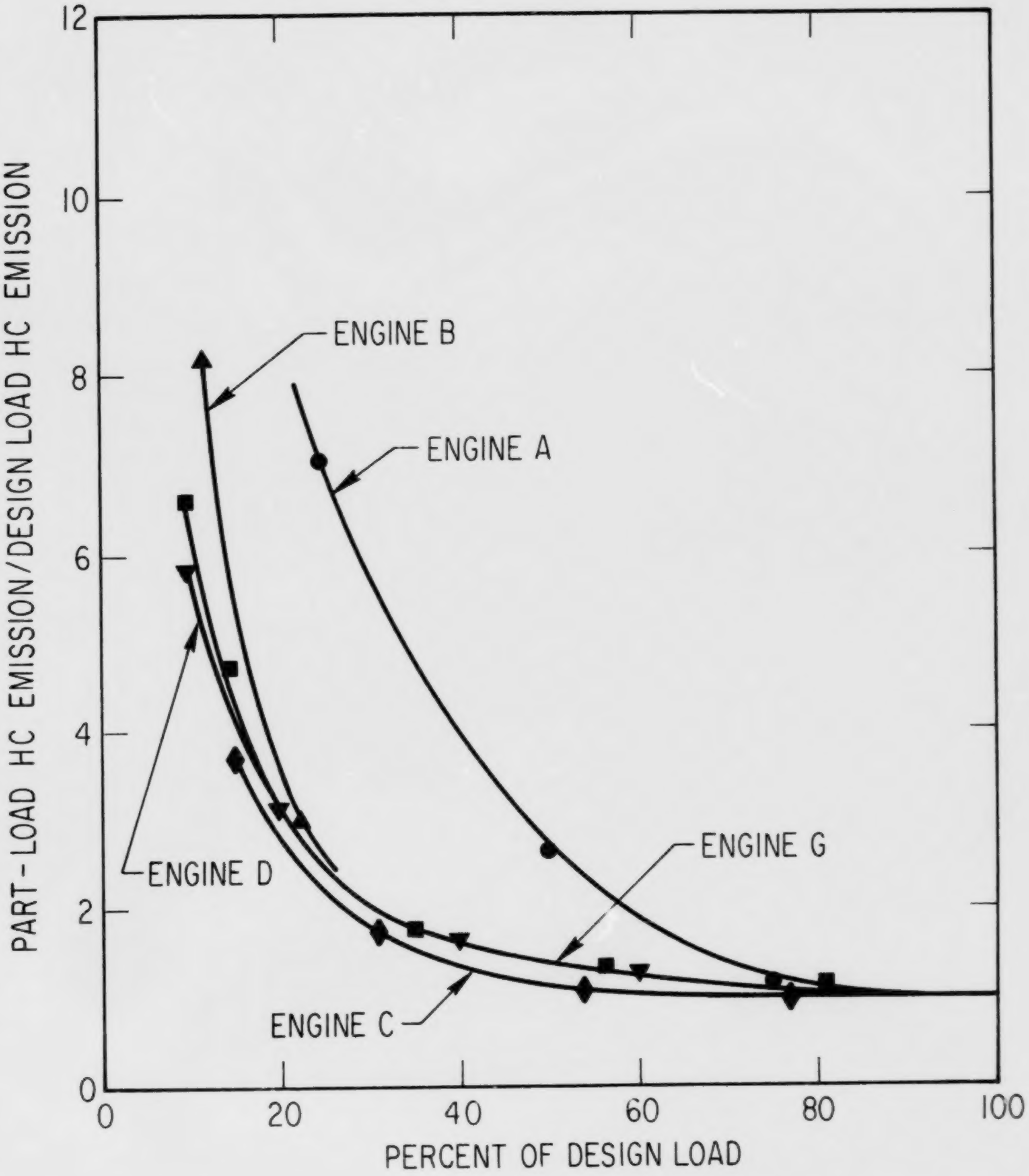

Figure B-67. Gas Turbine Test Data Part-Load Emissions

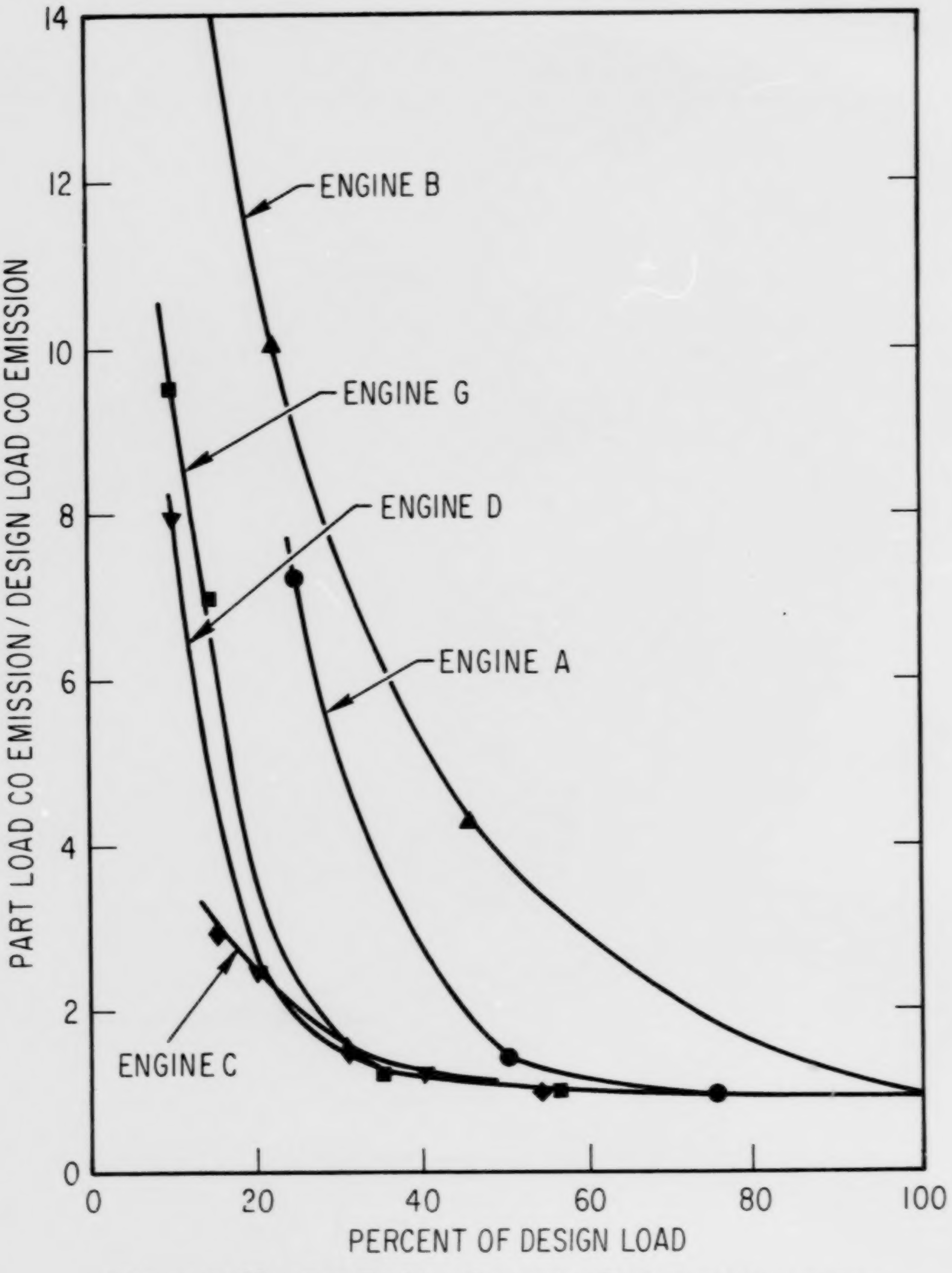

Figure B-68. Gas Turbine Test Data Part-Load Emissions

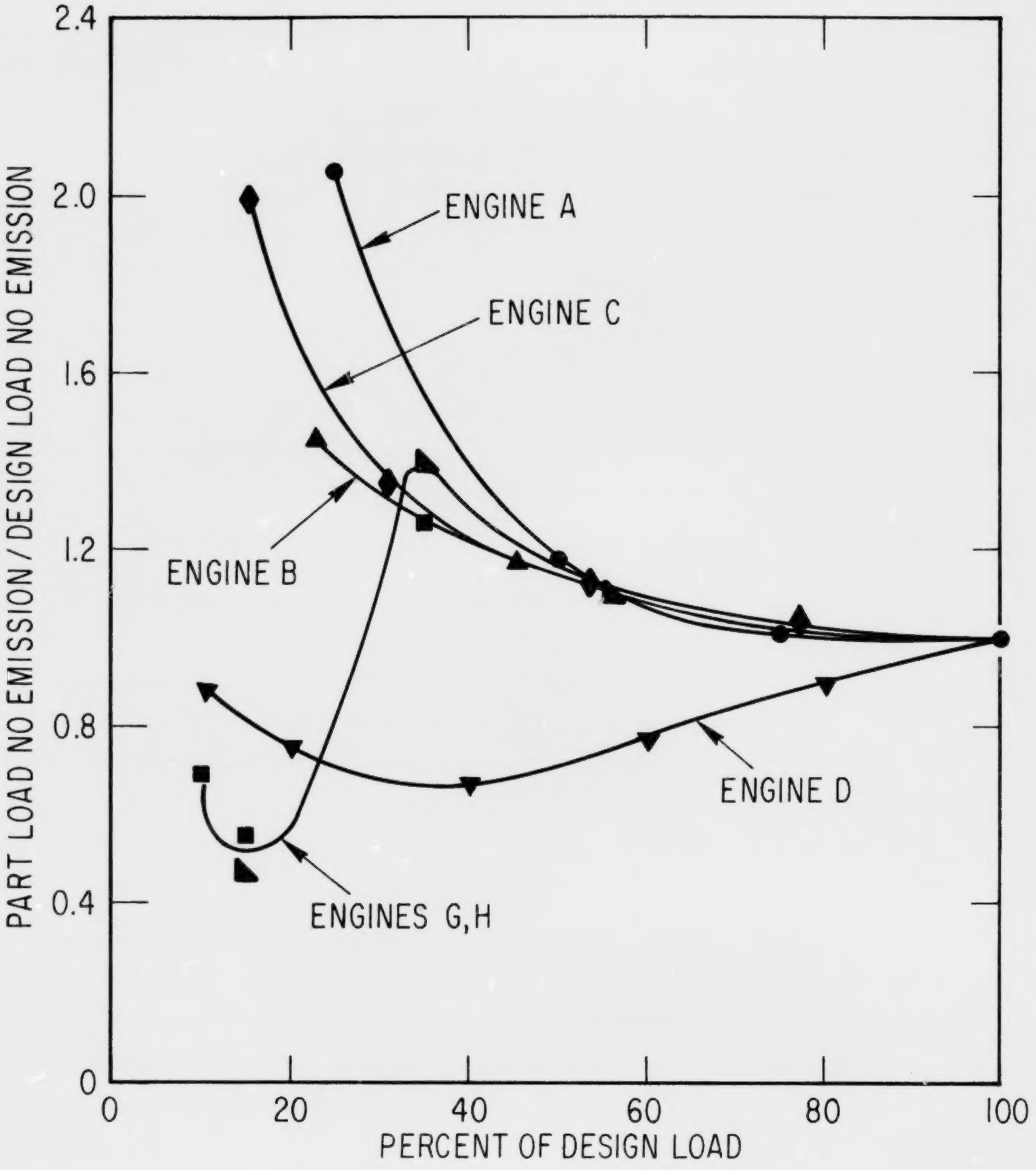

Figure B-69. Gas Turbine Test Data Part-Load Emissions

part-loads, the NO emissions increase again as a result of rapidly decreasing turbomachinery efficiencies. Since the General Motors Research GT-309 gas turbine was designed for automotive use, with exhaust emissions a design consideration, its part-load emission characteristics were selected for use in this study. The part-load specific mass emission factors for gas turbines are presented in Fig. B-70. It should be pointed out that the NO part-load curve could be modified somewhat by changing burner and turbine inlet temperatures.

The part-load emission characteristics for the projected technology are assumed to be identical to the present state-of-the-art characteristics. Thus the curves presented in Fig. B-70 are considered applicable to both state-of-the-art and projected technologies.

B.4.4 Cold Start Emissions

The effect of a cold start on gas turbine emissions was evaluated from the data published by Korth and Rose (Ref. B-81) and Cornelius et al (Ref. B-73). A Chrysler gas turbine automobile was road-tested by Korth and Rose over a composite 7.5-mi route at an average speed of approximately 25 mph. Based on three cold start and six hot start cycle tests, the ratios of cold start versus hot start emissions for HC, CO, and NO are 1.21, 1.17, and 0.89, respectively. These ratios are in reasonable agreement with the spark ignition engine factors.

According to Cornelius (Ref. B-73), the CO concentration is approximately 160 ppm for a cold cycle of the seven-mode test procedure and approximately 50 ppm for a hot cycle. This ratio agrees qualitatively with the data from Ref. B-81. Additional experimental work is required before the question of cold start versus hot start emissions from gas turbines can be adequately answered.

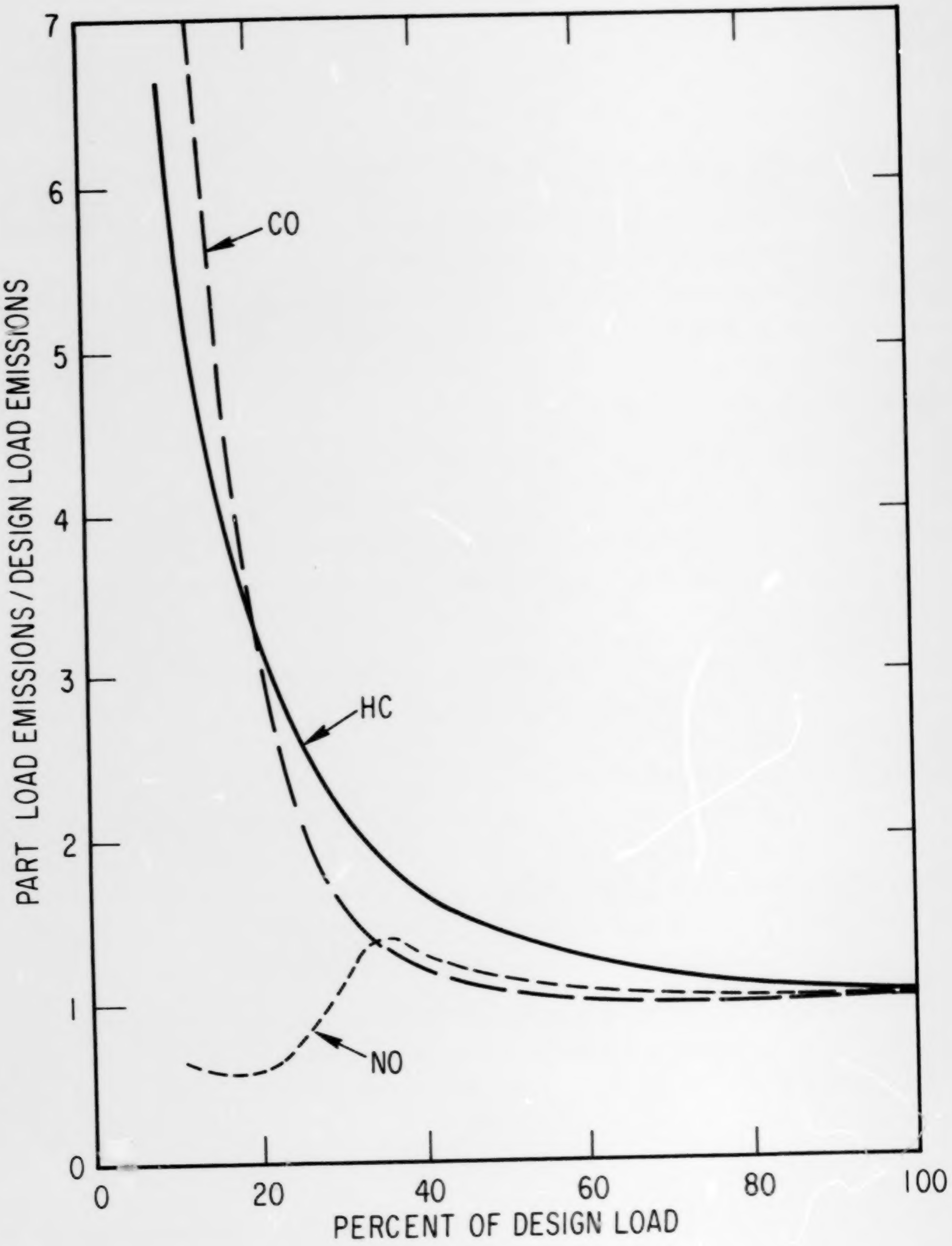

Figure B-70. Gas Turbines - HC, CO, NO, Emissions, Steady State Part-Load

B.4.5 Effect of Fuel on Gas Turbine Emissions

Although it is recognized that exhaust emissions may be affected by the type of fuel used in the burner, no attempt was made to use fuel type as a correlating parameter. Also, the reactivity of the hydrocarbon constituents was neglected in this study. Analysis by General Motors (Ref. B-73) indicates that the reactivity of the HC emissions from gas turbines is very comparable to that from gasoline engines.

B.4.6 Instrumentation

To assure validity of the test data obtained from the various sources, a brief review was made of the instrumentation and experimental techniques used in the tests. It is concluded that the data are accurate within the normal band of uncertainty.

Heated FID was used on all tests and as a result, condensation of the heavy hydrocarbon species was largely eliminated. Carbon monoxide was always measured by NDIR. Different techniques were used for NO. The phenol disulfonic acid procedure (PDS) was used on engine A and the grab sample was analyzed approximately 24 hr after the tests. A modified Saltzman method was used on engines B, C, and D, and NDIR on engines E and F. All three methods were used on engine G and good agreement was achieved over the whole range of engine operating conditions (Ref. B-74), provided adequate time was allowed before the Saltzman method was used.

It should be pointed out that the hydrocarbon emissions from gas turbines are often very low in concentration and the background HC level can no longer be neglected. Since this is not always recognized, some of the reported HC levels might be too high.

B.4.7 Other Pollutants

Although this study is only concerned with the emission of hydrocarbon, carbon monoxide, and nitric oxide, a few comments on the other pollutants emitted from gas turbines are in order. Often smoke can be observed in the exhaust of gas turbines, primarily at high loads. This is the result of locally fuel-rich zones in the combustor. Much progress to alleviate this problem has been made. For example, pre-vaporization of the fuel has been an effective method to reduce smoke. Aldehydes are believed to be related to lean combustion and to the temperature-time history of the combustion products (Ref. B-73). The only aldehyde data available are from engines A and G. In both cases the level is of the order of 2 ppm, which is the limit of sensitivity. Sulfur dioxide emission is directly related to the sulfur content in the fuel and control is achieved by limiting the allowable sulfur content. Control of smoke and sulfur dioxide appears to be well in hand. However, additional work is required to characterize the emissions of aldehydes from gas turbines and to develop methods which will effectively reduce these products.

B.5 RANKINE ENGINE EMISSIONS

B.5.1 General

The Rankine engine emission characteristics presented in this report were derived from test data published in the available literature. The emission data reported by Vickers et al (Ref. B-82) were obtained from an experimental burner/boiler test setup that was designed to simulate the operating conditions of the General Motors SE-101 automotive Rankine cycle engine. Emission data from the General Motors SE-124 steam car and from a Doble automobile, tested by General Motors, are reported by Vickers et al (Ref. B-83). Miner (Ref. B-84) presents emission data from a Williams steamer. The work of Burkland et al (Ref. B-85), Morgan and Raymond (Ref. B-86), and Altshuler and Caretto (Ref. B-87) was primarily concerned with burner and nozzle development or evaluation. Since exhaust emissions from Rankine cycle engines are strongly affected by the burner and boiler design, the configurations are briefly described.

B.5.2 Engine and Test Description

The General Motors steam engine SE-101 (Ref. B-82) is a closed Rankine cycle engine designed for 160 hp. Its maximum efficiency is approximately 15 percent. The boiler is a monotube design and is divided into three sections: an economizer, an evaporator, and a superheater. The burner is designed for high combustion efficiency, uniform temperature profile of the combustion gases leaving the burner, good off-design operating characteristics, and low emissions. No air preheater is used, since the combustion gas temperature at the boiler exhaust is relatively low. The specific heat release rate is 3.7×10^6 Btu/hr-ft^3. Since the burner is operated at ambient pressure, it is considerably larger than an equivalent gas turbine combustor. Depending upon load, the air/fuel ratio of the burner varies between approximately 25 and 40. The corresponding combustion gas temperatures at the boiler inlet are approximately 2500 and 1900°F, respectively. An air atomizing fuel nozzle is utilized on the engine. Kerosene was used on all emission tests.

The burner used with the General Motors SE-124 steam engine is a vortex type and uses air atomized fuel injection. The specific heat release rate was reduced to 950,000 Btu/hr-ft^3 in an effort to reduce HC and CO emissions. The burner is operated at constant fuel flow rate and power is controlled by means of OFF/ON operation.

A 1923 Doble automobile was also tested at General Motors (Ref. B-83). The burner of that engine was designed for a specific heat release rate of only 300,000 Btu/hr-ft^3. Thus, the residence time of the combustion gases is much longer than that of the SE-124, and particularly longer than that of the SE-101.

The Williams steamer was tested for emissions at the Mobil Oil Company Laboratories, Paulsboro, New Jersey. The car was operated on a chassis dynamometer over the California seven-mode driving cycle. Little detail was given about the engine except that the design was based upon the experience gained over the last 30 years.

A very extensive burner development program has been conducted by the Marquardt Company, Van Nuys, California (Ref. B-85), under contract to APCO. The Marquardt effort was primarily aimed at developing design criteria for continuous flow, low emission, external burners for use in Rankine cycle engines. Many component and operating variables were varied, including air/fuel ratio, air/fuel mixing, residence time of the combustion gases in the burner, and fuel type. The burners were designed for a heat release rate of 500,000 Btu/hr and are of cylindrical shape, having an outside diameter of 5 in. and a length of 36 in. The design specific heat release rate is 1.25×10^6 Btu/hr-ft^3, approximately one-third of that in the General Motors SE-101 burner and may, in part, explain the lower emissions of the Marquardt burner. A heat exchanger was installed at the end of the burner to simulate the cooling of the combustion gases in the boiler.

Three fuel injection configurations were analyzed in the Marquardt program. In the first configuration, fuel vapor is injected into a small mixing section and the premixed air/fuel mixture was then injected into the combustion chamber. The second injector has multiple slots arranged around the periphery at the inlet of the burner. Fuel vapor is injected through these openings radially inward, and the vapor jets are then broken up by the high-velocity air being injected axially through a small tube at the heat of the burner and by the recirculating gases. This configuration represents the sudden expansion (SUE) burner concept patented by Marquardt. The third injector is a pressure atomizing spray nozzle designed and manufactured for liquid fuels by the Spraying Systems Company. Three types of fuels were tested in the program: trimethylhexane, kerosene, and methane.

The emission data presented in Ref. B-86 are from a burner developed by Thermo Electron Corporation, Waltham, Massachusetts, for use in a 3 kw engine/generator set. The burner is designed for a specific heat release rate of 2.8×10^6 Btu/hr-ft^3. No other details are available.

A boiler designed by Bessler Boilers, Emeryville, California was used in the program conducted by Altshuler and Caretto (Ref. B-87). This boiler is a single-pass monotube type and is similar in design to the boiler used on the Doble steam cars. The integrated burner/boiler is 15 in. in diameter and 17 in. high. The volume of the burner is approximately 0.18 ft^3 and the specific heat release rate is approximately 1.1 x 10^6 Btu/hr-ft^3. Air is used to cool the inner wall of the burner before entering the combustion chamber. Four Monarch F-80 high-pressure fuel nozzles, having different flow rates and spray patterns, were used in the program. Axial location of the nozzles was varied and emission data were gathered for the optimum positions.

B.5.3 Combustion and Exhaust Emission Characteristics

Exhaust emission concentration measurements have been conducted by General Motors over a range of air/fuel ratios, air flow rates, burner air inlet temperature, and for a number of burner configurations. Some of the test results obtained by General Motors from the SE-101 burner testing are presented in Figs. B-71 and B-72. The effect of air/fuel ratio on hydrocarbon, carbon monoxide, and nitric oxide emission is shown in Fig. B-71 for an air inlet temperature of 100^oF and an air flow rate that is 60 percent of design. The HC and CO concentrations have a minimum at an air/fuel ratio of approximately 30. This is explained by two opposing effects. As air/fuel ratio increases, the combustion temperature decreases which tends to increase the exhaust concentration of these constituents as a result of thermal quenching of the reactions. However, the increasing concentration of oxygen has a tendency to reduce the concentration of CO. Sawyer (Ref. B-76) and Altshuler and Caretto (Ref. B-87) have come to similar conclusions. As expected, the nitric oxide concentration decreases with increasing air/fuel ratio, reflecting the slower rate of NO formation at lower temperature. Figure B-72 shows the part-load emission characteristics of the SE-101 burner for an air/fuel ratio of 25 and an air inlet temperature of 100^oF.

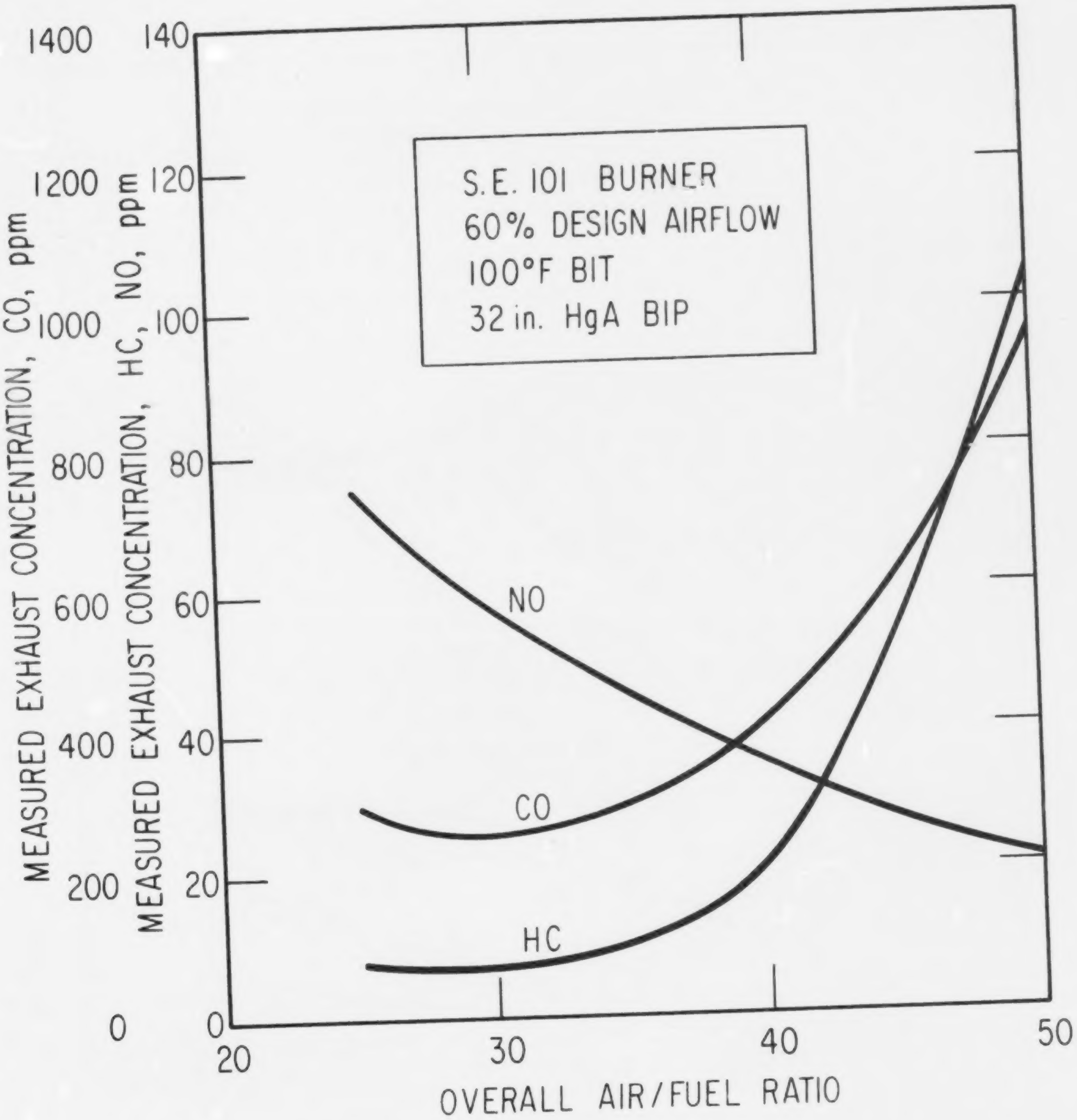

Figure B-71. Rankine Engines - General Motors Research SE-101 Burner Emissions (60 Percent Design Air Flow)

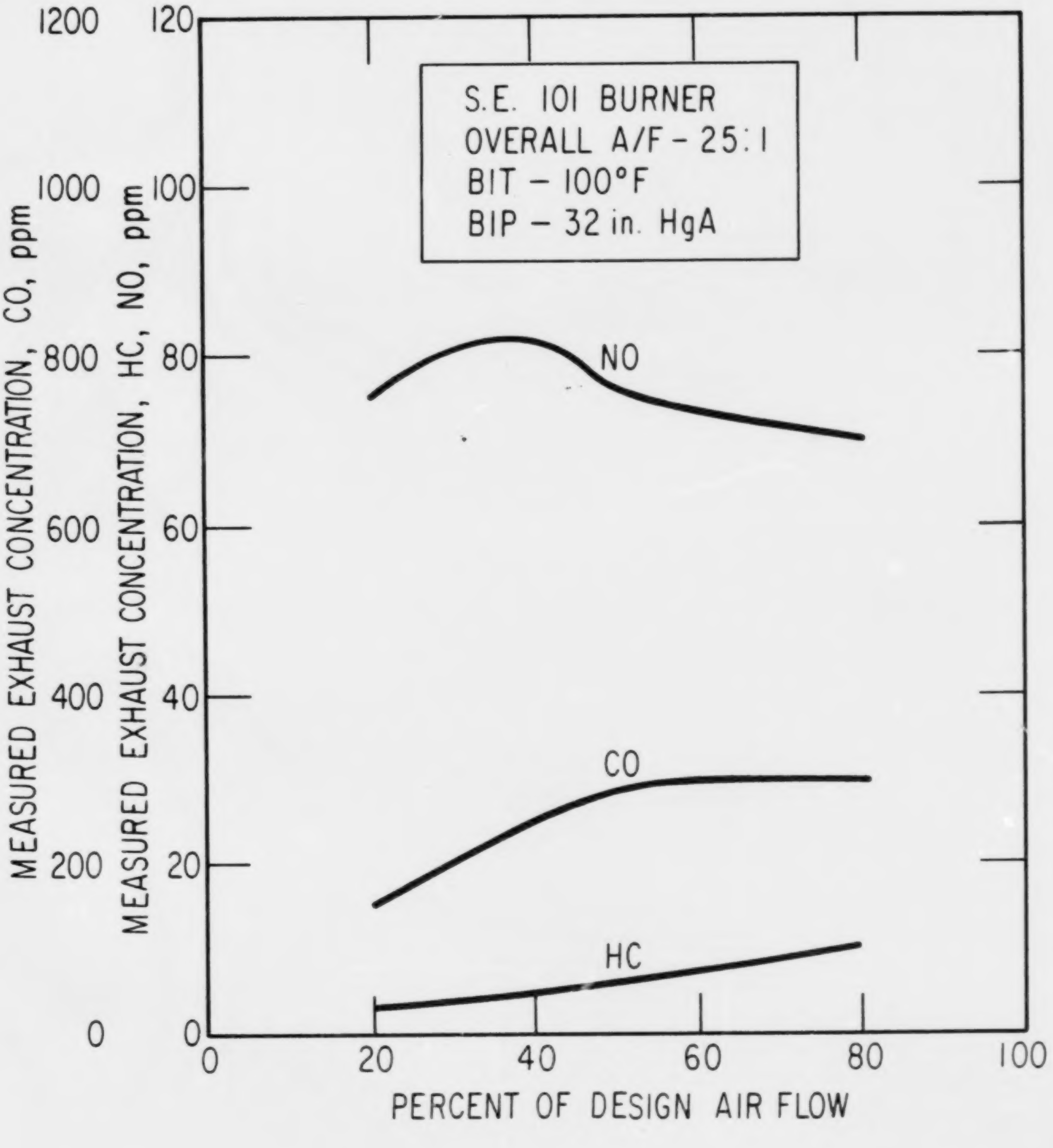

Figure B-72. Rankine Engines - General Motors Research SE-101 Burner Emissions (Air/Fuel Ratio = 25)

The HC and CO concentrations decrease somewhat as load is reduced. This might be explained by the longer residence time of the combustion gases in the burner as a result of the lower gas velocity obtained at lower air flow. The NO concentration remains essentially constant over the range of loads tested in the study. A comparison of these trends with the General Motors Stirling engine data discussed in the following section indicates similar trends for HC and NO. However, in the case of the Stirling engine, the CO concentration increases as load is reduced. Since the two burners are similar in design, this discrepancy is difficult to explain. The HC and CO concentrations of the Rankine cycle burner are higher and the NO concentrations lower than on the Stirling engine as a result of the lower burner air inlet temperatures used on the Rankine engine. It appears that the Rankine engine HC and CO emissions of the SE-101 engine could be reduced by increasing the residence time in the burner and by modifying the admission schedule of the secondary air. The HC concentration data presented by General Motors (Ref. B-82) were measured by FID and are reported in equivalent hexane.

The specific mass emissions listed in Table B-7 for a number of selected engine operating conditions of the SE-101 engine were computed from the data of Fig. B-71. Conversion of the concentration data to specific mass emissions was based on the assumption of a 15-percent engine efficiency and a fuel heat of combustion of 18,600 Btu/lb.

The HC and CO emissions obtained from the SE-101 automobile test program (Ref. B-83) are higher than those from the burner test facility (Ref. B-82). In the simulated test setup, only two preheater sections were used, and as a result, wall quenching effects were probably not adequately duplicated. This points out the importance of large combustor volumes so that the HC and CO reactions are completed at the boiler inlet.

Table B-7. Rankine Engine A - General Motors SE-101 Burner Emissions

Point No.	Air/Fuel Ratio	HC ppm Hexane	CO ppm	NO ppm	HC grams/ bhp-hr	CO grams/ bhp-hr	NO grams/ bhp-hr
A1	40	21	410	35	1.03	6.72	0.62
A2	30	6.5	250	57	0.24	3.11	0.76
A3	25	7	295	74	0.22	3.09	0.82

Table B-8. Rankine Engine Automobile Emissions, DHEW Driving Cycle, Hot Start

	HC, grams/mi	CO, grams/mi	NO, grams/mi	Ref.
GM. SE-101	1.0	8.0	2.2	B-84
GM. SE-124	0.3	1.0	1.7	B-84
Doble	1.4	3.9	2.0	B-84

Table B-9. Rankine Engine B - Williams Steam Car Emissions

	Concentration	Air/Fuel Ratio	Specific Mass Emissions, grams/bhp-hr
HC	20 ppm hexane	25	0.63
CO	500 ppm	25	5.2
NO	70 ppm	25	0.78

The General Motors SE-101 and SE-124 and the Doble steam car were tested at General Motors over the DHEW driving cycles. The hot start emission data obtained in these tests are presented in Table B-8. As indicated, the HC and CO emissions of the SE-101 are significantly lower than those from the other two cars. The NO emissions of all three cars are quite comparable. Although part of the improvement shown by the SE-124 is the result of the lower weight of that car, the beneficial effects of the lower specific heat release rate are quite apparent.

Data from the Williams steamer (Ref. B-84) and specific mass emissions computed on the basis of an engine efficiency of 15 percent are listed in Table B-9. The question of the instrumentation used on these tests could not be resolved.

Part of the data published by the Marquardt Company (Ref. B-85) are presented in Figs. B-73 through B-75. The emission concentration characteristics of the prevaporized, premixed, fuel injection configuration (Burner A) are shown in Fig. B-73 for a 50-percent design fuel (trimethylhexane, TMH) flow. The emissions are rather insensitive to variations in the overall burner equivalence ratio. The effect of primary zone equivalence ratio on emissions is also shown in Fig. B-73.

While HC and CO remain essentially constant, the NO concentration decreases considerably as the primary zone mixture is enriched (increasing equivalence ratio), emphasizing again the importance of primary zone design on the emissions of NO. As further discussed below, the HC concentrations reported by Marquardt are probably too low as a result of the measuring technique used in that program. The emission data obtained with the SUE burner, Fig. B-74, show similar trends. The SUE burner gives slightly lower CO and slightly higher NO values than Burner A.

The effect of load on the emissions from Burner A is illustrated in Fig. B-75 for TMH fuel and a primary zone equivalence ratio of 1.2.. The species concentrations plotted were corrected to stoichiometric. Unlike the General Motors data, HC and CO show a tendency to increase as load is reduced,

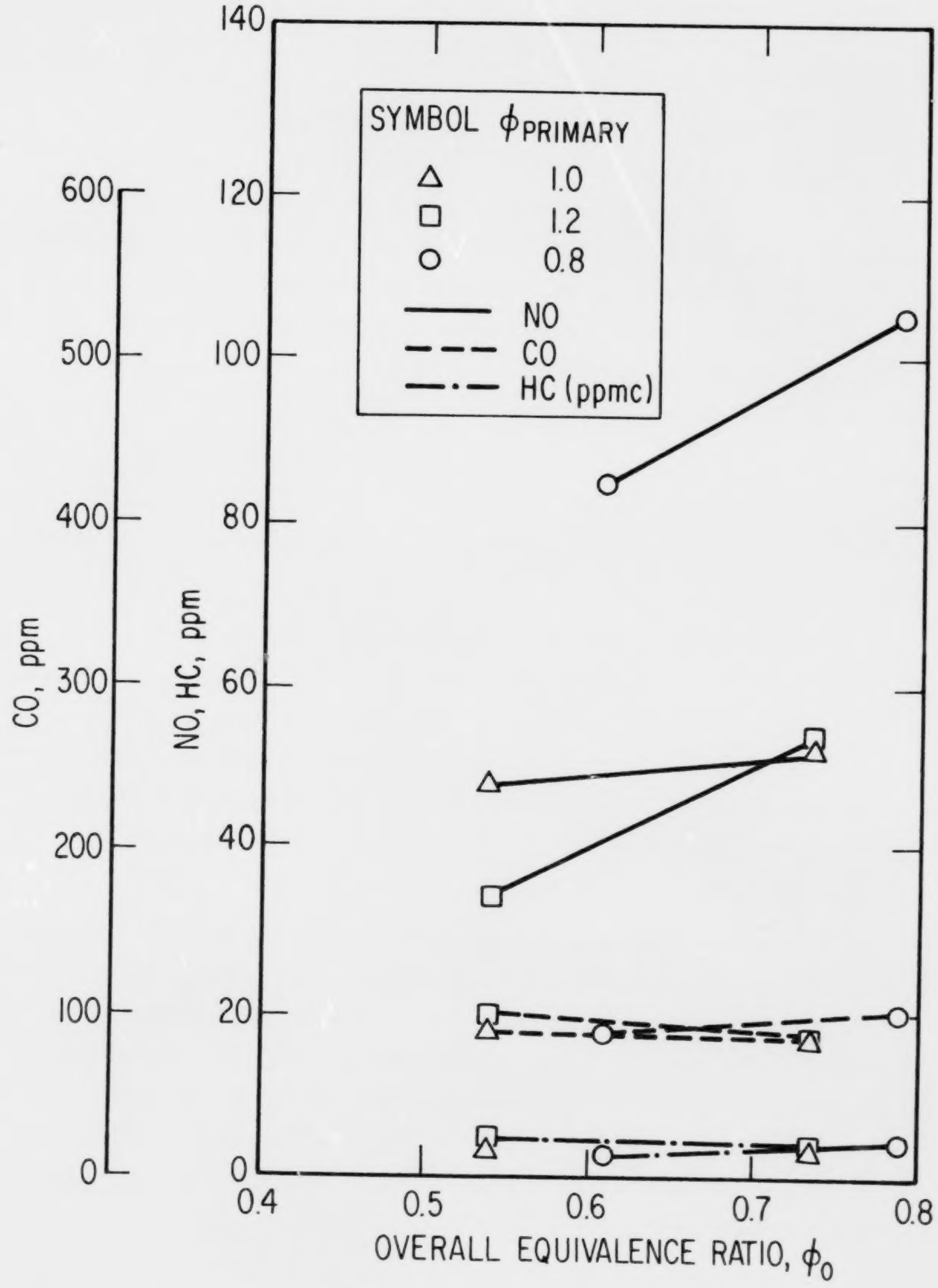

Figure B-73. Rankine Engines - Marquardt Burner A Emissions (Vaporized, Premixed Injection TMH Fuel, 50 Percent Design Flow)

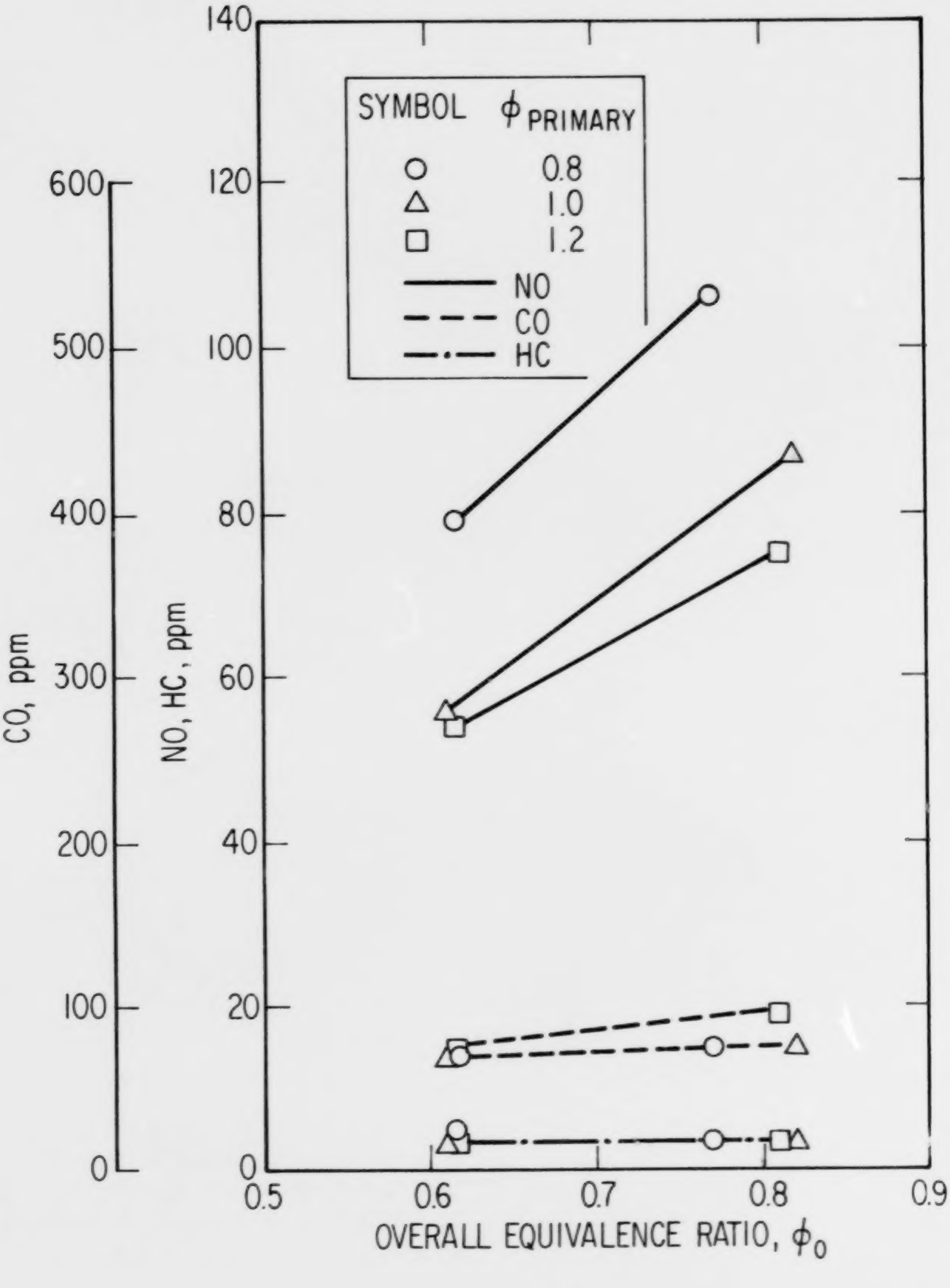

Figure B-74. Rankine Engines - Marquardt SUE Burner Emissions (Vaporized TMH Fuel, 50 Percent Design Flow)

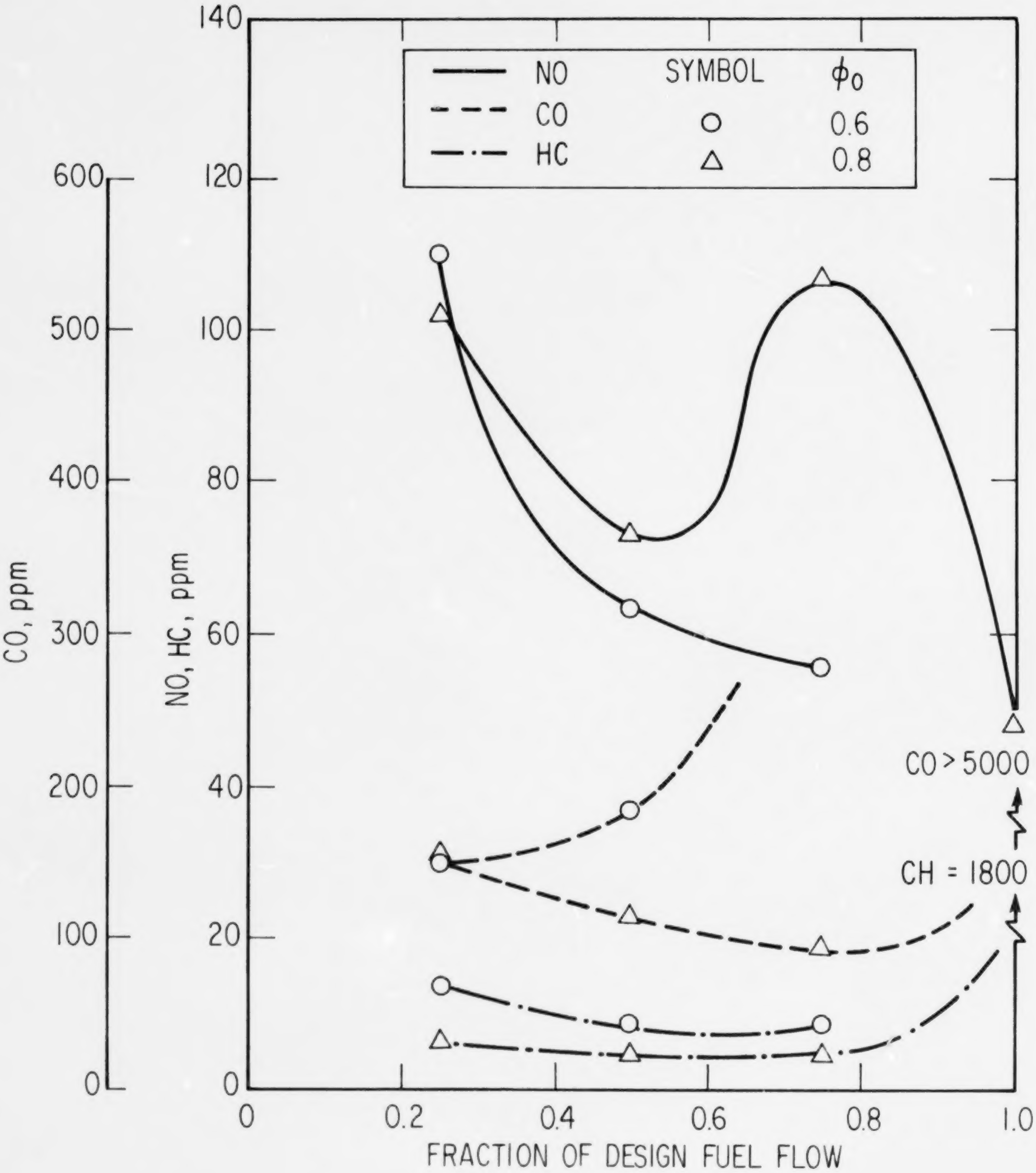

Figure B-75. Rankine Engines - Marquardt Burner A Emissions (TMH Fuel) while NO exhibits the opposite trend. Similar tendencies are shown by the other two burners used in the Marquardt program. Kerosene and methane resulted in comparable emission levels.

Specific mass emissions computed from the Marquardt data are presented in Table B-10. It should be emphasized that the HC data points are probably too low. This is further discussed in Section B. 5. 7.

Exhaust emission data obtained from Thermo Electron Corporation (TECO) (Ref. B-86) are depicted in Fig. B-76 as a function of percent excess air. These data are from the tests conducted with the design heat release rate of 105,000 Btu/hr. The CO concentration shows a minimum value which is believed to be the result of the combined effects of decreasing combustion temperature and increasing oxygen concentration obtained with increasing excess air. The HC concentration remains almost constant over a fairly wide range of mixture ratios and then increases sharply as more excess air is used. As expected, the NO concentration decreases with increasing excess air as a result of decreasing temperature and residence time. These trends are quite comparable to the General Motors data (Fig. B-71). It should be pointed out, however, that the HC concentrations measured by TECO are probably too low because an unheated FID setup was used. This is further discussed in Section B. 5. 7. The HC data reported by TECO are in equivalent CH_2.

Specific mass emissions computed from the TECO data are listed in Table B-11 for a number of air/fuel ratios. Thermo Electron Corporation also took data of a burner heat load of 50,000 Btu/hr. The measured emissions are considerably lower than those obtained at 105,000 Btu/hr. For instance, CO and NO are reduced by a factor of almost 3. Although the trend is correct, reflecting the longer residence time, the magnitude of these changes is somewhat unexpected and certainly much higher than that observed by General Motors and by Marquardt.

Table B-10. Rankine Engine C - Marquardt Burner Emissions, Vaporized, Premixed Injection TMH Fuel, 50 Percent Design Flow

Point No.	Air/Fuel Ratio	HC ppmc	CO ppm	NO ppm	HC grams/ bhp-hr	CO grams/ bhp-hr	NO grams/ bhp-hr
C1	27.2	5	100	35	0.028	1.13	0.42
C2	25	5	90	40	0.026	0.94	0.45
C3	21.4	5	85	51	0.022	0.76	0.49
C4	20	5	80	55	0.021	0.68	0.50

Table B-11. Rankine Engine D - Thermo Electron Corporation Burner Emissions

Point No.	Air/Fuel Ratio	HC ppmc	CO ppm	NO ppm	HC grams/ bhp-hr	CO grams/ bhp-hr	NO grams/ bhp-hr
D1	22.5	95	117	16	0.45	1.11	0.16
D2	21	45	72	24	0.20	0.63	0.23
D3	19.5	22	57	45	0.09	0.47	0.40
D4	18	14	60	84	0.053	0.456	0.68

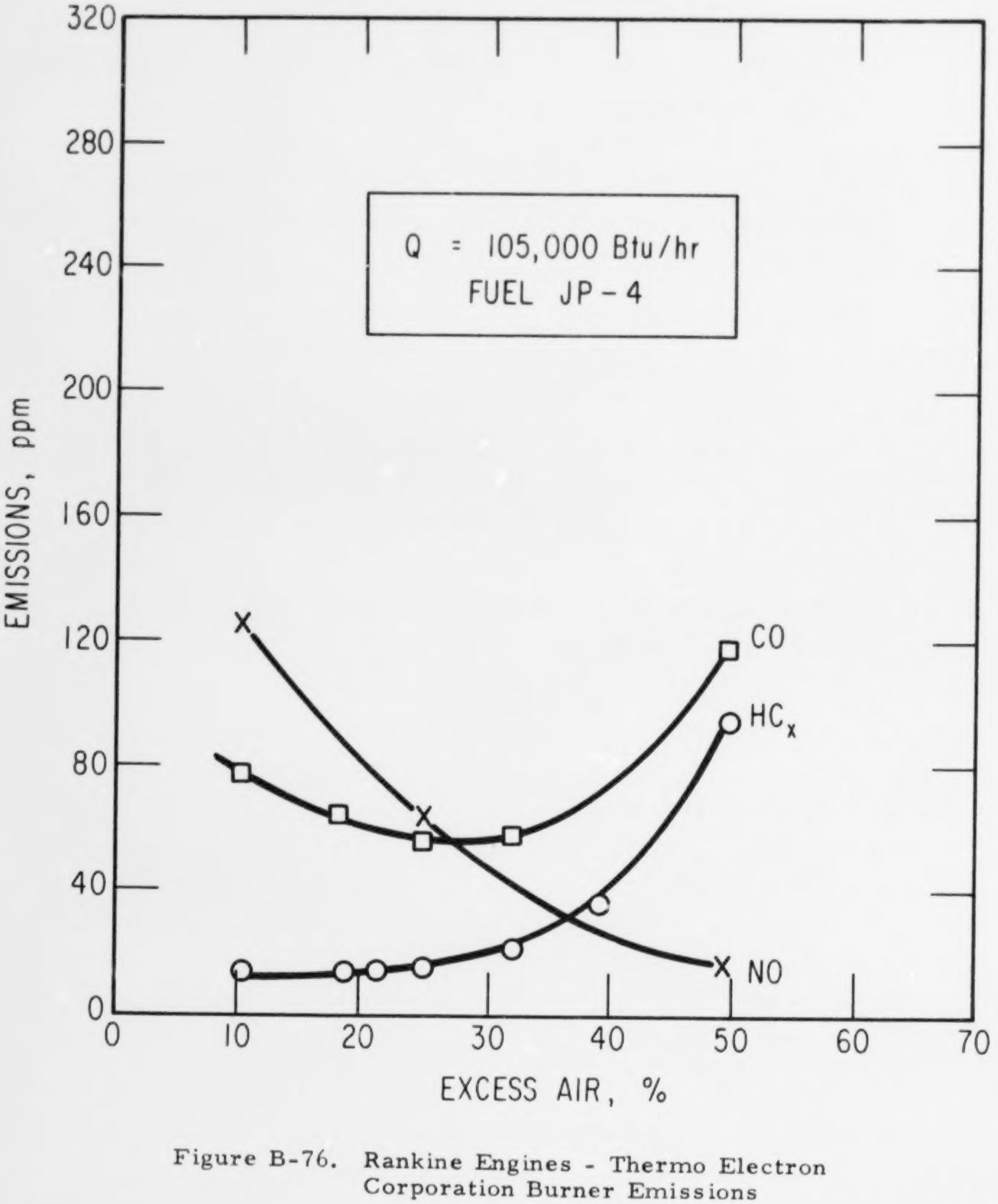

Figure B-76. Rankine Engines - Thermo Electron Corporation Burner Emissions

Data taken by Altshuler and Caretto (Ref. B-86) are plotted in Fig. B-77. These data were obtained with the 1.5-gal/hr-30^{o}R nozzle which showed the best emission characteristics. This nozzle has a design fuel flow rate of 1.5 gal/hr and a spray angle of 30 deg. The HC data are reported in terms of hexane and appear to be somewhat high. This may be due to inadequate fuel atomization and subsequent quenching at the boiler walls. Specific mass emissions for a number of operating points are presented in Table B-12.

B.5.4 Design Load Emissions

B.5.4.1 State-of-the-Art Technology

The Rankine engine exhaust emission concentration data, Figs. B-71 through B-77, were converted to specific mass emission numbers using a 15-percent engine efficiency and a fuel heating value of 18,600 Btu/hr. These data points which provided the basis for establishing design load emission characteristics of Rankine cycle engines are depicted in Figs. B-78 through B-80. The upper curves in these figures are considered representative of the present state-of-the-art technology.

As indicated in Fig. B-78, there is a large scatter in the HC data. Much better agreement is achieved in the NO and CO data. Inadequate HC measuring techniques were used in several of the programs and this may partly explain the large spread in the HC data. Also, the differences in burner specific heat release rates (residence time) have some effect on the emissions, particularly on HC and CO. In view of these uncertainties, it was decided to use the Stirling engine HC data discussed in Section B.6 as a guideline to establish the design load emission characteristics of Rankine engines. As discussed in Section B.6, the Stirling engine HC data are based on hot FID instrumentation.

The specific mass emissions are assumed constant for engine design power levels above 50 hp. Below that point, however, the specific mass emissions increase to reflect the reduction in engine component efficiencies.

Table B-12. Rankine Engine E - Bessler Boiler Emission Data

Point No.	Air/Fuel Ratio	HC ppm Hexane	CO ppm	NO ppm	HC grams/ bhp-hr	CO grams/ bhp-hr	NO grams/ bhp-hr
E1	37.5	28	75	30	1.29	1.16	0.50
E2	30	30	29	50	1.12	0.36	0.67
E3	25	36.5	33	65	1.14	0.34	0.73

Table B-13. Rankine Engine Automobile Cold Start Emissions

	f_{HC}	f_{CO}	f_{NO}
GM. SE-101	1.12	1.22	1.12
GM. SE-124	1.62	2.48	1.57
Doble 1923	2.32	1.73	1.43

f_{HC}, f_{CO}, f_{NO} = Ratio of emissions including engine warmup to emissions with warmed up engine

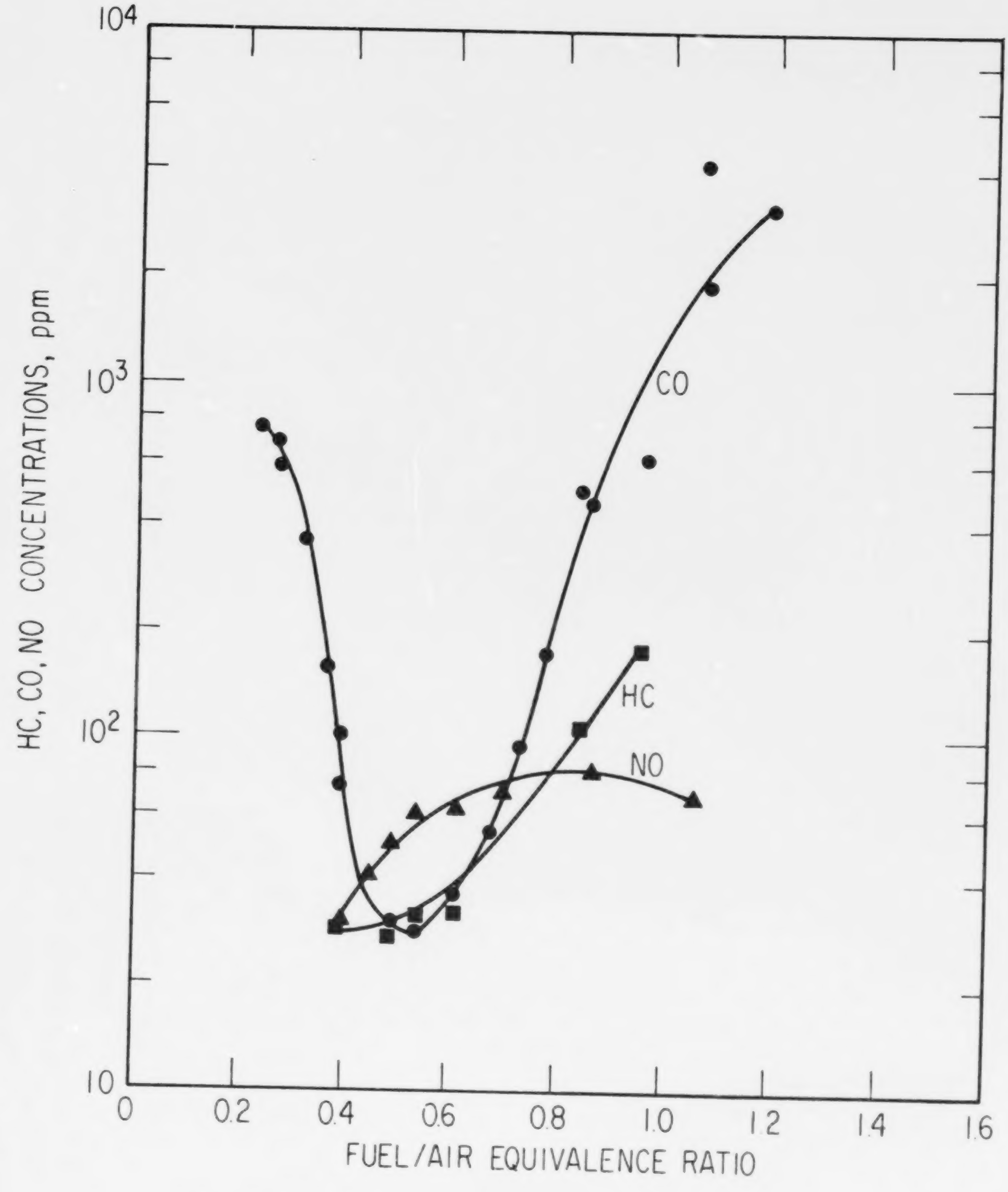

Figure B-77. Rankine Engines - Bessler Boiler Emission Data

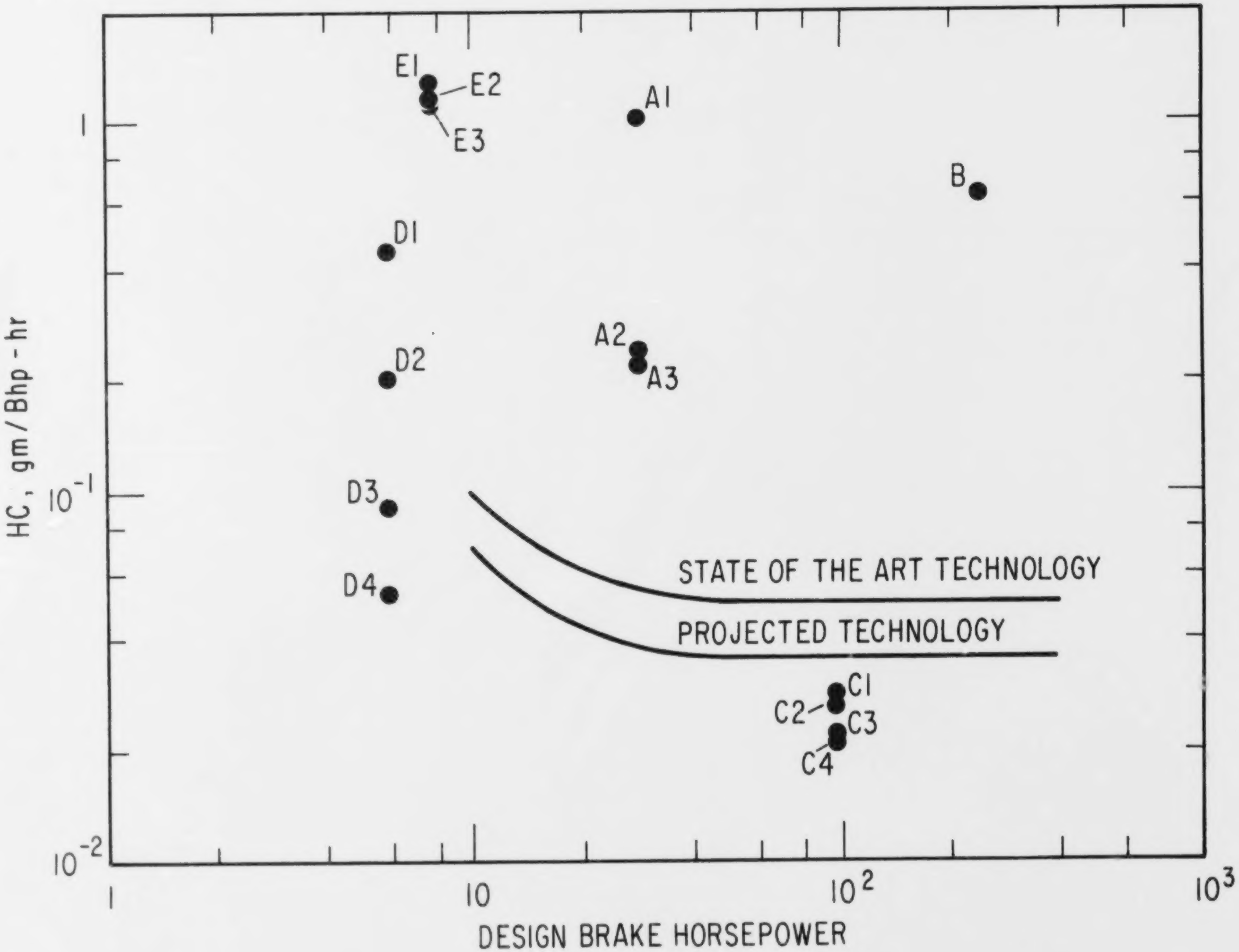

Figure B-78. Rankine Engines - Hydrocarbon Emission, Steady State Design Load

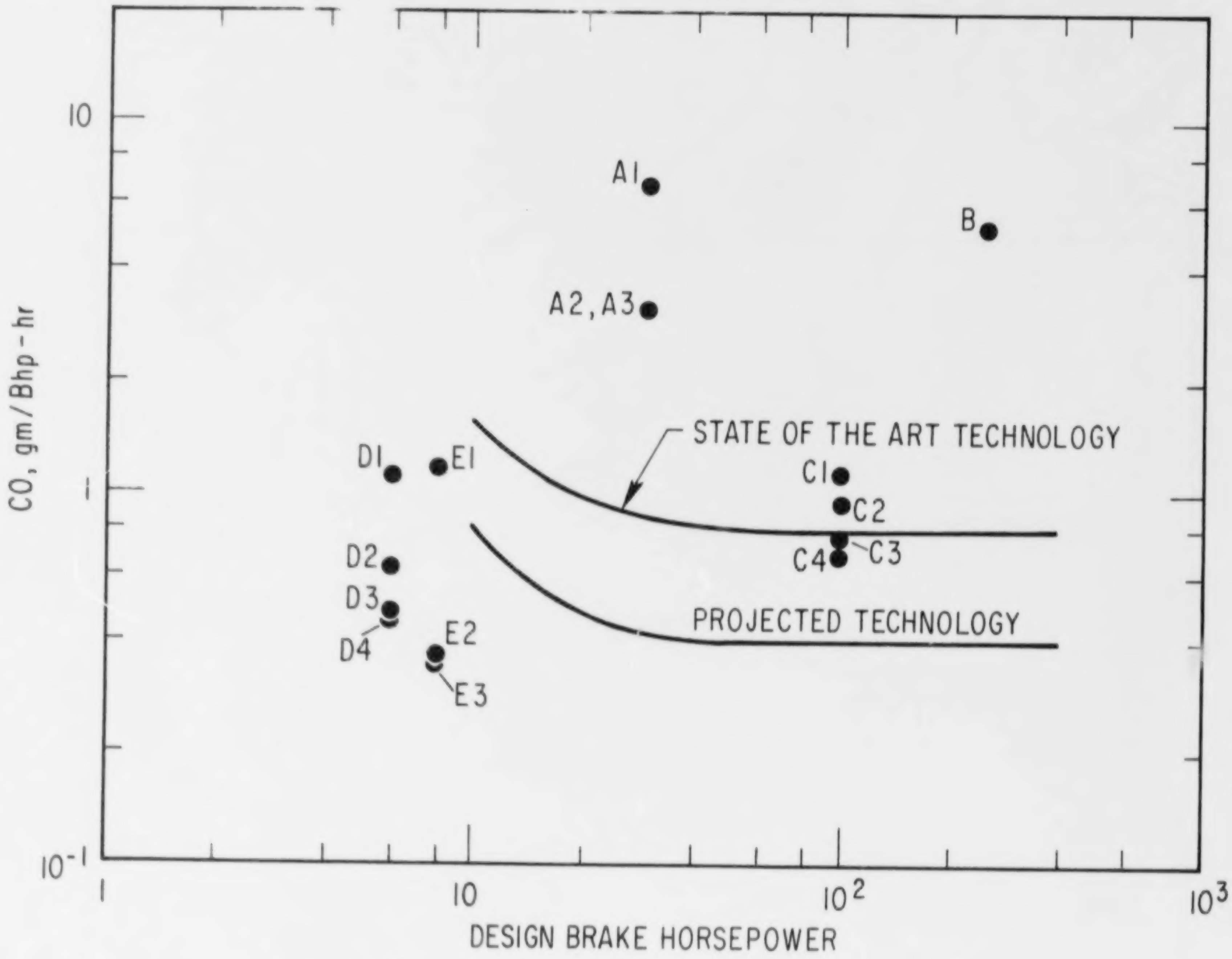

Figure B-79. Rankine Engines - Carbon Monoxide Emission, Steady State Design Load

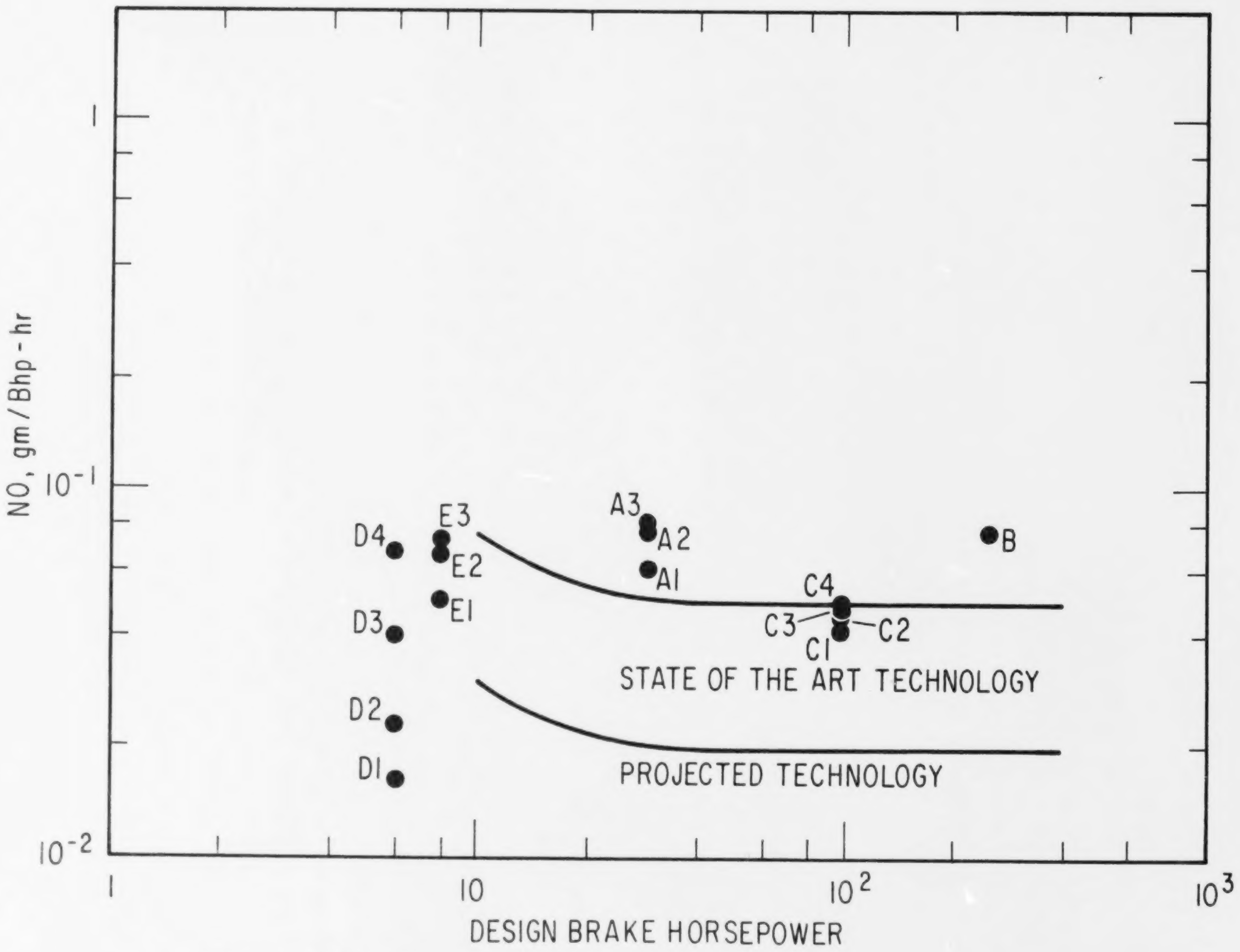

Figure B-80. Rankine Engines - Nitric Oxide Emission, Steady State Design Load

B.5.4.2 Projected Technology

The critical emission species of the Rankine cycle engine is NO. Both HC and CO emissions are already very low for the present state-of-the-art technology. Reduction of NO is believed to be possible by means of optimizing the primary and secondary zones of the burner and increasing residence time. In addition, exhaust gas recirculation may be feasible. This technique has been used successfully on the Philips Stirling engine (Section B.6). Based on these considerations, it is estimated that the NO emission for the projected technology can be reduced by a factor 2.5 from the present state-of-the-art technology value. The projected reduction in HC and CO is somewhat lower, reflecting the general tendency of obtaining higher HC and CO concentrations with the burner design modifications required for NO control.

Comparison of the design point specific mass emissions of the Rankine engines and the Stirling engines which are discussed in Section B.6 indicates that the HC emissions of the Rankine engines are higher by a factor of 3.3. This increase is the result of lower engine efficiency and higher HC concentrations obtained at the lower burner inlet air temperature of the Rankine engines. In addition, wall quenching effects are potentially more serious in the Rankine engine because of the relatively low temperature of the boiler. The CO follows the same trend as HC except that the wall quenching effects may be less serious and as a result the difference in the CO specific mass emissions is slightly less. The NO emissions of the Rankine engine are only moderately higher than those of the Stirling engine because of the compensating effects of engine efficiency and burner inlet air temperature.

Again, the specific mass emissions of the projected technologies are assumed to be constant for engine design power levels above 50 hp. Below that point the specific mass emissions increase.

B.5.5 Part-Load Emissions

There is little agreement in the part-load emission characteristics of the engines and burners tested (Refs. B-82 through B-87). The General Motors and Thermo Electron data indicate some reduction in the concentration of CO and HC with decreasing load. However, the Marquardt data show little change over a wide range of part-load conditions. For NO, there is reasonable agreement and very little change in NO concentration with load is observed.

Considering the lack of a sufficiently large data sample and the contradictory trends observed in the data, it was decided to use engine efficiency as a measure of the part-load emissions for both present state-of-the-art and projected technologies. The specific mass emissions of each species at part-load are then computed by multiplying the design load emissions obtained from Figs. B-78 through B-80 and the part-load factors presented in Fig. B-81. Obviously, this is a rather crude assumption and points out the need of reliable Rankine engine part-load emission data.

B.5.6 Cold Start Emissions

The only cold start emission information available is the data published by General Motors (Ref. B-83) for the General Motors SE-101 and SE-124 engines and the Doble steam car. In each case, the emissions were measured during engine warmup. Factors were derived from these data relating the total emissions, including warmup and hot DHEW cycle, to the emissions obtained during the hot DHEW cycle. These factors are presented in Table B-13. As indicated, the warmup emissions have only a small effect on the total emissions of the SE-101 engine, resulting from the fact that only a 2.8-min warmup period was required to achieve adequate steam pressure. In the case of the SE-124 and the Doble, the warmup emissions represent a significant portion of the total emissions, primarily because a much longer warmup time was required.

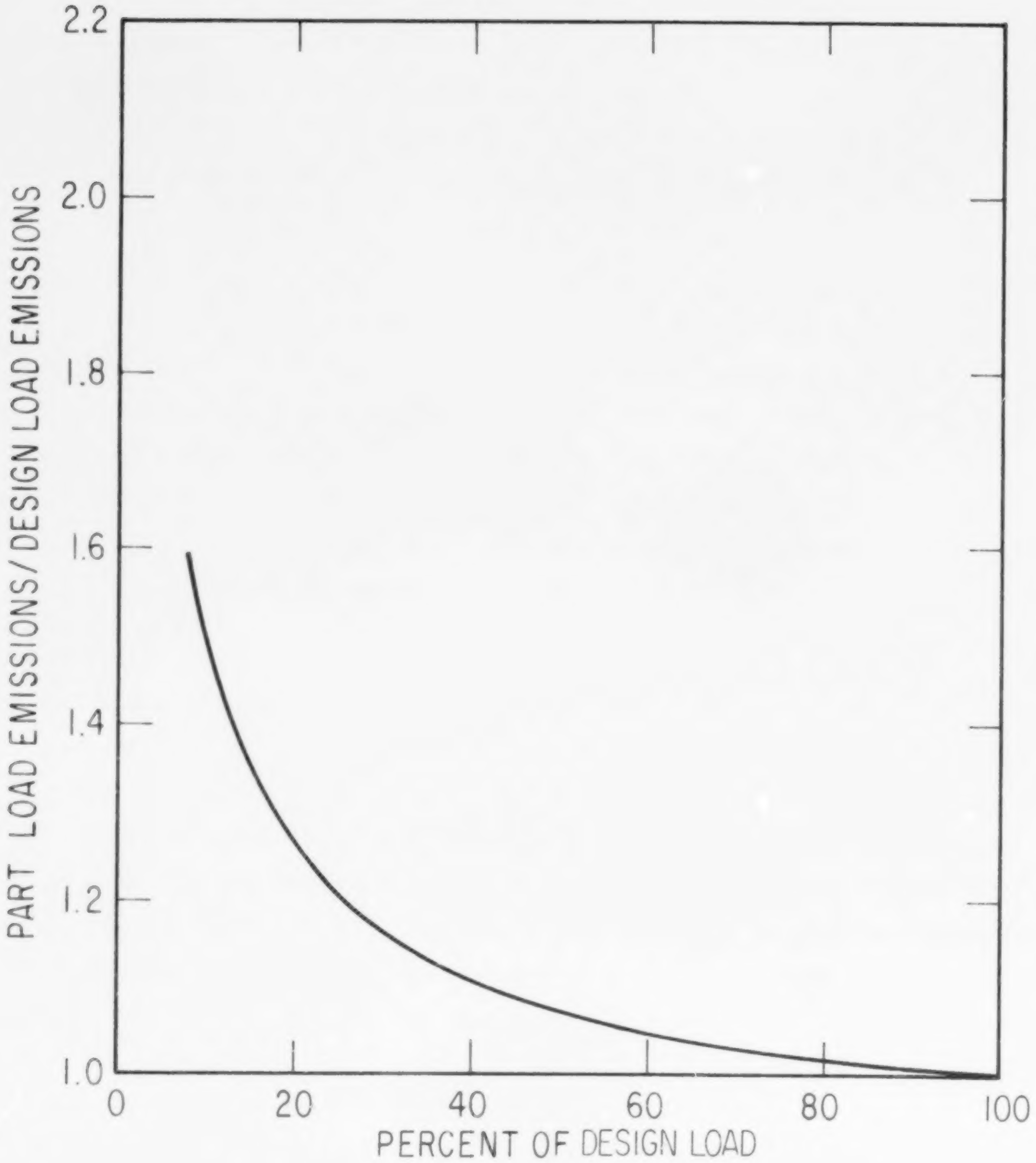

Figure B-81. Rankine Engines - HC, CO, NO, Emissions, Steady State Part-Load

B. 5. 7 Instrumentation

The difficulty of obtaining reliable exhaust emission data has been previously pointed out. General Motors has used the most accurate set of instruments commercially available, including low range NDIR for CO and NO, and hot FID for HC, which is mandatory when kerosene or other heavy fuels are used. Formaldehyde was determined by wet chemical analysis, and smoke was observed visually.

NDIR instrumentation was also used by Marquardt for measurement of CO and NO, and HC was determined by means of FID. However, to remove water vapor which primarily affects NO measurements, all the sample gas was run through an ice bath. As a result, an undetermined amount of the heavier HC constituents was condensed, and the HC data reported by Marquardt are considered too low and should be used with caution.

Thermo Electron Corporation has used NDIR to measure CO and NO and "cold" FID for HC. Thus, the HC data are considered too low.

Altshuler and Caretto used NDIR for the measurement of CO and NO. The exhaust gas sample used to determine CO and NO was run through a condensation trap to remove water vapor which affects the NO readings. Hot FID was used for HC analysis and that part of the sample gas was not cooled.

B. 5. 8 Other Pollutants

In addition to measuring the emissions of HC, CO, and NO, General Motors has made attempts to determine the odor and smoke characteristics of their engine. No offensive odor was detected so long as air/fuel ratio was below 40:1. Smoke was never observed at air/fuel ratios of 25:1 or higher.

B.6 STIRLING ENGINE EMISSIONS

B.6.1 General

Characterization of the exhaust emissions of Stirling engines are based upon emission data from two engines built and tested by General Motors Research Laboratories and by Philips Research Laboratories of the Netherlands. Although heat may be supplied to the engine from any type of high temperature energy source, the two engines considered were operated only on diesel fuel.

The General Motors Stirling engine is a single-cylinder engine rated at 10 hp (Ref. B-88). Its design speed is 3000 rpm and all tests discussed in this section were conducted at that speed. An air preheater is used to increase engine efficiency. The burner was designed for high combustion efficiency and uniform gas temperature distribution across the burner exit plane. The engine was tested at General Motors for emissions over a wide range of operating conditions using diesel fuel No. 2.

The Philips engine is also a single-cylinder configuration designed for 80 hp. The emission tests were conducted in the Netherlands using European diesel fuel (Ref. B-88). Two burner designs were considered. The standard slit burner demonstrated very good flame stability and uniform temperatures across the burner exit plane over a wide range of operating conditions. The advantage of the experimental louver burner is its ease of fabrication. Various amounts of EGR were used in the test program which was designed primarily to assess the effects of recirculation on NO emission.

B.6.2 Design Load Emissions

B.6.2.1 State-of-the-Art Technology

Generally, Stirling engines running on diesel fuel are designed to operate at air/fuel ratios of 20 or above. Under those conditions, burner temperature and oxygen concentration are sufficiently high to assure low emissions of hydrocarbon and carbon monoxide. The nitric oxide concentrations are high unless special provisions are made.

The exhaust emission data of the General Motors engine reported by Lienesch and Wade (Ref. B-88) for different engine operating conditions are listed in Table B-14. Also presented in that table are other important parameters which are required to convert the concentration data to specific mass emission numbers. The CO, NO, and NO_2 measurements were made by General Motors, both upstream and downstream of the air preheater. The downstream concentrations of CO are approximately half of the upstream values, indicating that additional reactions are occurring in the preheater. This trend is reasonable considering the high temperature of the exhaust gases entering the preheater and the kinetics of the CO oxidation reaction. The downstream nitric oxide concentrations were slightly lower than the corresponding upstream values on all tests. This is surprising since no significant changes in the NO_2 concentration were observed. Since the upstream versus downstream measurements of NO differ by only 10 percent, no further attempts were made to resolve this apparent discrepancy. Hydrocarbon concentrations were only measured upstream of the preheater and no background HC measurements were made. Since that level may have been as high as 1 ppm equivalent hexane, the HC values are probably on the high side. The CO concentrations are the downstream values. For NO, the upstream values were used primarily because the NO_2 concentrations, which were always less than 30 ppm, were not available. This approach is considered reasonable since the variations seem to be well within the normal band of test data uncertainty.

In addition to providing a basis for establishing Stirling engine emission characteristics, the data were used to assess the effects of various engine operating parameters on emissions. The data from tests A2 to A6, Table B-14, run at essentially constant air/fuel ratio, indicate that the HC emissions decrease with increasing burner inlet air temperature, while NO increases. This trend agrees with theoretical calculations. However, the

Table B-14. General Motors Research 10 hp Stirling Engine Emissions

Point No.	Brake, hp	Air Flow, lb/hr	Air/Fuel Ratio	Burner Air Inlet Temp., °F	HC ppm, Hexane	CO ppm	NO ppm	HC grams/bhp-hr	CO grams/bhp-hr	NO grams/bhp-hr
A1	2.48	114	27.1	80	6	365	80	0.375	7.6	1.78
A2	4.72	118	25.3	249	4	325	95	0.137	3.7	1.16
A3	4.84	118	25.7	440	2	45	120	0.067	0.5	1.43
A4	4.84	94.2	26.0	800	2	68	230	0.053	0.6	2.21
A5	4.75	78.3	24.5	994	1.5	68	380	0.034	0.51	3.07
A6	4.72	75.5	26.4	1210	1	75	475	0.022	0.55	3.7
A7	4.78	89.3	29.8	1200	---	47	320	-----	0.40	2.9
A8	4.84	109.5	35.2	1200	0.5	35	202	0.015	0.36	1.83
A9	4.83	136.1	39.6	1150	0.5	35	130	0.019	0.44	1.76
A10	4.91	58.1	20.2	1167	3	130	880	0.049	0.71	5.13
A11	9.65	137.7	25.4	1350	2	30	550	0.039	0.20	3.85
A12	9.69	108.5	19.9	1360	1.5	35	1160	0.023	0.18	6.4

CO emissions increase somewhat with increasing temperature, and that is difficult to explain. Since the CO level is sufficiently low to meet almost any future emission goals, no attempts were made to explain this trend. Tests A6 through A10 show the effect of air/fuel ratio on emissions at half-load for burner inlet air temperatures of approximately 1200°F. As expected, the NO concentration increases rapidly as air/fuel ratio is reduced, primarily as a result of increasing temperature and residence time. Since burner flow rate decreases with decreasing air/fuel ratio, the specific mass emissions increase at a slower rate. This is supported by the full load data from tests A11 and A12. At half-load, the HC and CO concentrations remain essentially constant over the air/fuel ratio range between approximately 30 and 40. Further reduction results in rapidly increasing HC and CO concentrations. As shown in Table B-14, the corresponding specific mass emissions decrease at a slower rate because of the reduction in air flow rate at lower air/fuel ratios.

Test data from the Philips engine is presented in Table B-15 (Ref. B-88). The engine was operated without and with EGR. Two burners, the slit burner and the louver burner, were used in the program. In all cases, a burner inlet air temperature of 1100°F was maintained. Hydrocarbon concentrations were not measured in this particular test series. Philips reports that the hydrocarbons of their burners are between 1 and 2 ppm equivalent hexane. A constant value of 2 ppm was used to compute the HC specific mass emission values listed in Table B-15 for the slit burner. This assumption is considered reasonable in view of the fact that the CO concentration of the slit burner increases only moderately as the recirculation rate is increased from 0 to 33 percent. In the case of the louver burner, the data show a significant reduction of the CO emissions as the air/fuel ratio is decreased from 22.4 to 20.3 (Tests B2 and B3). This appears abnormal and disagrees with the trends derived from the General Motors data.

Table B-15. Philips 80 hp Stirling Engine Emissions

Point No.	Burner Type	Brake, hp	Air Flow, lb/hr	Air/Fuel Ratio	Recirculation, Percent	HC ppm, Hexane	CO ppm	NO ppm	HC grams/bhp-hr	CO grams/bhp-hr	NO grams/bhp-hr
B1	Louver	29.3	272	20.3	100	≈ 2	761	47	0.026	5.25	0.21
B2	Louver	29.7	272	20.3	33	≈ 2	330	160	0.026	1.39	0.73
B3	Louver	28.0	272	22.4	0	≈ 2	811	263	0.027	3.62	1.25
B4	Slit	31.3	292	20.5	100	≈ 2	168	38	0.025	0.72	0.17
B5	Slit	31.3	292	20.9	33	≈ 2	122	40	0.025	0.52	0.18
B6	Slit	31.3	285	20.6	0	≈ 2	78	107	0.025	0.33	0.48

It should be pointed out that the CO measurement technique used by Philips is also sensitive to hydrocarbons and, as a result, the reported CO values are on the high side. However, considering the low hydrocarbon content of the exhaust, the error appears to be small. The NO_x concentrations are the sum of all the oxides of nitrogen species measured by Philips and were used to compute NO specific mass emissions.

The Philips data indicate that EGR represents a feasible and effective method towards control of NO emissions for Stirling engines without adversely affecting the emissions of HC and CO. The slit burner has superior emission characteristics and slightly better efficiency. Specific mass emissions and fuel consumption of the Philips engine are lower than on the General Motors engine. To some degree, this reflects the inherently higher efficiency of the larger Philips engine.

The specific mass emission data presented in Tables B-14 and B-15 are also shown graphically in Figs. B-82 through B-84. The upper curves in these figures are considered a reasonable representation of the present state-of-the-art technology. As in the case of the other heat engines, the specific mass emissions are considered constant for design power levels above 50 hp. Below that point the specific mass emissions are assumed to increase to reflect the deterioration of engine efficiency. It should be pointed out that several of the HC and CO data points in Figs. B-82 and B-83 are actually below the selected state-of-the-art curves. The reason is that the corresponding NO emissions are excessive. This points out the importance of selecting the proper combination of engine operating parameters in order to minimize all emissions. Since HC and CO are inherently low, attention must be primarily focused on NO. The curves reflect this approach.

B.6.2.2 Projected Technology

It is apparent that nitric oxide presents the principal emission problem in Stirling engines. Based on the trends derived from the data, a number of approaches can be suggested, including burner modifications, EGR, lower

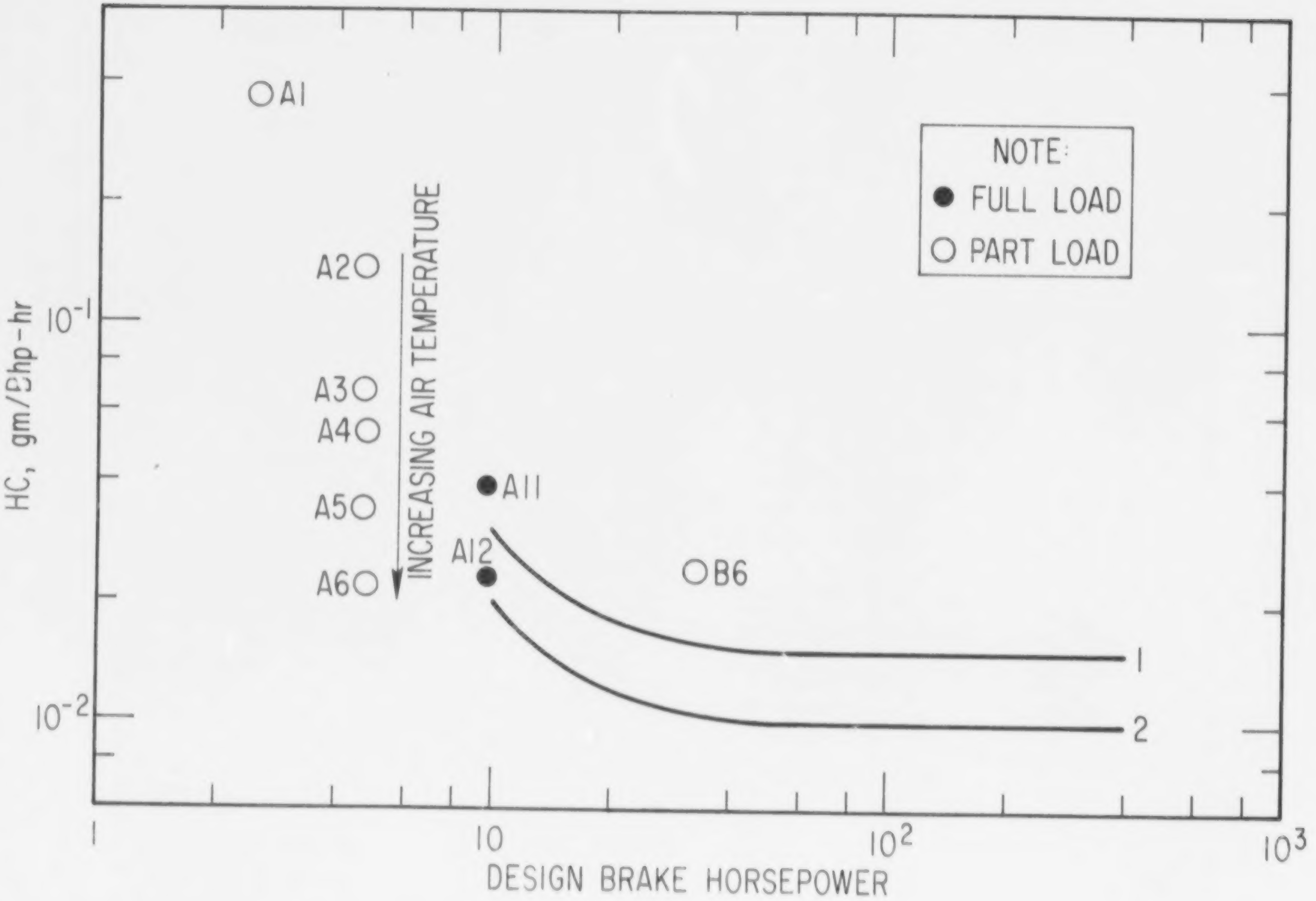

Figure B-82. Stirling Engines - Hydrocarbon Emission, Steady State Design Load

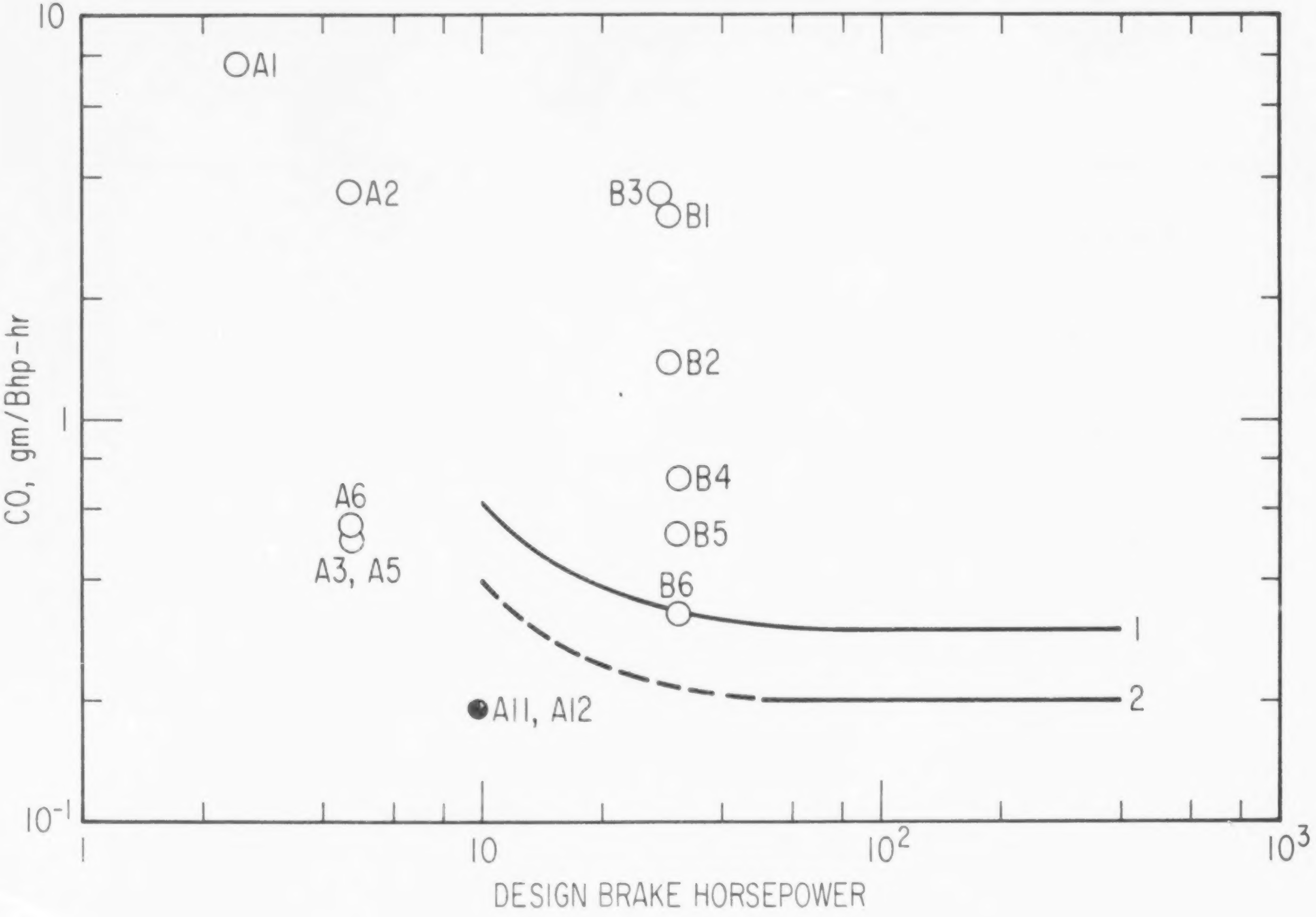

Figure B-83. Stirling Engines - Carbon Monoxide Emission, Steady State Design Loa

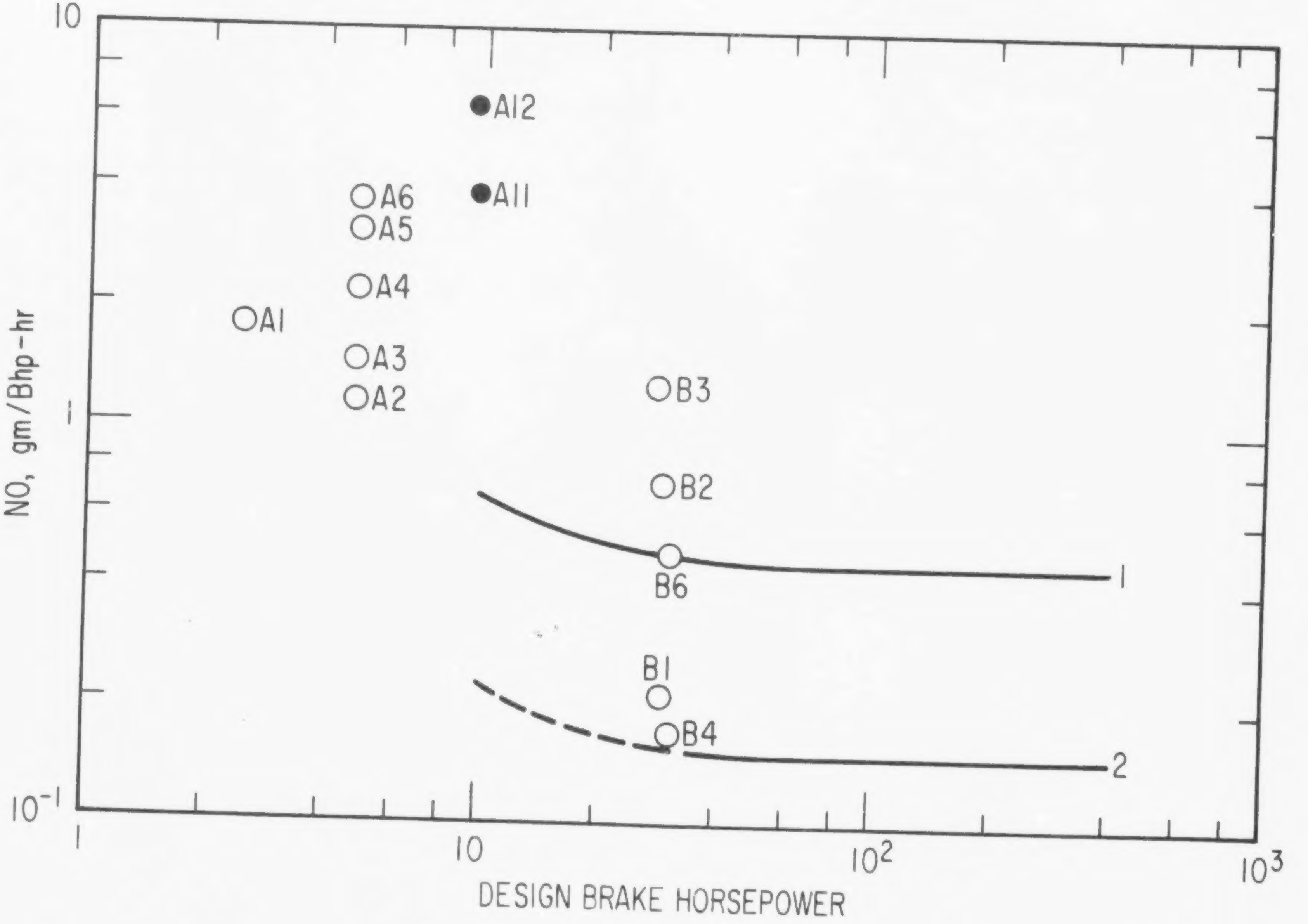

Figure B-84. Stirling Engines - Nitric Oxide Emission, Steady State Design Load burner inlet air temperature, and reduction of residence time of the gases in the primary zone of the burner.

As shown by Philips, the slit burner has much lower NO emissions than the louver burner. It is conceivable that the NO emissions could be further reduced by means of additional burner modifications. Incorporation of EGR has been shown to be an effective method in reducing NO emissions from Stirling engines. As previously pointed out, the addition of EGR results in lower combustion temperatures and, for a given burner design, lower residence time of the gases in the primary zone of the burner. Reduction of burner inlet air temperature and/or increase of the air/fuel ratio also result in lower NO emissions. This has been demonstrated by both General Motors and Philips. Although effective from an NO emissions point of view, both methods show a tendency towards higher fuel consumption and HC and CO emissions. Since NO formation in the burner is kinetically controlled, a reduction in the residence time tends to reduce formation and concentration of nitric oxide.

It appears that the methods outlined above are potentially effective in lowering exhaust emission in Stirling engines. Further optimization of these approaches, separately and in combination, is required to determine the most desirable burner configurations with respect to exhaust emissions, fuel consumption, and engine operation.

With these considerations in mind, the projected specific mass emission curves were drawn in Figs. B-82 through B-84. The projected NO emissions are by a factor of 3 lower than the corresponding present state-of-the-art values. Since the various approaches aimed at reducing NO have tendency to increase the HC and CO emissions, it is assumed that the projected HC and CO emissions are reduced by only a factor of 1.5.

B.6.3 Part-Load Emissions

Lacking sufficient test data, a meaningful part-load emission study could not be conducted for the Stirling engine. To account for at least some of the part-load effects, it was decided to use the cycle efficiency versus percent of design load correlation as the basis for estimating the emissions at part-load. The same approach was used to characterize the part-load emissions of Rankine engines. The recommended part-load emission factors are presented in Fig. B-85 in terms of the ratio of part-load emission to design-load emission versus percent of design load. These factors are applicable to HC, CO, and NO, for both present state-of-the-art and projected technologies. The absolute value of the emissions at a certain part-load point is then computed by multiplying the emission factors from Fig. B-85 and the design load specific mass emissions from Figs. B-82 through B-84. This approach is approximate, at best, and points out the need of a comprehensive Stirling engine emission test program.

B. 6. 4 Cold Start Emissions

There is no information available to characterize the cold start emissions of Stirling engines. Obviously, these factors have to be resolved before a complete assessment can be made of the emissions from Stirling engines.

B. 6. 5 Instrumentation

The significance of an evaluation of the test procedures and instrumentation used in emission test programs has been previously stated.

In the General Motors tests,* HC was measured by means of a hot FID setup. A sample line temperature of 375°F was maintained, which provides a reasonable compromise between additional oxidation of the hydrocarbons to be recorded and condensation of the heavy components. Continuous NDIR instruments were used for NO and CO. The NO_2 was measured by means of continuous NDUV. This set of instrumentation represents the most reliable presently available.

A somewhat different approach was taken by Philips. The hydrocarbons were measured with electrically-heated FID. Wet chemical methods were used to determine CO and NO. The CO was determined by first removing all

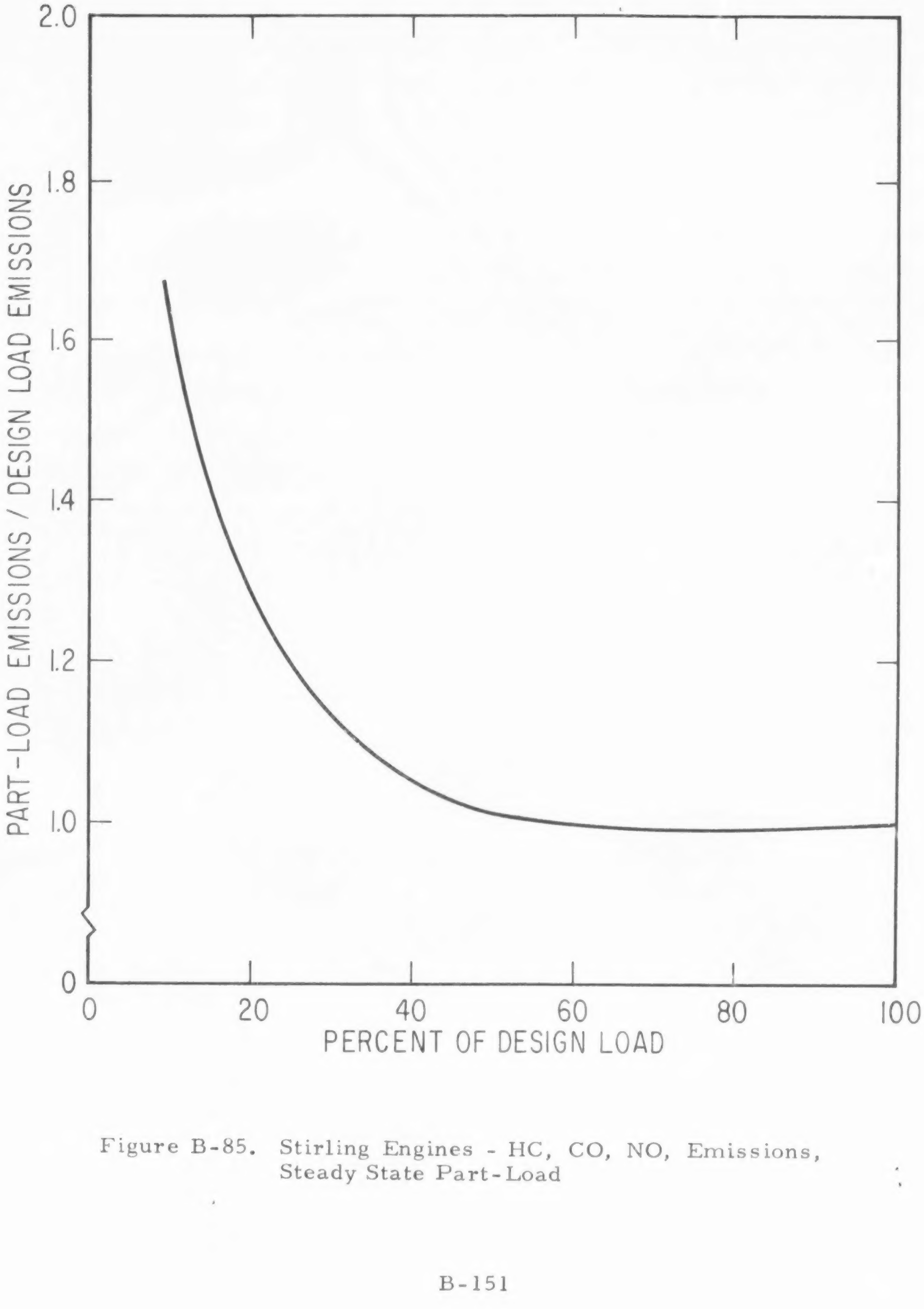

Figure B-85. Stirling Engines - HC, CO, NO, Emissions, Steady State Part-Load the CO_2 contained in the exhaust sample and then burning all the carbon compounds, including HC. Then the CO_2 was measured and converted analytically to CO. Since the HC concentrations in the exhaust of Stirling engines are very low, the error resulting from the oxidation of the HC species is small and the reported CO concentrations are considered accurate. The oxides of nitrogen species are determined through conversion into ammonia. The ammonia content of the solution is then determined spectrophotometrically. At the NO_x concentration levels of Stirling engine exhausts, this method is sufficiently accurate.

B. 6. 6 Other Pollutants

Little information is available on smoke and odor from the Stirling engine exhaust. According to Ref. B-88, the General Motors engine is smoke-free at all operating conditions, including cold start. Also, no odor was detected. The Philips engine shows some smoke during warmup. However, it appears that this problem might be alleviated by means of burner modification and/or variation of the air/fuel ratio during warmup.

B.7 REFERENCES

B-1. Kiyoshi Matsumoto, Tadahide Toda, and Hidetaka Nohira, Oxides of Nitrogen from Smaller Gasoline Engine, SAE Paper 700145, Automotive Engineering Congress, Detroit, Michigan (12-16 January 1970).

B-2. Personal Communication with K. Nakajima, Toyota Motor Co., Ltd., Lyndhurst, New Jersey.

B-3. Personal Communication with Engine Manufacturer.

B-4. Personal Communication with C. Marks, General Motors Research, Warren, Michigan.

B-5. Personal Communication with G. Gelb, TRW Systems, Redondo Beach, California.

B-6. Personal Communication with R. Hurn, Bureau of Mines, Bartlesville, Oklahoma.

B-7. H. K. Newhall and I. A. El Messiri, A Combustion Chamber Designed for Minimum Engine Exhaust Emissions, SAE Paper 700491, Mid-Year Meeting, Detroit, Michigan (17-22 May 1970).

B-8. W. A. Daniel, Flame Quenching at the Walls of An Internal Combustion Engine, Sixth Symposium (International) on Combustion, Reinhold Publishing Co., New York (1956).

B-9. W. A. Daniel, Why Engine Variables Affect Exhaust Hydrocarbon Emissions, SAE Paper 700108, Automotive Engineering Congress, Detroit, Michigan (12-16 January 1970).

B-10. L. J. Papa, Gas Chromatography - Measuring Exhaust Hydrocarbons Down to Parts per Billion, SAE Paper 670494, Mid-Year Meeting, Chicago, Illinois (15-19 May 1967).

B-11. E. S. Starkman, Theory, Experiment and Rationale in the Generation of Pollutants by Combustion, 12th Symposium (International) on Combustion, Poitiers, France (14-20 July 1968).

B-12. R. F. Sawyer, Fundamental Processes Controlling the Air Pollution Emissions from Turbojet Engines, AIAA Paper No. 69-1040, AIAA 6th Annual Meeting and Technical Display, Anaheim, California (20-24 October 1969).

B-13. H. K. Newhall and S. M. Shahed, Kinetics of Nitric Oxide Formation in High Pressure Flames, Submitted to the Combustion Institute for the 13th Symposium (International) on Combustion.

B-14. P. Eyzat and J. C. Guibet, A New Look at Nitrogen Oxides Formation in Internal Combustion Engines, SAE Paper 680124, Automotive Engineering Congress, Detroit, Michigan (8-12 January 1968).

B-15. G. A. Lavoie, J. B. Heywood, and J. C. Keck, Experimental Study of Nitric Oxide Formation in Internal Combustion Engines, Department of Mechanical Engineering, Massachusetts Institute of Technology, Fluid Mechanics Laboratory Publication No. 69-10 (November 1969).

B-16. H. K. Newhall and E. S. Starkman, Direct Spectroscopic Determination of Nitric Oxide in Reciprocating Engine Cylinders, SAE Paper 670122, Automotive Engineering Congress, Detroit, Michigan (9-13 January 1967).

B-17. L. S. Caretto, L. J. Muzio, R. F. Sawyer, and E. S. Starkman, The Role of Kinetics in Engine Emission of Nitric Oxide, Paper presented at AICHE/IMIQ Meeting, Denver, Colorado (September 1970).

B-18. T. A. Huls and H. A. Nickol, Influence of Engine Variables on Exhaust Oxides of Nitrogen Concentrations from a Multi-cylinder Engine, SAE Paper 670482, Mid-Year Meeting, Chicago, Illinois (15-19 May 1967).

B-19. D. F. Hagen and G. W. Holiday, The Effects of Engine Operating and Design Variables on Exhaust Emissions, SAE Paper 486C, Combined National Automobile and Production Meetings of the SAE, Detroit, Michigan (12-16 March 1962).

B-20. M. W. Jackson, W. M. Wiese, and I. T. Wentworth, The Influence of Air-Fuel Ratio, Spark Timing and Combustion Chamber Deposits on Exhaust Hydrocarbon Emissions, SAE Paper 486A, National Automobile Week, Detroit, Michigan (12-16 March 1962).

B-21. W. S. Fagley, M. V. Sink, and C. M. Heinen, Maintenance and the Automobile Exhaust, SAE Paper 29V, SAE Annual Meeting, Detroit, Michigan (12-16 January 1959).

B-22. I. H. Freeman and R. C. Stahman, Vehicle Performance and Exhaust Emission, Carburetion vs. Timed Fuel Injection, SAE Paper 650863, National Fuel and Lubricants Meeting, Tulsa, Oklahoma (2-4 November 1965).

B-23. D. L. Hittler and L. R. Hamkins, Emission Control by Engine Design and Development, SAE Paper 680110, Automotive Engineering Congress, Detroit, Michigan (8-12 January 1968).

B-24. L. Eltinge, F. J. Marsee, A. J. Warren, Potentialities of Further Emissions Reduction by Engine Modifications, SAE Paper 680123, Automotive Engineering Congress, Detroit, Michigan (8-12 January 1968).

B-25. J. H. Jones and J. C. Gagliardi, Vehicle Exhaust Emission Experiments Using a Premixed and Preheated Air Fuel Charge, SAE Paper 670485, Mid-Year Meeting, Chicago, Illinois (15-19 May 1967).

B-26. E. Bartholomew, Potentialities of Emission Reduction by Design of Induction Systems, SAE Paper 660109, Automotive Engineering Congress, Detroit, Michigan (10-14 January 1966).

B-27. D. A. Trayser and F. A. Creswick, Effect of Induction System Design on Automotive Engine Emissions, Presented at the ASME Winter Annual Meeting, Los Angeles, California (16-20 November 1969).

B-28. T. A. Huls, P. S. Myers, and O. A. Uyehara, Spark Ignition Engine Operation and Design for Minimum Exhaust Emission, SAE Paper 660405, Mid-Year Meeting, Detroit, Michigan (6-10 June 1966).

B-29. H. W. Schwochert, Performance of a Catalytic Converter on Nonleaded Fuel, SAE Paper 690503, Mid-Year Meeting, Chicago, Illinois (19-23 May 1969).

B-30. D. P. Osterhaut, K. I. Jagel, and W. J. Koehl, The IIEC Program-A Progress Report, ASTM Workshop on Effects of Automotive Emission Requirements on Gasoline Characteristics, Toronto, Ontario, Canada (24 June 1970).

B-31. R. D. Kopa, Control of Automotive Exhaust Emission by Modifications of the Carburetion System, SAE Paper 660114, Automotive Engineering Congress, Detroit, Michigan (10-14 January 1966).

B-32. H. K. Newhall, Control of Nitrogen Oxides by Exhaust Recirculation-A Preliminary Theoretical Study, SAE Paper 670495.

B-33. J. D. Benson, Reduction of Nitrogen Oxides in Automobile Exhaust, SAE Paper 690019, International Automotive Engineering Congress, Detroit, Michigan (13-17 January 1969).

4 OF 5

PB

201646

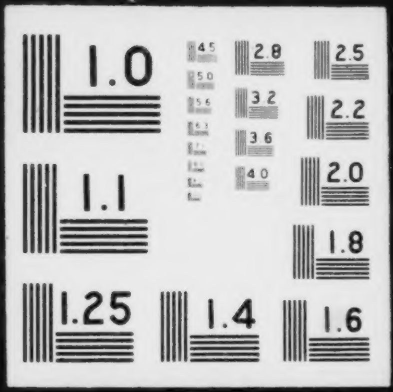
1.0
4.5
5.0
5.6
6.3
7.1
8.0
9.0
2.8
3.2
3.6
4.0
2.5
2.2
2.0
1.1
1.8
1.25
1.4
1.6

B-34. W. Glass, F. R. Russell, D. T. Wade, and D. M. Hollabaugh, Evaluation of Exhaust Recirculation for Control of Nitrogen Oxides Emissions, SAE Paper 700146, Automotive Engineering Congress, Detroit, Michigan (12-16 January 1970).

B-35. J. E. Nicholls, I. A. El Messiri, and H. K. Newhall, Inlet Manifold Water Injection for Control of Nitrogen Oxides - Theory and Experiment, SAE Paper 690018, International Automotive Engineering Congress, Detroit, Michigan (13-17 January 1969).

B-36. J. J. Mikita and E. N. Cantwell, Exhaust Manifold Thermal Reactors - A Solution to the Automotive Emission Problem, 68th Annual Meeting of the National Petroleum Refiners Association, San Antonio, Texas (5-8 April 1970).

B-37. E. N. Cantwell, I. T. Rosenlund, W. J. Barth, F. L. Kinnear, and S. W. Ross, A Progress Report on the Development of Exhaust Manifold Reactors, SAE Paper 690139, International Automotive Engineering Congress, Detroit, Michigan (13-17 January 1969).

B-38. W. Glass, D. S. Kim, and B. J. Kraus, Synchrothermal Reactor System for Control of Automotive Exhaust Emission, SAE Paper 700147 Automotive Engineering Congress, Detroit, Michigan (12-16 January 1970).

B-39. D. E. Cole and C. Jones, Reduction of Emissions from the Curtiss-Wright Rotating Combustion Engine with an Exhaust Reactor, SAE Paper 700074, Automotive Engineering Congress, Detroit, Michigan (12-16 January 1970).

B-40. E. Mitchell, J. M. Cobb, and R. A. Frost, Design and Evaluation of a Stratified Charge Multifuel Military Engine, SAE Paper 680042, Automotive Engineering Congress, Detroit, Michigan (8-12 January 1968).

B-41. R. W. McJones, R. J. Corbell, Natural Gas Fueled Vehicles Exhaust Emissions and Operational Characteristics, Automotive Engineering Congress, Detroit, Michigan (12-16 January 1970).

B-42. M. C. Baxter, G. W. Leck III, and P. E. Mizelle, Total Emissions Control Possible with LP-Gas Vehicle, SAE Paper 680529, West Coast Meeting, San Francisco, California (12-15 August 1968).

B-43. C. D. Tyree and K. J. Springer, Studies of Emissions from Gasoline Powered Vehicles Above 6000 lb Gross Vehicle Weight, Final Report No. AR-752 (July 1970).

B-44. Personal Communication with Prof. David E. Cole, University of Michigan, Ann Arbor, Michigan.

B-45. Personal Communication with T. Ashby, APCO, Ypsilante, Michigan (November 1970).

B-46. Personal Communication with G. Gelb, TRW Systems, Redondo Beach, California (December 1970).

B-47. Personal Communication with C. Marks, General Motors Research Laboratories, Warren, Michigan (November 1970).

B-48. Personal Communication with W. Marshall, Bureau of Mines, data to be published by W. Marshall.

B-49. Personal Communication with one Engine Manufacturer.

B-50. Personal Communication with Test Laboratory.

B-51. C. T. Hare and K. J. Springer, Measurement of Diesel Exhaust Emissions using EMA Procedures, Final Report No. AR-749, Project 11-2814-01 (30 June 1970).

B-52. Personal Communication with Mr. J. L. Dooley, McCulloch Corporation, Los Angeles, California.

B-53. Personal Communication.

B-54. V. S. Yumlu and A. W. Carey, Jr., Exhaust Emission Characteristics of Four-Stroke, Direct Injection, Compression Ignition Engines, SAE Paper 680420, Mid-Year Meeting, Detroit, Michigan (20-24 May 1968).

B-55. J. M. Perez and E. W. Landen, Exhaust Emission Characteristics of Precombustion Chamber Engines, SAE Paper 680421, Mid-Year Meeting, Detroit Michigan (20-24 May 1968).

B-56. M. H. Saadawi, Air Pollutants in Diesel Engine Exhaust, Parts I and II, Department of Engineering, University of California at Los Angeles, Report No. 65-32 (February 1966).

B-57. W. F. Marshall and R. W. Hurn, Factors Influencing Diesel Emissions, SAE Paper 680528, West Coast Meeting, San Francisco, California (12-15 August 1968).

B-58. Cooperative Evaluation of Techniques for Measuring Hydrocarbons in Diesel Exhaust, Coordinating Research Council, Inc., New York, CRC Report No. 431 (February 1970).

B-59. R. W. Hurn and W. F. Marshall, Techniques for Diesel Emission Measurement, SAE Paper No. 680418, Mid-Year Meeting, Detroit, Michigan (20-24 May 1968).

B-60. H. W. Pearsall, Measuring the Total Hydrocarbons in Diesel Exhaust, SAE Paper 670089, Automotive Engineering Congress, Detroit, Michigan (9-13 January 1967).

B-61. J. H. Johnson, E. J. Sienicki, and O. F. Zeck, A Flame Ionization Technique for Measuring Total Hydrocarbons in Diesel Exhaust, SAE Paper No. 680419, Mid-Year Meeting, Detroit, Michigan (20-24 May 1968).

B-62. K. J. Springer, An Investigation of Diesel-Powered Vehicle Odor and Smoke, Part III, Final Report No. AR-695, Contract No. PH 22-68-23.

B-63. K. J. Springer and C. T. Hare, Four Years of Diesel Odor and Smoke Control Technology Evaluations -- A Summary, ASME Paper No. 69-AW/APC-3, ASME Winter Annual Meeting, Los Angeles, California (16-20 November 1969).

B-64. J. W. Vogh, "Nature of Odor Components in Diesel Exhaust," Journal of the Air Pollution Control Association, vol. 19, no. 10, pp. 773-777 (October 1969).

B-65. D. F. Merrion, Effect of Design Revisions on Two-Stroke-Cycle Diesel Engine Exhaust, SAE Paper 680422, Mid-Year Meeting, Detroit, Michigan (20-24 May 1968).

B-66. N. A. Henein and J. A. Bolt, The Effect of Some Fuel and Engine Factors on Diesel Smoke, SAE Paper 690557, National West Coast Meeting, Seattle, Washington (11-14 August 1969).

B-67. K. C. Tessier and H. E. Bachman, Fuel Additives for the Suppression of Diesel Exhaust Odor and Smoke, Part I: Proposed Mechanism for Smoke Suppression, ASME Paper No. 68-WA/DGP-4, ASME Winter Annual Meeting and Energy Systems Exposition, New York (1-5 December 1968).

B-68. Personal Communication with Manufacturer.

B-69. Exhaust Emissions from Williams Research Corporation Gas Turbine Engines, Report No. WR-ER8 (18 June 1970).

B-70. Personal Communication with A. J. Feeney, Williams Research Corporation, Walled Lake, Michigan.

B-71. Personal Communication with Solar, A Division of International Harvester Company, San Diego, California.

B-72. W.A. Turunen and J.S. Collman, The General Motors Research GT-309 Gas Turbine Engine, SAE Paper 650714, Combined Powerplant and Transportation Meeting, Cleveland, Ohio (18-21 October 1965).

B-73. W. Cornelius, D. L. Stivender, and R. E. Sullivan, A Combustion System for a Vehicular Regenerative Gas Turbine Featuring Low Air Pollutant Emissions, SAE Paper 670936, Combined Fuels and Lubricants, Powerplant and Transportation Meeting, Pittsburgh, Pennsylvania (30 October to 3 November 1967).

B-74. W. Cornelius and W.R. Wade, The Formation and Control of Nitric Oxide in a Regenerative Gas Turbine Burner, SAE Paper 700708, Combined National Farm, Construction, and Industrial Machinery and Powerplant Meeting, Milwaukee, Wisconsin (14-17 September 1970).

B-75. R. F. Sawyer, Emissions Characteristics of Vehicular Gas Turbine Engines, ASME Winter Annual Meeting, New York (30 November 1970).

B-76. R. F. Sawyer, D.P. Teixeira, and E.S. Starkman, "Air Pollution Characteristics of Gas Turbine Engines," Transaction of the ASME Journal of Engineering for Power (October 1969).

B-77. D.S. Smith, R.F. Sawyer, and E.S. Starkman, "Oxides of Nitrogen from Gas Turbines," Journal of the Air Pollution Control Association, vol. 18, no. 1 (January 1968).

B-78. R. F. Sawyer, Fundamental Processes Controlling the Air Pollution Emissions from Turbojet Engines, AIAA Paper No. 69-1040, AIAA 6th Annual Meeting and Technical Display, Anaheim, California (20-24 October 1969).

B-79. A. W. Bell, N. Bayard de Volo, and B.P. Breen, Nitric Oxide Reduction by Controlled Combustion Processes, Paper No. WSCI-70-5, Western States Section, Combustion Institute, Spring Meeting (20-21 April 1970).

B-80. Personal Communication with W. Cornelius, C. Amann, and W. Wade, General Motors Research Laboratories, Warren, Michigan.

B-81. M. W. Korth and A. H. Rose, Jr., Emissions from a Gas Turbine Automobile, SAE Paper 680402, Mid-Year Meeting, Detroit, Michigan (20-24 May 1968).

B-82. P. T. Vickers, C. A. Amann, H. R. Mitchell, and W. Cornelius, The Design Features of the GM SE-101 - A Vapor Cycle Powerplant, SAE Paper 700163, Automotive Engineering Compress, Detroit, Michigan (12-16 January 1970).

B-83. P. T. Vickers, J. R. Mondt, W. H. Haverdink, and W. R. Wade, General Motors Steam Powered Cars - Emissions, Fuel Economy and Performance, SAE Paper 700670, National West Coast Meeting, Los Angeles, California (24-27 August 1970).

B-84. S. S. Miner, Developments in Automotive Steam Powerplants, SAE Paper 690943, International Automotive Engineering Congress, Detroit, Michigan (13-17 January 1969).

B-85. C. V. Burkland, W. B. Lee, G. Bahn, and R. Carlson, Study of Continuous Flow Combustion Systems for External Combustion Vehicle Powerplants, Final Report under Contract CPA 22-69-128, The Marquardt Corporation, Van Nuys, California (June 1970).

B-86. D. T. Morgan and R. J. Raymond, Conceptual Design-Rankine Cycle Power System with Organic Working Fluid and Reciprocating Engine for Passenger Vehicles, Thermo Electron Corporation Report No. TE 4121-133-70 (June 1970).

B-87. S. L. Altshuler and L. S. Caretto, The Air Pollution Characteristics of a Prototype Automotive Steam Generator (To be Published).

B-88. J. H. Lienesch and W. R. Wade, Stirling Engine Progress Report: Smoke, Odor, Noise and Exhaust Emissions, SAE Paper 680081, Automotive Engineering Congress, Detroit, Michigan (8-12 January 1968).

APPENDIX C

VEHICLE EXHAUST EMISSIONS TEST PROGRAM

CONTENTS

C. VEHICLE EXHAUST EMISSIONS TEST PROGRAM. C-1

- C.1 Introduction C-1
- C.2 Test Vehicles C-1
- C.3 Test Program. C-4
  - C.3.1 Driving Cycle Tests C-4
  - C.3.2 Steady-State Tests C-7
  - C.3.3 Vehicle Modifications C-8
    - C.3.3.1 Catalytic Converter. C-8
    - C.3.3.2 Turbocharger C-9
- C.4 Instrumentation C-9
  - C.4.1 Exhaust Emissions C-9
  - C.4.2 Engine Parameters C-10
    - C.4.2.1 Fuel Flow C-10
    - C.4.2.2 Power Output C-10
    - C.4.2.3 Manifold Pressure C-11
    - C.4.2.4 Engine Speed C-11
    - C.4.2.5 Exhaust Gas Temperature C-11
- C.5 Results C-11
  - C.5.1 Comparison of Mass Emissions by Various Driving Cycles C-12
    - C.5.1.1 Comparison of Bag Results with Calculated Values C-12
    - C.5.1.2 Comparison of Seven-Mode Cycle with DHEW Cycle C-12
  - C.5.2 Cold Start Emissions C-12
  - C.5.3 Diesel Catalyst C-15
  - C.5.4 Steady-State Results C-15
- C.6 References C-16

TABLES

C-1. Engine Specifications for Test Vehicles C-2

C-2. Vehicle Specifications for Test Vehicles C-3

C-3. Test Results for Seven-Mode Driving Cycle C-5

C-4. Test Results for DHEW Driving Cycle C-6

FIGURES

C-1. Comparison of Cold Start Automotive Diesel Exhaust Emissions by Different Methods C-13

C-2. Comparison of Cold Start Exhaust Emissions for Ford Pinto by Different Methods C-14

APPENDIX C

VEHICLE EXHAUST EMISSIONS TEST PROGRAM

C.1 INTRODUCTION

As part of the overall study of Hybrid Heat Engine/Electric System Vehicles, an automobile exhaust emission test program was conducted at Scott Research Laboratories, San Bernardino, California. The objective of the program was primarily to obtain data on exhaust emissions from automotive engines of less than 100 hp during cold start, hot start, and steady-state operating conditions. Three prechamber-type diesel engines were used in the program, and the effects of a turbocharger and a catalytic converter on exhaust emissions were investigated. A domestic subcompact automobile with a spark ignition engine was also used.

The automobiles were operated on a chassis dynamometer over the seven-mode and DHEW driving cycles and under a number of steady-state engine operating conditions.

Scott Research Laboratories was selected as the test facility primarily because of their prior experience with diesel-powered vehicles gained during the 1970 MIT/Cal Tech Clean Air Car Race.

C.2 TEST VEHICLES

Four vehicles were used in the test program: three with compression-ignition (diesel) engines and one with a spark ignition gasoline engine. The engine and vehicle specifications are given in Tables C-1 and C-2, respectively.

The diesel-powered vehicles were domestic automobiles that had their factory-installed gasoline engines replaced by small foreign-manufactured diesel engines. The diesel conversions were made by the Wilcap Company, Torrance, California, which contributed the Valiant/Daihatsu and the

Table C-1. Engine Specifications of Test Vehicles[a]

Vehicle	Mustang/Daihatsu	Valiant/Daihatsu	Cadillac/Peugeot	Ford Pinto
Manufacturer	Daihatsu Kogyo Co., Osaka, Japan	Daihatsu Kogyo Co.	Peugeot-Lille, Paris, France	Ford of Germany, Cologne, Germany
Model	DE, four-cycle diesel	DG, four-cycle diesel	XDP 6.90, four-cycle diesel	Four-cycle, overhead cam
Displacement	138.5 cu in. (2270 cc)	145 cu in. (2500 cc)	193.3 cu in. (3168 cc)	122 cu in. (2000 cc)
Cylinders	Four, OHV	Four, OHV	Six, OHV	Four, OHV
Bore and Stroke	3.34 × 3.94 in. (85 × 100 mm)	3.46 × 4.09 in. (88 × 104 mm)	3.543 × 3.267 in. (90 × 83 mm)	3.574 × 3.092 in. (90.8 × 77 mm)
Compression Ratio	18.5 : 1	20 : 1	22.8 : 1	8.6 : 1
Rated Horsepower	63 at 3600 rpm	75 at 3800 rpm	106 at 4000 rpm	100 at 5600 rpm
Maximum Torque	107 ft-lb_f at 2000 rpm	126 ft-lb_f at 2000 rpm	147 ft-lb_f at 1950 rpm	120 ft-lb_f at 3600 rpm
Cooling	Water, no fan	Water, with fan	Water, with fan	Water, with fan
Fuel Supply	Injection, Bosch, throttled nozzle	Injection, Bosch, throttled nozzle	Injection, roto-diesel	Carburetion, Weber-design by Holly
Governor	Pneumatic	Pneumatic	Mechanical	NA
Weight	470 lb_f	528 lb_f	525 lb_f	297 lb_f
Combustion Chamber	Swirl type	Swirl type	Ricardo "Comet V"	Modified hemisphere
Ignition System	Glow plugs for starting	Glow plugs for starting	Glow plugs for starting	Bosch; Autolite spark plugs
Electrical System	12 V	12 V	12 V	12 V

[a]From Refs. C-1 – C-4.

Table C-2. Vehicle Specifications for Test Vehicles[a]

Vehicle	Mustang/Daihatsu	Valiant/Daihatsu	Cadillac/Peugeot	Ford Pinto
Body	1965 Ford Mustang	1969 Plymouth Valiant	1963 Cadillac Sedan de Ville	1971 Ford Pinto
Transmission:	Four-speed manual (Ford)	Three-speed automatic (Chrysler)	Three-speed automatic (Chrysler)	Three-speed automatic (Ford)
Gear Ratios	3.16, 2.21, 1.41, 1.00	2.45, 1.45, 1.00	2.45, 1.45, 1.00	2.46, 1.46, 1.00
Torque Converter	NA	Yes	Yes	No
Overdrive	No	30% reduction	No	No
Differential	3.23 : 1 at rear axle	3.80 : 1 at rear axle	3.21 : 1 at rear axle	3.81 : 1 at rear axle
Tires	6.50 × 13	7.00 × 13	J78 × 15	6.00 × 13
Weight	3000 lb_f, loaded	3200 lb_f, loaded	5000 lb_f, loaded	2500 lb_f, GVW
Odometer Miles				
Vehicle	150,000	18,000	82,000	1,900
Engine	52,000	18,000	1,200	1,900
Turbocharger	12,000	NA	NA	NA

[a] From Refs. C-1 – C-4.

Cadillac/Peugeot for the test program. The Mustang/Daihatsu was acquired on a rental basis. The Ford Pinto with the gasoline engine was provided by two new car dealers* who agreed to support the program.

C. 3 TEST PROGRAM

A rather extensive test plan was delineated at the beginning of the program. However, some modifications had to be made in the original plan as circumstances and results dictated. The test plan accomplished two objectives: (a) it established the seven-mode and DHEW driving cycle emissions for both cold and hot starts, and (b) it established the steady-state engine emissions over a wide range of engine operating conditions.

In accordance with the Federal Testing Procedure, indolene-30, with a specific gravity of 0.746 at 61°F, was used as the fuel in the spark ignition engine tests. ARCO Supreme (Atlantic Richfield Co.), with a specific gravity of 0.859 at 77°F, was used as the diesel fuel.

C. 3. 1 Driving Cycle Tests

Results of the seven-mode and DHEW driving cycle tests, together with the emission data for the four vehicles, are listed in Tables C-3 and C-4, respectively. All of the driving cycle tests except one were made from cold starts. Since the federal test procedures do not call for repetitive use of the DHEW driving cycle, one hot start DHEW driving cycle was made for direct comparison with the cold start DHEW cycle for the Valiant/Daihatsu with catalyst installed. The seven-mode cold start test with the Mustang/Daihatsu with turbocharger was made with a 4-hr cold soak (instead of the usual 12 hr) in order to duplicate the procedure used in the Clean Air Car Race.

In accordance with the specified procedure, continuous emission readings were taken during the seven-mode tests. In addition, bag samples were taken using the constant volume sampling procedure (CVS) described in the

---

*See Appendix F.4.

Table C-3. Test Results for Seven-Mode Driving Cycle

Vehicle	Start	Gas	Calculated per CACR, grams per mile	Total Bag Sample, grams per mile	Bag A,[a] grams per mile	Bag B,[b] grams per mile	Bag C,[c] grams per mile
Mustang/Daihatsu With Turbocharger	Cold	HC[d] CO NO_x[e]	1.16 2.15 1.44	NV[f] 2.87 2.25	NV[f] 2.87 1.62	NV[f] 2.87 1.99	NV[f] 2.87 2.09
Mustang/Daihatsu With Turbocharger	Hot	HC[d] CO NO_x[e]	1.16 2.08 1.51	- - -	- - -	- - -	- - -
Mustang/Daihatsu Without Turbocharger	Cold	HC[d] CO NO_x[e]	2.01 2.87 2.07	NV[f] 6.47 1.80	NV[f] 3.23 1.54	NV[f] 3.23 1.48	NV[f] 3.23 1.38
Valiant/Daihatsu Without Catalyst	Cold	HC[d] CO NO_x[e]	0.26 0.81 1.89	NV[f] 2.89 2.47	NV[f] 2.89 2.00	NV[f] 2.89 2.00	NV[f] 1.45 2.00
Ford Pinto	Cold	HC[d] CO NO_x[e]	1.63 50.67 1.91	3.94 80.96 3.32	6.33 112.76 2.21	4.45 98.30 2.90	2.87 72.28 3.79
Ford Pinto	Hot	HC[d] CO NO_x[e]	1.91 35.94 2.38	- - -	- - -	- - -	- - -

[a] Taken during first cycle.

[b] Taken during second cycle.

[c] Taken during third cycle.

[d] Hot FID as propane; however, bag samples were cold FID.

[e] As NO_2.

[f] Bag results not considered valid for diesels.

Table C-4. Test Results for DHEW Driving Cycle

Vehicle	Start	Gas	Total Bag Sample, grams per mile	Bag A,[a] grams per mile	Bag B,[b] grams per mile
Mustang/Daihatsu With Turbocharger	Cold	HC[c]	NV[d]	NV[d]	NV[d]
		CO	3.20	3.20	3.20
		NO_x[e]	2.79	1.79	2.26
Mustang/Daihatsu Without Turbocharger	Cold	HC[c]	NV[d]	NV[d]	NV[d]
		CO	3.26	3.26	6.52
		NO_x[e]	2.52	2.25	3.11
Valiant/Daihatsu Without Catalyst	Cold	HC[c]	NV[d]	NV[d]	NV[d]
		CO	3.20	3.20	3.20
		NO_x[e]	3.05	2.79	3.89
Valiant/Daihatsu With Catalyst	Cold	HC[c]	NV[d]	NV[d]	NV[d]
		CO	3.20[f]	3.20[f]	3.20[f]
		NO_x[e]	3.44	2.54	4.02
Valiant/Daihatsu With Catalyst	Hot	HC[c]	NV[d]	NV[d]	NV[d]
		CO	0[f]	0[f]	0[f]
		NO_x[e]	3.42	2.52	3.63
Cadillac/Peugeot	Cold	HC[c]	NV[d]	NV[d]	NV[d]
		CO	3.20	3.20	3.20
		NO_x[e]	3.52	2.84	5.68
Ford Pinto	Cold	HC[c]	2.76	5.71	3.33
		CO	76.82	141.00	96.02
		NO_x[e]	2.79	2.52	4.89

[a] Taken during first 143 sec.

[b] Taken between 143 and 340 sec.

[c] Cold FID as propane.

[d] Bag results not considered valid for diesels.

[e] As NO_2.

[f] Least detectable level (0.01%).

Federal Register of 15 July 1970 (Ref. C-5). The DHEW driving cycle presented in that document was used in the program. Although a revised DHEW cycle was presented in the Federal Register of 10 November 1970 (Ref. C-6), close examination revealed that the revisions were minor and did not justify delay of the test program until the new driving charts became available.

For both the Mustang and Valiant, the chassis dynamometer was set at an inertia load of 3000 lb_f and a road load of 8 hp. The road load was determined by making a manifold pressure reading at 50 mph cruise on the highway and then duplicating that reading with the vehicle on the dynamometer rollers. For the Pinto, this same procedure indicated an inertia load of 2500 lb_f and a road load of 4 hp.

For the Cadillac, the dynamometer load settings were arbitrarily matched with those of the Mustang and Valiant since the primary objective was to obtain a valid comparison of the engines and not the vehicles.

C.3.2 Steady-State Tests

The objective of these tests was to determine the engine specific mass emissions over a wide range of engine operating conditions for use in the analysis and evaluation of hybrid heat engine/electric vehicle systems. The tests were made at four different engine speeds (3000, 2400, 1800, and 1400 rpm), with a variation in load at each speed from full throttle to approximately 10 percent load to provide four or five load settings at each rpm. The emissions were also monitored at idle speed.

Attempts to operate the vehicles at their rated engine speeds were unsuccessful. At wide-open throttle and rated speed, the engine temperature reached the boiling point before the emission levels were completely stabilized because of inadequate auxiliary fan capacity. Since no temperature problems were experience at 3000 rpm, this speed was selected as maximum.

At full load, approximately 3 min were required for the diesels and approximately 5 min for the gasoline engine emissions to stabilize. At part load, approximately 2 min were required.

Wheel horsepower is measured on the chassis dynamometer, whereas engine brake horsepower is required to convert the measured pollutant specie concentrations to specific mass emission numbers. In view of the uncertainties in the drive train efficiency at the various speed and load conditions, the computed specific mass emissions are only approximate.

C.3.3 Vehicle Modifications

C.3.3.1 Catalytic Converter

It was originally planned to test the Pinto, as well as one of the diesels, with and without a catalytic converter in the exhaust system. However, it was not possible to obtain the proper catalytic device for the Pinto in time to include it in the program.

A catalytic converter for diesel exhaust (Model 4D23S) was obtained from Engelhard Industries, Newark, N. J., and installed in the Valiant/Daihatsu exhaust system after completion of the driving cycle and steady-state tests without catalyst. Engelhard advised that the catalyst required a minimum operating temperature of about 375°F. Therefore, it was installed as close as possible to the exhaust manifold.

The previous tests made with the Valiant/Daihatsu were repeated, with exception of the seven-mode driving cycle. Instead, a hot and a cold DHEW cycle tests were run.

It was subjectively observed that the strong diesel exhaust odor usually present was not detected when the vehicle was tested with the catalytic converter in the system.

C.3.3.2 Turbocharger

The first tests with the Mustang were made with an AiResearch (Model TO-4) turbocharger installed in the system. The pneumatic governor control was arranged such that the turbocharger operated at about 30 percent maximum manifold pressure. The earlier tests were repeated with the turbocharger removed and with the engine operating in its standard configuration. The most notable difference, other than power output, was in the amount of particulates trapped in the filters of the emission detectors. With the turbocharger in the system, the amount of smoke (particulates) was significantly reduced.

C.4 INSTRUMENTATION

In addition to the instrumentation required to monitor exhaust emissions, measurements of several engine parameters were made that permitted correlation of vehicle exhaust emissions with engine characteristics.

C.4.1 Exhaust Emissions

The exhaust species monitored were CO, CO_2, HC, NO, and NO_2. The CO, CO_2, and NO were measured with nondispersive infrared (NDIR) detectors; the NO_2 was measured with a nondispensive ultraviolet (NDUV) detector. The hydrocarbons were measured with both a heated flame ionization detector (FID) and an NDIR detector. Detection of the diesel exhaust species requires that the FID have a heated sample line and a heated detector in order that the heavier hydrocarbons found in the exhaust gases do not condense before reaching the detector. Continuous on-line monitoring of all emission species was carried out for both the driving cycles and steady-state tests. In addition, bag sample readings were made for the driving cycles in accordance with federal procedures for CVS. Multiple bag samples were also taken. This provided values for segments as well as totals for the driving cycle tests and made it possible to examine the exhaust emission characteristics during engine warmup. Bag A was used for the first cycle and bags B and C for the following two cycles of the seven-mode test. For the DHEW cycle, bag A was used to monitor the emissions during the first 143 sec of the cycle and bag B for the period between 143 and 340 sec.

The readings obtained from the bag samples for the hydrocarbons in the diesel exhaust were inaccurate because of condensation of the heavy hydrocarbons in the bag. The conversion of the NO to NO_2 in the bag samples was also quite apparent, even though sample readings were taken immediately at the end of the test cycles.

C.4.2 Engine Parameters

The engine operating parameters recorded for the driving cycle tests were fuel consumption, fuel and intake air temperature, humidity, and barometric pressure. Air flow rate, power output, engine speed, manifold pressure, and exhaust gas temperature were also recorded for the steady-state tests.

C.4.2.1 Fuel Flow

The total fuel consumption was recorded for each of the driving-cycle tests. For the steady-state tests, the fuel flow rates were measured by measuring the fuel volume consumed in a known period of time after a stable point was attained. A sufficient volume of fuel was consumed in 1 min to permit a reading that was approximately 2 percent accurate. However, at idle speed, 5 min were required before a measurement could be made.

C.4.2.2 Power Output

The horsepower at the rear wheels was measured with a newly calibrated Clayton chassis dynamometer with 20-in. rollers. Since this load includes both dynamometer friction and the power absorbed by the absorption unit, a calibration curve was made at 50 and 40 mph in accordance with the procedure outlined in the Federal Register.

C.4.2.3 Manifold Pressure

The manifold pressure gauges already installed in the Mustang and Valiant were used to measure manifold pressure. However, a standard pressure gauge was installed in the Pinto. Manifold pressure measurements were not made with the Peugeot engine because of its characteristic to admit a full charge of air on each suction stroke.

C.4.2.4 Engine Speed

Both the Mustang and Valiant had tachometers previously installed. The tachometer readings on the vehicle instruments were checked by using a Strobotac in conjunction with the crankshaft pulley. However, for the Cadillac/Peugeot, only the Strobotac was used.

For the steady-state tests made with the Pinto, the engine speed was measured by using an electric tachometer connected to the engine's ignition system.

C.4.2.5 Exhaust Gas Temperature

For the Valiant, a chromel-alumel thermocouple was installed at the inlet to the catalytic converter for measurement of exhaust gas temperature. The temperature history of at least one driving cycle was recorded.

C.5 RESULTS

The mass emission data for the seven-mode driving cycle and the DHEW driving cycle for the various test vehicles are listed in Tables C-3 and C-4, respectively. Values are given for individual bag samples as well as for total bag samples in order to illustrate the trend in the various emissions as a function of engine temperature during warmup. Data are not shown for the hydrocarbon measurements obtained from the bag readings for the diesels because they were not considered to be quantitatively valid. Moreover, the HC levels were too close to the background levels (in some cases the background bag even gave higher readings) to derive any meaningful qualitative results.

Data reduction for the steady-state tests was not completed in time to be included in this preliminary report. However, the results will be included in the final report. The data presented should not be considered final until publication of the Scott Research Laboratories final report (Ref. C-7).

C.5.1 Comparison of Mass Emissions by Various Driving Cycles

Figure C-1 shows the emission levels measured for the diesel-powered vehicles in the two driving cycles. In addition, the seven-mode data are shown for two different methods of calculation. Figure C-2 shows the equivalent data for the gasoline-powered vehicle.

C.5.1.1 Comparison of Bag Results with Calculated Values

The seven-mode cycle emissions were determined by the current method of calculation as well as by CVS bag sampling techniques. The current method utilizes data on pollutant species concentration combined with weighting factors for the various modes. In general, the calculated seven-mode results were lower than those obtained from the bag readings. Similar observations have been made by other investigators for spark ignition engines. For the Pinto, the observed difference was more pronounced than for the diesel-powered automobiles.

C.5.1.2 Comparison of Seven-Mode Cycle with DHEW Cycle

Comparison of the bag data from the two driving cycles indicates that the seven-mode and DHEW cycles yield similar results for the diesels. For the Pinto, the DHEW cycle HC and NO_x emissions are somewhat lower and the CO levels are about the same.

C.5.2 Cold Start Emissions

Comparison of the emission levels from the different bags shows that the CO emissions appear to be the same for the diesels whether hot or cold. However, it should be stressed that the measured CO levels were near the sensitivity threshold of the available NDIR instrument; hence, the observed

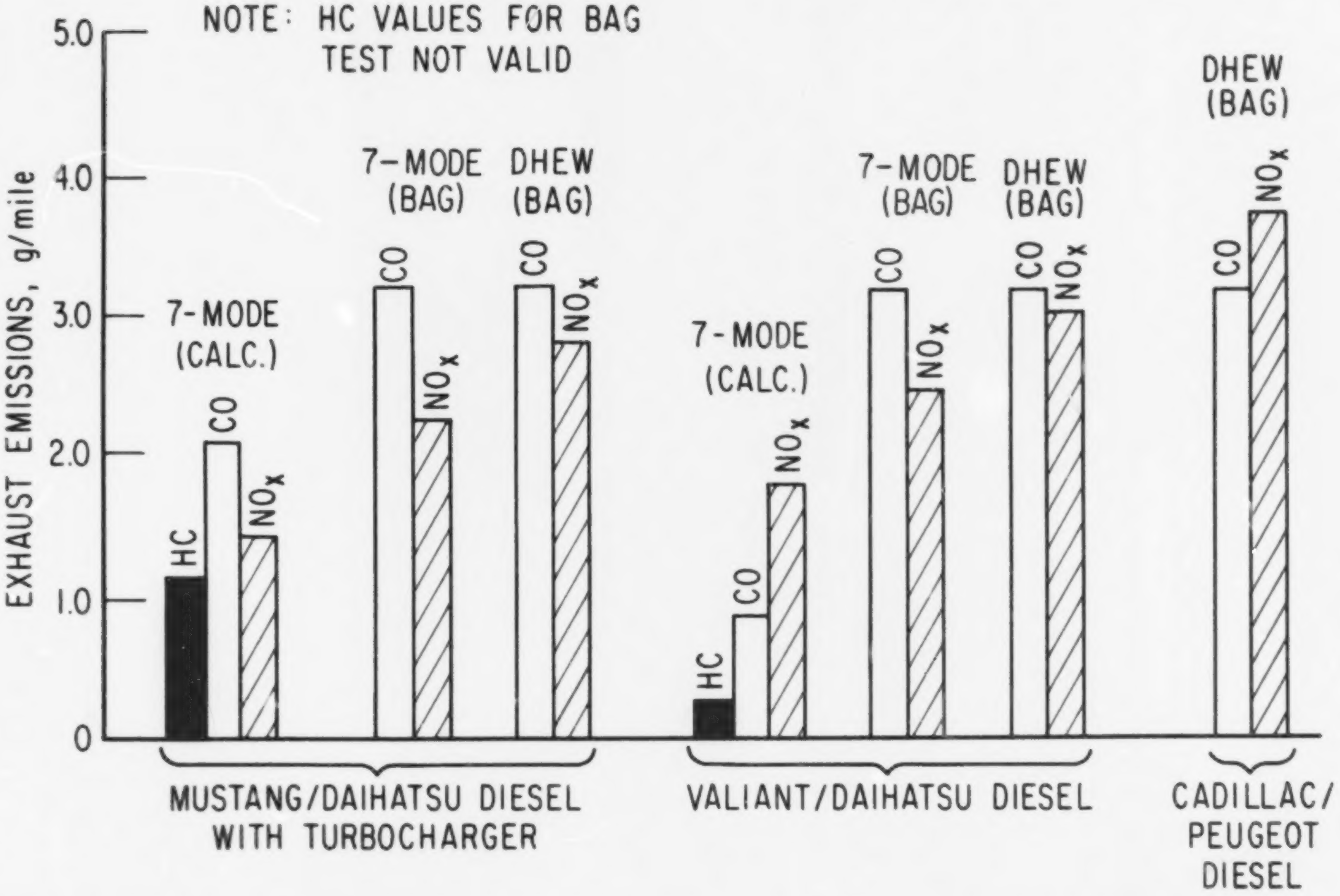

Figure C-1. Comparison of Cold Start Automotive Diesel Exhaust Emissions by Different Methods

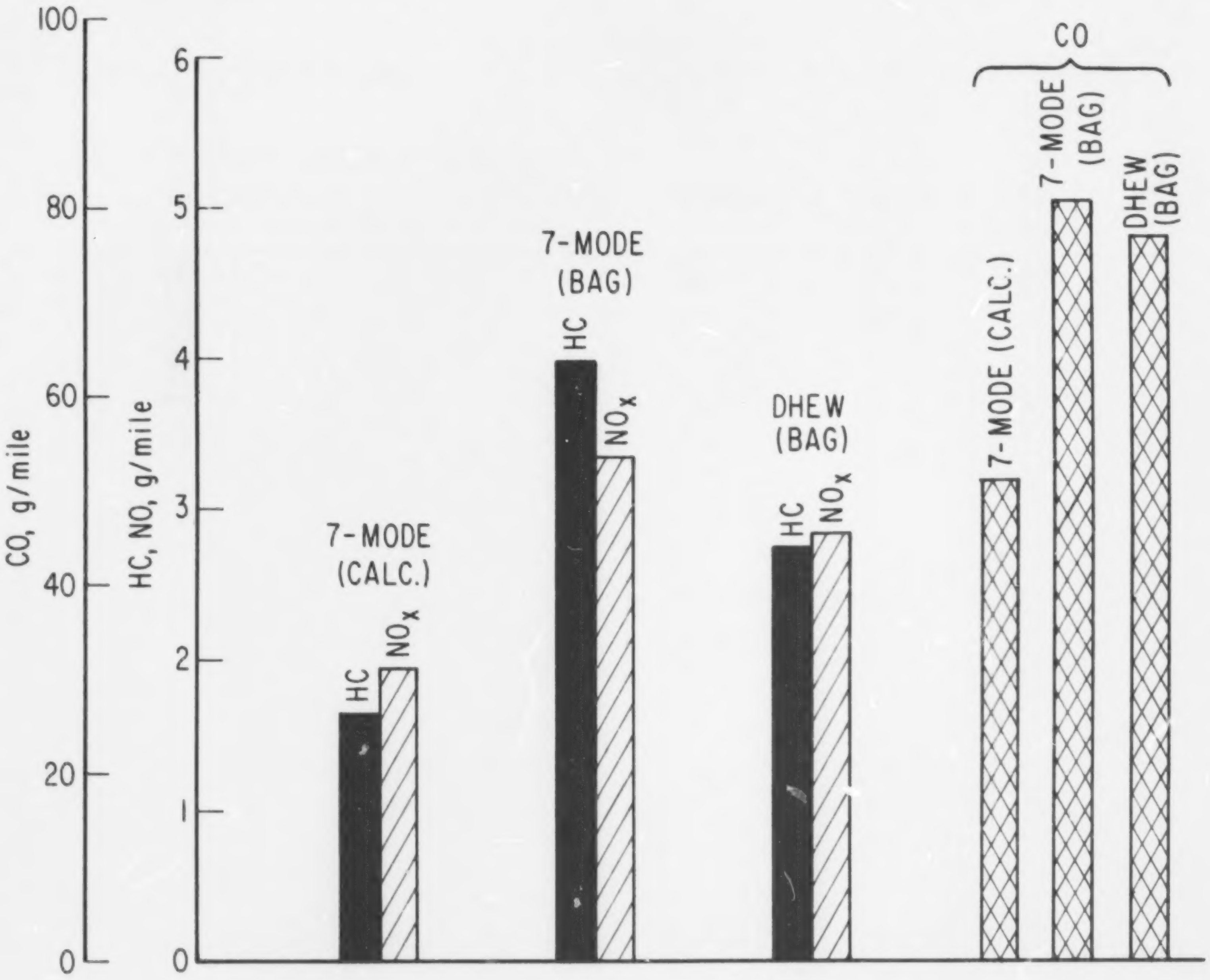

Figure C-2. Comparison of Cold Start Exhaust Emissions for Ford Pinto by Different Methods insensitivity of CO emissions to engine warmup should be a tentative conclusion. Since the HC bag data for the diesels are not valid because of condensation of the heavier HC molecules in the sample line, no conclusion can be made regarding HC based on the bag data. The calculated seven-mode cycle emissions indicate that there is no change in HC levels between hot and cold start tests.

For the Pinto, as expected, a definite decrease is shown in the CO and HC emissions during the warmup period.

As expected, the NO_x emissions increased for all engines during the warm-up period. However, the observed changes were greater for the Pinto. For the DHEW cycle, bag B contained data taken at the greatest rate of acceleration and the highest cruise level. The increasing high temperatures are reflected in the results.

In general, the data indicate that the diesel engine stabilizes faster than the spark ignition engine, and that the cold start effects are less severe. The same trend was observed during the steady-state runs. The Pinto results indicate that it was operating with a rich mixture during warmup because of the extremely high CO emission levels.

C.5.3 Diesel Catalyst

When the exhaust emissions were measured for the Valiant with a catalytic converter in the exhaust system, there was essentially no change observed in the NO_x level, as was expected with this particular catalyst. However, the HC and CO emissions were reduced significantly, although Table C-4 shows 3.2 g/mi for CO for the cold start test, which is the least detectable level of the instruments used.

As mentioned previously, the strong diesel odor usually present was quite mild when the catalyst was installed.

C.5.4 Steady-State Results

Data reduction for the steady-state tests was not completed in time to be included in this report.

C.6 REFERENCES

C-1. Workshop Manual, Model DE, Daihatsu Kogyo Company, Osaka, Japan.

C-2. Workshop Manual, Model DG, Daihatsu Kogyo Company, Osaka, Japan.

C-3. Technical Data Brochure, Societe Commerciale de Moteurs - C. L. M., Model XDP 6.90.

C-4.[*] Private Communication, Jim Rhodes, Resident Engineer, Ford Motor Company, Pico Rivera, California.

C-5. Federal Register (Department of Health, Education and Welfare, 15 July 1970), Vol. 35, No. 136.

C-6. Federal Register (Department of Health, Education and Welfare, 10 November 1970), Vol. 35, No. 219.

C-7. Diesel-Powered Passenger Car Emission Tests, Final Report, Project No. 2933, Scott Research Laboratories, Inc., San Bernardino, California (to be published).

---

[*] Not available outside The Aerospace Corporation.

APPENDIX D

EMISSION DRIVING CYCLE PERFORMANCE CHARACTERISTICS AND DESIGN DRIVING CYCLES

CONTENTS

D. EMISSION DRIVING CYCLE PERFORMANCE CHARACTERISTICS AND DESIGN DRIVING CYCLES D-1

D. 1 Introduction D-1

D. 2 Results of Emission Cycle Analysis D-1

D. 2. 1 Emission Cycles D-1

D. 3 Design Driving Cycles D-43

TABLES

D-1. Design Driving Cycle for Family Car. D-44

D-2. Design Driving Cycle for Commuter Car D-45

D-3. Design Cycle for Low-speed Delivery Van D-46

D-4. Design Driving Cycle for High-speed Van D-46

D-5. Design Driving Cycle for Low-speed Intracity Bus D-47

D-6. Design Driving Cycle for High-speed Intracity Bus. D-48

APPENDIX D

EMISSION DRIVING CYCLE PERFORMANCE CHARACTERISTICS AND DESIGN DRIVING CYCLES

D. 1 INTRODUCTION

An emission driving cycle is a set of velocity-time points which defines a velocity profile for use in determining vehicle exhaust emissions. This is in contrast to a design driving cycle which was used to verify that vehicle performance is sufficient to meet APCO specifications and maximum driving demands. An analysis of the operation of a family car, a commuter car, a delivery van and an intracity bus over their respective emission driving cycles was performed in order to determine the horsepower, energy and torque levels involved. These data are useful to insure that power/drive-train designs are adequate to meet the demands of these cycles. Also, they may be used in making preliminary exhaust emission estimates. Plots of the results are presented here. In addition, the design cycles used in this study are presented in tabular form in Section D. 4.

D. 2 RESULTS OF EMISSION CYCLE ANALYSIS

An analysis of the emission driving cycles for each class of vehicle studied was performed as discussed in Section 5. Vehicle powerplant output torque, horsepower, and energy requirements for each cycle were calculated using a computer program to solve the equations involved. Graphs of the computed results are presented.

D. 2. 1 Emission Cycles

D. 2. 1. 1 DHEW Cycle

			Page
Fig.	D-1.	Velocity Profile - DHEW Emission Cycle	D-4
	D-2.	Acceleration Profile - DHEW Emission Cycle	D-5
	D-3.	Distance Profile - DHEW Emission Cycle	D-6

D.2.1.2 New York City Comprehensive Cycle

Page

Fig. D-4. Velocity Profile - New York City Emission Cycle D-7

D-5. Acceleration Profile - New York City Emission Cycle D-8

D-6. Distance Profile - New York City Emission Cycle D-9

D.2.1.3 Delivery Van Emission Cycle (High and Low Speed)

Fig. D-7. Velocity Profile - Delivery Van Emission Cycle D-10

D-8. Acceleration Profile - Delivery Van Emissions Cycle D-11

D-9. Distance Profile - Delivery Van Emission Cycle D-12

D.2.1.4 High-speed Bus Emission Cycle

Fig. D-10 Velocity Profile - High-speed Bus Emission Cycle D-13

D-11 Acceleration Profile - High-speed Bus Emission Cycle D-14

D-12 Distance Profile - High-speed Bus Emission Cycle D-15

D.2.1.5 Low-speed Bus Emission Cycle

Fig. D-13. Velocity Profile - Low-speed Bus Emission Cycle D-16

D-14. Acceleration Profile - Low-speed Bus Emission Cycle D-17

D-15. Distance Profile - Low-speed Bus Emission Cycle D-18

D.2.2 Power Versus Time

Fig. D-16. Power Requirements - DHEW Emission Cycle - Family Car D-19

D-17. Power Requirements - DHEW Emission Cycle - Commuter Car D-20

D-18. Power Requirements - Delivery Van Emission Cycle D-21

D-19. Power Requirements - High-speed Bus Emission Cycle D-22

D-20. Power Requirements - Low-speed Bus Emission Cycle D-23

D.2.3 Cumulative Energy (to Wheels) Versus Time

Page

Fig. D-21. Energy Requirements - DHEW Emission Cycle - Family Car D-24

D-22. Energy Requirements - DHEW Emission Cycle - Commuter Car D-25

D-23. Energy Requirements - Delivery Van Emission Cycle D-26

D-24. Energy Requirements - High-speed Bus Emission Cycle D-27

D-25. Energy Requirements - Low-speed Bus Emission Cycle D-28

D.2.4 Torque (Shaft) Versus Time

Fig. D-26. Torque Requirements - DHEW Emission Cycle - Family Car D-29

D-27. Torque Requirements - DHEW Emission Cycle - Commuter Car D-30

D-28. Torque Requirements - Delivery Van Emission Cycle D-31

D-29. Torque Requirements - High-speed Bus Emission Cycle D-32

D-30. Torque Requirements - Low-speed Bus Emission Cycle D-33

D.2.5 Total Road Resistance (Rolling Plus Aerodynamic Drag) Versus Time

Fig. D-31. Road Resistance - DHEW Emission Cycle - Family Car D-34

D-32. Road Resistance - DHEW Emission Cycle - Commuter Car D-35

D-33. Road Resistance - Delivery Van Emission Cycle D-36

D-34. Road Resistance - High-speed Bus Emission Cycle D-37

D-35. Road Resistance - Low-speed Bus Emission Cycle D-38

D.2.6 Family Car (New York City Comprehensive Cycle)

Fig. D-36. Family Car - Power Requirements - New York City Emission Cycle D-39

D-37. Family Car - Energy Requirements - New York City Emission Cycle D-40

D-38. Family Car - Torque Requirements - New York City Emission Cycle D-41

D-39. Family Car - Road Resistance - New York City Emission Cycle D-42

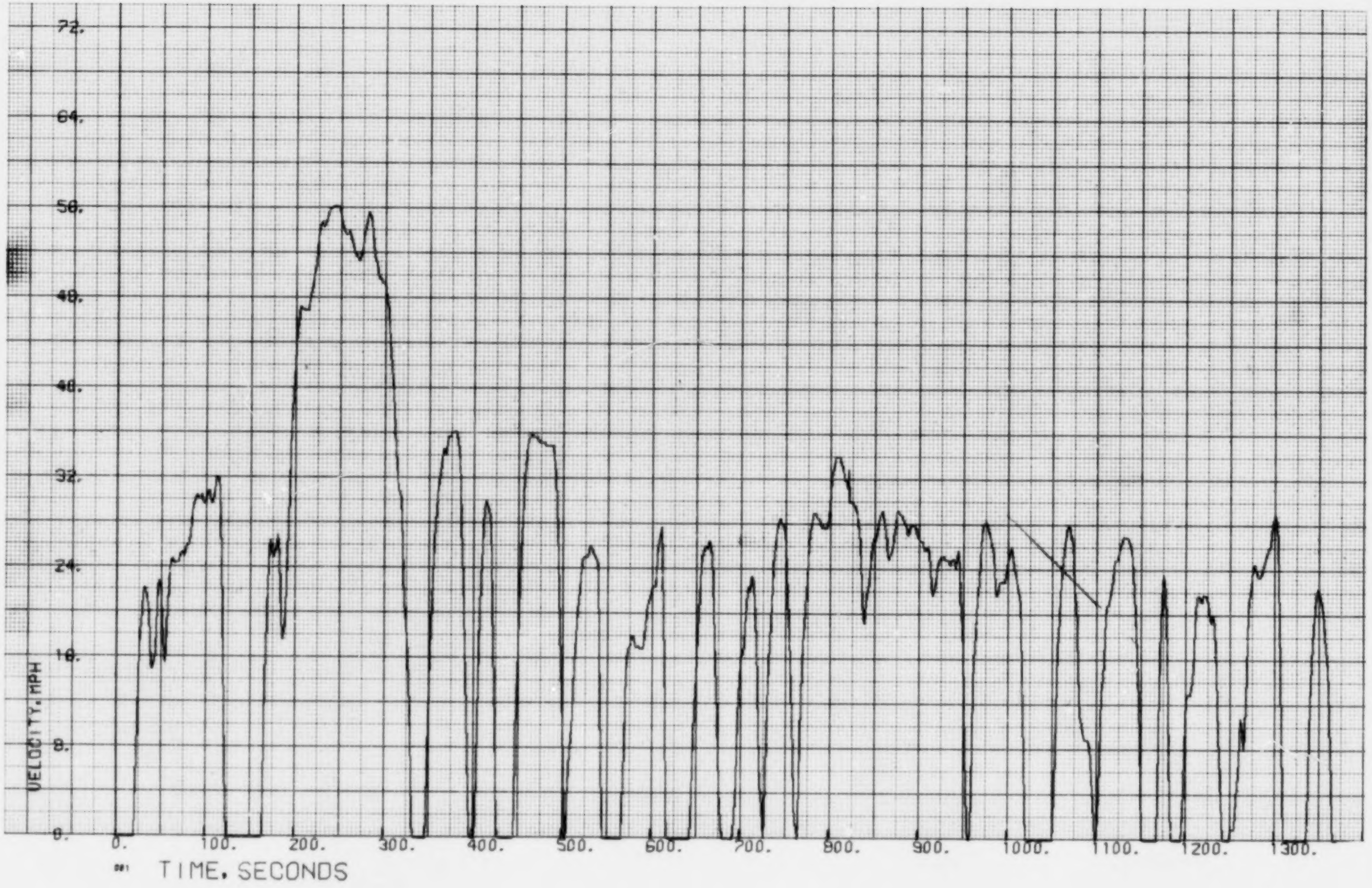

Figure D-1. Velocity Profile - DHEW Emission Cycle

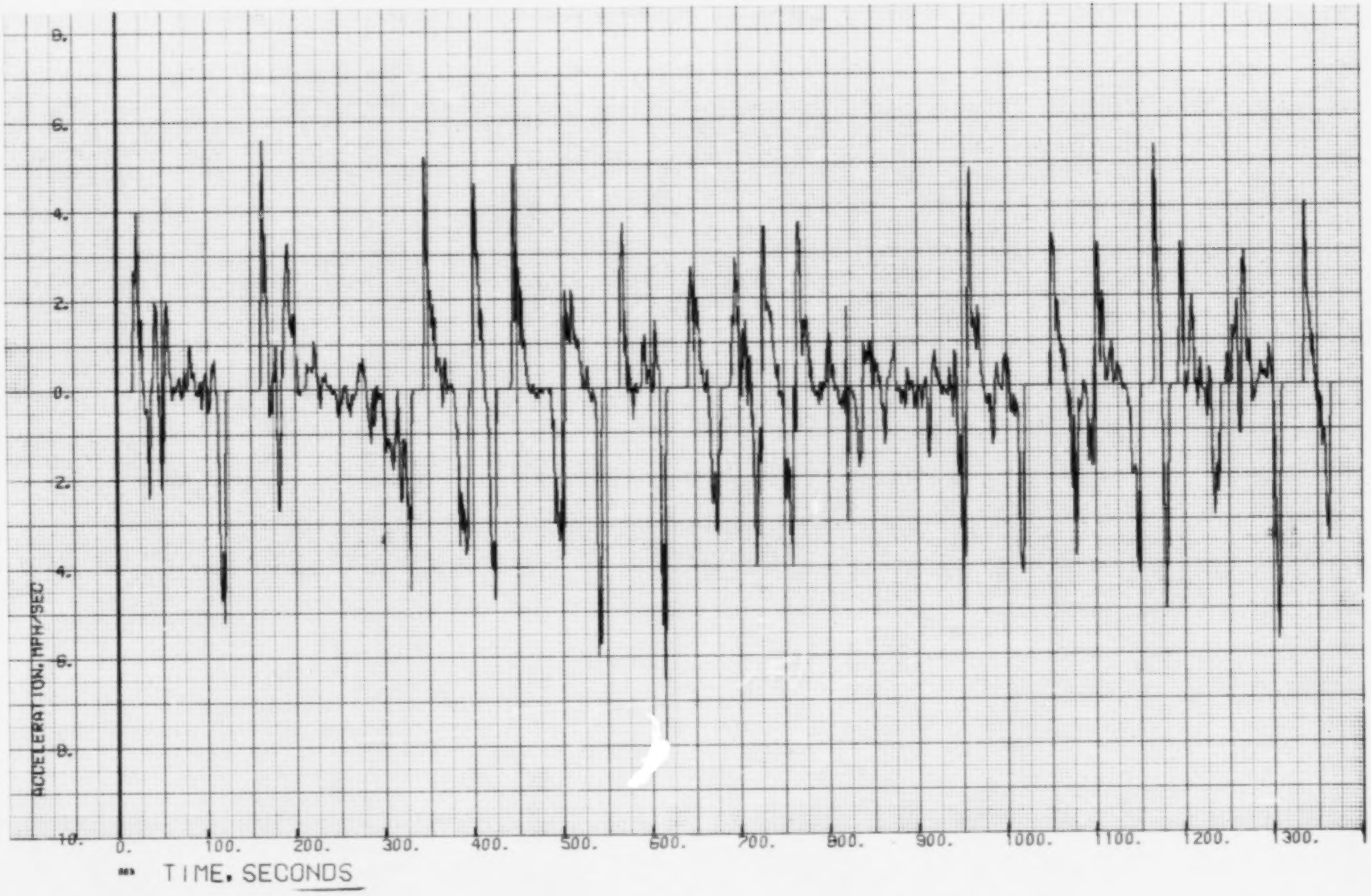

Figure D-2. Acceleration Profile - DHEW Emission Cycle

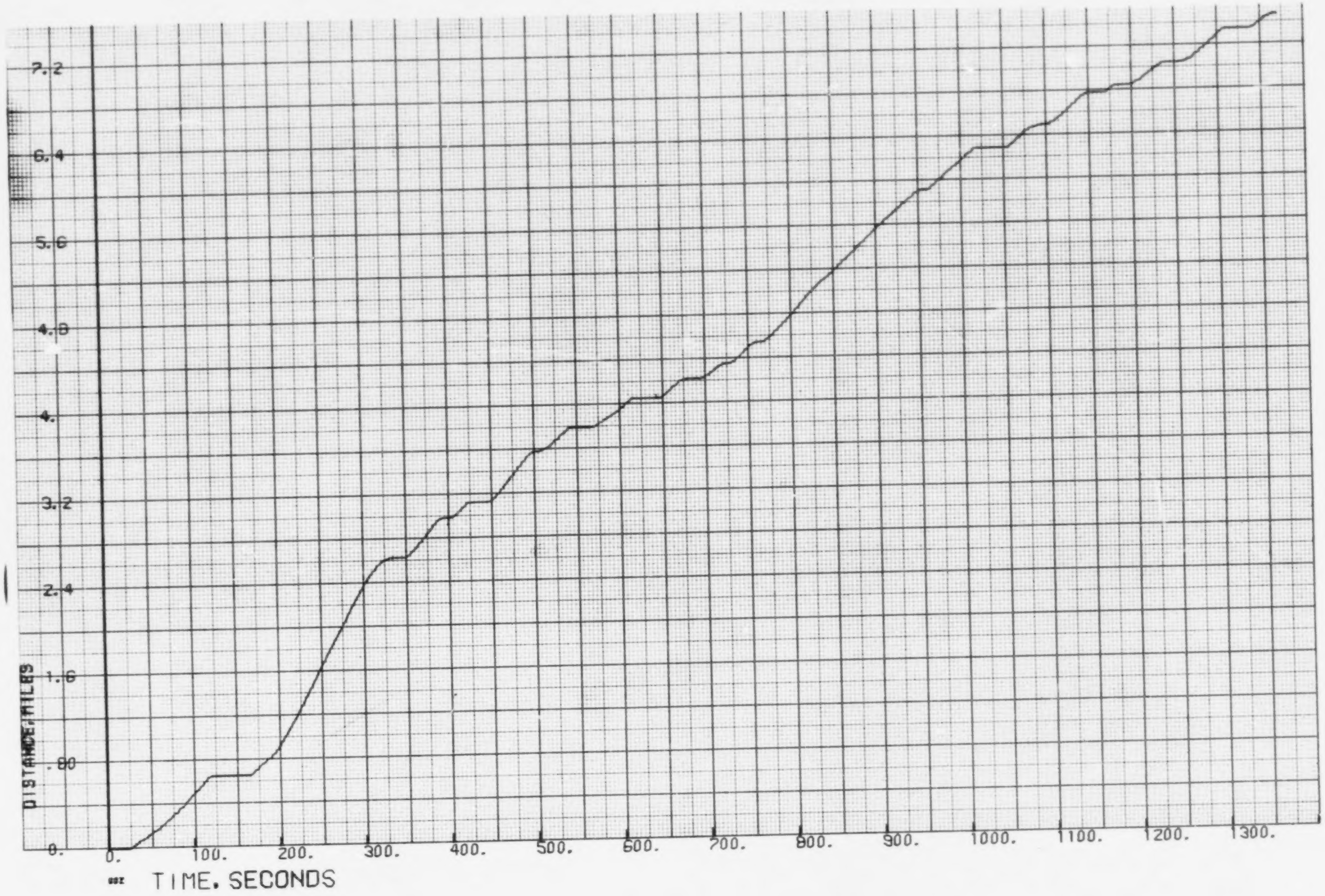

Figure D-3. Distance Profile - DHEW Emission Cycle

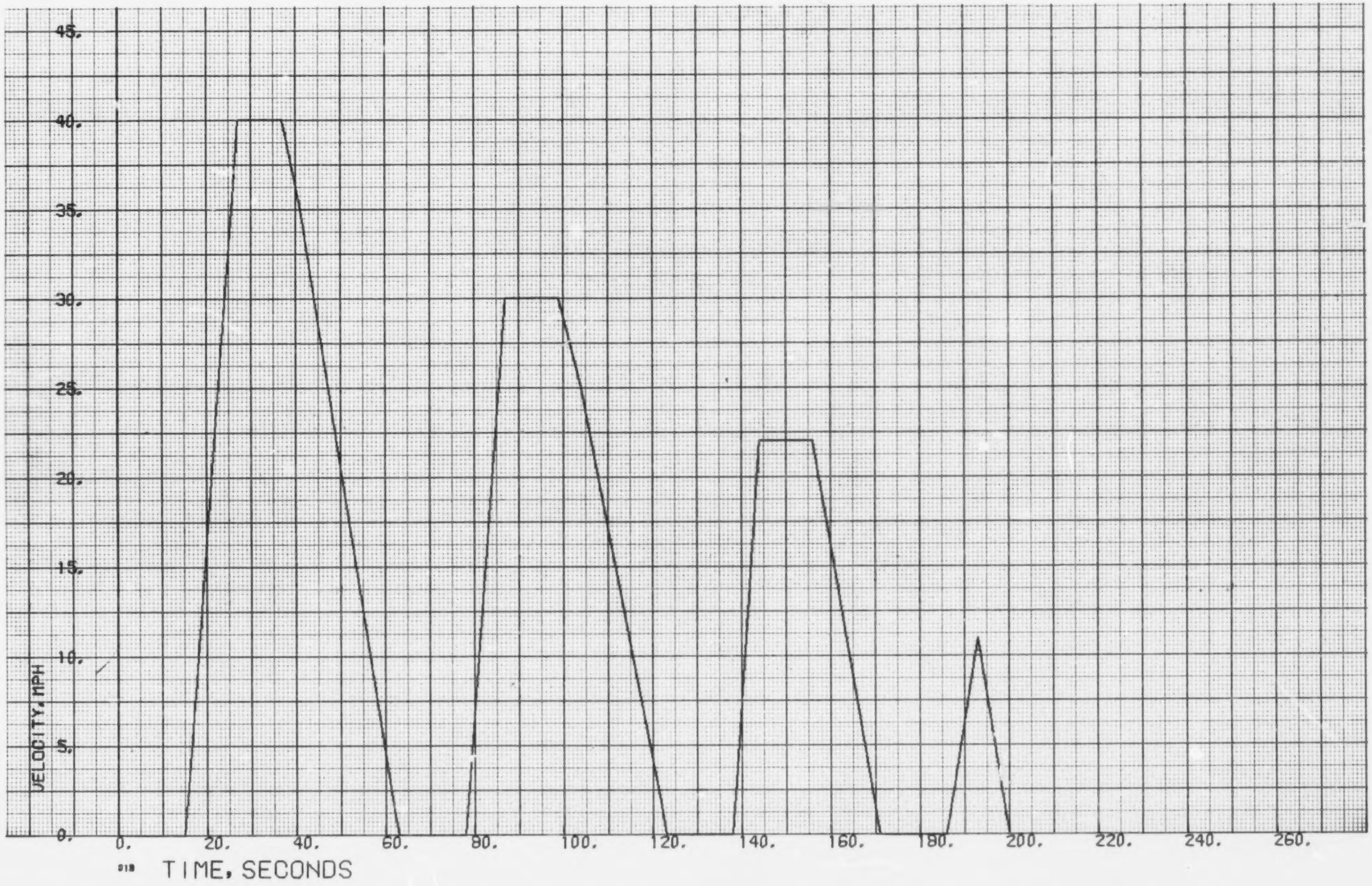

Figure D-4. Velocity Profile - New York City Emission Cycle

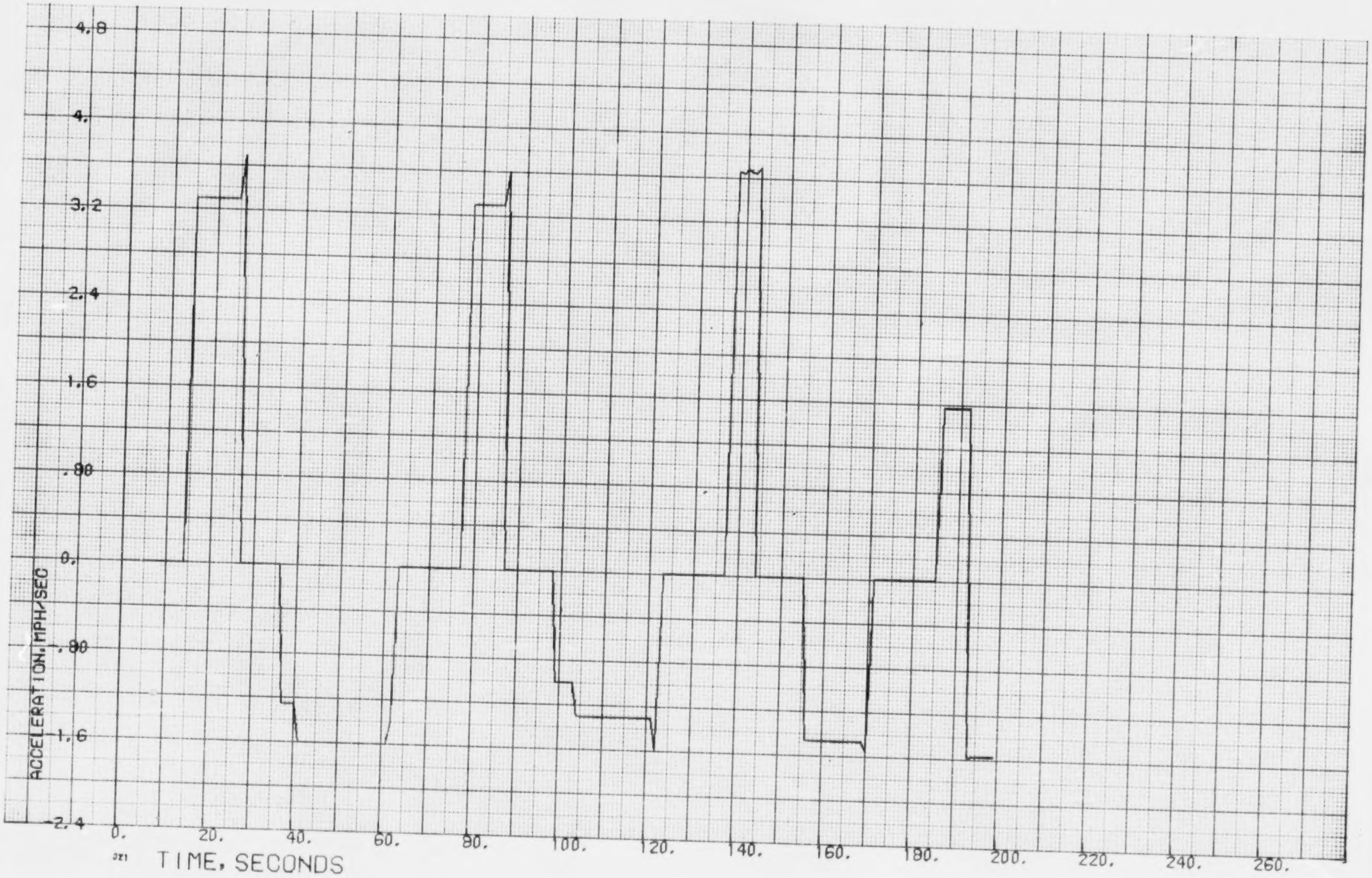

Figure D-5. Acceleration Profile - New York City Emission Cycle

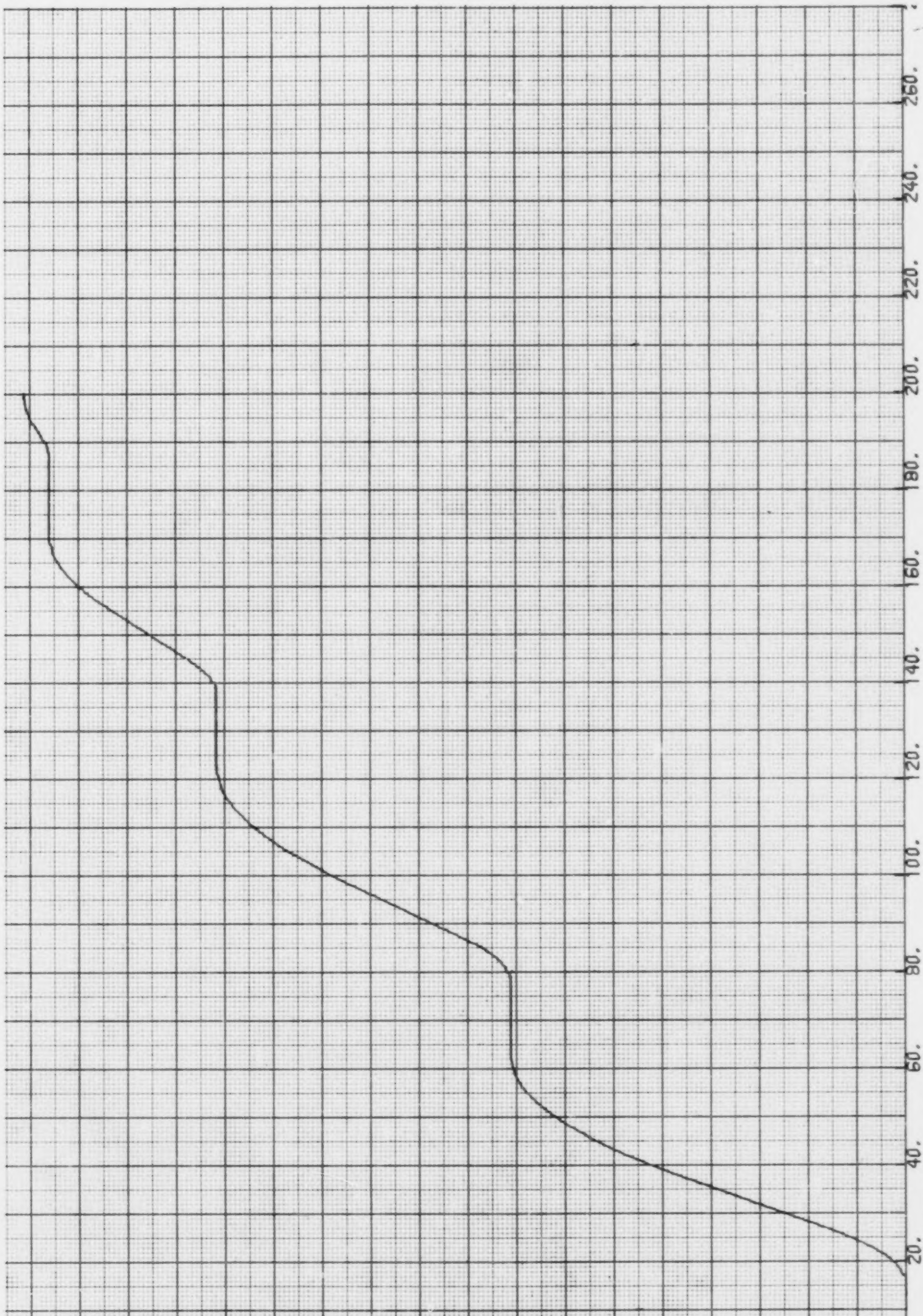

Figure D-6. Distance Profile - New York City Emission Cycle

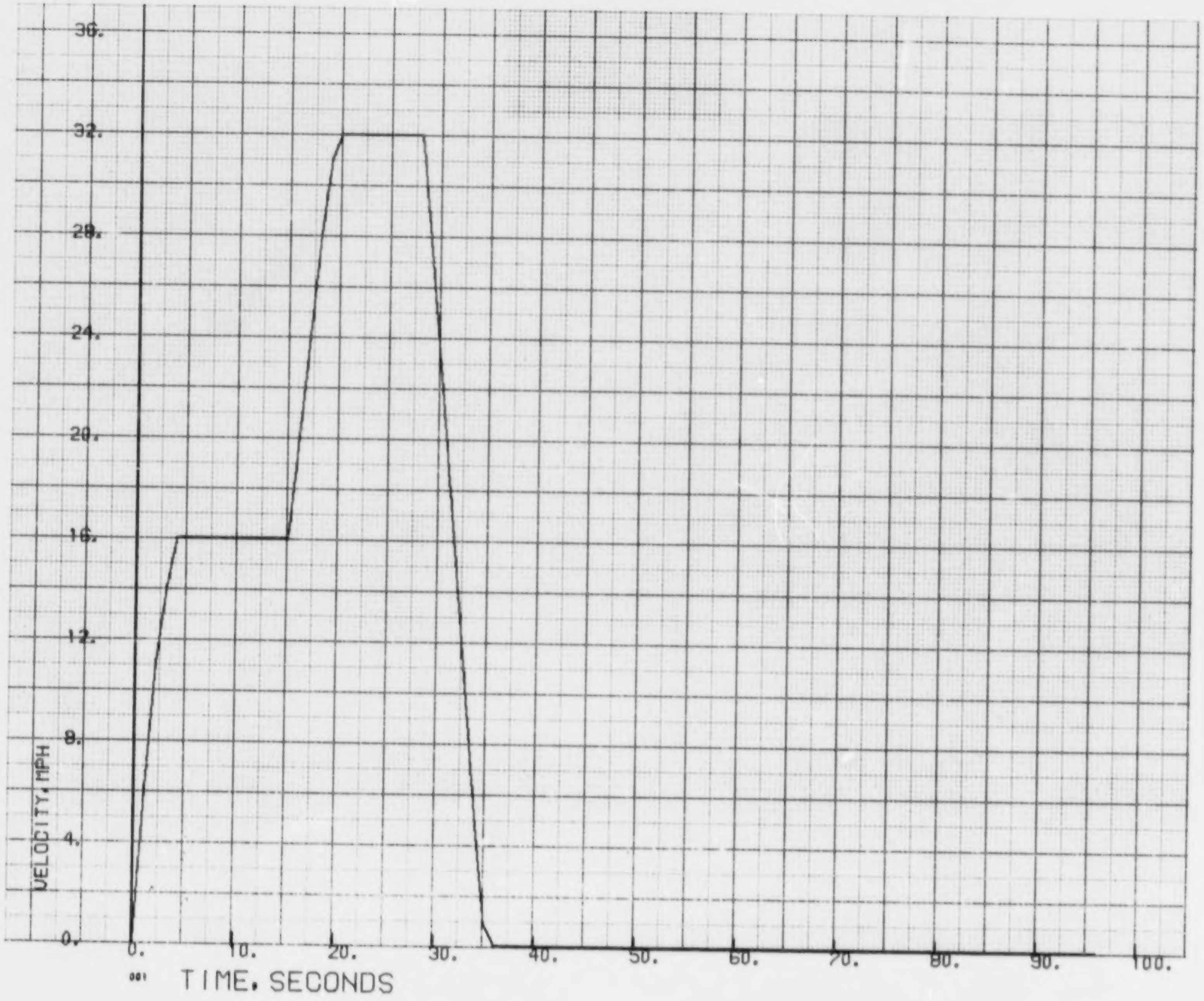

Figure D-7. Velocity Profile - Delivery Van Emission Cycle

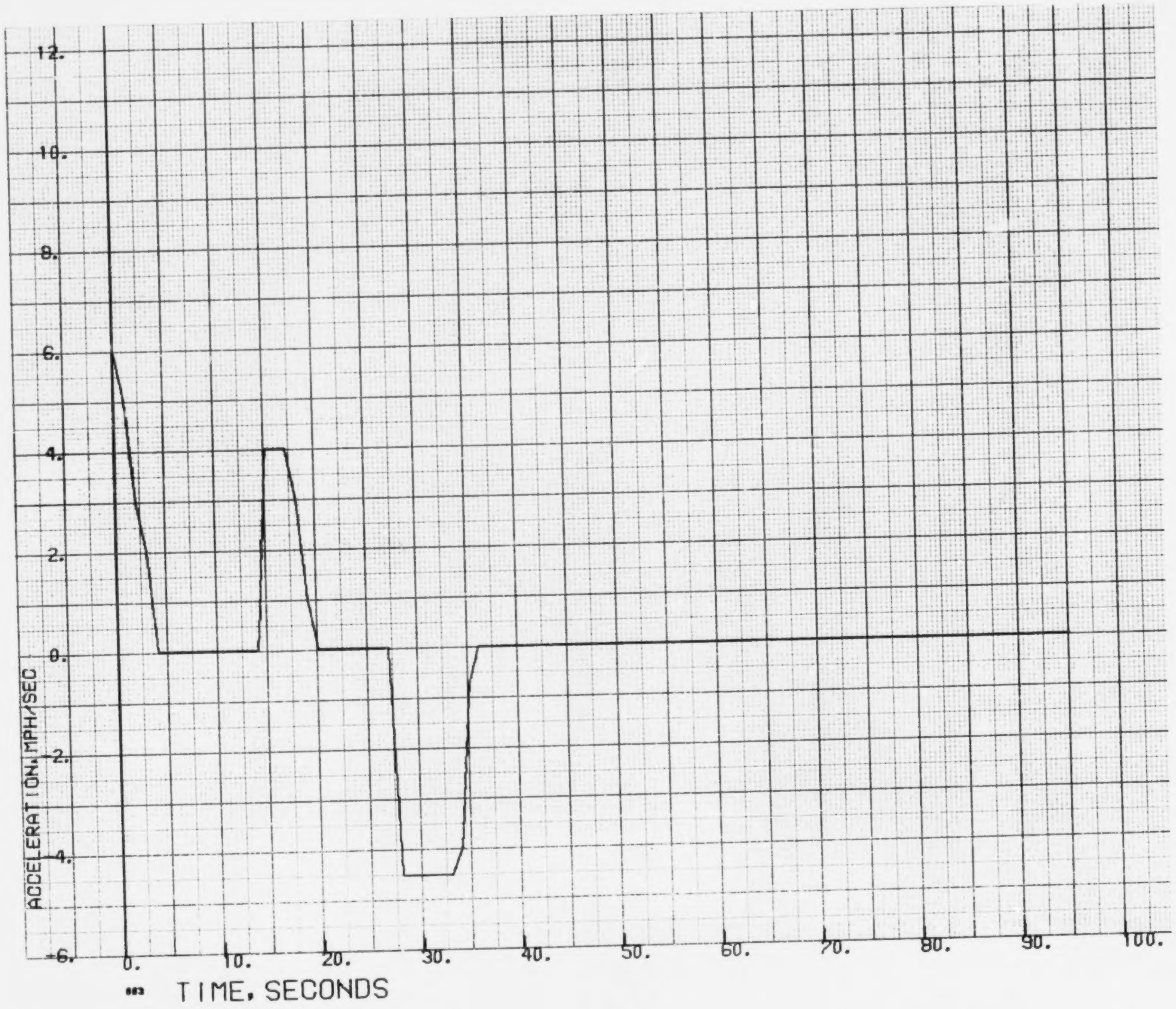

Figure D-8. Acceleration Profile - Delivery Van Emission Cycle

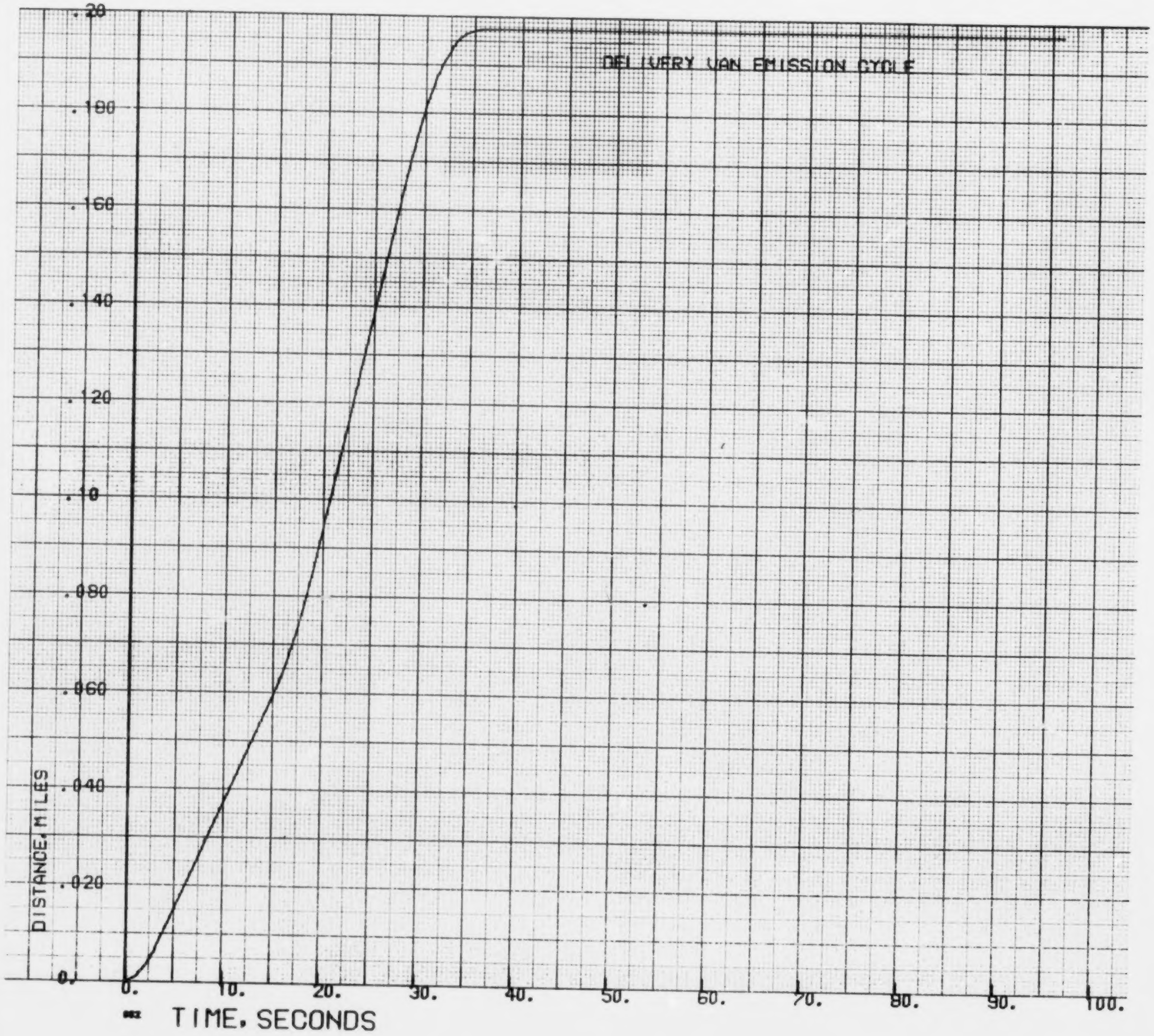

Figure D-9. Distance Profile - Delivery Van Emission Cycle

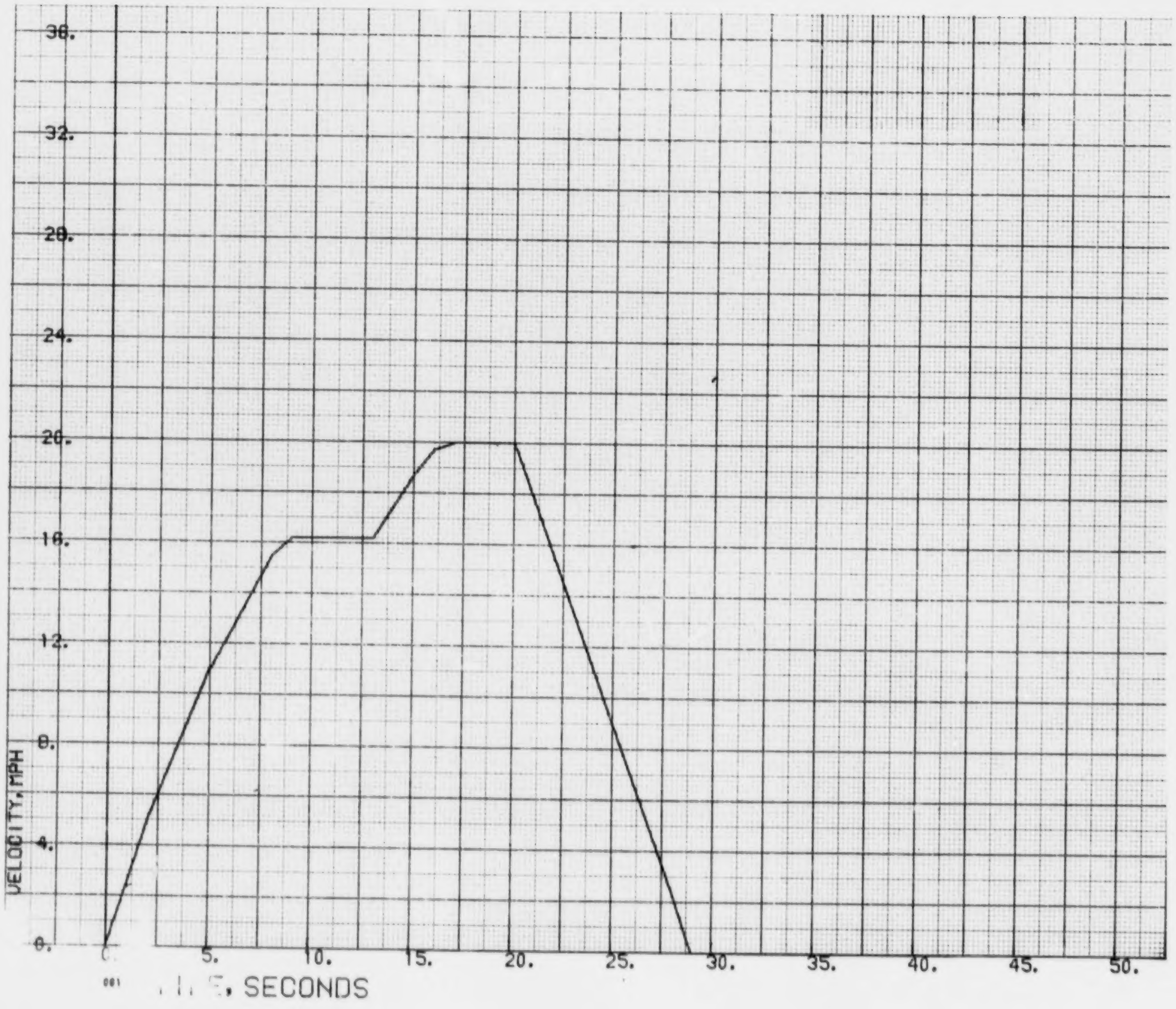

Figure D [illegible] Velocity Profile - Hi[illegible]speed Bus Emission Cycle

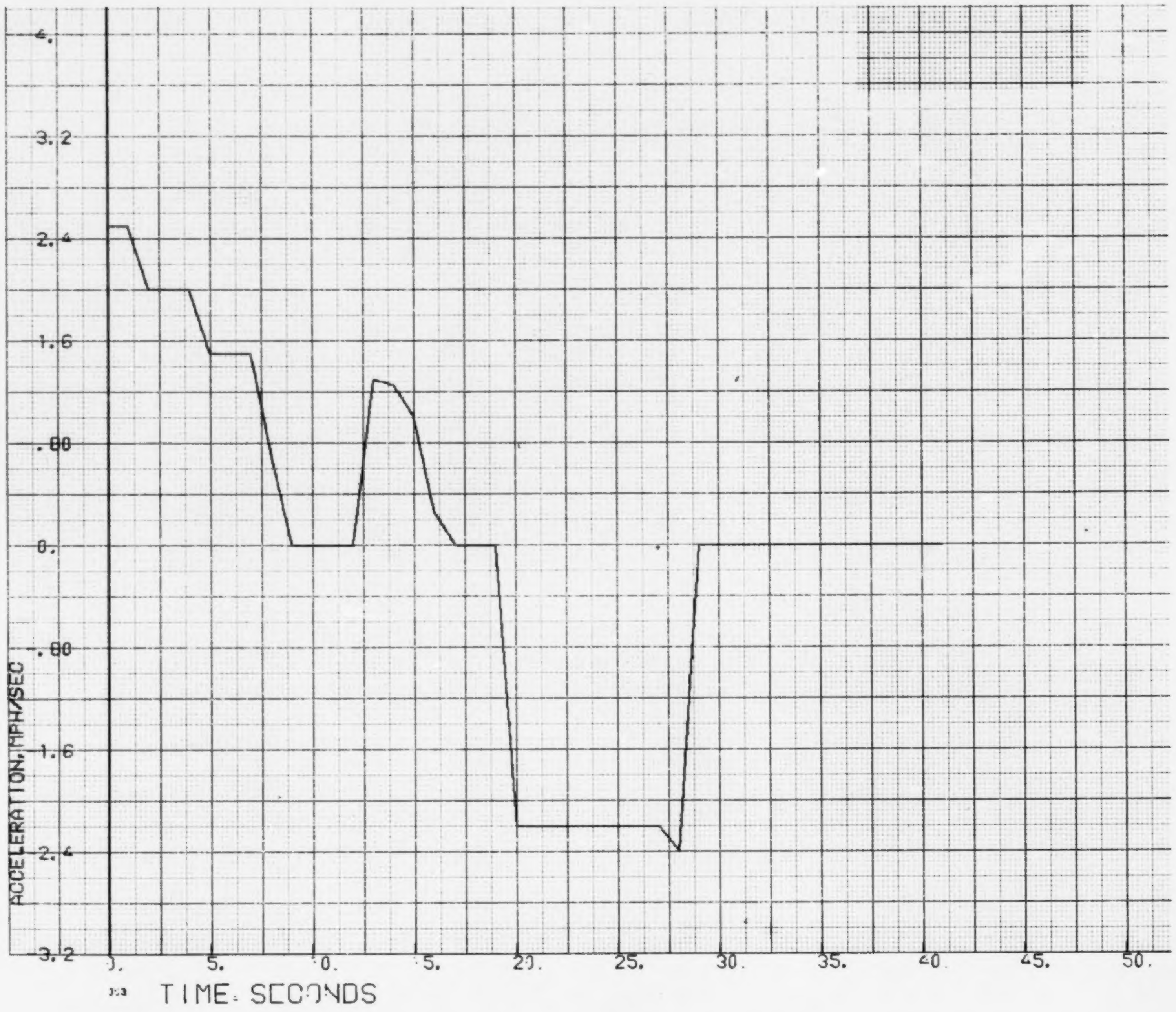

Figure D-11. Acceleration Profile - High-speed Bus Emission Cycle

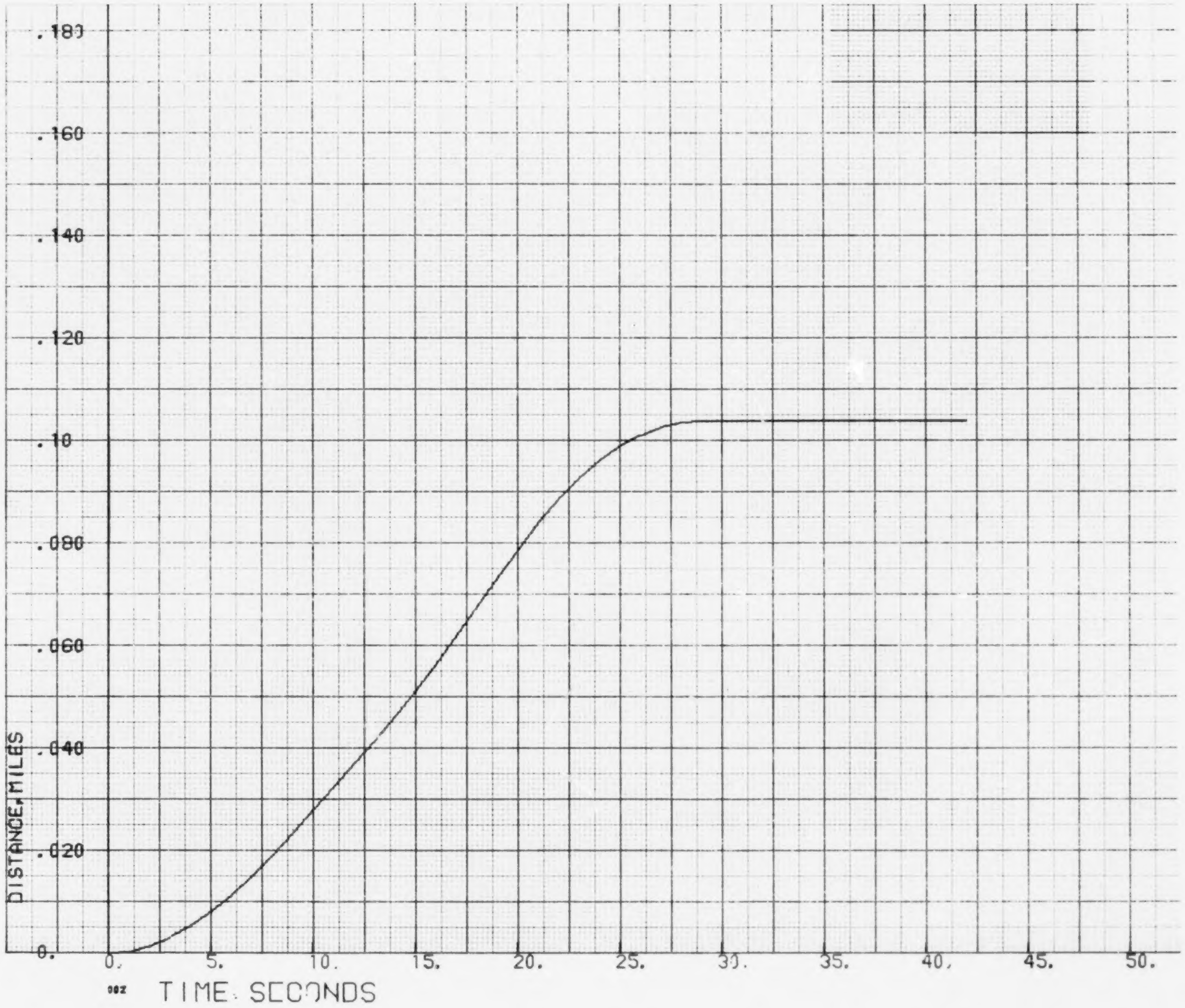

Figure D-12. Distance Profile - High-speed Bus Emission Cycle

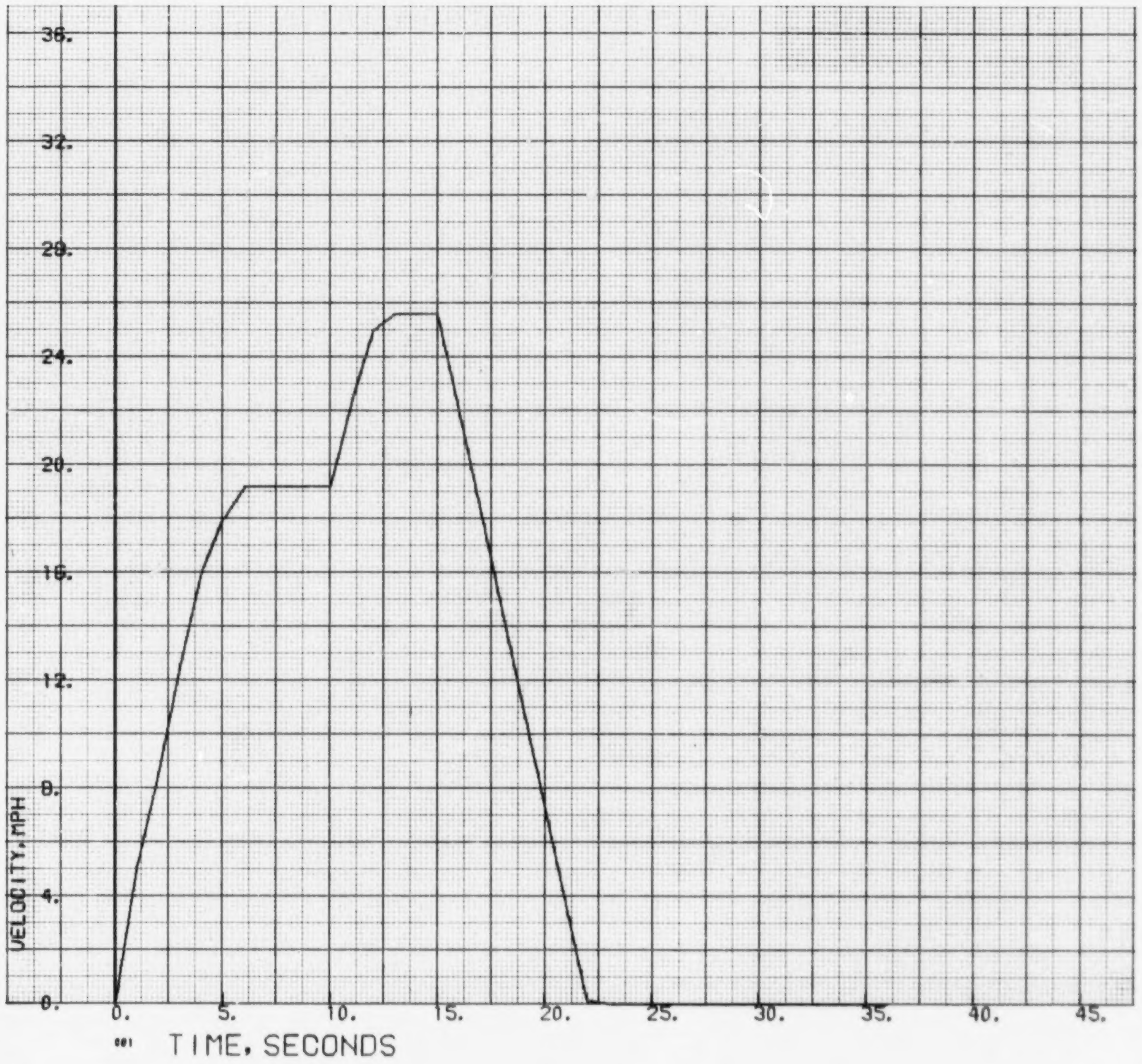

Figure D-13. Velocity Profile - Low-speed Bus Emission Cycle

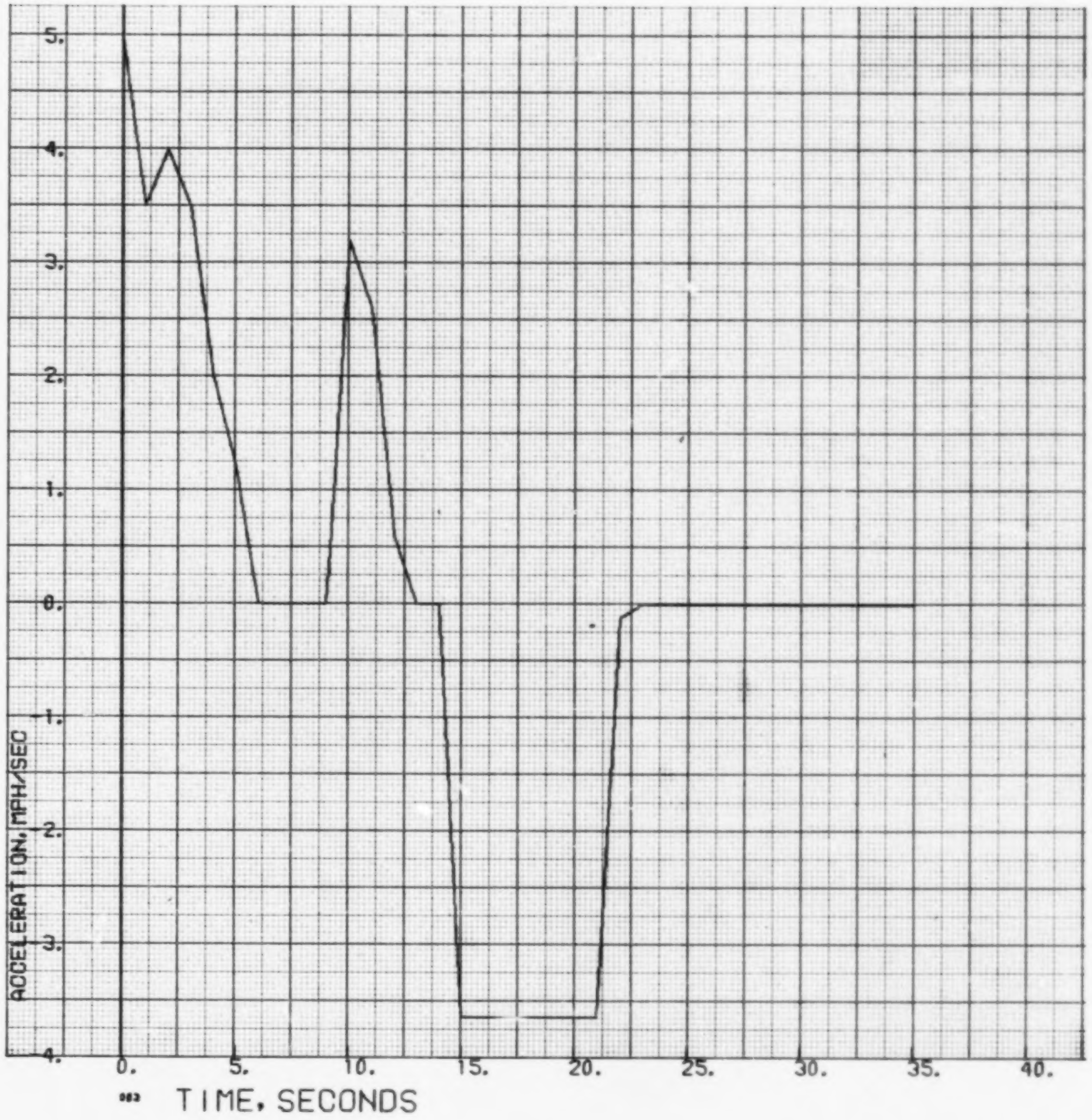

Figure D-14. Acceleration Profile - Low-speed Bus Emission Cycle

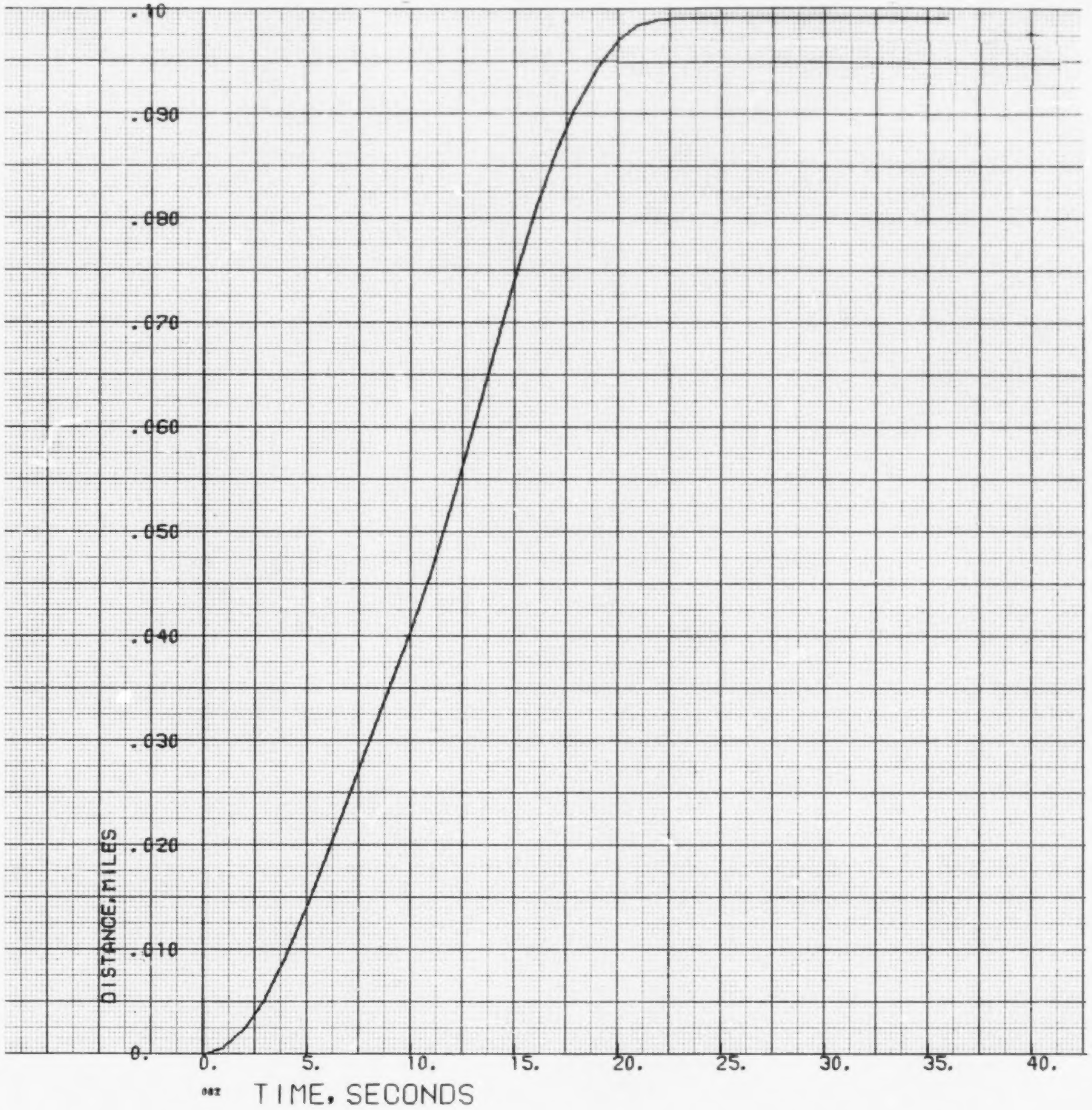

Figure D-15. Distance Profile - Low-speed Bus Emission Cycle

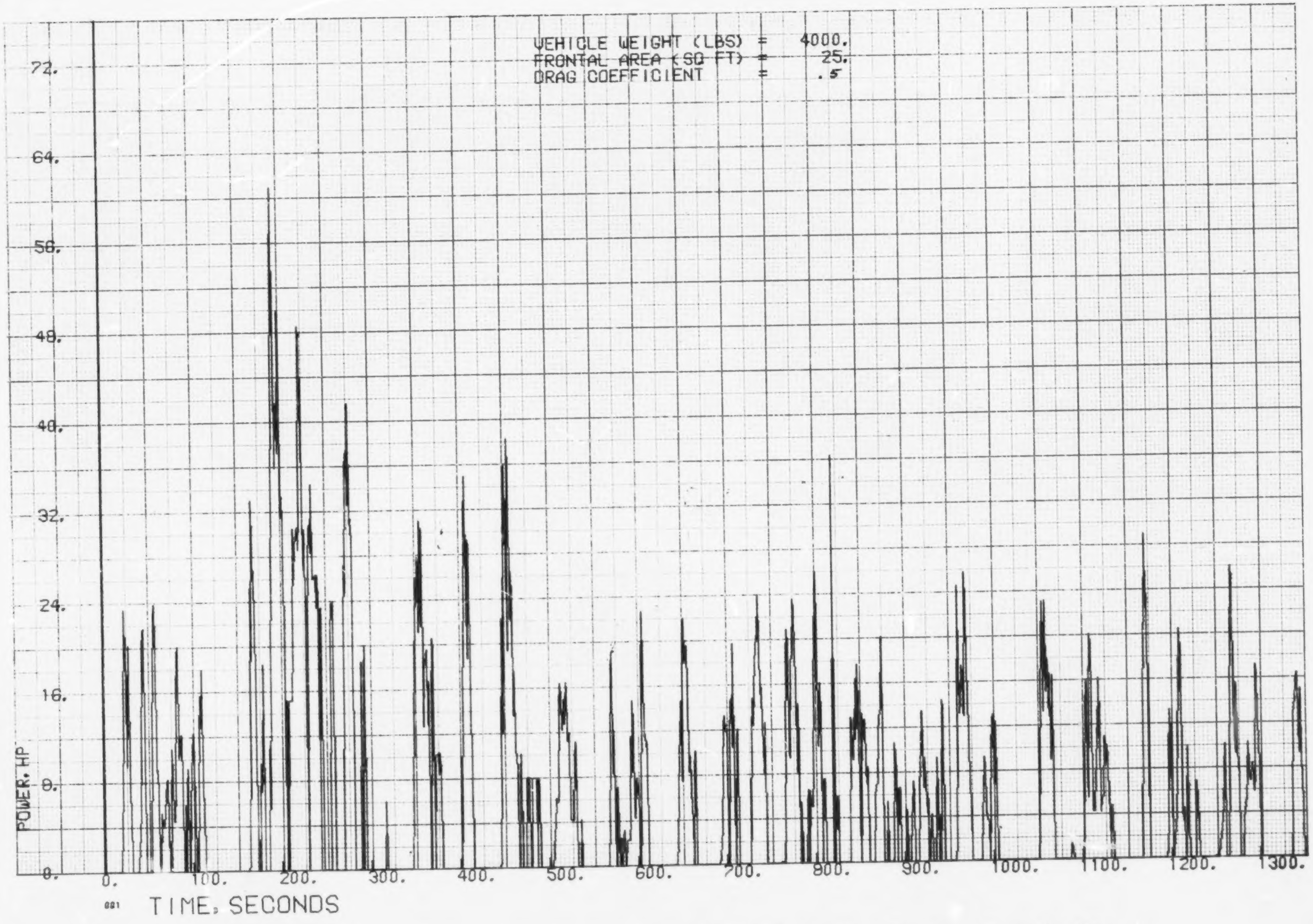

Figure D-16. Power Requirements - DHEW Emission Cycle - Family Car

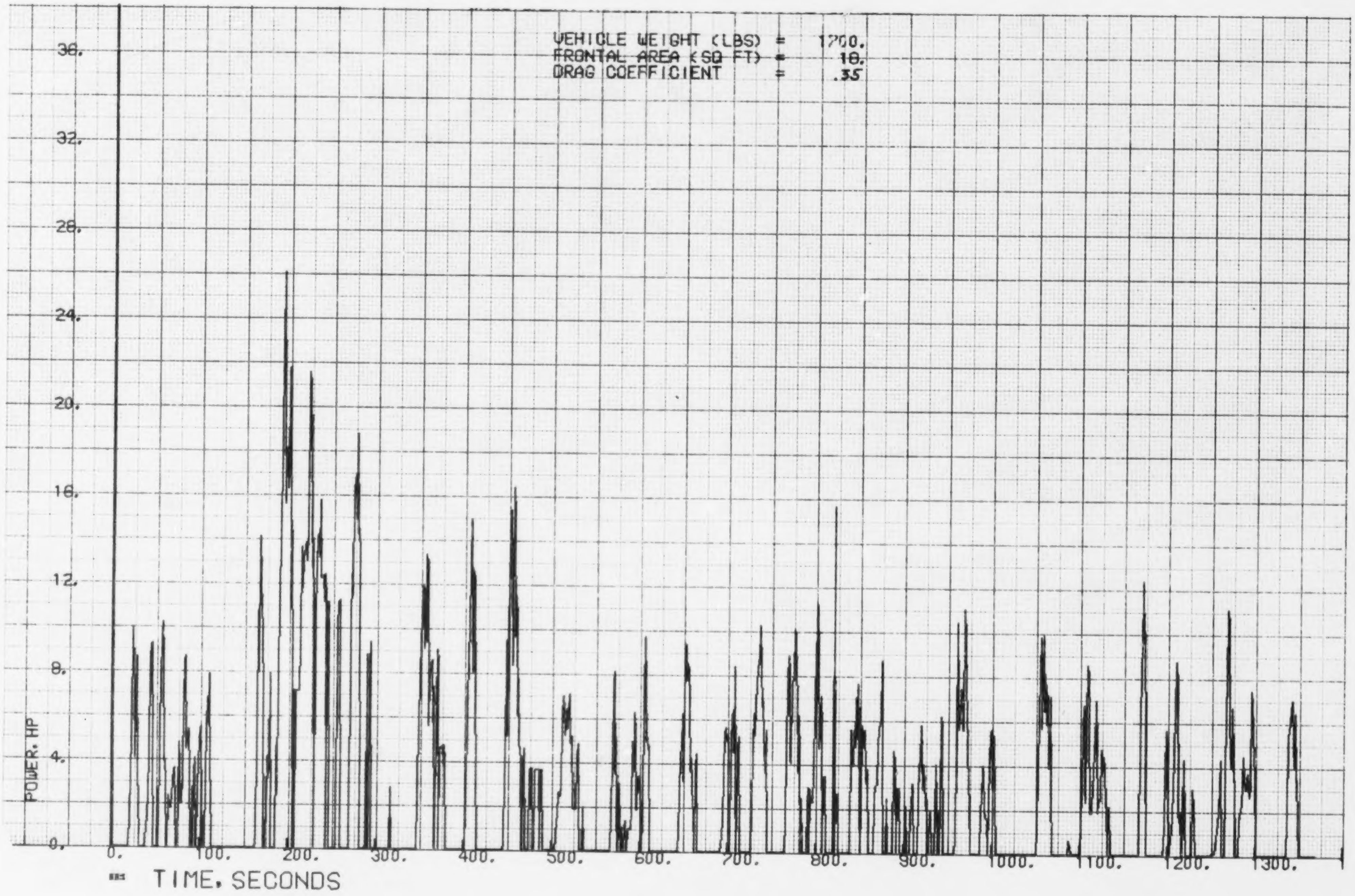

Figure D-17. Power Requirements - DHEW Emission Cycle - Commuter Car

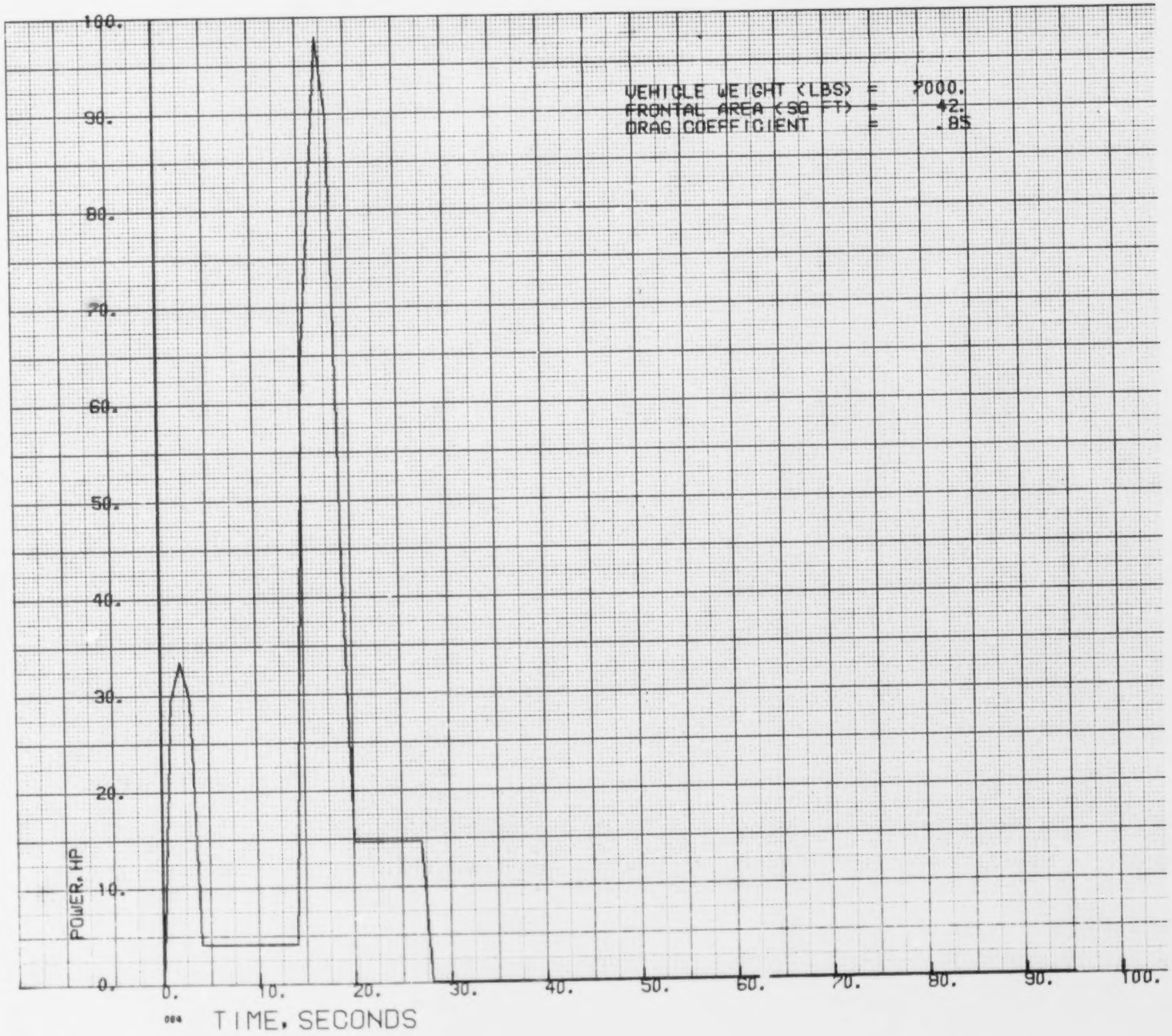

Figure D-18. Power Requiremer)elivery Van Emission Cycle

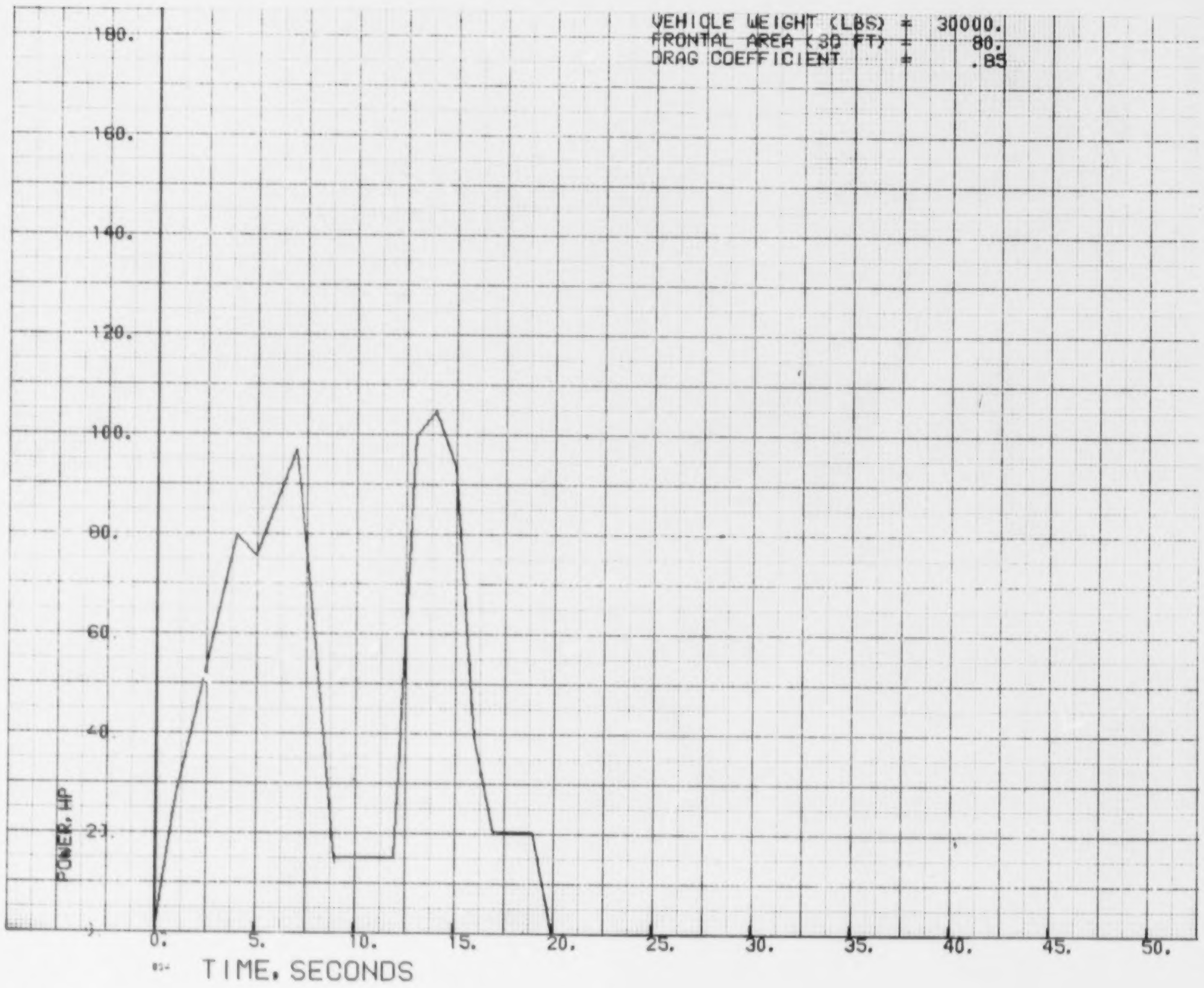

Figure D-19. Power Requirements - High-speed Bus Emission Cycle

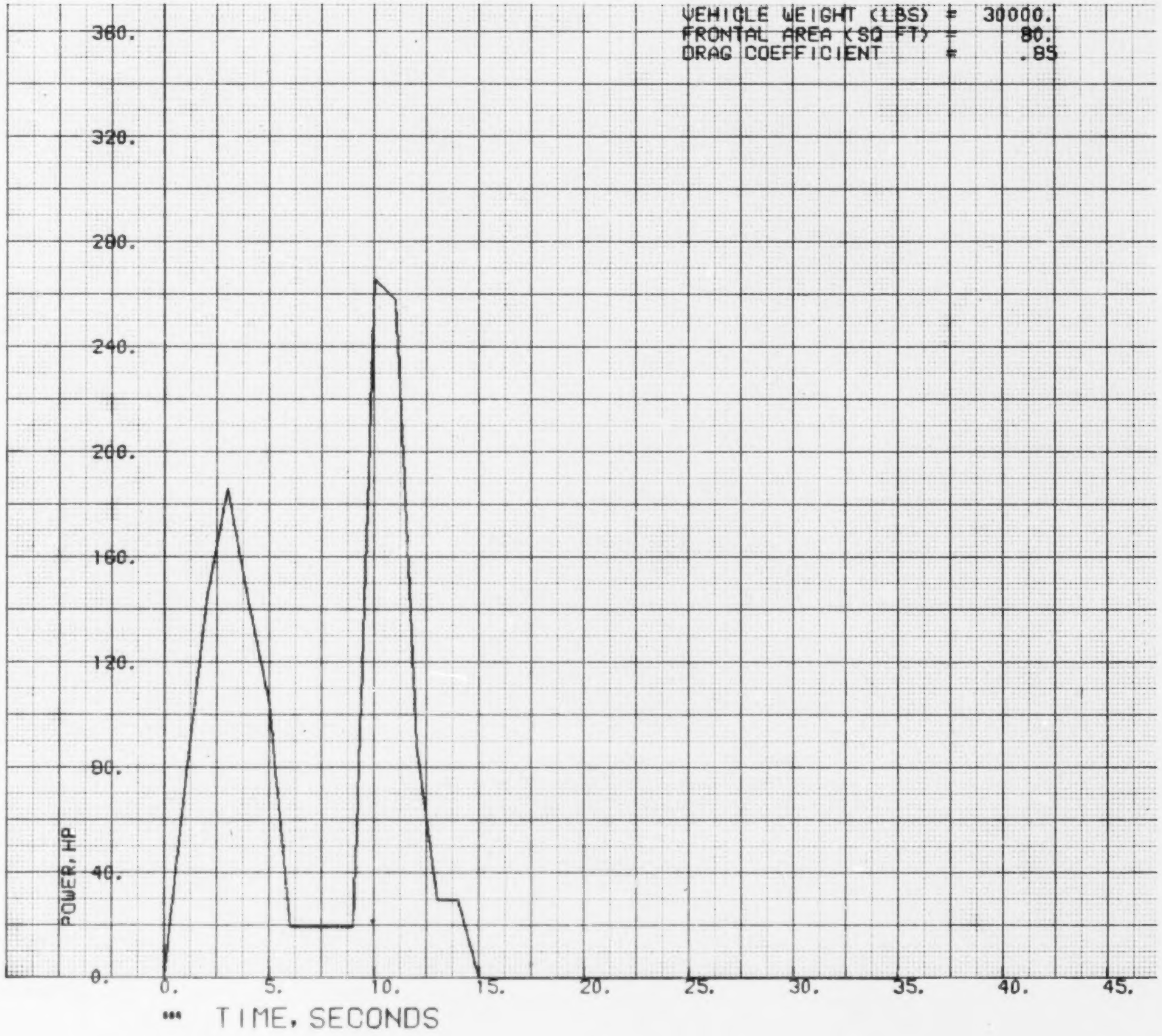

Figure D-20. Power Requirements - Low-speed Bus Emission Cycle

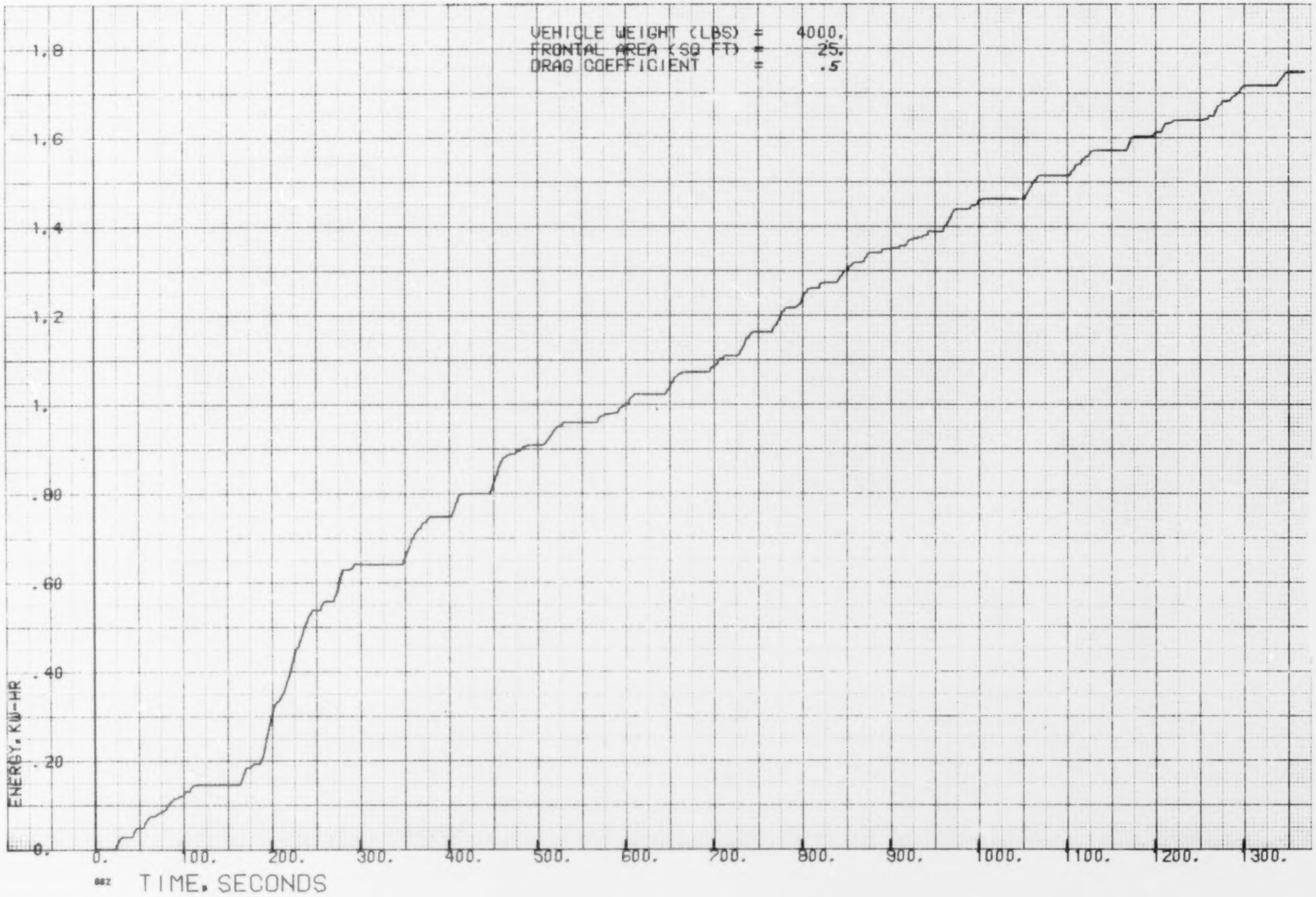

Figure D-21. Energy Requirements - DHEW Emission Cycle - Family Car

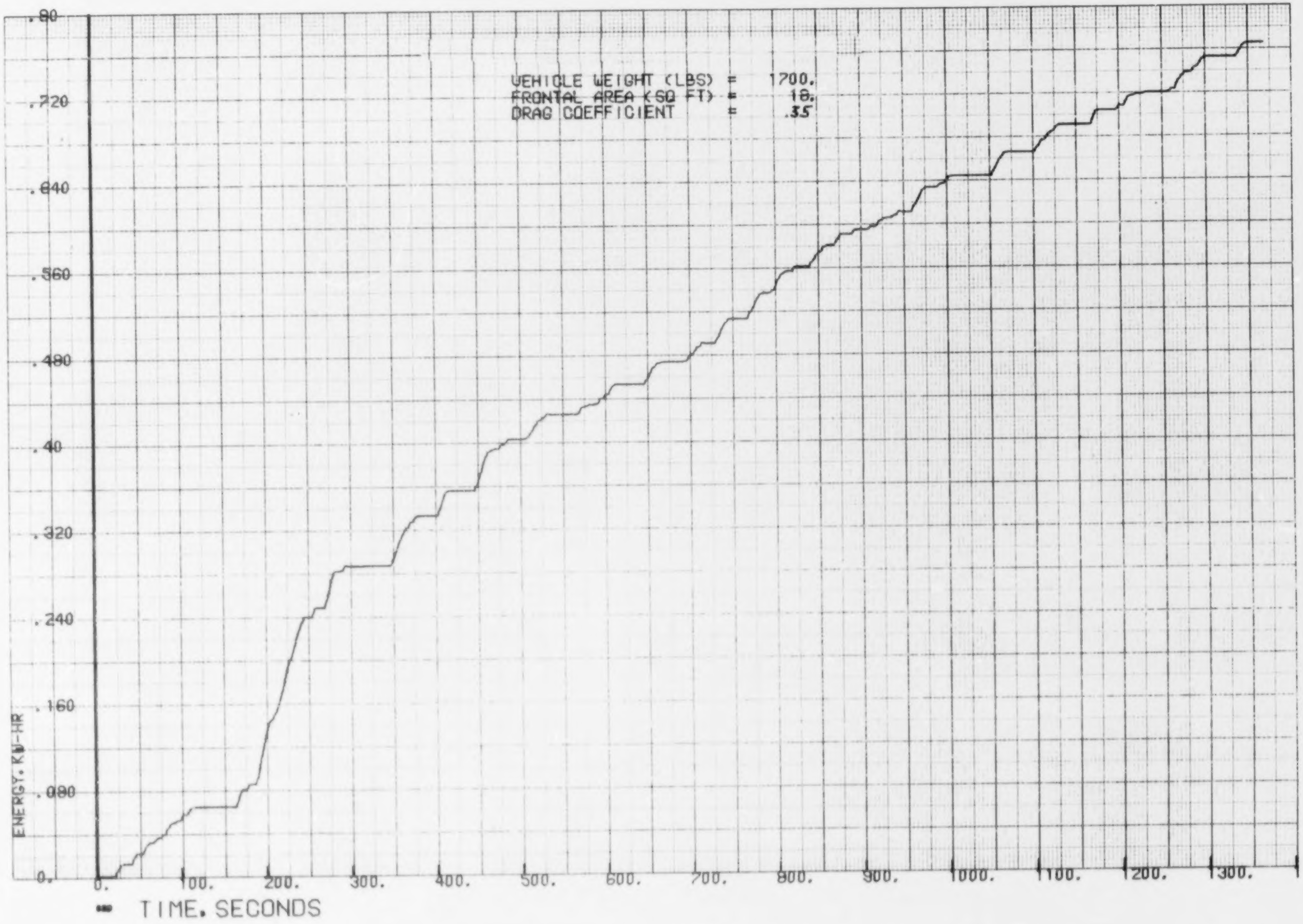

Figure D-22. Energy Requirements - DHEW Emission Cycle - Commuter Car

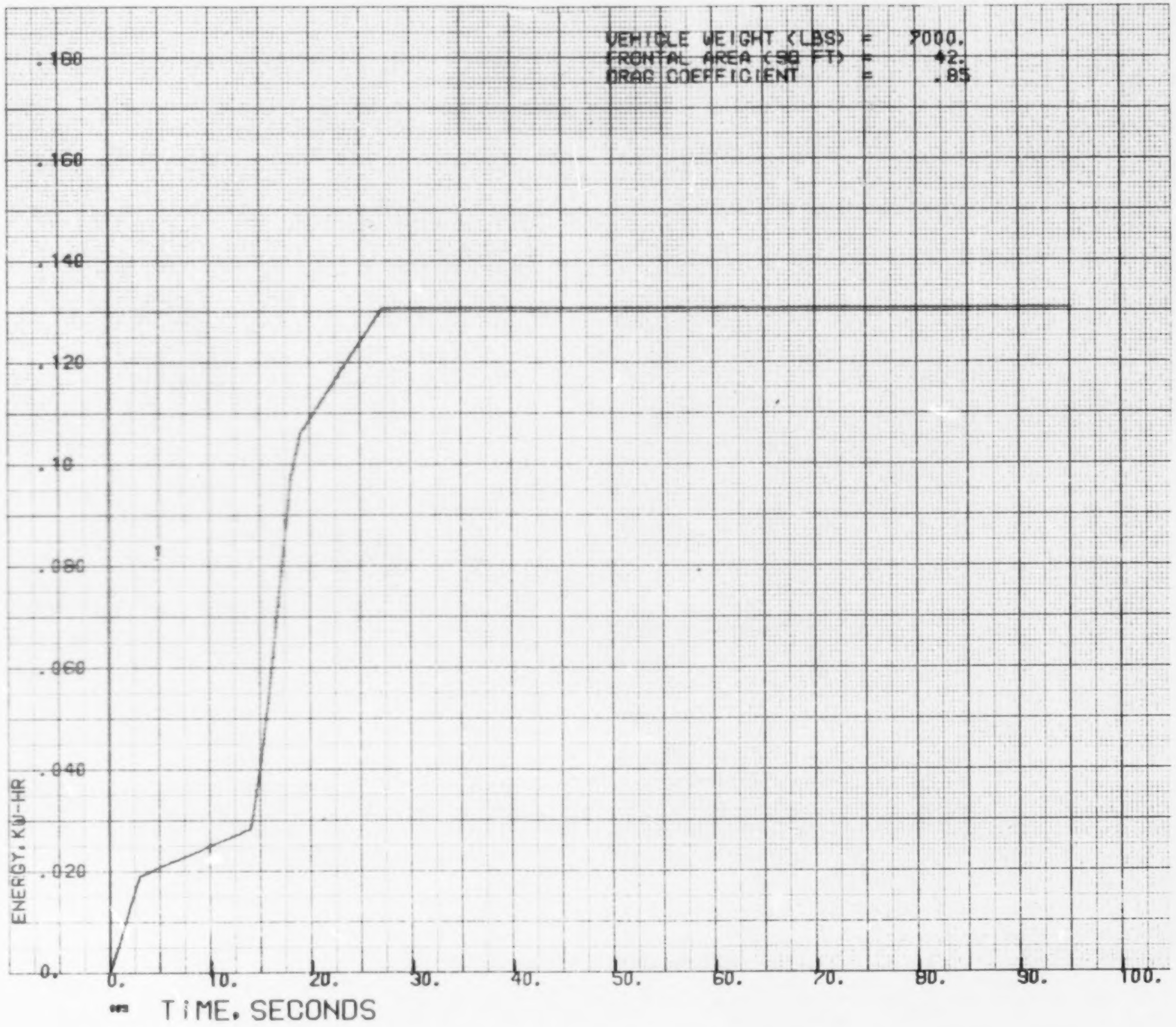

Figure D-23. Energy Requirements - Delivery Van Emission Cycle

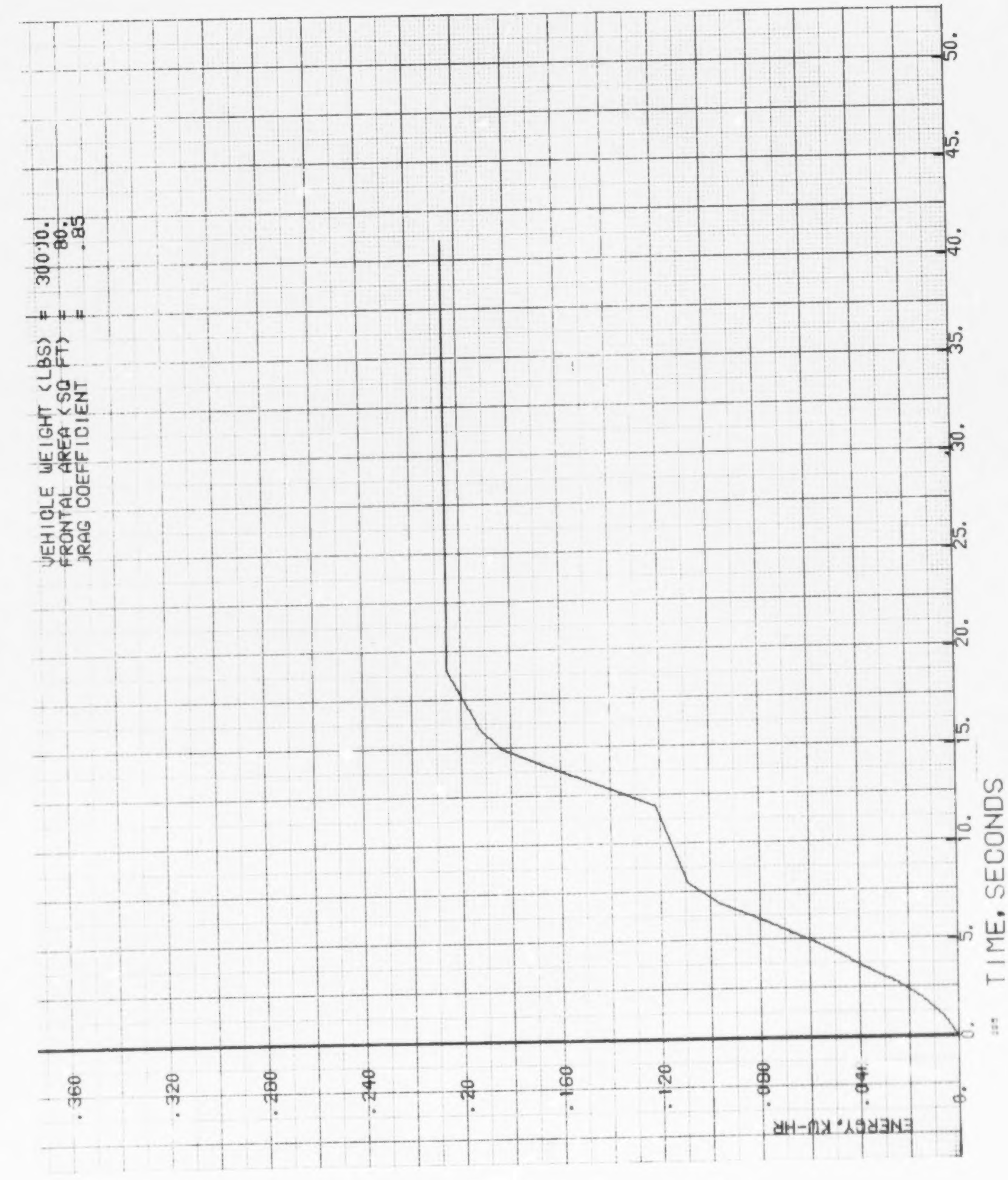

Figure D-24. Energy Requirements - High-speed Bus Emission Cycle

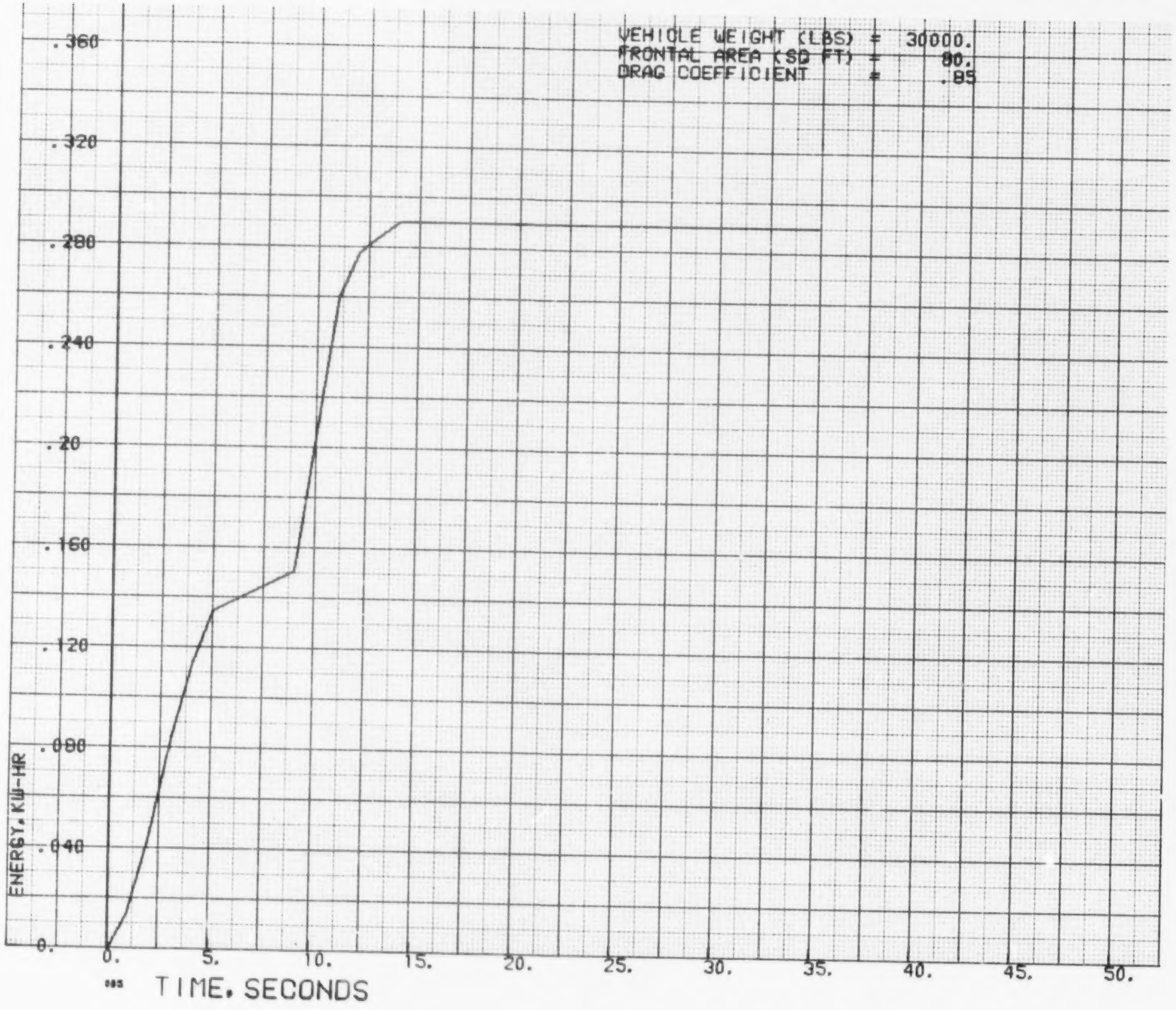

Figure D-25. Energy Requirements - Low-speed Bus Emission Cycle

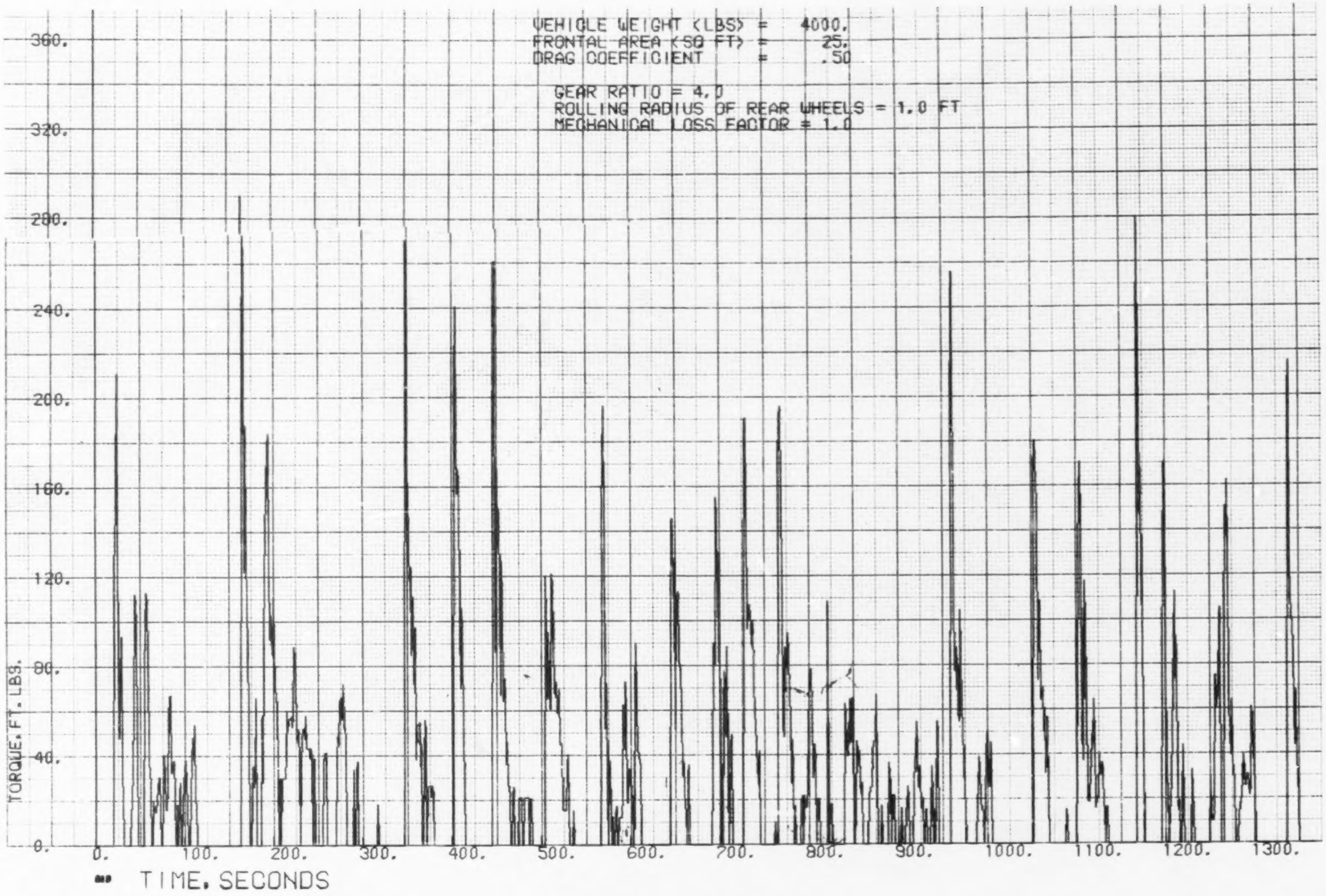

Figure D-26. Torque Requirements - DHEW Emission Cycle - Family Car

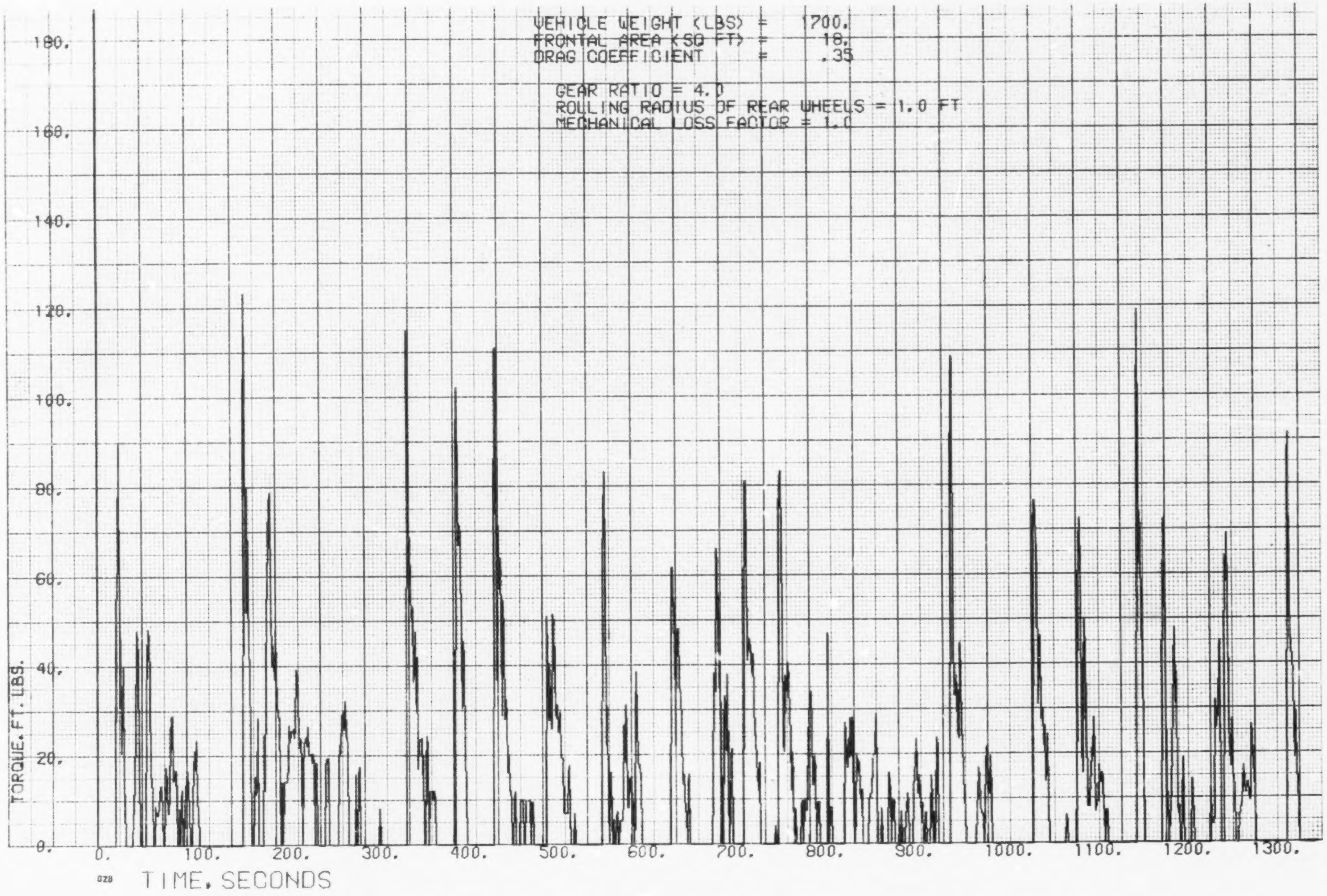

Figure D-27. Torque Requirements - DHEW Emission Cycle - Commuter Car

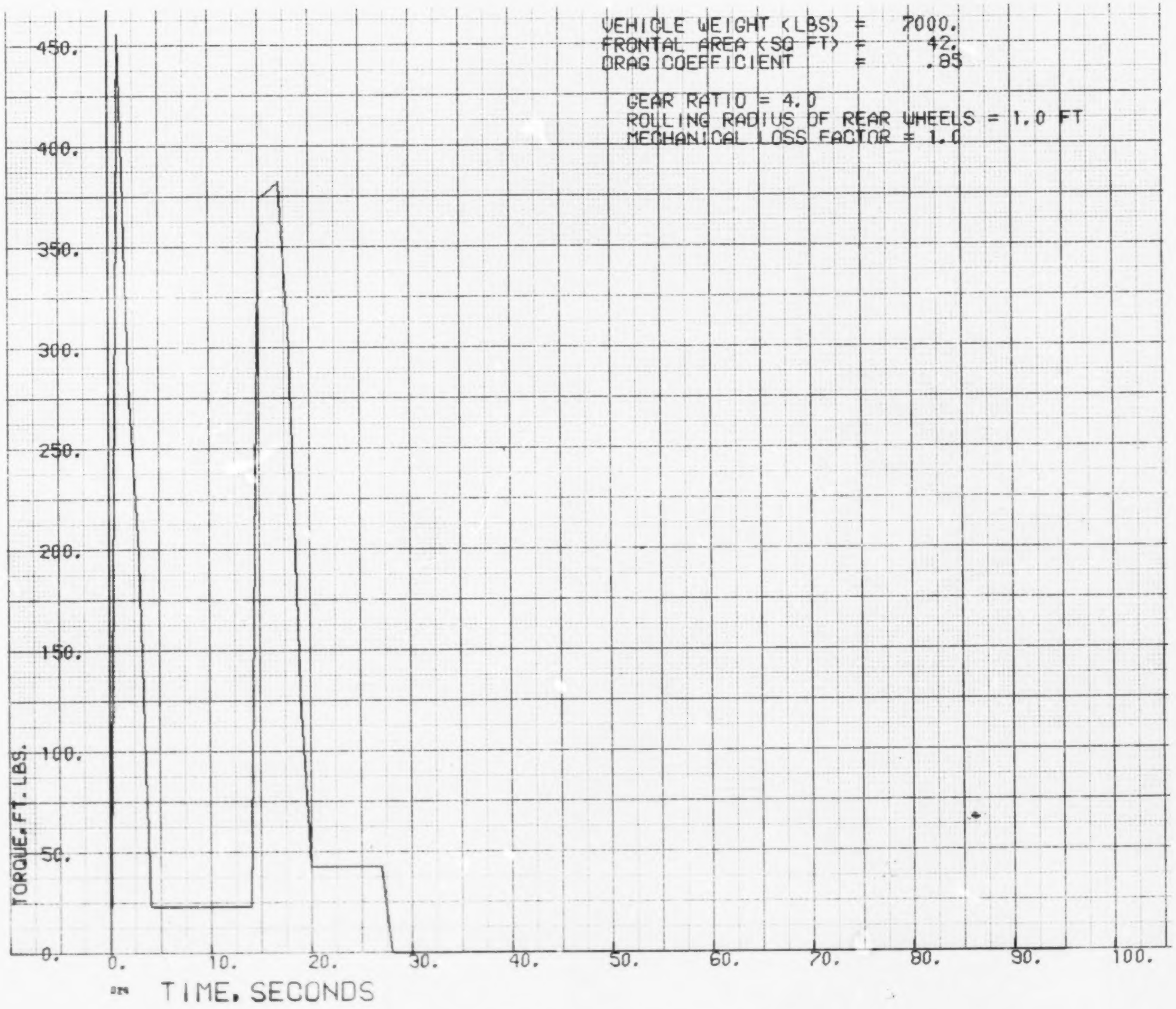

Figure D-28. Torque Requirements - Delivery Van Emission Cycle

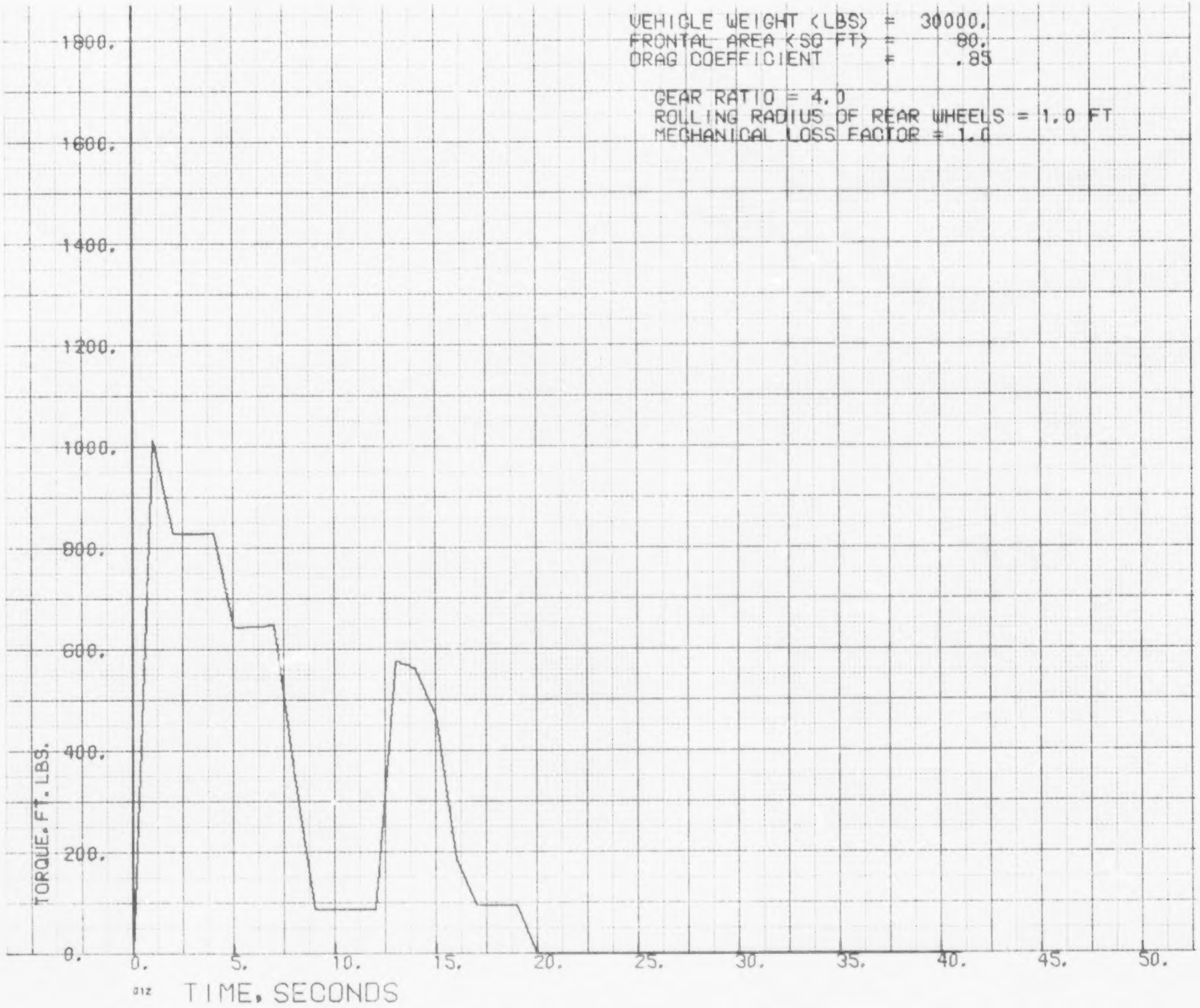

Figure D-29. Torque Requirements - High-speed Bus Emission Cycle

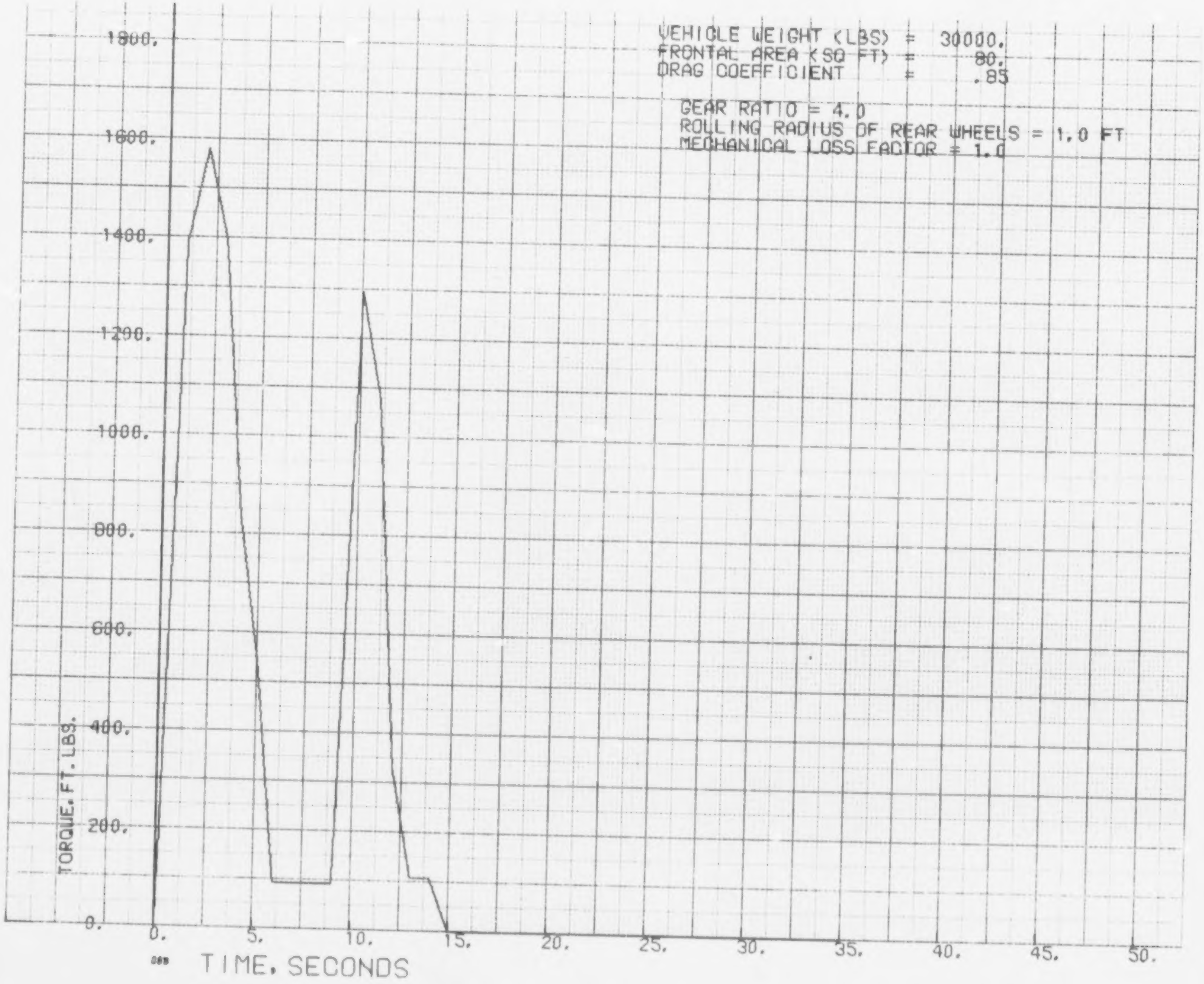

Figure D-30. Torque Requirements - Low-speed Bus Emission Cycle

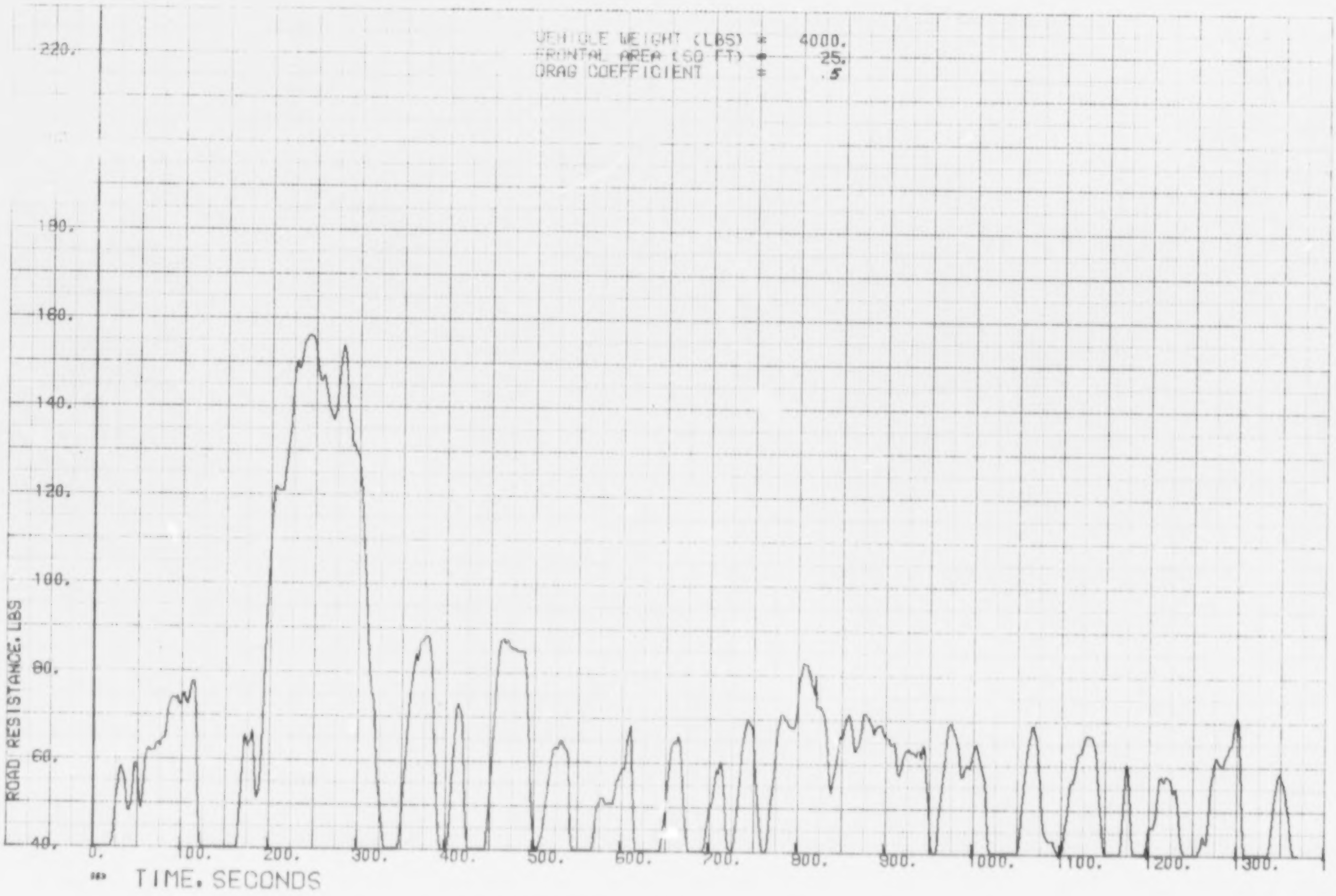

Figure D-31 Road Resistance - DHEW Emission Cycle - Family Car

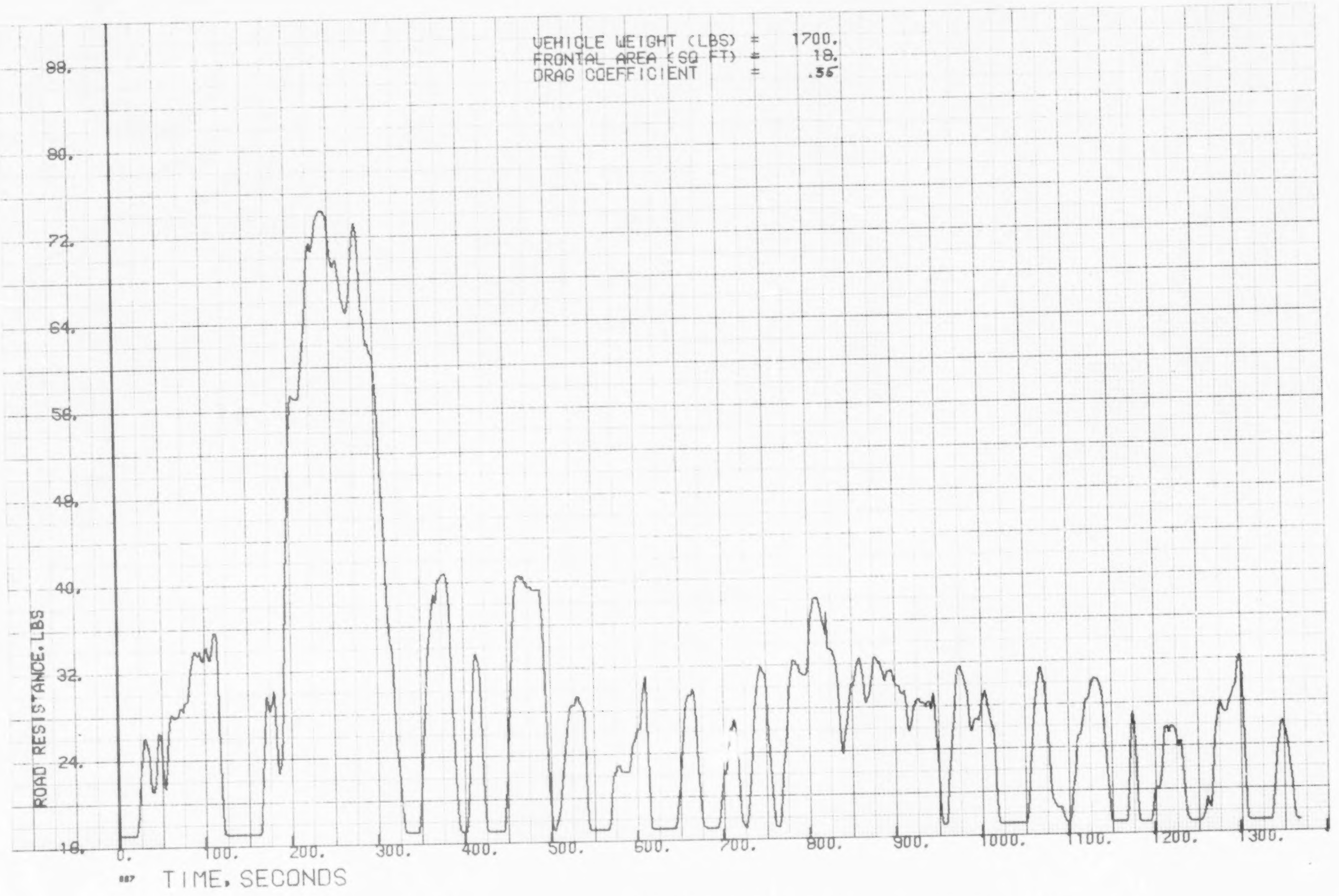

Figure D-32. Road Resistance - DHEW Emission Cycle - Commuter Car

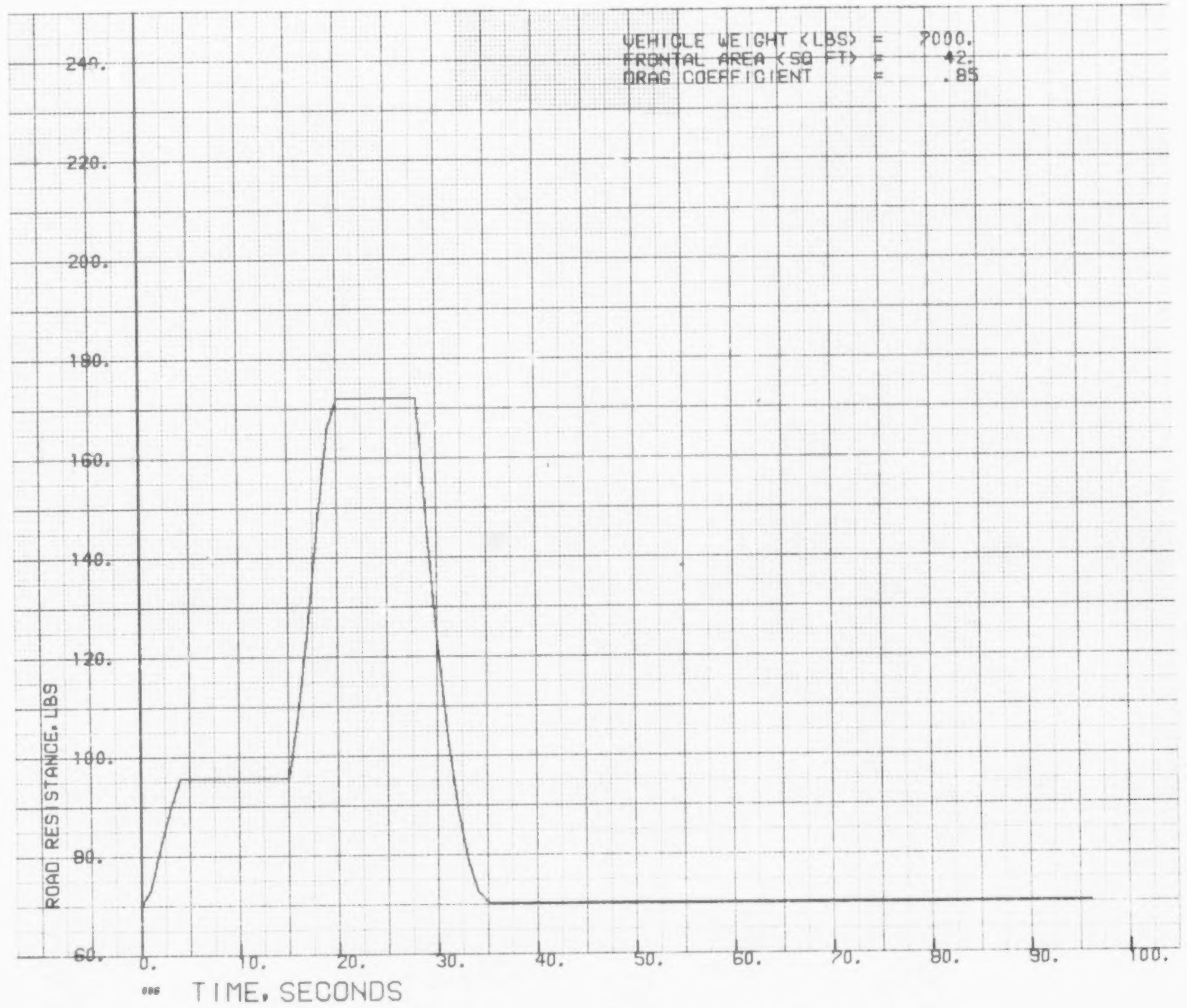

Figure D-33. Road Resistance - Delivery Van Emission Cycle

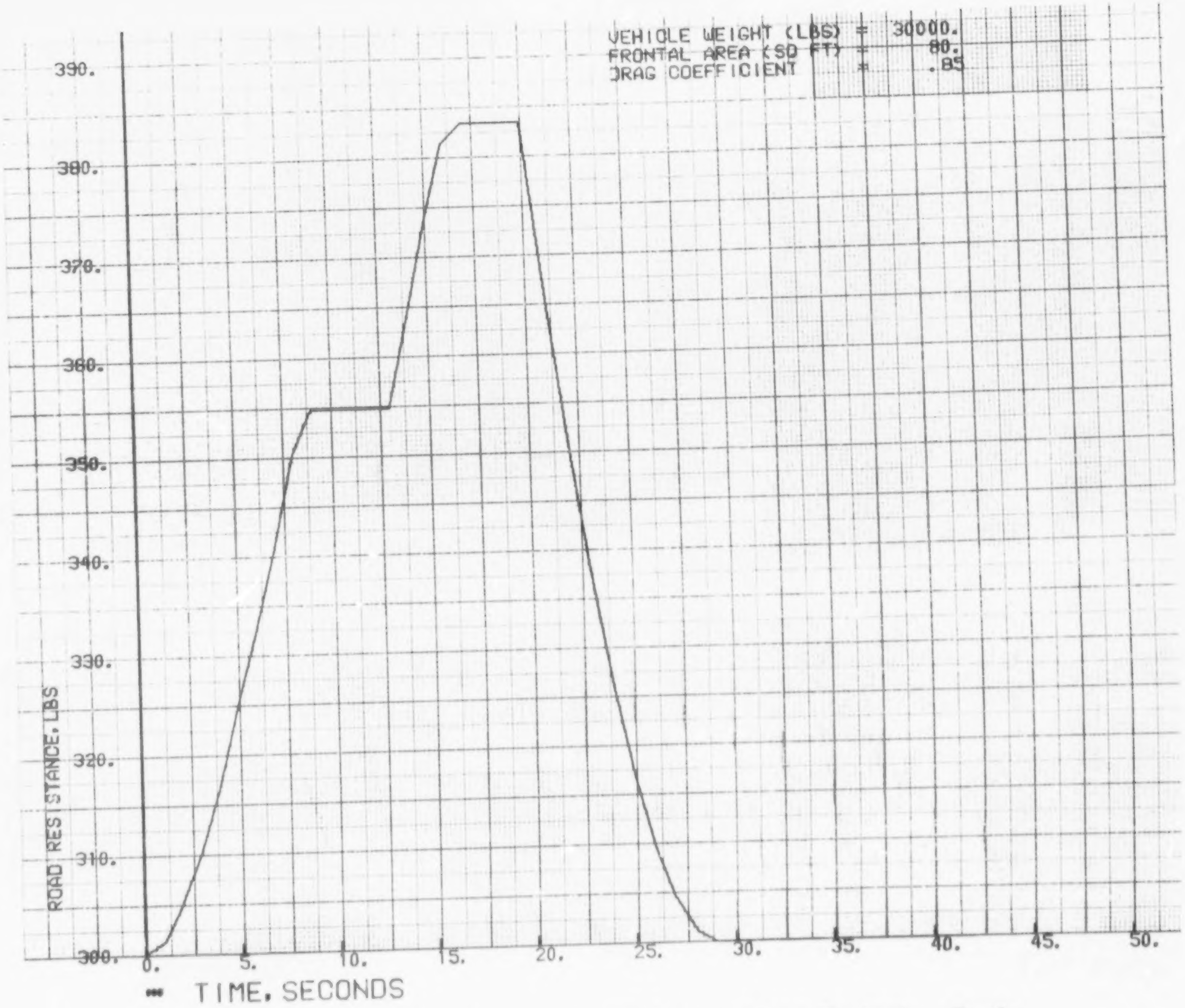

Figure D-34. Road Resistance - High-speed Bus Emission Cycle

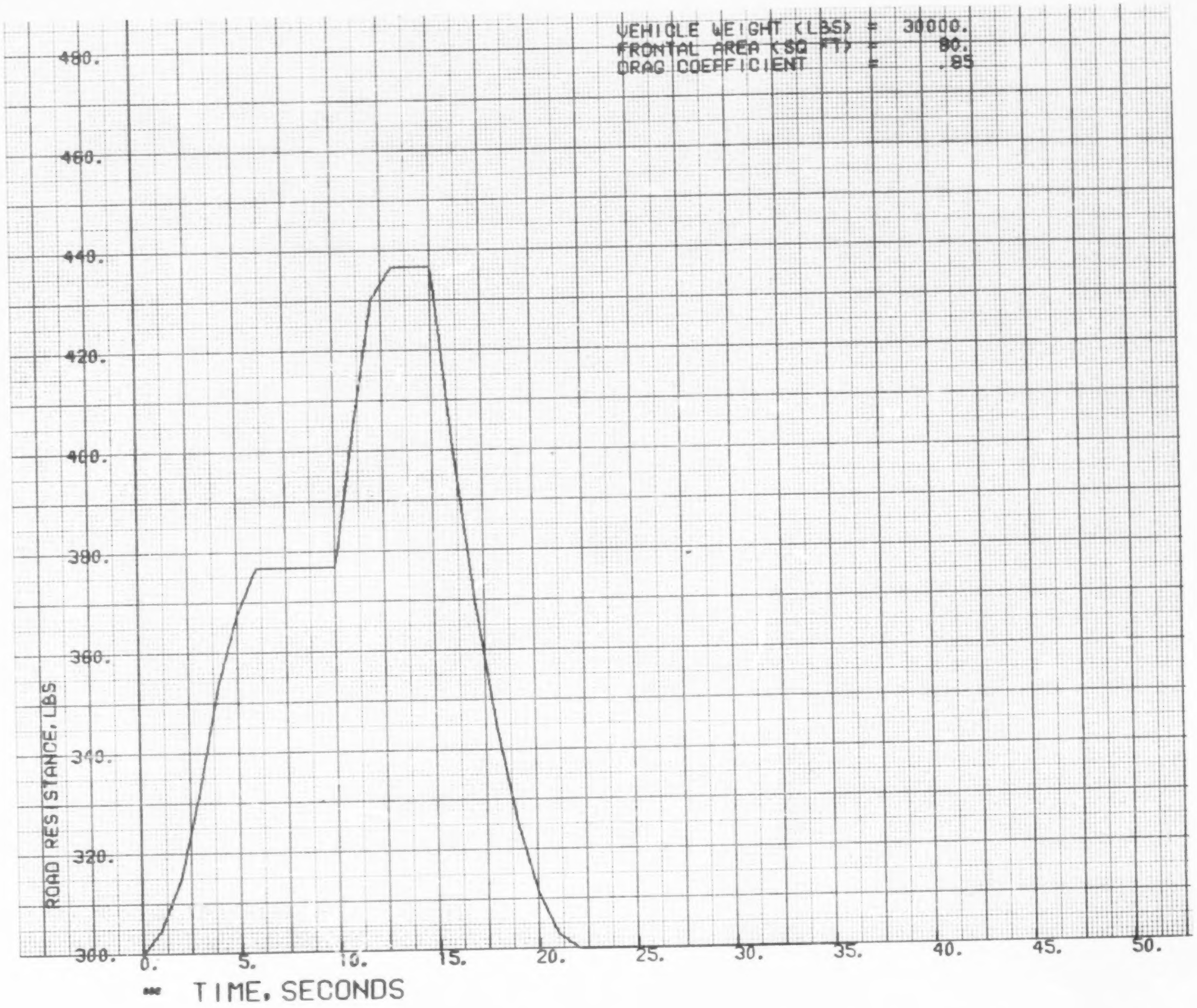

Figure D-35. Road Resistance - Low-speed Bus Emission Cycle

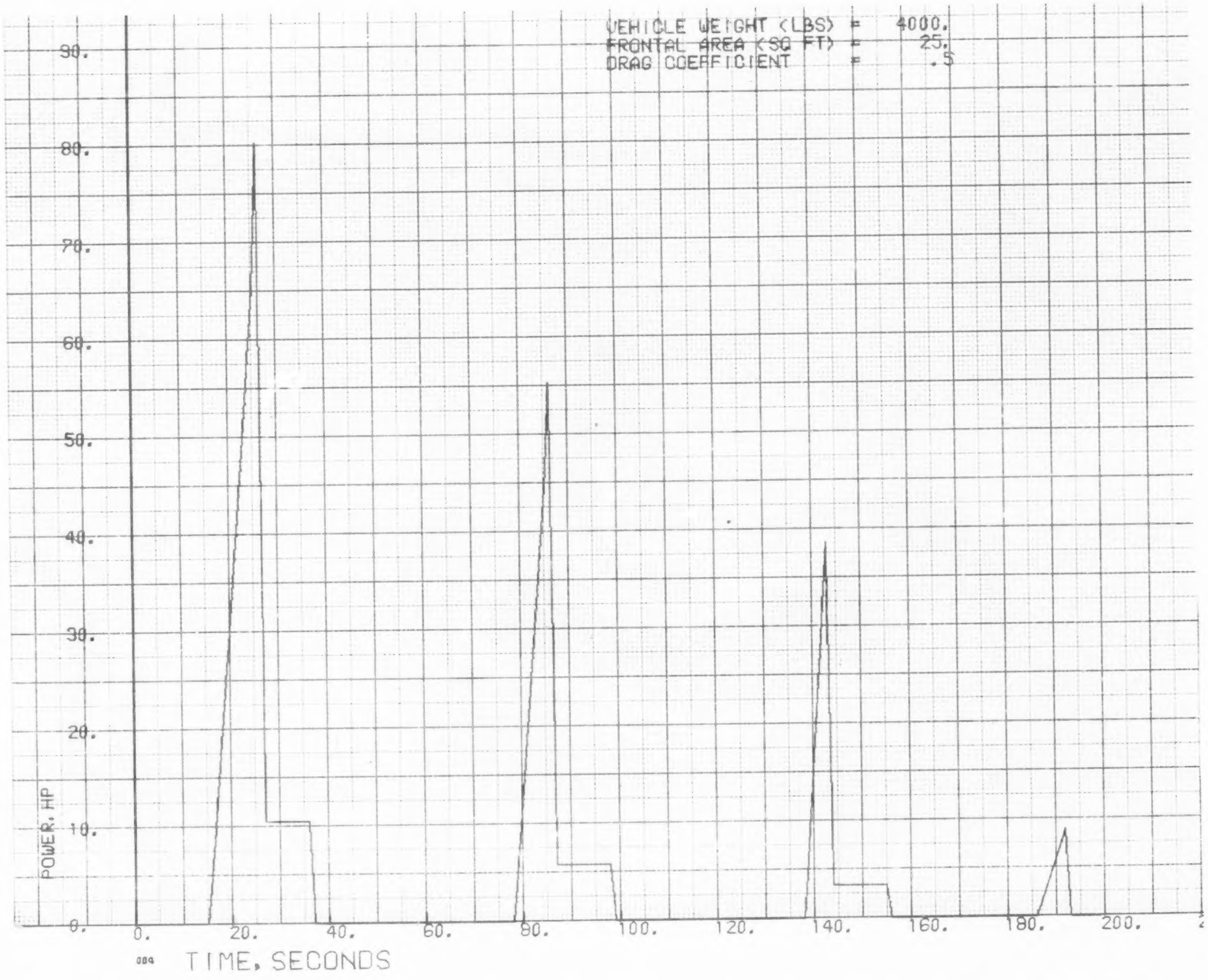

Figure D-36. Family Car - Power Requirements - New York City Emission Cycle

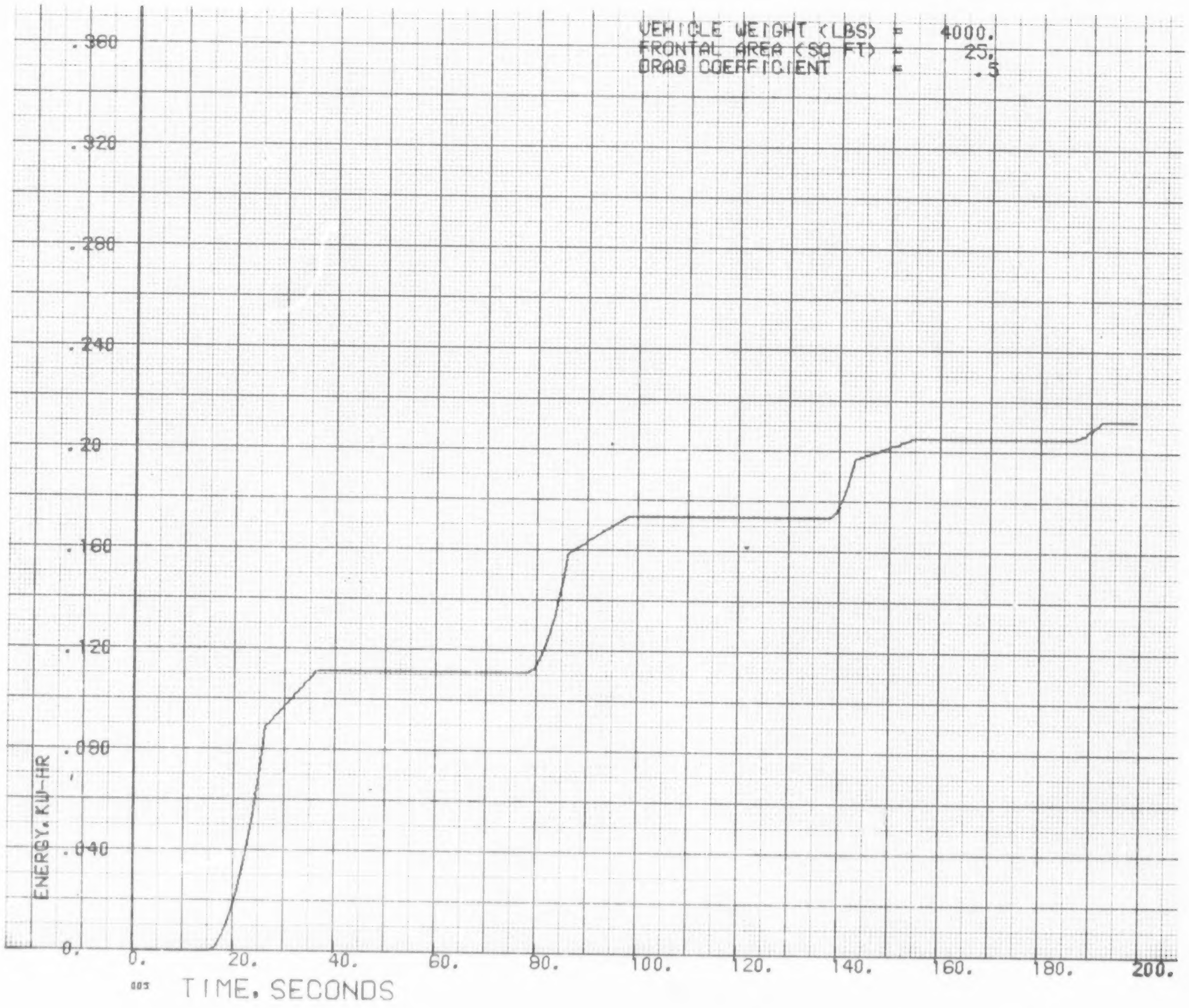

Figure D-37. Family Car - Energy Requirements - New York City Emission Cycle

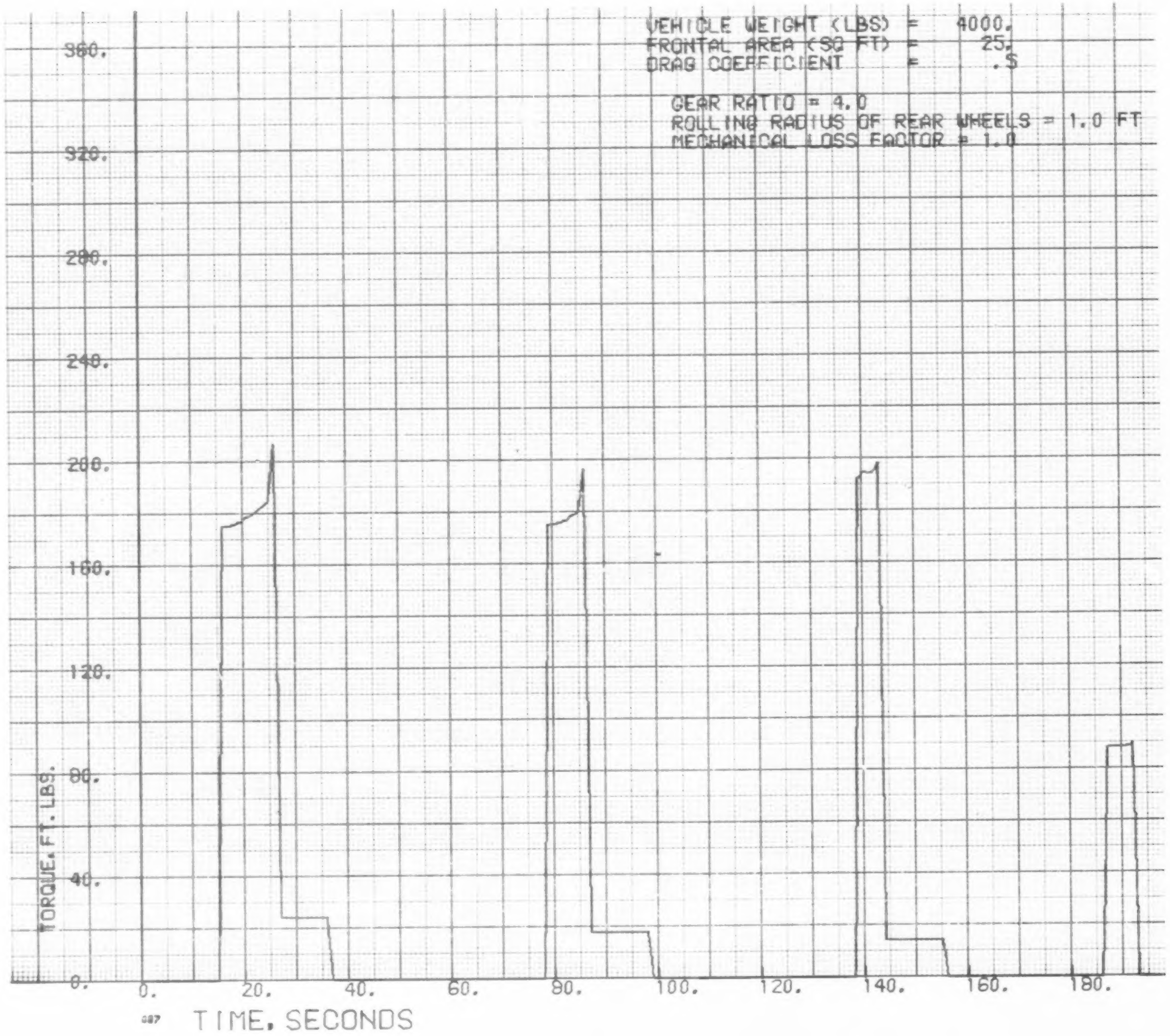

Figure D-38. Family Car - Torque Requirements - New York City Emission Cycle

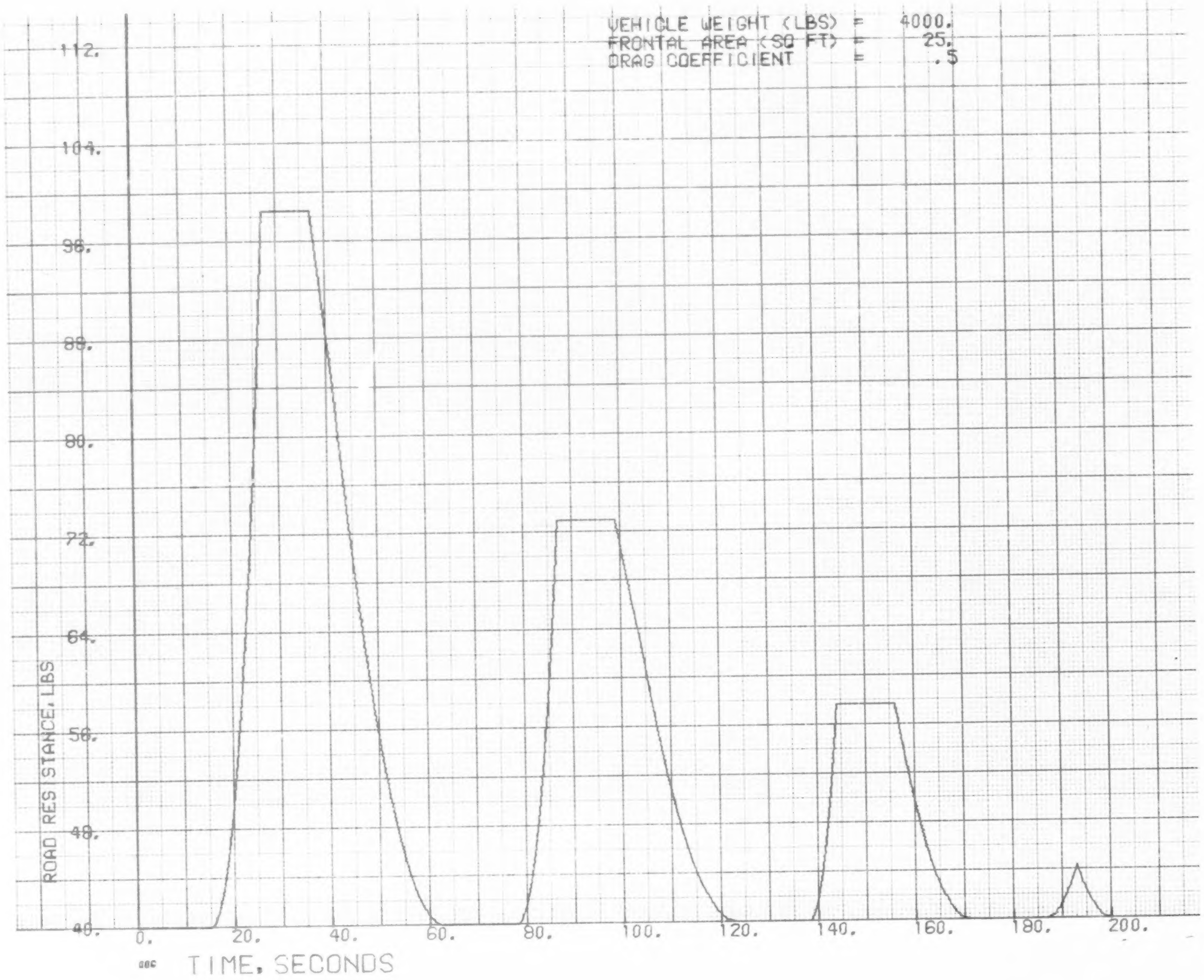

Figure D-39. Family Car - Road Resistance - New York City Emission Cycle

D.3 DESIGN DRIVING CYCLES

Design driving cycles were used in the present study to size power train components as discussed in Section 4. The respective driving cycles for each type of vehicle are presented in Tables D-1 through D-6.

In order to increase the total number of computer simulations that could be performed within the time constraints of the present study, reduce the turnaround time between simulations, and reduce the overall computer costs. Each of the design driving cycles presented in the tables was abbreviated. This was achieved by reducing the duration of the maximum speed cruise and range demonstration events to 1 sec each and by reducing the constant speed operation on a grade event to 60 sec.

Table D-1. Design Driving Cycle for Family Car

Event	Elapsed Time, sec	Speed, mph	Grade, sin θ
Maximum Accleration to Maximum Cruise Speed	0	0.0	0.0
	1	8.5	0.0
	2	16.8	0.0
	3	24.7	0.0
	4	31.2	0.0
	5	37.2	0.0
	6	42.2	0.0
	7	46.7	0.0
	8	50.5	0.0
	9	54.0	0.0
	10	57.0	0.0
	11	59.6	0.0
	12	62.1	0.0
	13	64.2	0.0
	14	66.4	0.0
	15	68.4	0.0
	16	70.2	0.0
	17	72.0	0.0
	18	73.6	0.0
	19	75.1	0.0
	20	76.5	0.0
	21	77.7	0.0
	22	78.5	0.0
	23	79.2	0.0
	24	79.8	0.0
	25	80.0	0.0
Maximum Cruise Speed for ~5% of Range* (~10 Miles)	26 ↓ 475	80.0 ↓ 80.0	0.0 ↓ 0.0
Slow Down to Cruise Speed for Range Demonstration	476 ↓ 479	76.0 ↓ 68.0	0.0 ↓ 0.0
Range Demonstration at Constant Speed (~182 Miles)	480 ↓ 10,330	66.5 ↓ 66.5	0.0 ↓ 0.0
Slow Down for Grade	10,331 ↓ 10,340	62.0 ↓ 40.0	0.0 ↓ 0.0
Maintain Constant Speed on Grade (~8 Miles)	10,341 ↓ 11,060	40.0 ↓ 40.0	0.119 ↓ 0.119
Slow to Rest	11,061 ↓ 11,075	40.0 ↓ 0.0	0.0 ↓ 0.0

*Total Distance at End of Cycle ~ 200 Miles

Table D-2. Design Driving Cycle for Commuter Car

Event	Elapsed Time, sec	Speed, mph	Grade, sin θ
Maximum Acceleration to Maximum Cruise Speed	0	0.0	0.0
	1	7.0	0.0
	2	13.0	0.0
	3	19.0	0.0
	4	24.9	0.0
	5	30.1	0.0
	6	34.6	0.0
	7	38.0	0.0
	8	41.5	0.0
	9	44.5	0.0
	10	47.3	0.0
	11	49.8	0.0
	12	52.1	0.0
	13	54.1	0.0
	14	56.1	0.0
	15	57.8	0.0
	16	59.8	0.0
	17	60.0	0.0
	18	62.3	0.0
	19	63.7	0.0
	20	64.9	0.0
	21	66.0	0.0
	22	67.0	0.0
	23	68.0	0.0
	24	69.0	0.0
	25	70.0	0.0
Maximum Cruise Speed for ~5% of Range* (~2.5 Miles)	26	70.0	0.0
	↓	↓	↓
	155	70.0	0.0
Slow Down to Cruise Speed for Range Demonstration	156	66.0	0.0
	157	62.0	0.0
	158	60.0	0.0
Range Demonstration at Constant Speed (~43.5 Miles)	159	59.4	0.0
	↓	↓	↓
	2,795	59.4	0.0
Slow Down for Grade	2,796	55.4	0.0
	↓	↓	↓
	2,805	33.0	0.0
Maintain Constant Speed on Grade (~4 Miles)	2,806	33.0	0.119
	↓	↓	↓
	3,240	33.0	0.119
Slow to Rest	3,241	30.0	0.0
	↓	↓	↓
	3,250	0.0	0.0

*Total Distance at End of Cycle ≈ 50 Miles

Table D-3. Design Cycle for Low-speed Delivery Van

Event	Elapsed Time, sec	Speed, mph	Grade, sin θ
Maximum Acceleration to Maximum Cruise Speed	0	0.0	0.0
	1	6.5	0.0
	2	12.2	0.0
	3	17.3	0.0
	4	21.9	0.0
	5	25.9	0.0
	6	29.6	0.0
	7	32.9	0.0
	8	35.8	0.0
	9	38.5	0.0
	10	40.0	0.0
Maximum Cruise Speed and Range Demonstration* (~59.5 Miles)	11 ↓ 5,365	40.0 ↓ 40.0	0.0 ↓ 0.0
Slow Down for Grade	5,366 ↓ 5,375	40.0 ↓ 8.0	0.0 ↓ 0.0
Maintain Constant Speed on Grade (~0.5 Mile)	5,376 ↓ 5,600	8.0 ↓ 8.0	0.196 ↓ 0.196
Slow to Rest	5,601 ↓ 5,605	8.0 ↓ 0.0	0.0 ↓ 0.0

*Total Distance at End of Cycle = 60 Miles.

Table D-4. Design Driving Cycle for High-speed Van

Event	Elapsed Time, sec	Speed, mph	Grade, sin θ
Maximum Acceleration to Maximum Cruise Speed	0	0.0	0.0
	1	6.5	0.0
	2	12.2	0.0
	3	17.3	0.0
	4	21.9	0.0
	5	25.9	0.0
	6	29.6	0.0
	7	32.9	0.0
	8	35.8	0.0
	9	38.5	0.0
	10	41.0	0.0
	11	43.2	0.0
	12	45.3	0.0
	13	47.2	0.0
	14	48.9	0.0

Table D-4. Design Driving Cycle for High-speed Van (Continued)

Event	Elapsed Time, sec	Speed, mph	Grade, sin θ
Maximum Acceleration to Maximum Cruise Speed (cont)	15	50.5	0.0
	16	51.9	0.0
	17	53.3	0.0
	18	54.5	0.0
	19	55.7	0.0
	20	56.7	0.0
	21	57.7	0.0
	22	58.0	0.0
	23	59.5	0.0
	24	60.3	0.0
	25	61.0	0.0
	26	61.7	0.0
	27	62.3	0.0
	28	62.9	0.0
	29	63.4	0.0
	30	63.9	0.0
	31	64.4	0.0
	32	65.0	0.0
Maximum Speed Cruise and Range Demonstration* (~59.5 Miles)	33 ↓ 3, 328	65.0 ↓ 65.0	0.0 ↓ 0.0
Slow Down for Grade	3, 329	61.0	0.0
	3, 339	21.0	0.0
	3, 343	8.0	0.0
Maintain Constant Speed on Grade (~0.5 Mile)	3, 344 ↓ 3, 568	8.0 ↓ 8.0	0.196 ↓ 0.196
Slow to Rest	3, 569 ↓ 3, 573	6.2 ↓ 0.0	0.0 ↓ 0.0

*Total Distance at End of Cycle ~ 60 Miles.

Table D-5. Design Driving Cycle for Low-speed Intracity Bus

Event	Elapsed Time, sec	Speed, mph	Grade, sin θ
Maximum Acceleration to Maximum Cruise Speed	0	0.0	0.0
	1	4.4	0.0
	2	8.6	0.0
	3	12.4	0.0
	4	16.0	0.0
	5	19.3	0.0
	6	22.3	0.0
	7	25.0	0.0
	8	27.5	0.0

Table D-5. Design Driving Cycle for Low-speed Intracity Bus (Continued)

Event	Elapsed Time, sec	Speed, mph	Grade, sin θ
Maximum Acceleration to Maximum Cruise Speed (cont)	9	29.7	0.0
	10	31.7	0.0
	11	33.4	0.0
	12	35.0	0.0
	13	36.4	0.0
	14	37.7	0.0
	15	38.8	0.0
	16	39.7	0.0
	17	40.0	0.0
Maximum Speed Cruise and Range Demonstration * (~199 Miles)	18	40.0	0.0
	↓	↓	↓
	17,930	40.0	0.0
Slow Down for Grade	17,935	23.0	0.0
	17,940	6.0	0.0
Maintain Constant Speed on Grade (~0.5 Mile)	17,941	6.0	0.196
	↓	↓	↓
	18,240	6.0	0.196
	18,241	6.0	0.0
Slow to Rest	18,245	0.0	0.0
	18,250	19.0	0.0

*Total Distance at End of Cycle = 200 Miles.

Table D-6. Design Driving Cycle for High-speed Intracity Bus

Event	Elapsed Time, sec	Speed, mph	Grade, sin θ
Maximum Acceleration to Maximum Cruise Speed	0	0.0	0.0
	1	3.3	0.0
	2	6.1	0.0
	3	8.6	0.0
	4	10.7	0.0
	5	12.5	0.0
	6	14.2	0.0
	7	15.6	0.0
	8	16.9	0.0
	9	18.1	0.0
	10	19.1	0.0
	11	20.1	0.0
	12	21.0	0.0
	13	21.8	0.0
	14	22.5	0.0
	15	23.2	0.0
	16	23.8	0.0
	17	24.4	0.0
	18	25.0	0.0
	19	25.5	0.0

Table D-6. Design Driving Cycle for High-speed Intracity Bus (Continued)

Event	Elapsed Time, sec	Speed, mph	Grade, sin θ
Maximum Acceleration to Maximum Cruise Speed (cont)	20	25.9	0.0
	21	26.4	0.0
	22	26.9	0.0
	23	27.3	0.0
	24	27.8	0.0
	25	28.3	0.0
	26	28.8	0.0
	27	29.3	0.0
	30	29.8	0.0
	31	30.3	0.0
	32	30.7	0.0
	33	31.2	0.0
	34	32.2	0.0
	35	32.7	0.0
	36	33.2	0.0
	37	33.7	0.0
	38	34.2	0.0
	39	34.7	0.0
	40	35.2	0.0
	41	35.7	0.0
	42	36.2	0.0
	43	36.7	0.0
	44	37.2	0.0
	45	37.6	0.0
	46	38.1	0.0
	47	38.6	0.0
	48	39.1	0.0
	49	39.6	0.0
	50	40.0	0.0
	51	40.5	0.0
	52	41.0	0.0
	53	41.4	0.0
	54	41.9	0.0
	55	42.3	0.0
	56	42.8	0.0
	57	43.2	0.0
	58	43.6	0.0
	59	44.1	0.0
	60	44.5	0.0
	61	44.9	0.0
	62	45.3	0.0
	63	45.7	0.0
	64	46.1	0.0
	65	46.5	0.0
	66	46.9	0.0
	67	47.3	0.0
	68	47.7	0.0
	69	48.0	0.0
	70	48.4	0.0
	71	48.8	0.0
	72	49.1	0.0
	73	49.5	0.0
	74	49.8	0.0
	75	50.1	0.0
	76	50.4	0.0
	77	50.8	0.0
	78	51.1	0.0
	79	51.4	0.0
	80	51.7	0.0
	81	52.0	0.0

Table D-6. Design Driving Cycle for High-speed Intracity Bus (Continued)

Event	Elapsed Time, sec	Speed, mph	Grade, sin θ
Maximum Acceleration to Maximum Cruise Speed (cont)	82	52.3	0.0
	83	52.5	0.0
	84	52.8	0.0
	85	53.1	0.0
	86	53.4	0.0
	87	53.6	0.0
	88	53.9	0.0
	89	54.1	0.0
	90	54.3	0.0
	91	54.6	0.0
	92	54.8	0.0
	93	55.0	0.0
	94	55.2	0.0
	95	55.5	0.0
	96	55.7	0.0
	97	55.9	0.0
	98	56.1	0.0
	99	56.2	0.0
	100	56.4	0.0
	101	56.6	0.0
	102	56.8	0.0
	103	57.0	0.0
	104	57.1	0.0
	105	57.3	0.0
	106	57.4	0.0
	107	57.6	0.0
	108	57.7	0.0
	109	57.9	0.0
	110	58.0	0.0
	111	58.2	0.0
	112	58.3	0.0
	113	58.4	0.0
	114	58.5	0.0
	115	58.7	0.0
	116	58.8	0.0
	117	58.9	0.0
	118	59.0	0.0
	119	59.1	0.0
	120	59.2	0.0
	121	59.3	0.0
	122	59.4	0.0
	123	59.5	0.0
	124	59.6	0.0
	125	59.7	0.0
	126	59.8	0.0
	127	59.9	0.0
	128	60.0	0.0
Maximum Cruise Speed and Range Demonstration	129	60.0	0.0
	↓	↓	↓
	11,948	60.0	0.0

Table D-6. Design Driving Cycle for High-speed Intracity Bus (Concluded)

Event	Elapsed Time, sec	Speed, mph	Grade, sin θ
Slow Down for Grade	11, 949	59.0	0.0
	11, 954	42.0	0.0
	11, 959	26.0	0.0
	11, 964	10.0	0.0
Maintain Constant Speed on Grade (~1.0 Mile)	11, 965	10.0	0.10
	↓	↓	↓
	12, 324	10.0	0.10
Slow to Rest	12, 325	8.0	0.0
	12, 329	0.0	0.0

*Total Distance at End of Cycle ≈ 200 Miles.

APPENDIX E

HEAT ENGINE DATA COMPILATION AND COMPARISON

TABLES

E-1. Spark Ignition Engines (Reciprocating) E-3

E-2. Spark Ignition Engines (Rotary) E-5

E-3. Compression Ignition Engines E-5

FIGURES

E-1. Comparison of SFC Maps - Toyota Versus Ref. E-1. . . . E-10

E-2. Comparison of SFC Maps - Toyota Versus Ford E-11

E-3. Comparison of S. I. Engine WOT SFC Characteristics . . . E-12

E-4. Comparison of SFC Maps - Comet Versus Ref. E-3 . . . . E-13

E-5. Comparison of SFC Maps - Comet Versus Mercedes . . . E-14

E-6. Comparison of CI Engine Optimum SFC Characteristics. . E-15

APPENDIX E

HEAT ENGINE DATA COMPILATION AND COMPARISON

A listing of the internal combustion engines used as a data base for the plots of SFC, weight, and volume shown in Section 8 is provided in Tables E-1 through E-3 (The external combustion engines are identified in Section 8.). Additionally, Figs. E-1 through E-6 are presented to provide justification for the selection of certain engines as being representative of a given heat engine type (See Section 8).

The validity of using the Toyota data (Toyota Corona 3RC, 115.7 CID engine) to represent typical S. I. engine fuel consumption characteristics (Section 8.2.2) was examined. Comparison plots of data from other sources are shown in Figs. E-1, E-2, and E-3. Figure E-1 is an overlay on Fig. 8-4 of a "typical carbureted engine" SFC map obtained from Ref. E-1. The bumps in the rpm curves near the wide open throttle (WOT) point may be noted. These are a characteristic of the particular device used for power enrichment (power jet or economizer). In general, the shapes of the two sets of curves are in good agreement, although the optimum SFC for the Ref. E-1 engine is flatter than the Toyota characteristic.

Another overlay of an SFC map is shown in Fig. E-2. These data, from Ref. E-2, are for a Ford engine (model and year unspecified). Again, there is general agreement with the Toyota characteristics.

The rpm envelopes shown in Figs. E-1 and E-2 represent the sum total of information acquired on optimum throttle SFC. However, a great deal of SFC data for wide open throttle operation was obtained. These data are shown with the Toyota WOT characteristic in Fig. E-3. Considerable variation between engines is evident; however, the Toyota curve falls nicely within the extremes of the data scatter. This may indirectly provide some additional confidence in the use of Fig. 8-7 as a representative sample of S. I. engine optimum throttle performance.

The validity of using the Comet data as a representative sample of diesel engine performance (Section 8.3.2) is examined in Figs. E-5, E-6, and E-7. In Fig. E-5, the Comet SFC map is compared with data identified as being typical of small, automotive-type diesels (Ref. E-3). The comparison indicates excellent agreement.

Figure E-6 compares the Comet (turbulence chamber, TC) engine with a Mercedes-Benz 123 CID (precombustion chamber, PC) engine rated 55 hp at 4400 rpm (Ref. E-4). At the higher speeds it will be noted that the Mercedes data indicate higher SFC and that there is an increasing disparity in the position of comparable percent rpm curves. This trend may reflect a characteristic difference in the performance of the two combustion chamber types (PC versus TC), or it may simply be due to the fact that the Mercedes is rated at a higher speed than Comet (4400 versus 3500 rpm). If the latter, the effects observed in Fig. E-6 could easily be explained in terms of friction losses. It is noted that when the data are compared at equal rpm (instead of percent rpm) the relation between the SFC characteristics for the two engines improves considerably.

In Fig. E-7, the Comet optimum SFC characteristic is compared with the optimum curves for eight different divided chamber engines (all automotive), including the PC-type Mercedes discussed under Fig. E-6. It can be seen that the Comet curve falls well within the scatter of data over the complete power range. At the high end of the power range where a true representation of performance has significance, the Comet curve approximates a mean fit to the data spread.

Table E-1. Spark Ignition Engines (Reciprocating)

KEY

A	Automobile	DI	Direct Injection
I	Industrial	TC	Turbulence Chamber
B	Bus	PC	Precombustion Chamber
T	Truck	*	Indicates Data Plotted

Make	Model	Application	Rated[1] HP	Rated RPM	Displacement, in.^{3}	Weight, lb	Volume, ft^3	Minimum SFC, lb/hp-hr
Alfa-Romeo	Giulia 1300	A	89	6000	79	260*		
American Motors	Hornet	A	128	4400	199	470*	13.5*	
American Motors	Gremlin	A	135	4000	232	437*		
American Motors	Jeep/155	A	136	4200	225	410*	14.4*	0.500*
American Motors	Hornet SST	A	145	4300	232	485*	13.5*	0.454*
American Motors	Ambassador	A	150	3800	258	491*		0.467*
American Motors	Ambassador SST	A	210	4400	304	593		0.434*
American Motors	AMX	A	245	4400	360	594*		0.454*
American Motors	Jeep F4	A	75	4000	134	390	8.85*	0.510*
American Motors	Jeep L4	I	60	4000	134	344	7.70*	0.568*
Briggs/Stratton	200400	I	8	3600	20.3	74	2.38*	
Briggs/Stratton	243430	I	10	3600	23.9	96	3.03*	
Briggs/Stratton	320420	I	14	3600	32.4	116	3.47*	
Chrysler	Dart	A	230	4500	318	535*		
Datsun	J	A	67	5200	79.3	306*	7.99*	0.441*
Datsun	L-13	A	77	6000	79.1	282*		
Datsun	L-16	A	96	5600	97.3	290*		
Ford	091GF	I	58	4000	91	267		0.480*
Ford	104GF	I	70	4000	104	267	8.01	0.470*
Ford	Saab	A	83	5200	104	267*		
Ford	134	I	48.5	2800	134	489		0.500*
Ford	172	I	68	2800	172	489		0.500*
Ford	170	T, B	105	4200	170	360	18.11*	
Ford	Mustang	A	120	4000	200	337*		0.501*
Ford	Galaxie	A	150	4000	240	473*		0.500*

(1)Refers to bare engine peak power output at the engine flywheel

Table E-1. Spark Ignition Engines (Reciprocating) (Continued)

Make	Model	Application	Rated(1) HP	Rated RPM	Displacement, in.^{3}	Weight, lb	Volume, ft^3	Minimum SFC, lb/hp-hr
Ford	6-300	T, B, I	165	3600	300	438		0.505*
Ford	330HD	T, B, I	190	4000	330	720		0.475*
Ford	391EHD	T, B, I	235	4000	391	721		0.500*
Ford	V8-477	T, I	253	3400	477	1044		0.500*
Ford	V8-534	T, I	266	3200	534	1044		0.480*
General Motors	Nova	A	90	4000	153	350*	10.5*	
General Motors	Camaro	A	140	4500	230	444*	16.2*	
General Motors	Vega	A	90		140	285*		
General Motors	Vega	A	110		140	290*		
General Motors	Corvette	A	300	4800	350	607*		
Onan	N4-MS-NH-3	I	25	3600	60	112	3.93*	0.584*
Onan	CCKA	I	16.5	3600	49.8	148	3.81*	0.713*
Opel	19US	A	90	5200	115.8			0.542*
Opel	11S	A	59	5600	65.8			0.491*
Tecumseh	HH120	I	12		27.7	107	2.68*	
Toyota	Corona	A	90	4600	115.7	386*		0.478*
Toyota	Corona MK II	A	108	5500	113.4	382*		
Toyota	Corolla	A	60	6000	65.6	217*		
Universal	AF-UJ	M	30	3500	64.5	247	5.61*	
Universal	UF-HF	M	70	3500	141	391	9.61*	
Volkswagen	122	I	40	3600	72.7	206	11.63*	
Volkswagen	124A	I	53	3600	96.7	235	11.40*	
Volkswagen	126A	I	53	3600	96.7	220	11.75*	
Volkswagen	1200	A	36	3700	72.74	198*		
Volkswagen	1500	A	65	4600	96.6	277*		
Volkswagen	1600	A	53	4200	96.6	253*		
Waukesha	ICK	I	17	3200	61.3	195	3.88*	
Waukesha	FC	T, I	34	2600	133	290	8.91*	
Wisconsin	VG4D	I	37	2400	154	410	14.40*	

(1) Refers to bare engine peak power output at the engine flywheel

Table E-2. Spark Ignition Engines (Rotary)

Make	Model	Application	Rated[1] HP	Rated RPM	Displace- ment, in.^{3}	Weight, lb	Volume, ft^3	Minimum SFC, lb/hp-hr
Curtiss-Wright	RC1-6.6	I	6.55	5500	6.6	34*	2.0*	0.68*
Curtiss-Wright	RC1-9.8	I	8	4700	9.8	37*	2.3*	0.71*
Curtiss-Wright	RC1-18.5	I	20	5000	18.5	56*	3.2*	0.69*
Curtiss-Wright	RC2-20	I	40	4500	40	120*	4.8*	0.604*
Curtiss-Wright	RC2-28	I	55	4500	56	136*	6.6*	0.604*
Curtiss-Wright	RC2-30-10A	A	110	7000	60	225*	6.4*	0.48*
Curtiss-Wright	RC2-30	A	128.5	5500	60	285*	6.4*	0.51*

Table E-3. Compression Ignition Engines

Make	Model	Type	Application	Rated[1] HP	Rated RPM	Displace- ment, in.^{3}	Weight lb	Volume, ft^3	Minimum SFC, lb/hp-hr
American Marc	AC-1	TC	I	9	2500	35	205*	7.45*	
American Marc	WC-1	PC	I	9	2500	35	213*	8.16*	
American Marc	AC-2	TC	I	18	2500	72	360*	13.60*	
American Marc	WC-2	PC	I	18	2500	72	360*	13.54*	
American Marc	WD-2	TC	I	28	2500	94	365*	19.68*	
American Marc	3015	DI		15	3000	41	210*	4.57*	
American Marc	3020	DI		20	3000	46	212*	4.62*	
American Marc	3030	DI		30	3000	82	324*	7.12*	
American Marc	3040	DI		40	3000	91	335*	7.23*	
Caterpillar	1140	DI	T, B	150	3200	522	1196*	23.78*	
Caterpillar	1145	DI	T, B	175	3200	522	1196*	23.78*	
Caterpillar	1150	DI	T, B	200	3000	573	1196*	23.78*	
Caterpillar	1160	DI	T, B	225	2800	636	1196*	23.78*	
Caterpillar	73	PC	T	250	2200	638	1940	45.83*	
Caterpillar	1674TA	PC	T	270	2200	638	2260	46.06*	

---

[1] Refers to bare engine peak power output at the engine flywheel

Table E-3. Compression Ignition Engines (Continued)

Make	Model	Type	Application	Rated HP[1]	Rated RPM	Displacement, in.^{3}	Weight lb	Volume, ft^3	Minimum SFC, lb/hp-hr
Chrysler-Nissan	CN432	TC	T	61	4000	132	474*	11.17*	0.452*
Chrysler-Nissan	CN633	TC	T	92	4000	198	662*	14.93*	0.448*
Comet	MK V	TC	A	83	3500	173			0.403*
Cummins	V6-140	DI	T, B	140	3300	352	1145*		
Cummins	V-352	DI	I	140	3300	352	1175		0.400*
Cummins	V6-155	DI	T	155	3300	378	1195*		
Cummins	C-464	DI	I	168	2500	464	1580		0.430*
Cummins	V8E-170	DI	T	170	3300	470	1380*		0.396*
Cummins	V8-185	DI	T, B	185	3300	470	1380*		0.400*
Cummins	V-470	DI	I	185	3300	470	1410		0.400*
Cummins	H-743	DI	I	190	2000	743	3100		0.385*
Cummins	V6E-195	DI	T	195	2500	588	1640*		
Cummins	V-588	DI	I	200	2600	588	1790		0.370*
Cummins	V6-200	DI	T	200	2600	588	1640*		
Cummins	V8-210	DI	T	210	3300	504	1460*		0.390*
Cummins	N-743	DI	I	220	2100	743	2470		0.365*
Cummins	NH-230	DI	I	230	2100	855	2430		0.371*
Cummins	V8-235	DI	T	235	2400	785	2080*		
Cummins	N-855	DI	I	250	2100	855	2590		0.435*
Cummins	V-785	DI	I	265	2600	785	2180		0.370*
Cummins	V8E-265	DI	T	265	2600	785	2080*		
Cummins	NHCT-270	DI	I	270	2100	855	2540		0.362*
Cummins	NHTF-295	DI	T	295	2300	855	2510*		
Cummins	V-903	DI	T, B	320	2600	903	2160*		0.362*
Cummins	NHF-240	DI	T	340	2300	855	2430*		
Cummins	NT-350	DI	T	350	2100	855	2750*		
Deutz	F1L110	TC	I	14	3000	39	242*		
Deutz	F2L310	TC	I	28	3000	78	330*		
Deutz	F2L812	TC	I	29	2300	104	617*		

---

(1) Refers to bare engine peak power output at the engine flywheel

Table E-3. Compression Ignition Engines (Continued)

Make	Model	Type	Application	Rated HP[1]	Rated RPM	Displacement, in.^{3}	Weight lb	Volume, ft^3	Minimum SFC, lb/hp-hr
Deutz	F2L912	DI	I	32	2300	115	618*		
Deutz	F3L812	TC	T, B, I	50	2800	156	661*	15.51*	
Deutz	F3L912	DI	T, B, I	60	2800	173	660*	13.83*	
Deutz	F4L812	TC	T, B, I	67	2800	207	694*	18.81*	
Deutz	F4L912	DI	T, B, I	80	2800	230	695*	15.74*	
Deutz	F6L812	TC	T, B, I	100	2800	311	903*	25.23*	
Deutz	F6L912	DI	T, B, I	120	2800	345	904*	22.34*	
Daihatsu	D-138	TC	A	63	3600	138	470*		0.444*
Daihatsu	D-154	TC	A	74	3800	154	528		0.425*
Ford	158-D	DI	I	36.5	2000	158	684*		
Ford	144	DI	I	46	2400	144	596		0.399*
Ford	172	DI	I	59.5	2400	172	596		0.408*
GMC	DH478	DI	T, B	165	2800	478	1056*	22.34*	
GMC	DH637	DI	T	210	2800	637	1270*	27.08*	
Henschel	4R1010	TC	T	88	3400	192	706*		
Henschel	6R1010	TC	T	126	3400	287	882*		
International	D-354	DI	T	131	2800	354	1095*		0.375*
International	DV-462	DI	T	160	3000	461	1220*	30.44*	
International	DV-550	DI	T	180	3000	549	1270*	30.44*	
International	DV-550	DI	T	200	3000	549	1270*	30.44*	
Isuzu	B110	PC	I	19.3	2600	67			0.493*
Isuzu	C201	TC	I	36.5	2600	122			0.459*
Isuzu	C221	TC	T	48.7	3000	135			0.459*
Isuzu	DA220	PC	I	68	2200	249			0.459*
Isuzu	D400	PC	T	74	2800	243			0.482*
Isuzu	DA120	PC	T, B	103.4	2200	374			0.426*
Isuzu	DA640	PC	T, B	111.5	2400	399			0.426*
Leyland	100	PC	T	42	3500	91	403*		0.440*
Leyland	120	PC	T	68	3500	102	570*		0.410*

---

(1) Refers to bare engine peak power output at the engine flywheel

Table E-3. Compression Ignition Engines (Continued)

Make	Model	Type	Application	Rated HP[1]	Rated RPM	Displacement, in.^{3}	Weight lb	Volume, ft^3	Minimum SFC, lb/hp-hr
Leyland	200	DI	T	69	2400	230	862*		0.380*
Leyland	300	DI	T	89	2400	312	1080*		0.380*
Leyland	310	DI	T	110	2400	345	1080*		0.380*
Leyland	400	DI	T	134	2400	399	1181*		0.365*
Leyland	401	DI	T	149.5	2600	399	1181*		0.365*
Leyland	AV505	DI	T	162	2400	502	1365*		
Leyland	500	DI	T	183	2600	500	1659*		0.375*
Leyland	AV691	DI	T	215	2200	690	1890		0.355*
Leyland	680	DI	T	216	2200	677	2000*		0.372*
Leyland	AV760	DI	T	236	2200	761	1904		0.350*
Leyland	801V	DI	T	291	2600	800	2050*		0.368*
Leyland	AV1100	DI	T	310	1900	1087	3375		0.357*
Mack	END864C	DI	T	270	2300	864			0.348*
Mercedes-Benz	DM636	PC	I	43	3500	108	355		0.428*
Mercedes-Benz	DM621	PC	A	55	4350	122			0.420*
Mercedes-Benz	DM314	DI	T, B, I	80	2800	231	660	11.52*	0.362*
Mercedes-Benz	DM352	DI	T, B, I	126	2800	346	850	16.55*	0.359*
Mercedes-Benz	DM355	DI	I	235	2000	707	1780		0.337*
Nissan	SD20	TC	T, B, A	63.5	4000	121	412*		
Nissan	SD22	TC	T, B, A	70	4000	132	412*		
Nissan	SD33	TC	T, B, A	105	4000	198	606*		
Nissan	ND601	DI	A	140	2800	418	1345*		
Nissan	PD601	DI	T	190	2300	629	1885*		0.370*
Onan	DJA	PC	I	7	2400	30	228	4.86*	
Onan	DJBA	PC	I	15	2400	60	270	5.90*	
Onan	DJC	PC	I	28	2400	120	438	9.49*	
Perkins	4-108	PC	T	60	4000	107	450*	6.66*	
Perkins	4-203	PC	T	70	2600	203	635*		
Perkins	4-203C	PC	T	71	2600	203	635*		

(1) Refers to bare engine peak power output at the engine flywheel

Table E-3. Compression Ignition Engines (Concluded)

Make	Model	Type	Application	Rated HP[1]	Rated RPM	Displacement, in.^{3}	Weight lb	Volume, ft^3	Minimum SFC, lb/hp-hr
Perkins	4-154	PC	T	80	3600	154	555*	11.86*	
Perkins	4-236	DI	T	88	2600	236	740*		
Perkins	6-354	DI	T	131	2800	354	1020*	22.92*	
Perkins	V8-510	DI	T	185	2800	511	1550*	25.12*	
Peugot	XDP4.88	TC	A	68	4500	119	396*		0.440*
Peugot	XDP4.90	TC	A	75	4500	129	413*		0.438*
Peugot	XDP6.90	TC	A	106	4000	193	591*		0.432*
Witte	100	PC	I	26.3	1800	100			0.400*
Witte	120	PC	I	31	1800	120			0.400*

---

(1) Refers to bare engine peak power output at the engine flywheel

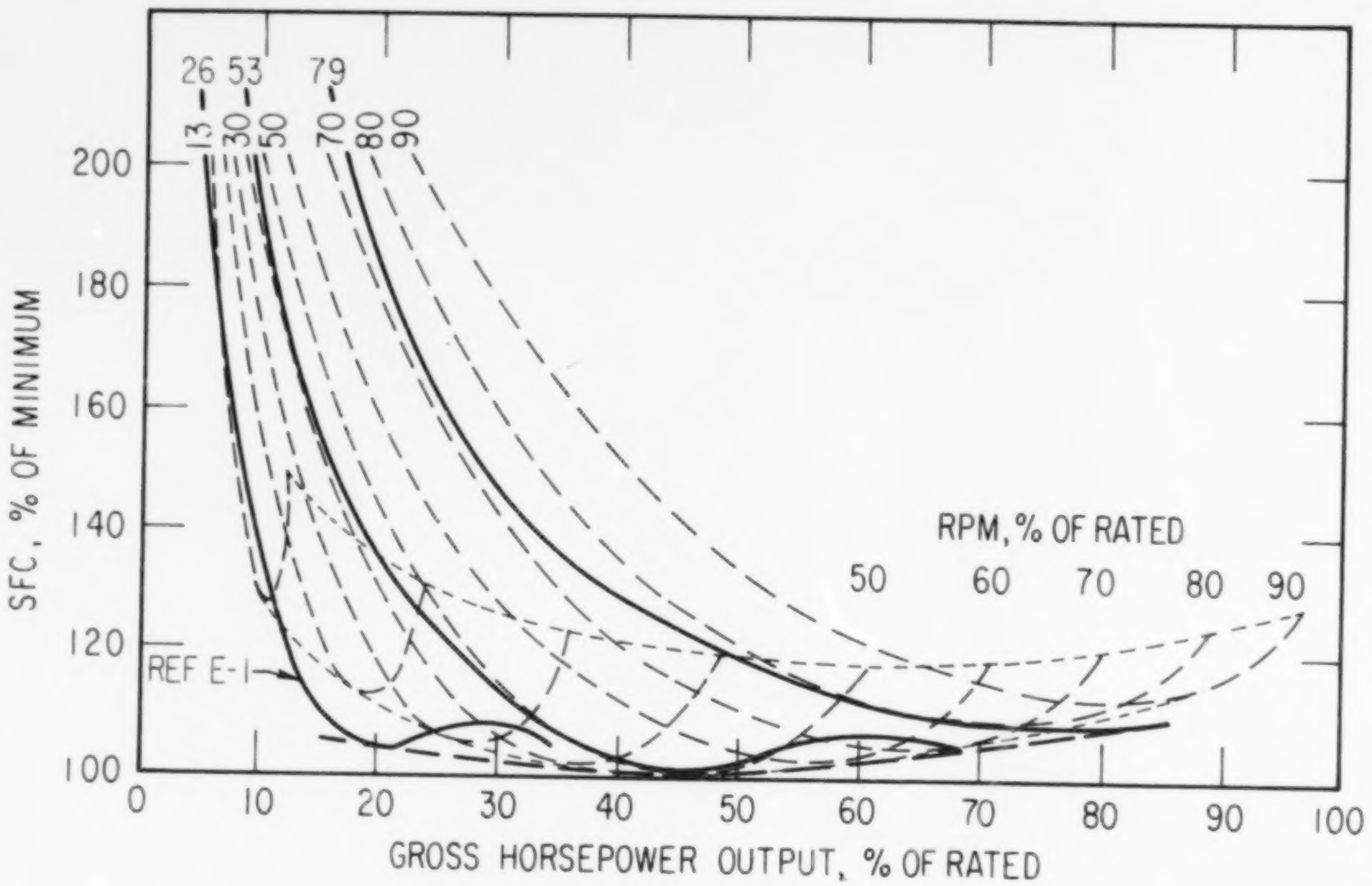

Figure E-1. Comparison of SFC Maps - Toyota Versus Ref. E-1

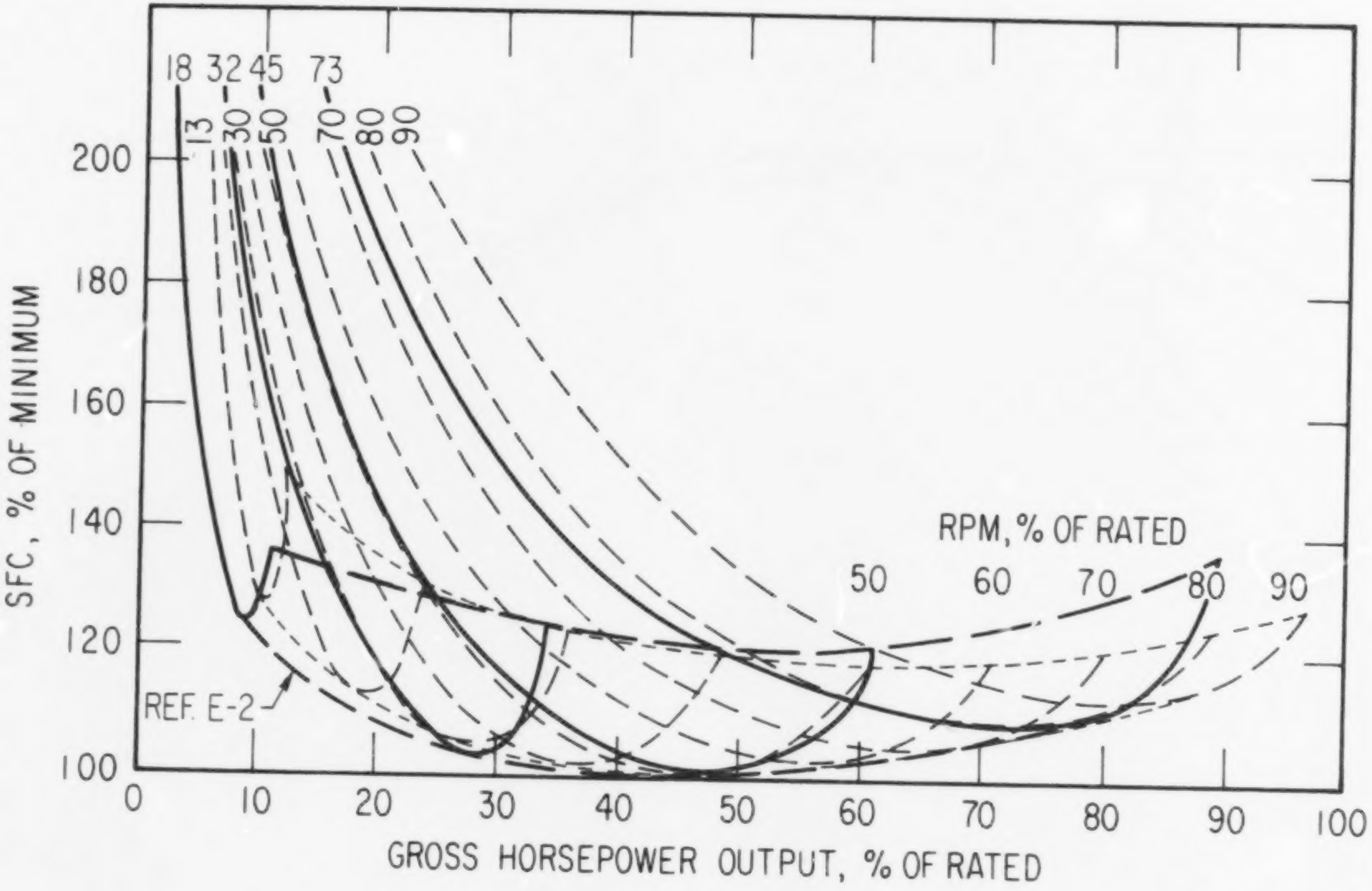

Figure E-2. Comparison of SFC Maps - Toyota Versus Ford (Ref. E-2)

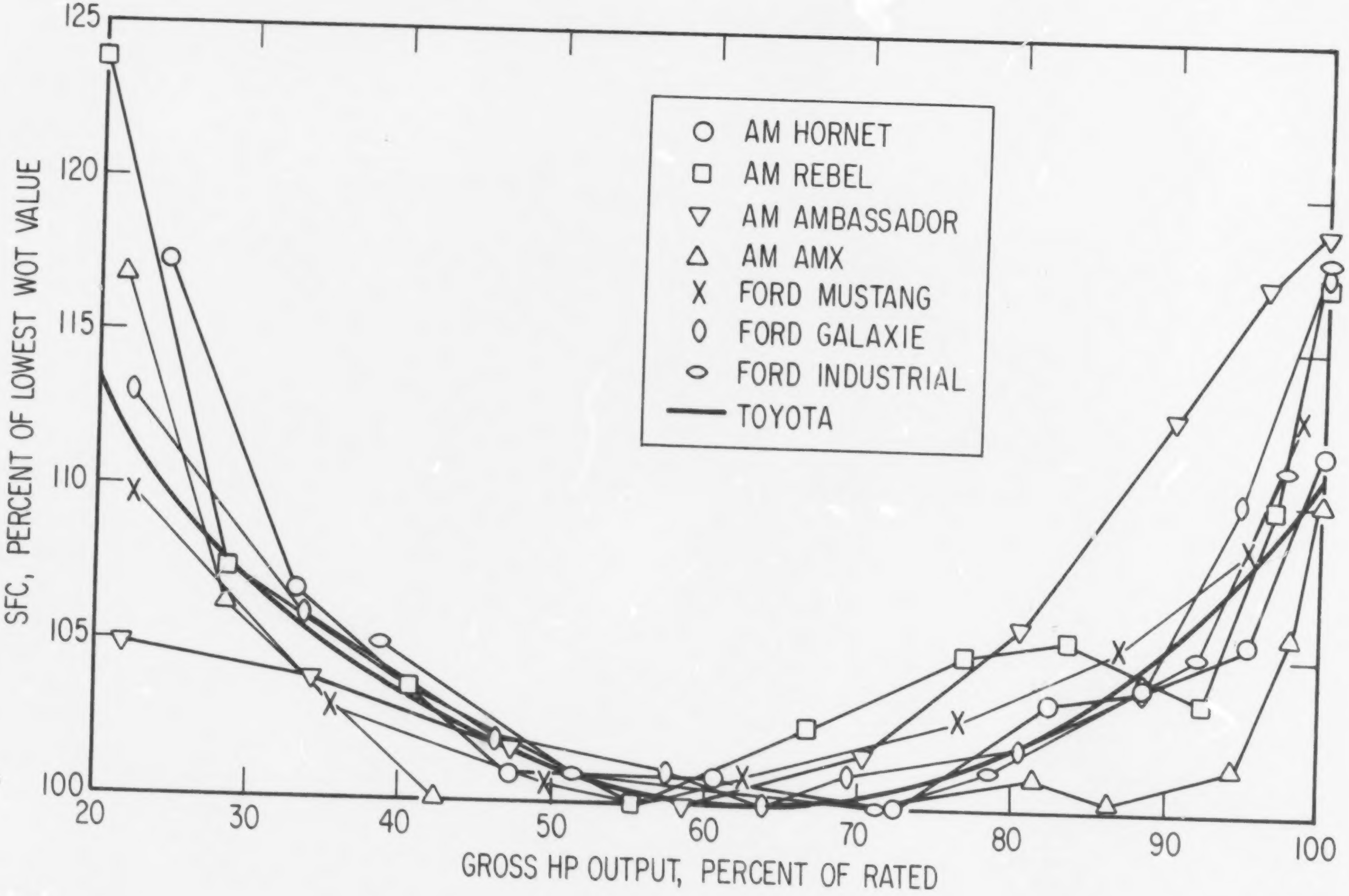

Figure E-3. Comparison of S. I. Engine WOT SFC Characteristics

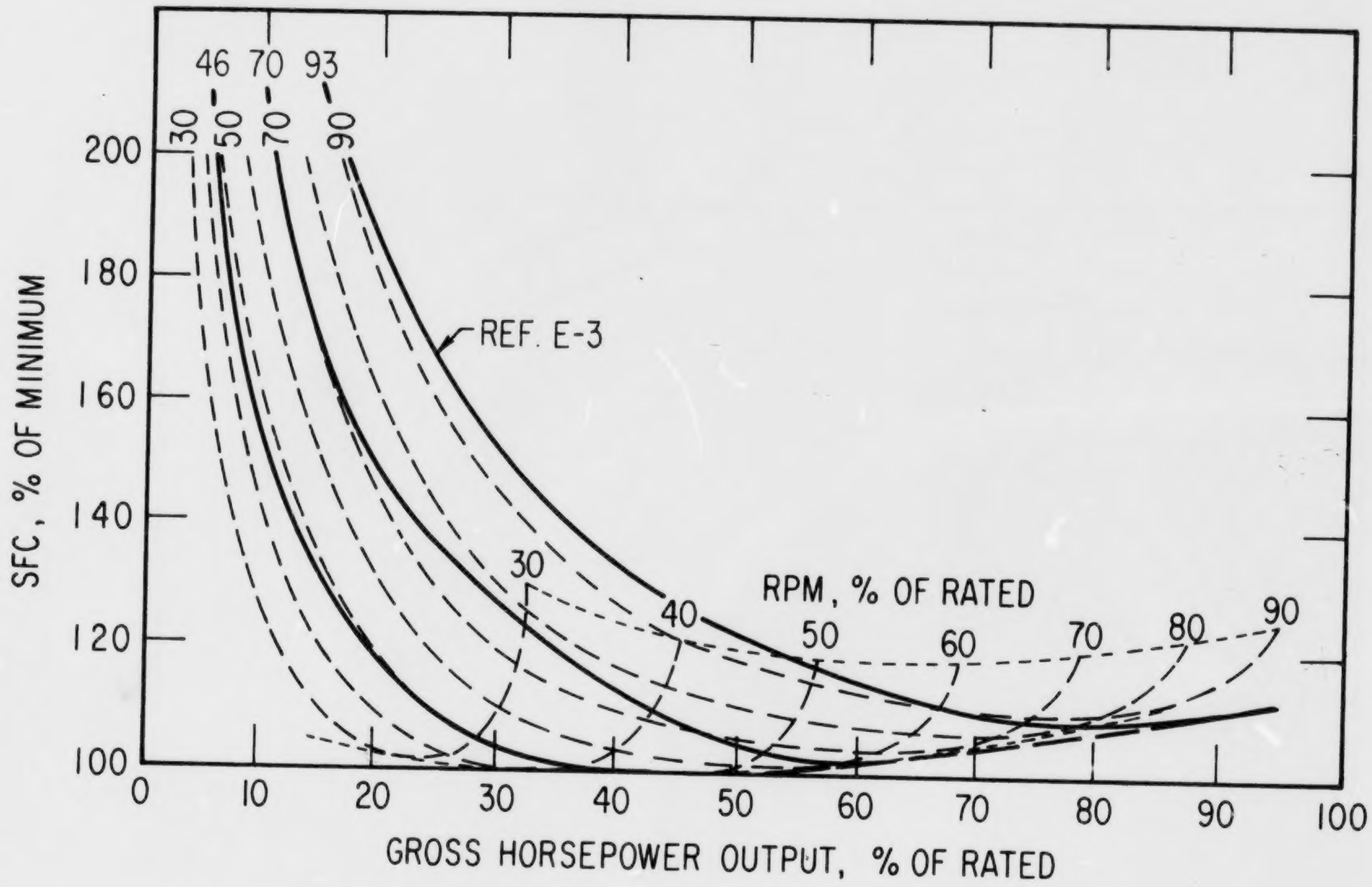

Figure E-4. Comparison of SFC Maps - Comet Versus Ref. E-3

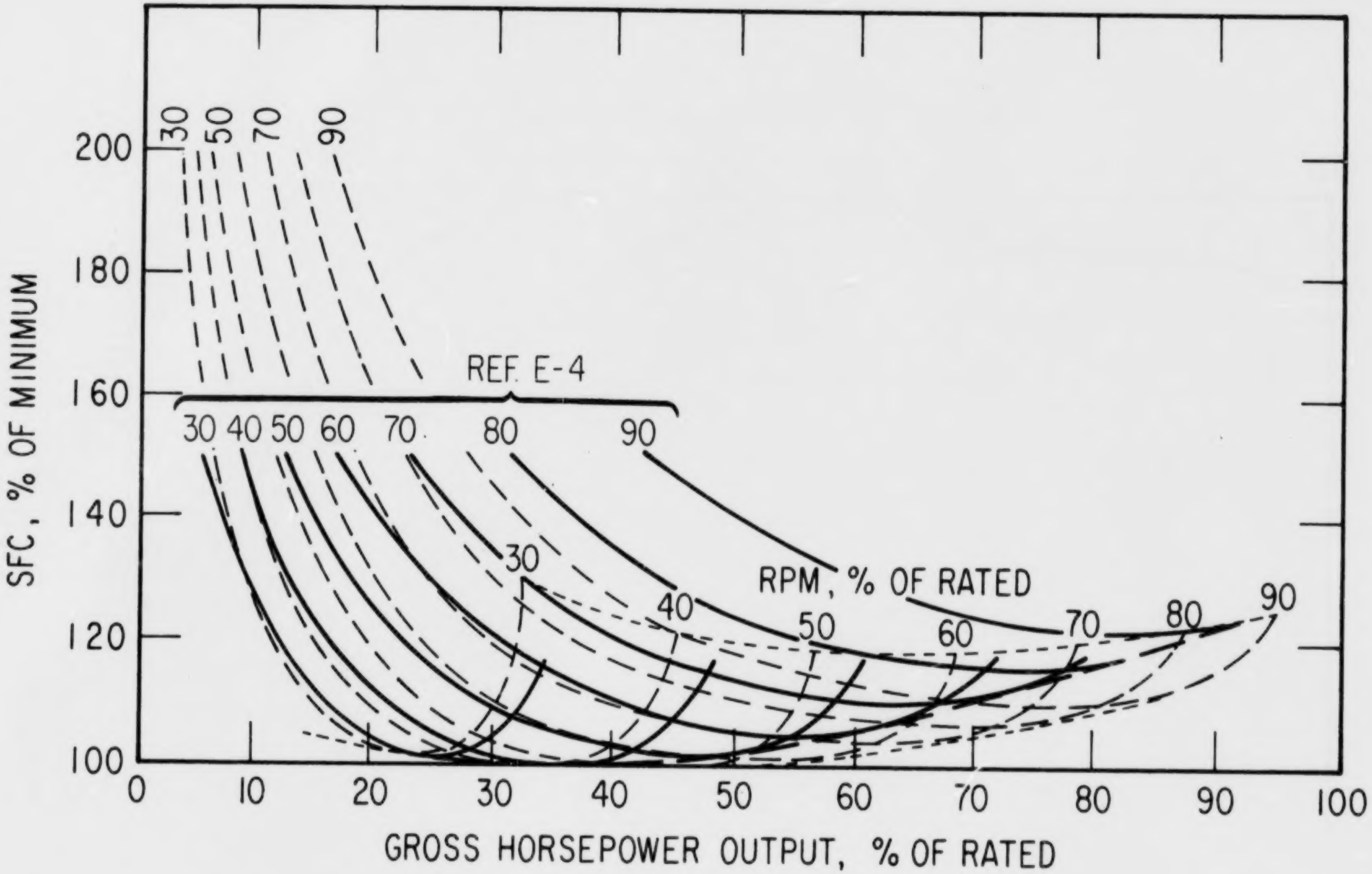

Figure E-5. Comparison of SFC Maps - Comet Versus Mercedes (Ref. E-4)

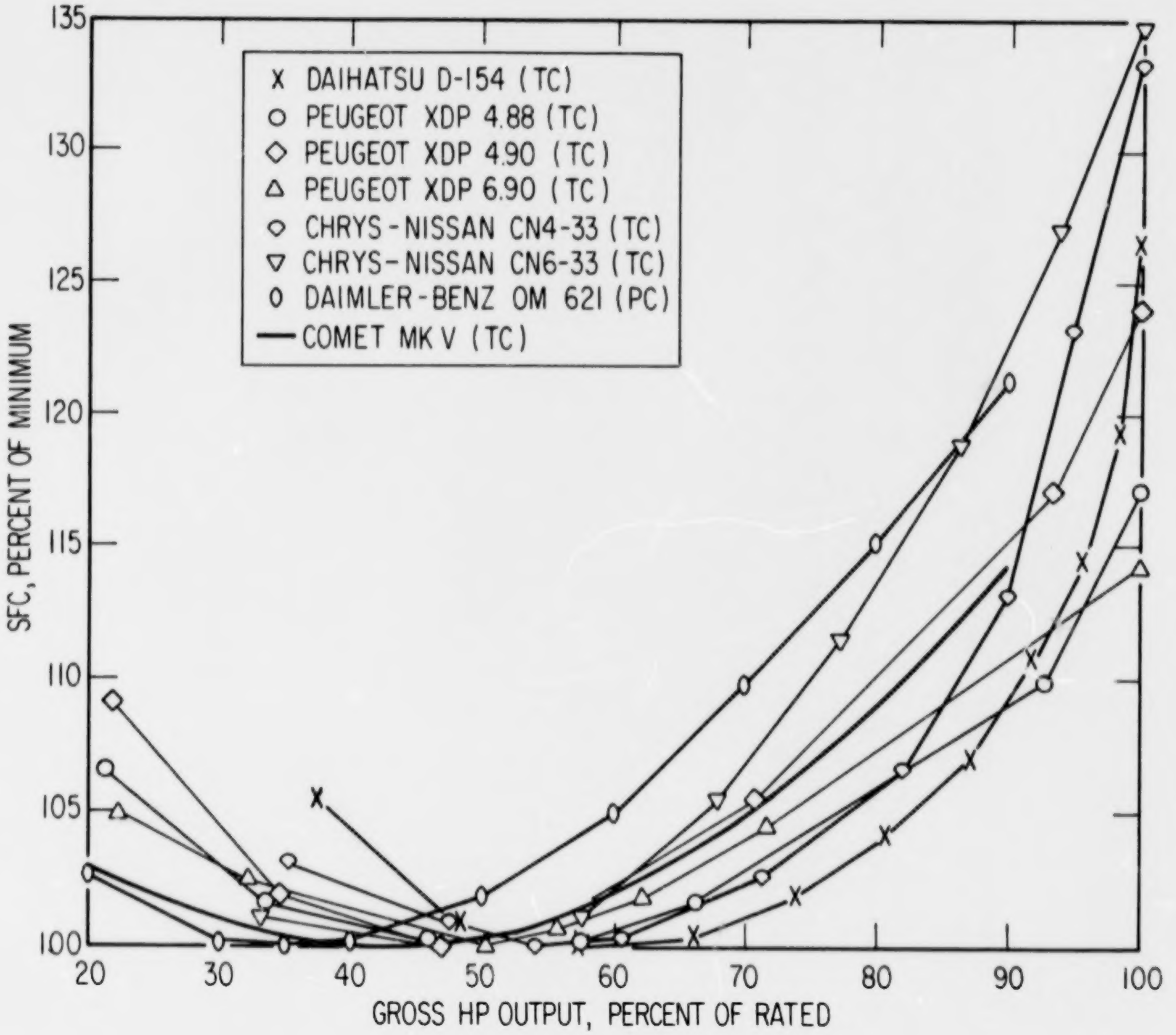

Figure E-6. Comparison of CI Engine Optimum SFC Characteristics

REFERENCES

E-1. Bishop and Simko, A New Concept of Stratified Charge Combustion - the Ford Combustion Process (FCP), SAE Paper No. 680041 (January 1968).

E-2. D. N. Hwang, Fundamental Parameters of Vehicle Fuel Economy and Acceleration, SAE Paper No. 690541 (30 October 1968).

E-3. E. F. Obert, Internal Combustion Engines, International Textbook Company, Scranton Pennsylvania (December 1968).

E-4. E. Eisele, Daimler-Benz Passenger Car Diesel Engines - Highlights of 30 Years of Development, SAE Paper No. 680089 (January 1968).

APPENDIX F

ACKNOWLEDGMENTS TO SOURCES OF SUBSYSTEMS/COMPONENT DATA

CONTENTS

F. ACKNOWLEDGMENTS TO SOURCES OF SUBSYSTEMS/COMPONENT DATA F-1

F.1 Electrical System - Motor, Generator, and Control Systems F-1

F.2 Electrical System - Battery Characteristics and Operation F-4

F.3 Heat Engine Performance Characteristics and Operation F-8

F.4 Heat Engine Exhaust Emissions F-11

APPENDIX F

ACKNOWLEDGMENTS TO SOURCES OF SUBSYSTEMS/COMPONENT DATA

This appendix acknowledges the data of great value to this study that were provided by individuals in industry, universities, and government agencies.

F.1 ELECTRICAL SYSTEM – MOTOR, GENERATOR, AND CONTROL SYSTEMS

Data Source	Primary Contact	Remarks
Aeroflex Labs. Newport Beach, Calif.	W.S. Roth M. Ruderman	Data on brushless dc motors.
Airsupply Co. Santa Monica, Calif. Representing Hartman Electrical Mfg. Co. Mansfield, Ohio	R.J. Leckey H.T. Fuller	Data on relays and provisions for protection of motors.
Bose Corp. Natick, Mass.	S. Hendryx T. Froeschle J. Veranth	Information on inverter state of the art.
Electric Fuel Propulsion Detroit, Mich.	R.R. Aronson	Information on electric vehicles and electric motor performance curves.
Electric Motion Control Pasadena, Calif.	D. Middlebrook H. deJong	Information on new smooth acceleration drive system without semiconductors. Demonstration of model.
Ford Motor Co. Dearborn, Mich.	W.H. Koch	Electric vehicle test results and numerous discussions on motor operation and selection criteria.

Data Source	Primary Contact	Remarks
Fort Belvoir Army Res. and Dev. Labs., Virginia	R.E. Hopkins	Information on ac motors, inverters, and motor mounted in wheel. Review of motor operation, selection criteria, and advance design considerations for Army hybrid vehicle.
Garrett Corp. AiResearch Mfg. Div. Los Angeles, Calif.	K.M. Chirgwin	Information on separately excited motors and controls.
General Electric Co. Erie, Pa.	W.G. Brighton	Information on motors applied to or proposed for electric vehicles.
General Motors Research Labs. Warren, Mich.	R.W. Johnston, et al.	Results of research efforts on ac induction motor-inverter for electric vehicles.
Gulton Industries Metuchen, N.J.	V. Wouk	Information on electric motor drive systems in Europe and design criteria for Gulton all-electric car.
Massachusetts Institute of Technology Cambridge, Mass.	R.D. Thornton	Extensive information on research in electric vehicle design and advance design techniques for power train components.

Data Source	Primary Contact	Remarks
Minicars, Inc. Goleta, Calif.	D. Friedman I. Barpal J. Anton	Data on design considerations and component data for hybrid vehicle parallel configuration.
Permag Pacific Los Angeles, Calif. Representing Indiana General and Arnold Engineering	D. Warburton	Data on permanent magnets.
TRW Systems Redondo Beach, Calif.	N.A. Richardson G.H. Gelb T.C. Wang B. Berman	Design considerations and data on hybrid vehicle parallel configuration. Numerous discussions on design philosophy, system operation, and component performance characteristics.
Univ. of California Los Angeles, Calif.	G.A. Hoffman	Data on future electric cars.

F.2 ELECTRICAL SYSTEM – BATTERY CHARACTERISTICS AND OPERATION

Data Source	Primary Contact	Remarks
Allis-Chalmers Mfg. Co. Milwaukee, Wis.	E. Pischotti	Data on metal-air battery.
Argonne National Lab. Argonne, Ill.	E.J. Cairns	Data on alkali-metal battery.
Atomics International Canoga Park, Calif.	L. Heredy L.R. McCoy	Data on nickel-zinc and lithium-sulfur batteries.
Battelle Memorial Inst. Columbus, Ohio	J. McCallum	General battery technology.
Bell Telephone Lab. Murry Hill, N.J.	L.D. Babusci R.V. Biagetti	Data on lead-acid battery.
Dartmouth College Hanover, N.H.	D. Ragone	Advice on battery selection, design and technology.
Dow Chemical Co. Midland, Mich.	R.P. Ruh	Advanced battery technology.
Eltra Corp. C&D Battery Div. Plymouth Meeting, Pa.	J. Macres (Costa Mesa, Calif.)	Lead-acid battery data and technology.
Eagle-Picher Co. Joplin, Mo.	E. Broglio F. Dittman P. Eddy E. Morse M. Barr (Los Angeles)	Data on lead-acid, nickel-zinc, and nickel-cadmium batteries.
E.S.B. Corp. Carl Norberg Res. Lab. Yardley, Pa.	G. Frysinger J. Smyth J. Norberg (Philadelphia)	Lead-acid battery data and technology.

Data Source	Primary Contact	Remarks
Fort Belvoir Army Res. and Dev. Labs., Virginia	H. Barger R. Hopkins J. Huff J. MacDonald J. O'Sullivan	Battery data and technology.
Fort Monmouth Army Electronics Command, New Jersey	M. Sulkes	Nickel-zinc battery technology.
General Electric Co. Gainsville, Fla.	G. Rampel L. Nuttall (Lynn, Mass.) R. Casler (Los Angeles)	Data on nickel-cadmium, nickel-zinc, and metal-air batteries.
General Motors Corp. Allison Div. Indianapolis, Ind.	L. Johnson	Lead-acid battery technology.
Globe-Union, Inc. Milwaukee, Wis.	V. Halsall W. Towle	Data on lead-acid battery.
Gould-National Battery Co. Minneapolis, Minn.	S.S. Nielsen K. Christianson D. Douglas	Data on lead-acid battery.
Gulton Industries Metuchen, N.J.	C. Laurie C. Rosen W. Ryder R. Shair V. Wouk	Data on nickel-zinc, lead-acid and lithium halogen batteries.
Lead Industries Assn. New York, N.Y.	C.A. Baker	Data on lead-acid battery.
Mallory Battery Co. Ruben Labs. New Rochelle, N.Y.	S. Ruben	Lead-acid battery technology.
Massachusetts Institute of Technology Cambridge, Mass.	E. Gilliland R. Thornton	Data on nickel-zinc and lead-acid batteries.

Data Source	Primary Contact	Remarks
McCulloch Motors Los Angeles, Calif.	J. Bigby J. Dooley J. Orsino	Data on lead-acid and nickel-cadmium batteries. Change control data.
Standard Oil of Ohio Cleveland, Ohio	D.O. Maxwell	Advanced battery technology.
Textron Corp. Heliotek Div. Sylmar, Calif.	H. Sieger	Data on aluminum-chlorine battery.
TRW Systems Redondo Beach, Calif.	G. Gelb	Lead-acid and nickel-cadmium battery data and technology.
Tyco Labs. Waltham, Mass.	J. Giner R. Jasinski J. Perry	Battery technology.
Union Carbide Corp. Consumer Products Div. Parma, Ohio	R.J. Brodd	Battery technology.
Westinghouse Electric Corp. Redlands, Calif.	R. Bell C.W. Poole	Lead-acid battery technology.
Yuosa Battery (America), Inc. Gardena, California	S. Kawata	Lead-acid battery technology.

* *

Steering Committee on Secondary Battery Selection for Hybrid Vehicle:

Dept. of Defense

J. Lander, U.S. Air Force Aeropropulsion Laboratory, Dayton, Ohio
M. Sulkes, Fort Monmouth Army Electronics Command, New Jersey
R. Hopkins, J.R. Huff, Fort Belvoir Army Research and Development Laboratories, Virginia

Data Source	Primary Contact	Remarks
Steering Committee on Secondary Battery Selection for Hybrid Vehicle (Continued):		
L.R. Pollack, S. Szpak, Mare Island Naval Shipyard, Vallejo, Calif.		
J.C. White, U.S. Naval Research Laboratory, Washington, D.C.		
D. Icenhower, U.S. Naval Ship Research and Development Center, Annapolis, Md.		
Dept. of Health, Education and Welfare		
G. Hagey, C. Pax, Air Pollution Control Office, Ann Arbor, Mich.		
Dept. of Transportation		
R. Strombotne, Urban Mass Transport Administration, Washington, D.C.		
M. Solomon, Transportation Systems Center, Cambridge, Mass.		
NASA		
T. Hennigan, Goddard Space Flight Center, Greenbelt, Md.		
L. Rosenblum, H.J. Schwartz, Lewis Research Center, Cleveland, Ohio		
Civilian		
J. Kettler, D. Lapedes, The Aerospace Corporation, El Segundo, Calif.		
D.V. Ragone, Dartmouth College, Hanover, N.H.		

F.3 HEAT ENGINE PERFORMANCE CHARACTERISTICS AND OPERATION

Data Source	Primary Contact	Remarks
Aerojet-General Corp. Azusa, Calif.	R. Barrett	Data on organic Rankine engine.
American Motors Corp. Detroit, Mich.	P.A. Lundy	Data on American Motors engine and accessory products.
Barber-Nichols, Consulting Engineers Arvada, Colo.	R. Barber	Rankine engine technology.
Closed Cycle Systems Maspeth, N.Y.	D. Kelly	Data on Stirling engine.
Ford Motor Co. Engine and Foundry Div. Los Angeles, Calif.	F.E. Cashel	Performance and cost data on Ford Motor Co. industrial engine products.
Fort Belvoir Army Res. and Dev. Labs., Virginia	H. Barger R. Hopkins J. Huff J. MacDonald J. O'Sullivan	Heat engine controls data.
Garrett Corp., Signal Companies Los Angeles, Calif.	D. Furst H. Egli R. Hoffman	Gas turbine engine technology.
General Motors Corp. Chevrolet Motor Div. Warren, Mich.		Nova engine performance characteristics.
Lear Motors Corp. Reno, Nev.	E. Alford	Data on Rankine engine.

Data Source	Primary Contact	Remarks
Massachusetts Institute of Technology Cambridge, Mass.	E. Gilliland	Engine data.
McCulloch Motors Los Angeles, Calif.	J. Bigby J. Dooley J. Orsino	Data on diesel and Rankine engines.
Paxve, Inc. Costa Mesa, Calif.	E. Zwick	Data on Rankine engine.
R. J. Smith Consulting Engineer Midway City, Calif.	R.J. Smith	Rankine engine technology.
Rotron Research Corp. Woodstock, N.Y.	D. Carlson	Turbomachinery and engine technology.
Solar Aircraft San Diego, Calif.	M. Bull P. Carlson W. Compton W. Owens G. Backes	Gas turbine engine data and technology.
Southwest International Albuquerque, N.M.	P. Bencoe	Engine technology.
Sunstrand Corp. Rockford, Ill.	W. Heidrick	Rankine engine and transmission data and technology.
Steam Energy Systems Waltham, Mass.	L. Hoagland	Rankine engine technology and emission data.
Thermo Electron Eng. Co. Waltham, Mass.	D. Morgan	Rankine engine data and technology.

Data Source	Primary Contact	Remarks
United Aircraft Corp. Pratt and Whitney Aircraft Div. Hartford, Conn.	E. White P. Grevstad R. Kiefer (Los Angeles)	Data on gas turbine engine.
Univ. of Michigan Ann Arbor, Mich.	D. Patterson	Heat engine technology.
White Motor Corp. Torrance Calif.		Diesel engine smoke rating relationships and data.
Williams Research Corp. Walled Lake, Mich.	A.J. Feeney S. Williams	Gas turbine engine data and technology.

F. 4 HEAT ENGINE EXHAUST EMISSIONS

Data Source	Primary Contact	Remarks
Adam Opel Aktiengesellschaft Ruesselsheim, W. Germany	H. Zincke	Engine specifications for several Opel engines.
Automobile Club of Southern Calif. Los Angeles, Calif.	L. Bintz	Steady-state emission tests on two vehicles at various engine speeds and load conditions.
Calif. Air Resources Board Air Resources Lab. Los Angeles. Calif.	A. J. Hocker	Data on engine emissions during seven-mode driving cycle.
Caterpillar Tractor Co. Peoria, Ill.	R. D. Henderson	Information on Caterpillar diesel engine emissions.
Chaffee Motor Co. Hawthorne, Calif.	R. Crane	Donated Ford Pinto for test program at Scott Research Labs.
Clayton Mfg. Co. El Monte, Calif.	L. Tinkhaum	Engine emission data and information on chassis dynamometers and measuring techniques.
Cummins Engine Co. Columbus, Indiana	L. Eltinge	Present and projected diesel engine emission characteristics.

Data Source	Primary Contact	Remarks
Curtiss Wright Corp. Wood-Ridge, N. J.	C. Jones	Engine specifications and performance data for several Curtiss Wright Rotating Combustion (Wankel) engines.
Du Pont de Nemours Co. Los Angeles, Calif.	D. L. Pastell	Test data and general information on Du Pont low-emission vehicle.
Engine Manufacturers Assn. Chicago, Ill.	T. C. Young	Data on diesel engine emissions.
Engelhard Industries Newark, N. J.	J. Mooney	Catalytic converter provided for test program. General information on catalytic converter characteristics.
Environmental Protection Agency Air Pollution Control Office Ypsilante, Mich.	W. R. Stahmann T. Ashby	Data on cold start emissions.
Ford Motor Co. Pico Rivera, Calif.	J. Rhodes	Ford Pinto engine and vehicle data.

Data Source	Primary Contact	Remarks
General Motors Research Labs. Warren, Mich.	F. W. Bowditch C. Marks W. Cornelius C. A. Amann W. R. Wade P. T. Vickers T. H. Lievesch	Engine exhaust emission characteristics, part load emission data for spark ignition engine, operation and emission characteristics of the General Motors gas turbine, and emission characteristics of Rankine and Stirling engine burners.
Marquardt Co. Van Nuys, Calif.	C. V. Burkland	Discussions of Marquardt's study of external combustion engines.
Mercedes-Benz of North America, Inc. Fort Lee, N. J.	R. Theusner	Information on Mercedes-Benz OE 302 city bus with hybrid engine.
Minicars, Inc. Goleta, Calif.	D. Friedman, et al.	Discussions of the Minicar Hybrid Heat Engine/ Electric Vehicle.
Mobile Res. and Dev. Center Paulsboro, N. J.	P. W. Snyder	Emission data from the Inter-Industry Emission Control Program.

Data Source	Primary Contact	Remarks
Renault, Inc. Englewood Cliffs, N. Y.	F. Louis	Data on emission concentration vs engine speed and engine specifications for the Renault engine 810-20 (1289 cc).
Sierra Ford Co. San Bernardino, Calif.	K. Waddell	Donated Ford Pinto for test program at Scott Research Labs.
Solar Aircraft San Diego, Calif.	N. Tangedahl W. A. Compton	Emission test data from two Solar gas turbines and general information on gas turbine and combustor design.
Southwest Research Inst. San Antonio, Tex.	K. J. Springer	Reports on diesel and gasoline engine emissions and discussions of diesel engine test procedures and techniques.
Texaco, Inc. Beacon Research Labs. Beacon, N. Y.	E. Mitchell	Emission test data from Texaco Controlled Combustion System (TCCS).
Thermo Electron Corp. Waltham, Mass.	D. T. Morgan	Information on the Thermo Electron Rankine engine program.

Data Source	Primary Contact	Remarks
Thermo Mechanical Systems Co. Tarzana, Calif.	H. W. Welsh	General information on diesel and gasoline engine emissions. 13-mode emission data for several diesel engines.
TRW Systems Redondo Beach, Calif.	G. Gelb	Data on steady-state part load and cold start emissions from TRW Systems Hybrid Engine System.
Toyota Motor Co., Ltd. Lyndhurst, N. J.	K. Nakajima	Data on intake air volume vs RPM and manifold pressure for Toyota 115.7 C. D. engine.
U. S. Dept. Interior Bureau of Mines Bartlesville Petroleum Research Center Bartlesville, Okla.	R. Hurn W. F. Marshall	Data on emissions from a CFR engine operated with gasoline, propane, and methane over a wide range of air/fuel ratios. Data on parametric diesel engine emissions and general discussions on diesel engine emission characteristics.

Data Source	Primary Contact	Remarks
Universal Oil Products Research Center Des Plaines, Ill.	R. Allen	General discussion on performance of the UOP catalytic converter.
Univ. of Michigan Ann Arbor, Michigan	D. E. Cole	Discussions on state-of-the-art and projected automobile engine emissions.
Univ. of Wisconsin Madison, Wis.	H. K. Newhall O. A. Uyehara	Discussions on ante chamber and spark ignition engine operation and emission characteristics.
Wilcap Co. Torrance, Calif.	T. Capanna	Donated two diesel-powered vehicles for test program at Scott Research Labs.
Williams Research Corp. Walled Lake, Mich.	A. J. Feeney C. Hubin	Emission and performance test data from several Williams gas turbines and combustors.